

# **SAND REPORT**

SANDSAND2005-4446

Unlimited Release

Printed July 2005

## **Spent Fuel Sabotage Aerosol Ratio Program: FY 2004 Test and Data Summary**

Martin A. Molecke, Ken B. Sorenson, Theodore T. Borek III, Roy R. Dickey, John E. Brockmann, Daniel A. Lucero, Michael W. Gregson Richard L. Coats, Robert E. Luna, M.C. Billone, T. Burtseva, H. Tsai. Argonne, W. Koch, O. Nolte, B.A. Autrusson, O. Loiseau, T. Mo and F.I. Young,

Prepared by  
Sandia National Laboratories  
Albuquerque, New Mexico 87185 and Livermore, California 94550

Sandia is a multiprogram laboratory operated by Sandia Corporation, a Lockheed Martin Company, for the United States Department of Energy under Contract DE-AC04-94AL85000.

Approved for public release; further dissemination unlimited.



Issued by Sandia National Laboratories, operated for the United States Department of Energy by Sandia Corporation.

**NOTICE:** This report was prepared as an account of work sponsored by an agency of the United States Government. Neither the United States Government, nor any agency thereof, nor any of their employees, nor any of their contractors, subcontractors, or their employees, make any warranty, express or implied, or assume any legal liability or responsibility for the accuracy, completeness, or usefulness of any information, apparatus, product, or process disclosed, or represent that its use would not infringe privately owned rights. Reference herein to any specific commercial product, process, or service by trade name, trademark, manufacturer, or otherwise, does not necessarily constitute or imply its endorsement, recommendation, or favoring by the United States Government, any agency thereof, or any of their contractors or subcontractors. The views and opinions expressed herein do not necessarily state or reflect those of the United States Government, any agency thereof, or any of their contractors.

Printed in the United States of America. This report has been reproduced directly from the best available copy.

Available to DOE and DOE contractors from

U.S. Department of Energy  
Office of Scientific and Technical Information  
P.O. Box 62  
Oak Ridge, TN 37831

Telephone: (865)576-8401  
Facsimile: (865)576-5728  
E-Mail: [reports@adonis.osti.gov](mailto:reports@adonis.osti.gov)  
Online ordering: <http://www.doe.gov/bridge>

Available to the public from

U.S. Department of Commerce  
National Technical Information Service  
5285 Port Royal Rd  
Springfield, VA 22161

Telephone: (800)553-6847  
Facsimile: (703)605-6900  
E-Mail: [orders@ntis.fedworld.gov](mailto:orders@ntis.fedworld.gov)  
Online order: <http://www.ntis.gov/ordering.htm>



# Spent Fuel Sabotage Aerosol Ratio Program: FY 2004 Test and Data Summary

Martin A. Molecke, Materials Transportation Testing and Analysis, Dept. 6141  
Ken B. Sorenson, Dept. 6142, Theodore T. Borek III, Dept. 1823,  
Roy R. Dickey, Dept. 2554, John E. Brockmann and Daniel A. Lucero, Dept. 9117  
Michael W. Gregson and Richard L. Coats, Dept. 6783  
Sandia National Laboratories\*, P.O. Box 5800, Albuquerque, NM 87185-0718, USA  
Robert E. Luna, Consultant  
M.C. Billone, T. Burtseva, and H. Tsai, Argonne National Laboratory, USA  
W. Koch and O. Nolte, Fraunhofer Institut für Toxikologie und Experimentelle Medizin, Germany  
G. G. Pretzsch, F. Lange, and W. Brücher, Gesellschaft für Anlagen- und Reaktorsicherheit, Germany  
B.A. Autrusson and O. Loiseau, Institut de Radioprotection et de Surete Nucleaire, France  
N. Slater-Thompson and R.S. Hibbs, U.S. Department of Energy  
T. Mo and F.I. Young, U.S. Nuclear Regulatory Commission

## ABSTRACT

This multinational, multi-phase spent fuel sabotage test program is quantifying the aerosol particles produced when the products of a high energy density device (HEDD) interact with and explosively particulate test rodlets that contain pellets of either surrogate materials or actual spent fuel. This program has been underway for several years. This program provides data that are relevant to some sabotage scenarios in relation to spent fuel transport and storage casks, and associated risk assessments. The program also provides significant technical and political benefits in international cooperation. We are quantifying the Spent Fuel Ratio (SFR), the ratio of the aerosol particles released from HEDD-impacted actual spent fuel to the aerosol particles produced from surrogate materials, measured under closely matched test conditions, in a contained test chamber. In addition, we are measuring the amounts, nuclide content, size distribution of the released aerosol materials, and enhanced sorption of volatile fission product nuclides onto specific aerosol particle size fractions. These data are the input for follow-on modeling studies to quantify respirable hazards, associated radiological risk assessments, vulnerability assessments, and potential cask physical protection design modifications. This document includes an updated description of the test program and test components for all work and plans made, or revised, during FY 2004. It also serves as a program status report as of the end of FY 2004. All available test results, observations, and aerosol analyses plus interpretations – primarily for surrogate material Phase 2 tests, series 2/5A through 2/9B, using cerium oxide sintered ceramic pellets are included. Advanced plans and progress are described for upcoming tests with unirradiated, depleted uranium oxide and actual spent fuel test rodlets. This spent fuel sabotage – aerosol test program is coordinated with the international Working Group for Sabotage Concerns of Transport and Storage Casks (WGSTSC) and supported by both the U.S. Department of Energy and the Nuclear Regulatory Commission.

---

\* Sandia is a multi-program laboratory operated by Sandia Corporation, a Lockheed Martin Company, for the United States Department of Energy under contract DE-AC04-94-AL85000.

## **ACKNOWLEDGEMENTS**

The authors wish to acknowledge and express gratitude to the major contributions and support by multiple people to the ongoing conduct and updating of this surrogate/spent fuel sabotage and aerosol measurement test program. All of the participants of the international Working Group for Sabotage Concerns of Transport and Storage Casks are responsible for the continuing successes of this program. Most of the same people have also provided major technical inputs to the writing of this report, analyses of the data within, plus designs and fabrication for many of the test components. We also recognize Marc Hagan, explosives technician, and Manny Vigil, Sandia National Laboratories (retired, consultant) for providing significant guidance on the science of the explosive components and processes.

## TABLE OF CONTENTS

<b>SPENT FUEL SABOTAGE AEROSOL RATIO PROGRAM:</b>	
<b>FY 2004 TEST and DATA SUMMARY .....</b>	<b>3</b>
ABSTRACT.....	3
ACKNOWLEDGEMENTS.....	4
TABLE OF CONTENTS .....	5
FIGURES.....	7
TABLES .....	11
1. INTRODUCTION .....	13
2. DATA NEEDS.....	15
4. TEST COMPONENT DETAILS, PHASE 2.....	20
4.1 Surrogate Material Test Rodlets, Phase 2.....	20
4.1.1 Surrogate Cerium Oxide Pellets.....	20
4.1.2 Zircaloy 4 Cladding Tubes.....	21
4.1.3 Fission Product Dopant Disks.....	22
4.1.4 Other Phase 2 Surrogate Test Rods .....	24
4.2 Aerosol Collection/ Explosive Containment Test Chambers .....	25
4.3 Aerosol Particle Sampling System.....	28
5. PHASE 3 and PHASE 4 TEST COMPONENTS.....	32
5.1 Phase 3 Depleted Uranium Oxide Test Rodlets.....	32
5.2 Phase 4 Spent Fuel Test Rodlets.....	34
5.2.1 High-Burnup, H.B. Robinson Spent Fuel Test Rodlets .....	35
5.2.2 Lower Burnup, Surry Spent Fuel Test Rodlets.....	37
6. TEST CONDUCT AND AVAILABLE RESULTS.....	38
6.1 Phase 2 Tests 2/5A through 2/5G, Variables and Observations .....	38
6.2 Phase 2 Tests 2/7A and 2/7B, Variables and Observations .....	41
6.4 Phase 2 Tests 2/6A and 2/6B, Variables and Observations .....	43
6.5 Phase 2 Test Results and Observations.....	44
6.5.1 Target Rodlet Disruptions.....	44
6.5.1.1 Pellet Disruption and Blowback Material/Rod Debris, and Impact Debris.....	45
6.5.1.2 Particle Impact Debris.....	47
6.5.2 Instrumentation Results, Temperatures and Pressures.....	47
6.5.3 Phase 2 Test Aerosol Particle Data.....	51
6.5.3.1 Particle Stratification Within Aerosol Sampling Chamber.....	51
6.5.3.2 Aerosol Results for Cerium Oxide.....	53
6.5.3.3 Aerosol Results for Zirconium.....	57
6.5.3.4 Aerosol Results for Fission Product Dopants .....	58
6.6 Phase 2 / Phase 3 Cross-Over Tests and Results .....	63
7. GIF FACILITY ISSUES AND REQUIREMENTS .....	66
7.1 Anticipated GIF Testing Schedule.....	68
7.2 Additional Nuclear Facility Concerns .....	69
7.3 Post-test Off-Site Transport of Spent Fuel Test Chambers .....	70
8. TEST PROGRAM SUMMARY.....	72
APPENDIX A, Aerosol and Particle Analysis Results .....	77
A.1 Aerosol Particle Measurements, Phase 2 Tests.....	77

A.1.1	Aerosol Fraction Analyses and Results, Tests 2/1A – 2/4B .....	77
A.1.5A	Test 2/5A, Aerosol Fraction Analyses and Results.....	77
	Test 2/5A Impact Debris Particle Sampling and Results.....	80
	Test 2/5A Rod Debris Particle Sampling and Results .....	80
A.1.5B	Test 2/5B Analyses and Results .....	81
	Test 2/5B Elemental Analysis of Impact Debris.....	81
A.1.5C	Test 2/5C Analyses and Results .....	83
A.1.5D	Test 2/5D Analyses and Results.....	85
A.1.5E	Test 2/5E Analyses and Results.....	85
	Test 2/5E Elemental Analysis of Impact Debris.....	88
A.1.5F	Test 2/5F Analyses and Results.....	90
A.1.5G	Test 2/5G Analyses and Results.....	90
	Test 2/5G Elemental Analysis of Impact Debris .....	94
A.1.6A	Test 2/6A Analyses and Results.....	96
A.1.6B	Test 2/6B Analyses and Results .....	108
A.1.7B	Test 2/7B Analyses and Results .....	120
A.1.8A	Test 2/8A Analyses and Results.....	120
A.1.8B	Test 2/8B Analyses and Results .....	123
A.1.8C	Test 2/8C Analyses and Results .....	126
A.1.8D	Test 2/8D Analyses and Results.....	135
A.1.9A	Test 2/9A Analyses and Results.....	144
A.1.9B	Test 2/9B Analyses and Results .....	146
REFERENCES .....		147
DISTRIBUTION.....		150

## FIGURES

Figure 2.1 Schematic of SFR Correlations, Source-Term Estimation, and Modeling Process ...	16
Figure 4.1 Phase 2 Test Rodlet, Pellets, Tubing, and Rod Holders, Test 2/5G .....	22
Figure 4.2 Pressurized Test Rodlets for Tests 2/6A and 2/6B .....	22
Figure 4.3 Fission product-doped cerium oxide pellets (dopant in wells), Test 2/4A .....	23
Figure 4.4 Fission Product Dopant Disks, Adjacent to Central Pellet, Test 2/5E .....	23
Figure 4.5 German HLW Glass Test Rodlet for Tests 2/7A .....	25
Figure 4.6 Phase 2 Aerosol Collection-Explosive Containment Test Chamber (open) .....	26
Figure 4.9 Phase 4 Test Chamber (transparent drawing) .....	26
Figure 4.8 Phase 3 Test Chamber and Aerosol Sampling Systems .....	26
Figure 4.7 Explosive-Aerosol Test Process .....	27
Figure 4.10 Marple Aerosol Impactor, disassembled (showing individual stages and one fiberglass substrate) .....	28
Figure 4.11 Aerosol Particle Sampling System .....	30
Figure 4.12 Gelman Filter Bank Sequential Samplers .....	30
Figure 4.13 Schematic of Aerosol Sampling System, High & Low, with Gelman Filters .....	31
Figure 5.1 Schematic of Phase 3 DUO <sub>2</sub> Test Rodlet, DUR-4 .....	33
Figure 5.2 DUO <sub>2</sub> Pellets and Dopant Disks for Test 3/1 .....	33
Figure 5.3 Photograph of Phase 3 DUO <sub>2</sub> Test Rodlets .....	33
Figure 5.4 H.B. Robinson Spent Fuel Test Rodlet Design, Argonne National Laboratory .....	36
Figure 5.5 Surry Spent Fuel Test Rodlet Design, Argonne National Laboratory .....	36
Figure 6.1 Test 2/5A Aerosol Sampling Apparatus .....	38
Figure 6.2 Test 2/7A and 2/7B Aerosol Apparatus .....	42
Figure 6.3 Test 2/7A Post-Test Chamber and Participants .....	42
Figure 6.4 Post-test Glass Target Rodlet, Test 2/7A .....	42
Figure 6.5 Test 2/5E Post-test Rodlet .....	45
Figure 6.6 Test 2/5E Post-test Rodlet Ends .....	45
Figure 6.7 Test 2/5F Post-test Rodlet, Bent .....	45
Figure 6.8 Test 2/5G Post-test Rodlet .....	45
Figure 6.9 Test 2/6A Post-test Rodlet .....	46
Figure 6.10 Test 2/6A Post-test Rodlet and Test 2/6B Rodlet .....	46
Figure 6.11 Test 2/6A Post-test Rodlet Ends .....	46
Figure 6.12 Test 2/8C Post-test Rodlet .....	46
Figure 6.13 Test 2/8D Post-test Rodlet Ends .....	46
Figure 6.14 Test 2/9A Post-test Rodlet .....	46
Figure 6.15 Test 2/9A Post-test Rodlet Ends .....	46
Figure 6.16 Test 2/5G Rod Debris, 500 μm fraction .....	48
Figure 6.19 Test 2/6A Impact Debris, 1000 μm fraction .....	48
Figure 6.17 Test 2/5G Rod Debris, 250 μm fraction .....	48
Figure 6.20 Test 2/6A Impact Debris, 250 μm fraction .....	48
Figure 6.18 Test 2/5G Rod Debris, 100 μm fraction .....	48
Figure 6.21 Test 2/6A Impact Debris, 74 μm fraction .....	48
Figure 6.22 Test 2/8A and 2/8B Measured Temperatures .....	49
Figure 6.23 Test 2/8D Measured Temperatures .....	49
Figure 6.24 Test 2/6B Measured Temperatures .....	49
Figure 6.25 Test 2/5D Pressure Measurement, Aerosol Chamber .....	51

Figure 6.26 Test 2/8A and 2/8B Measured Pressures.....	51
Figure 6.27 Phase 2 Test Results for CeO <sub>2</sub> Respirable Fraction .....	54
Figure 6.28 Phase 2 Test 2/4A CeO <sub>2</sub> Cumulative Fraction .....	55
Figure 6.29 Phase 2 Test 2/4B CeO <sub>2</sub> Cumulative Fraction .....	55
Figure 6.30 Phase 2 Test 2/5A CeO <sub>2</sub> Cumulative Fraction .....	55
Figure 6.31 Phase 2 Test 2/5E CeO <sub>2</sub> Cumulative Fraction.....	55
Figure 6.32 Phase 2 Test 2/5G CeO <sub>2</sub> Cumulative Fraction .....	56
Figure 6.33 Phase 2 Test 2/6A CeO <sub>2</sub> Cumulative Fraction.....	56
Figure 6.34 Phase 2 Test 2/6B CeO <sub>2</sub> Cumulative Fraction.....	56
Figure 6.35 Phase 2 Test 2/8C CeO <sub>2</sub> Cumulative Fraction.....	56
Figure 6.36 Phase 2 Test 2/8D CeO <sub>2</sub> Cumulative Fraction.....	56
Figure 6.37 Phase 2 Test Results for Zirconium Respirable Fraction .....	58
Figure 6.38 Phase 2 Test Results for Cesium Dopant Respirable Fraction .....	59
Figure 6.39 Differential Enhancement Factor for Cesium on Glass Aerosol Particles .....	60
Figure 6.40 Copper and Cesium Size Distribution on HLW Glass, Test 2/7B .....	61
Figure 6.41 Test 2/9A Aerosol Sampler Temperatures .....	64
Figure 6.42 Test 2/9A Aerosol Sampler Pressures .....	64
Figure 6.43 Test 2/9B Aerosol Sampler Temperatures .....	64
Figure 6.44 Test 2/9B Aerosol Sampler Pressures .....	64
Figure 8.1 Sandia GIF Floor Plan.....	67
Figure 8.2 Eastward cross-sectional view of the GIF .....	67
Figure A1.5.1 Test 2/5B, Weight Percent Distribution of Metals in Impact Sieved Fractions ...	83
Figure A1.5.2 Test 2/5C, Weight Percent Distribution of Metals in Impact Sieved Fractions ...	84
Figure A1.5.3 Test 2/5E Marple Metals Analysis Distribution, milligrams.....	87
Figure A1.5.4 Test 2/5E Marple Fission Product Dopant Analysis Distribution, milligrams.....	88
Figure A1.5.5 Test 2/5E, Weight Percent Distribution of Metals in Impact Sieved Fractions ...	89
Figure A1.5.6 Test 2/5E, Weight % Distribution of Fission Product Dopants, Sieved Impact Debris.....	90
Figure A1.5.7 Test 2/5G Marple Metals Analysis Distribution, milligrams .....	93
Figure A1.5.8 Test 2/5G Marple Fission Product Dopant Analysis Distribution, milligrams ....	93
Figure A1.5.9 Test 2/5G, Weight Percent Distribution of Metals in Impact Sieved Fractions...	95
Figure A1.5.10 Test 2/5G, Weight % Distribution of Fission Product Dopants, Sieved Impact Debris.....	95
Figure A1.6.1 Test 2/6A Marple 2935 (high) Particle Size Distribution.....	96
Figure A1.6.2 Test 2/6A Marple 2938 (high) Particle Size Distribution.....	96
Figure A1.6.3 Test 2/6A Marple 2937 (low) Particle Size Distribution.....	96
Figure A1.6.4 Test 2/6A Marple 2941 (low) Particle Size Distribution.....	96
Figure A1.6.5 Test 2/6A Marple Impactors Mass Concentration.....	96
Figure A1.6.6 Test 2/6A Gelman Filters Mass Concentration .....	96
Figure A1.6.7 Test 2/6A, Marple #2935 (high) Metals Analysis Distribution, milligrams .....	99
Figure A1.6.8 Test 2/6A, Marple #2935 (high) Fission Product Dopant Analysis Distrib., mg.	99
Figure A1.6.9 Test 2/6A, Marple #2937 (low) Metals Analysis Distribution, milligrams.....	102
Figure A1.6.10 Test 2/6A, Marple #2937 (low) Fission Product Dopant Analysis Distrib, mg	102
Figure A1.6.11 Test 2/6A, Marple #2941 (low) Metals Analysis Distribution, milligrams.....	105
Figure A1.6.12 Test 2/6A, Marple #2941 (low) Fission Product Dopant Analysis Distrib, mg	105
Figure A1.6.13 Test 2/6A Weight % Distribution of Metals in Impact Debris.....	107
Figure A1.6.14 Test 2/6A Weight % Distribution of Fission Products in Impact Debris .....	107

Figure A1.6.15	Test 2/6B Marple 2935 (high) Particle Size Distribution.....	108
Figure A1.6.16	Test 2/6B Marple 2938 (high) Particle Size Distribution.....	108
Figure A1.6.17	Test 2/6B Marple 2937 (low) Particle Size Distribution.....	108
Figure A1.6.18	Test 2/6B Marple 2941 (low) Particle Size Distribution.....	108
Figure A1.6.19	Test 2/6B Marple Impactors Mass Concentration.....	108
Figure A1.6.20	Test 2/6B Gelman Filters Mass Concentration.....	108
Figure A1.6.21	Test 2/6B, Marple #2935 (high) Metals Analysis Distribution, milligrams.....	111
Figure A1.6.22	Test 2/6B, Marple #2935 (high) Fission Product Dopant Analysis Distrib, mg .....	111
Figure A1.6.23	Test 2/6B, Marple #2937 (low) Metals Analysis Distribution, milligrams.....	114
Figure A1.6.24	Test 2/6B, Marple #2937 (low) Fission Product Dopant Analysis Distrib, mg	114
Figure A1.6.25	Test 2/6B, Marple #2941 (low) Metals Analysis Distribution, milligrams.....	117
Figure A1.6.26	Test 2/6B, Marple #2941 (low) Fission Product Dopant Analysis Distrib, mg	117
Figure A1.6.27	Test 2/6B Weight % Distribution of Metals in Impact Debris.....	119
Figure A1.6.28	Test 2/6B Weight % Distribution of Fission Products in Impact Debris .....	119
Figure A1.8.1	Test 2/8A Marple 2935 (high) Particle Size Distribution.....	122
Figure A1.8.2	Test 2/8A Marple 2938 (high) Particle Size Distribution.....	122
Figure A1.8.3	Test 2/8A Marple 2937 (low) Particle Size Distribution.....	122
Figure A1.8.4	Test 2/8A Marple 2941 (low) Particle Size Distribution.....	122
Figure A1.8.5	Test 2/8A Marple Impactors Mass Concentration.....	122
Figure A1.8.6	Test 2/8A Gelman Filters Mass Concentration .....	122
Figure A1.8.7	Test 2/8A Weight % Distribution of Metals in Impact Debris.....	123
Figure A1.8.8	Test 2/8A Weight % Distribution of Fission Products in Impact Debris .....	123
Figure A1.8.9	Test 2/8B Marple 2935 (high) Particle Size Distribution.....	124
Figure A1.8.10	Test 2/8B Marple 2938 (high) Particle Size Distribution.....	124
Figure A1.8.11	Test 2/8B Marple 2937 (low) Particle Size Distribution.....	124
Figure A1.8.12	Test 2/8B Marple 2941 (low) Particle Size Distribution.....	124
Figure A1.8.13	Test 2/8B Marple Impactors Mass Concentration.....	124
Figure A1.8.14	Test 2/8B Gelman Filters Mass Concentration.....	124
Figure A1.8.15	Test 2/8B Weight % Distribution of Metals in Impact Debris.....	126
Figure A1.8.16	Test 2/8B Weight % Distribution of Fission Products in Impact Debris .....	126
Figure A1.8.17	Test 2/8C Marple 2935 (high) Particle Size Distribution.....	127
Figure A1.8.18	Test 2/8C Marple 2938 (high) Particle Size Distribution.....	127
Figure A1.8.19	Test 2/8C Marple 2937 (low) Particle Size Distribution.....	127
Figure A1.8.20	Test 2/8C Marple 2941 (low) Particle Size Distribution.....	127
Figure A1.8.21	Test 2/8C Marple Impactors Mass Concentration.....	127
Figure A1.8.22	Test 2/8C Gelman Filters Mass Concentration.....	127
Figure A1.8.23	Test 2/8C, Marple #2935 (high) Metals Analysis Distribution, milligrams.....	130
Figure A1.8.24	Test 2/8C, Marple #2935 (high) Fission Product Dopant Analysis Distrib, mg	130
Figure A1.8.25	Test 2/8C, Marple #2937 (low) Metals Analysis Distribution, milligrams.....	133
Figure A1.8.26	Test 2/8C, Marple #2937 (low) Fission Product Dopant Analysis Distrib, mg	133
Figure A1.8.27	Test 2/8C Weight % Distribution of Metals in Impact Debris.....	135
Figure A1.8.28	Test 2/8C Weight % Distribution of Fission Products in Impact Debris .....	135
Figure A1.8.29	Test 2/8D Marple 2935 (high) Particle Size Distribution.....	136
Figure A1.8.30	Test 2/8D Marple 2938 (high) Particle Size Distribution.....	136
Figure A1.8.31	Test 2/8D Marple 2937 (low) Particle Size Distribution.....	136
Figure A1.8.32	Test 2/8D Marple 2941 (low) Particle Size Distribution.....	136

Figure A1.8.33 Test 2/8D Marple Impactors Mass Concentration.....	136
Figure A1.8.34 Test 2/8D Gelman Filters Mass Concentration .....	136
Figure A1.8.35 Test 2/8D, Marple #2935 (high) Metals Analysis Distribution, milligrams ....	139
Figure A1.8.36 Test 2/8D, Marple #2935 (high) Fission Product Dopant Analysis Distrib, mg	139
Figure A1.8.37 Test 2/8D, Marple #2937 (low) Metals Analysis Distribution, milligrams.....	142
Figure A1.8.38 Test 2/8D, Marple #2937 (low) Fission Product Dopant Analysis Distrib, mg	142
Figure A1.8.39 Test 2/8D Weight % Distribution of Metals in Impact Debris.....	144
Figure A1.8.40 Test 2/8D Weight % Distribution of Fission Products in Impact Debris .....	144
Figure A1.9.1 Test 2/9A Marple #1 Particle Size Distribution .....	145
Figure A1.9.2 Test 2/9A Marple #2 Particle Size Distribution .....	145
Figure A1.9.3 Test 2/9A Marple #3 Particle Size Distribution .....	145
Figure A1.9.4 Test 2/9A Marple #4 Particle Size Distribution .....	145
Figure A1.9.5 Test 2/9A Marple Impactors Mass Concentration.....	145
Figure A1.9.6 Test 2/9B Marple #1 Particle Size Distribution.....	146
Figure A1.9.7 Test 2/9B Marple #2 Particle Size Distribution.....	146
Figure A1.9.8 Test 2/9B Marple #3 Particle Size Distribution.....	146
Figure A1.9.9 Test 2/9B Marple #4 Particle Size Distribution.....	146
Figure A1.9.10 Test 2/9B Marple Impactors Mass Concentration.....	146

## TABLES

Table 3.1 Phase 2 Tests: CeO <sub>2</sub> Surrogate Test Matrix.....	17
Table 3.2 Phase 2 / Phase 3 Crossover Tests: Phase 3 Chamber + CeO <sub>2</sub> Surrogate .....	18
Table 3.3 Phase 3 Tests: Advanced DUO <sub>2</sub> Surrogate Test Matrix.....	18
Table 3.4 Phase 4 Tests: Actual Spent Fuel Test Matrix.....	19
Table 4.1 Cerium Oxide Surrogate Pellet Specifications, as Fabricated .....	21
Table 4.2 Fission Product Dopant Chemicals, per Test.....	24
Table 6.1 General Test and Aerosol Particle Sampler Information, FY 2004.....	39
Table 6.2 Observed Post-Test Rodlet Disruptions, Phase 2 Tests.....	44
Table 6.3 Phase 2 Test Results for CeO <sub>2</sub> Respirable Fraction.....	54
Table 6.4 Phase 2 Test Results for Zirconium Respirable Fraction .....	57
Table 6.5 Phase 2 Test Results for Cesium Dopant Respirable Fraction .....	59
Table A1.1 General Test and RESPICON Particle Sampler Information .....	77
Table A1.5.1 Test 2/5A Respicon Respirable Fraction (0-4 μm stage) Analyses .....	78
Table A1.5.2 Test 2/5A Respicon Thoracic Fraction (4-10 μm stage) Analyses.....	78
Table A1.5.3 Test 2/5A Respicon Inhalable Fraction (10-100 μm stage) Analyses .....	79
Table A1.5.4 Test 2/5A Distribution of Fission Product Dopants on Respicon Filters.....	79
Table A1.5.5 Test 2/5A Distribution of Cerium on Respicon Filters.....	80
Table A1.5.6 Test 2/5A, Weight Distribution of Remaining Impact Debris .....	80
Table A1.5.7 Test 2/5A, Weight Distribution of Ceria Rod Debris .....	81
Table A1.5.8 Test 2/5B, Weight Distribution of Impact Debris.....	81
Table A1.5.9 Test 2/5B, Elemental Analysis wt% of Sieved Impact Debris .....	82
Table A1.5.10 Test 2/5C, Weight Distribution of Impact Debris.....	83
Table A1.5.11 Test 2/5C, Elemental Analysis wt% of Sieved Impact Debris .....	84
Table A1.5.12 Test 2/5E, Marple Particle Elemental Analyses, Stages 0-3.....	85
Table A1.5.13 Test 2/5E, Marple Particle Elemental Analyses, Stages 4-7.....	86
Table A1.5.14 Test 2/5E, Marple Particle Elemental Analyses, Stages 8-9.....	86
Table A1.5.15 Test 2/5E, Marple Particle Cerium and Fission Product Distributions.....	87
Table A1.5.16 Test 2/5E, Weight Distribution of Impact Debris.....	88
Table A1.5.17 Test 2/5E, Elemental Analysis Wt% of Sieved Impact Debris.....	89
Table A1.5.18 Test 2/5G, Marple Particle Elemental Analyses, Stages 0-3 .....	91
Table A1.5.19 Test 2/5G, Marple Particle Elemental Analyses, Stages 4-7 .....	91
Table A1.5.20 Test 2/5G, Marple Particle Elemental Analyses, Stages 8-9 .....	92
Table A1.5.21 Test 2/5G, Marple Particle Cerium and Fission Product Distributions .....	92
Table A1.5.22 Test 2/5G, Weight Distribution of Impact Debris .....	94
Table A1.5.23 Test 2/5G, Elemental Analysis Wt% of Sieved Impact Debris .....	94
Table A1.6.1 Test 2/6A, Marple #2935 (high) Elemental Analyses, Stages 0-3.....	97
Table A1.6.2 Test 2/6A, Marple #2935 (high) Elemental Analyses, Stages 4-7.....	97
Table A1.6.3 Test 2/6A, Marple #2935 (high) Elemental Analyses, Stages 8-9.....	98
Table A1.6.4 Test 2/6A, Marple #2935 Particle Cerium and Fission Product Distributions .....	98
Table A1.6.5 Test 2/6A, Marple #2937 (low) Elemental Analyses, Stages 0-3.....	100
Table A1.6.6 Test 2/6A, Marple #2937 (low) Elemental Analyses, Stages 4-7.....	100
Table A1.6.7 Test 2/6A, Marple #2937 (low) Elemental Analyses, Stages 8-9.....	101
Table A1.6.8 Test 2/6A, Marple #2937 Particle Cerium and Fission Product Distributions ....	101
Table A1.6.9 Test 2/6A, Marple #2941 (low) Elemental Analyses, Stages 0-3.....	103
Table A1.6.10 Test 2/6A, Marple #2941 (low) Elemental Analyses, Stages 4-7.....	103

Table A1.6.11	Test 2/6A, Marple #2941 (low) Elemental Analyses, Stages 8-9.....	104
Table A1.6.12	Test 2/6A, Marple #2941 Particle Cerium and Fission Product Distributions ..	104
Table A1.6.13	Test 2/6A, Weight Distribution of Impact Debris .....	106
Table A1.6.14	Test 2/6A, Elemental Analysis. Wt% of Sieved Impact Debris .....	106
Table A1.6.15	Test 2/6B, Marple #2935 (high) Elemental Analyses, Stages 0-3.....	109
Table A1.6.16	Test 2/6B, Marple #2935 (high) Elemental Analyses, Stages 4-7.....	109
Table A1.6.17	Test 2/6B, Marple #2935 (high) Elemental Analyses, Stages 8-9.....	110
Table A1.6.18	Test 2/6B, Marple #2935 Particle Cerium and Fission Product Distributions ..	110
Table A1.6.19	Test 2/6B, Marple #2937 (low) Elemental Analyses, Stages 0-3.....	112
Table A1.6.20	Test 2/6B, Marple #2937 (low) Elemental Analyses, Stages 4-7.....	112
Table A1.6.21	Test 2/6B, Marple #2937 (low) Elemental Analyses, Stages 8-9.....	113
Table A1.6.22	Test 2/6B, Marple #2937 Particle Cerium and Fission Product Distributions ..	113
Table A1.6.23	Test 2/6B, Marple #2941 (low) Elemental Analyses, Stages 0-3.....	115
Table A1.6.24	Test 2/6B, Marple #2941 (low) Elemental Analyses, Stages 4-7.....	115
Table A1.6.25	Test 2/6B, Marple #2941 (low) Elemental Analyses, Stages 8-9.....	116
Table A1.6.26	Test 2/6B, Marple #2941 Particle Cerium and Fission Product Distributions ..	116
Table A1.6.27	Test 2/6B, Weight Distribution of Impact Debris.....	118
Table A1.6.28	Test 2/6B, Elemental Analysis. Wt% of Sieved Impact Debris .....	118
Table A1.7.1	Test 2/7B, Marple #2941 (low) Elemental Analyses, mg.....	120
Table A1.8.1	Test 2/8A, Weight Distribution of Impact Debris .....	121
Table A1.8.2	Test 2/8A, Elemental Analysis. Wt% of Sieved Impact Debris .....	121
Table A1.8.3	Test 2/8B, Weight Distribution of Impact Debris.....	125
Table A1.8.4	Test 2/8B, Elemental Analysis Wt% of Sieved Impact Debris .....	125
Table A1.8.5	Test 2/8C, Marple #2935 (high) Elemental Analyses, Stages 0-3.....	128
Table A1.8.6	Test 2/8C, Marple #2935 (high) Elemental Analyses, Stages 4-7.....	128
Table A1.8.7	Test 2/8C, Marple #2935 (high) Elemental Analyses, Stages 8-9.....	129
Table A1.8.8	Test 2/8C, Marple #2935 Particle Cerium and Fission Product Distributions ....	129
Table A1.8.9	Test 2/8C, Marple #2937 (low) Elemental Analyses, Stages 0-3.....	131
Table A1.8.10	Test 2/8C, Marple #2937 (low) Elemental Analyses, Stages 4-7.....	131
Table A1.8.11	Test 2/8C, Marple #2937 (low) Elemental Analyses, Stages 8-9.....	132
Table A1.8.12	Test 2/8C, Marple #2937 Particle Cerium and Fission Product Distributions ..	132
Table A1.8.13	Test 2/8C, Weight Distribution of Impact Debris.....	134
Table A1.8.14	Test 2/8C, Elemental Analysis. Wt% of Sieved Impact Debris .....	134
Table A1.8.15	Test 2/8D, Marple #2935 (high) Elemental Analyses, Stages 0-3.....	137
Table A1.8.16	Test 2/8D, Marple #2935 (high) Elemental Analyses, Stages 4-7.....	137
Table A1.8.17	Test 2/8D, Marple #2935 (high) Elemental Analyses, Stages 8-9.....	138
Table A1.8.18	Test 2/8D, Marple #2935 Particle Cerium and Fission Product Distributions ..	138
Table A1.8.19	Test 2/8D, Marple #2937 (low) Elemental Analyses, Stages 0-3.....	140
Table A1.8.20	Test 2/8D, Marple #2937 (low) Elemental Analyses, Stages 4-7.....	140
Table A1.8.21	Test 2/8D, Marple #2937 (low) Elemental Analyses, Stages 8-9.....	141
Table A1.8.22	Test 2/8D, Marple #2937 Particle Cerium and Fission Product Distributions ..	141
Table A1.8.23	Test 2/8D, Weight Distribution of Impact Debris .....	143
Table A1.8.24	Test 2/8D, Elemental Analysis Wt% of Sieved Impact Debris .....	143

# Spent Fuel Sabotage Aerosol Ratio Program: FY 2004 Test and Data Summary

## 1. INTRODUCTION

This document provides a detailed overview, results, and near-term plans for an ongoing, multi-national test program that is measuring aerosol particle data for some spent fuel sabotage scenarios relevant to spent fuel transport and storage casks. The casks used for spent nuclear fuel transport are extremely resistant to releasing any significant fraction of their contents, even in very severe accident conditions. However, in some credible sabotage scenarios, such as an attack employing high energy density devices (HEDDs), i.e., explosive armor-piercing weapons, it is possible that a small percentage of aerosolized particles from disrupted fuel pellet materials could be released. If released to the environment in a significant quantity, the particulated spent fuel respirable particles have the potential to cause radiological consequences. Measurement of the actual amounts, nuclide content, and size distribution of the released materials from spent fuel is essential for predicting the significance of the radiological impacts. These source-term data are the input for follow-on modeling studies to quantify respirable hazards, associated radiological risk assessments, vulnerability assessments, and potential cask physical protection design modifications. The need for accurately quantifying this information has been strongly supported by program participants in the U.S., Germany, France, and the U.K., as part of the international Working Group for Sabotage Concerns of Transport and Storage Casks (WGSTSC). WGSTSC partners need, and are helping coordinate this research to better understand potential radiological consequences, and to support subsequent risk assessments, detailed modeling, and to develop potential preventative measures from plausible sabotage events.

Sandia National Laboratories (SNL, Albuquerque, NM) Materials Transportation Testing and Analysis Department 6141, has the lead role for managing and performing this research program. Other SNL Departments providing required expertise, engineering, testing, and facilities are: Dept. 2554, Explosive Testing and Diagnostics; Center 6700, Radiation Sciences (Nuclear and Risk Technologies); Dept. 9117, Plasma, Aerosol, Non-continuum Processes; and, Dept. 1822, Materials Characterization, Analytical Chemistry.

Overall sabotage and transportation program support is provided by both the U.S. Department of Energy (DOE, Office of Civilian Radioactive Waste Management (OCRWM)/ Office of National Transportation, and National Nuclear Security Agency (NNSA)/ Office of International Safeguards) and the U.S. Nuclear Regulatory Commission (NRC, Offices of Nuclear Regulatory Research, and Nuclear Security and Incidence Response). Argonne National Laboratory (ANL), Energy Technology Division, has provided the detailed characterization and fabrication work for all spent fuel test rodlets to be used in this program. German participants, the Gesellschaft für Anlagen- und Reaktorsicherheit (GRS) and the Fraunhofer Institute of Toxicology and Experimental Medicine (ITEM), are providing supporting aerosol testing, expertise, and data analyses. The Institut de Radioprotection et de Surete Nucleaire (IRSN), France, has provided unirradiated depleted UO<sub>2</sub> (surrogate, DUO<sub>2</sub>) fuel test rodlets plus supporting modeling studies. The Office for Civil Nuclear Security (OCNS), in the UK, participates in a consultative role.

There are significant benefits for the continuing, successful conduct of this program for all participants involved:

- (1) The cooperation of U.S., German, French, and British organizations and governmental entities provides a significant policy benefit, considering that this project can lead to im-

proved safety of the environment from a postulated nuclear incident. The data generated from this program may be useful for determining how to counter or mitigate consequences of a terrorist threat with explosives and spent fuel.

(2) The spent fuel ratio and reliable aerosol particle source term data and information to be derived from these tests, analyses, and subsequent modeling efforts (e.g., near-field releases, radiological consequences and risk assessments) will provide enhanced interpretations and clarifications to both current and earlier data on surrogate test materials [Molecke et al., 2004a, Lange et al., 1994, Sandoval et al., 1983] and very limited actual spent fuel results [Schmidt et al., 1981, Alvarez et al., 1982].

(3) Through improved radiological and safety assessments, quantifications of respirable hazards, vulnerability assessments, and potential physical protection design modifications, an additional margin of safety to the environment may be provided from a plausible, albeit unlikely, sabotage scenario relevant to nuclear material transportation. These assessments may help guide transportation regulations and/or validate their current technical bases.

(4) The lack of adequate, detailed analyses based on representative and defensible data has required previous estimates of potential consequences of a sabotage attack to be very conservative. Therefore, the need exists to perform well designed experimental research to obtain technically defensible data on the generation of respirable aerosols formed from HEDD attack against spent nuclear fuel, SNF, and other, related radioactive materials. This need should be satisfied by the data output, and subsequent modeling analyses, originating from the current test program.

(5) This test program's analysis of aerosol release relevant to transportation and storage scenarios may be directly applied to the spent nuclear fuel surface and repository facility operations, thereby facilitating the important process of evaluating sabotage risk to the entire back end of the nuclear fuel cycle.

A major purpose of this document is to provide an update and extension to the FY 2003 document [Molecke et al., 2004a] that detailed this ongoing, multi-phase test program and the results obtained to date. We shall focus on new developments in test program design, test apparatus improvements, and document all the available data obtained over the past year. We shall present significant detail and test apparatus descriptions for the to-be initiated Phase 3 tests which include unirradiated, depleted uranium oxide and the upcoming, Phase 4, actual spent fuel aerosol-explosive tests.

The goals and objectives of this spent fuel sabotage aerosol measurements program and a summary of the historical background of related tests that built the foundation of the current test program were documented previously [Molecke et al., 2004a], and shall not be repeated herein.

## 2. DATA NEEDS

Aerosol particle testing requires sampling and measurement of the mass and physical characteristics of the aerosol particles produced from (spent fuel or surrogate rod) target-HEDD jet impact, with particle aerodynamic equivalent diameters (AED) up to 100  $\mu\text{m}$  (micrometers). The AED is defined by means of the settling velocity of a unit density sphere, and is equivalent to the particle geometric-diameter times the (particle density)<sup>1/2</sup>. For evaluations of aerosol and radiological consequences, there has always been a special emphasis on respirable particles, commonly defined as 0 to  $\leq 10 \mu\text{m}$  AED in size. Respirable particles also have been sub-categorized into the *respirable* fraction, 0 to  $\sim 4 \mu\text{m}$ , and the *thoracic* fraction,  $\sim 4$  to  $\sim 10 \mu\text{m}$  AED. Data from the coarser aerosol particles in the  $\sim 10$  to  $100 \mu\text{m}$  AED range, termed the *inhalable* fraction, are of interest primarily for radiological “ground-shine” (dispersion, soil contamination, potential ingestion) consequence estimates. Particles larger than  $100 \mu\text{m}$  are not considered to be aerosols. Multistage aerodynamic particle sizing devices (impactor collectors) are used to classify aerosol particles according to their aerodynamic diameter, and will be described later.

This experimental program is designed to measure two important features of the interaction of a HEDD (conical shaped charge, CSC) jet with spent fuel or surrogate material pellets contained within a Zircaloy-4™ cladding tube:

1. The measurement of a more accurate and precise value for the Spent Fuel Ratio (SFR) for respirable particles. The SFR is defined as:

$$\text{SFR} = [\text{spent fuel aerosol particle masses}] / [“\text{surrogate}” \text{ aerosol particle masses}]$$

The SFR determination is, essentially, the comparison of the respirable, aerosol particle data from irradiated fuel to unirradiated surrogate fuel. These data are obtained in paired experiments using the same apparatus, identical test conditions, and using the same HEDD. The SFR will be calculated from respirable, aerosol particles collected in multiple size ranges, from 0 up to about  $10 \mu\text{m}$ . There is special emphasis on the particle *respirable fraction*, defined as the mass of an element (i.e., U, Ce, Zr, Cs, etc.) in respirable particles (0 -  $10 \mu\text{m}$  AED) / mass of that element in the rod volume swept (particulated) by the HEDD; this is particularly relevant to far-field, airborne dispersion and consequence modeling studies. The measured SFR values provide a data bridge to previous large-scale surrogate (DUO<sub>2</sub>) cask tests [Lange et al., 1994, Sandoval et al., 1983] and consequence assessments. The SFR values permit scaling to other geometries, single fuel rod to rod bundles, by means of modeling.

The primary test benefit of using the ratio of respirable, aerosol particles for the SFR determination is that it is not necessary to recover and analyze all of the aerosolized materials produced; only the identical portions of aerosol particles from both the spent fuel and surrogate fuel tests must be obtained, analyzed, and compared. This ratio drives the requirement for use of identical-as-possible test apparatus and test conditions for multiple test phases and materials. In addition, by focusing on the spent fuel ratio determination, we can use test rodlets containing only a few actual or surrogate fuel pellets for aerosol particle production. Entire fuel assemblies or casks full of fuel assemblies do not need to be tested.

2. The measurement of enhancement or enrichment of volatile fission product nuclides like cesium and, to a lesser extent, ruthenium, preferentially sorbed onto specific, respirable particle size fractions in the sub- $\mu\text{m}$  to  $\mu\text{m}$  size range.

Figure 2.1 [Luna, 2004] conceptually illustrates how the measured SFR from the current test program can be used to correlate the available SFR data measurements (from Sandia and others) from small-scale tests, to larger-scale surrogate cask tests [Lange et al., 1994, Sandoval et al., 1983]. These data can be used to model source term releases from actual spent fuel casks. Aerosol test data plus follow-on modeling are needed to correlate, or scale, small-scale spent fuel rodlet results together with limited earlier, intermediate-to-large-scale surrogate results, to obtain reliable source term values representative of potential releases from a sabotage event on an actual, full-scale spent nuclear fuel transport or storage cask.

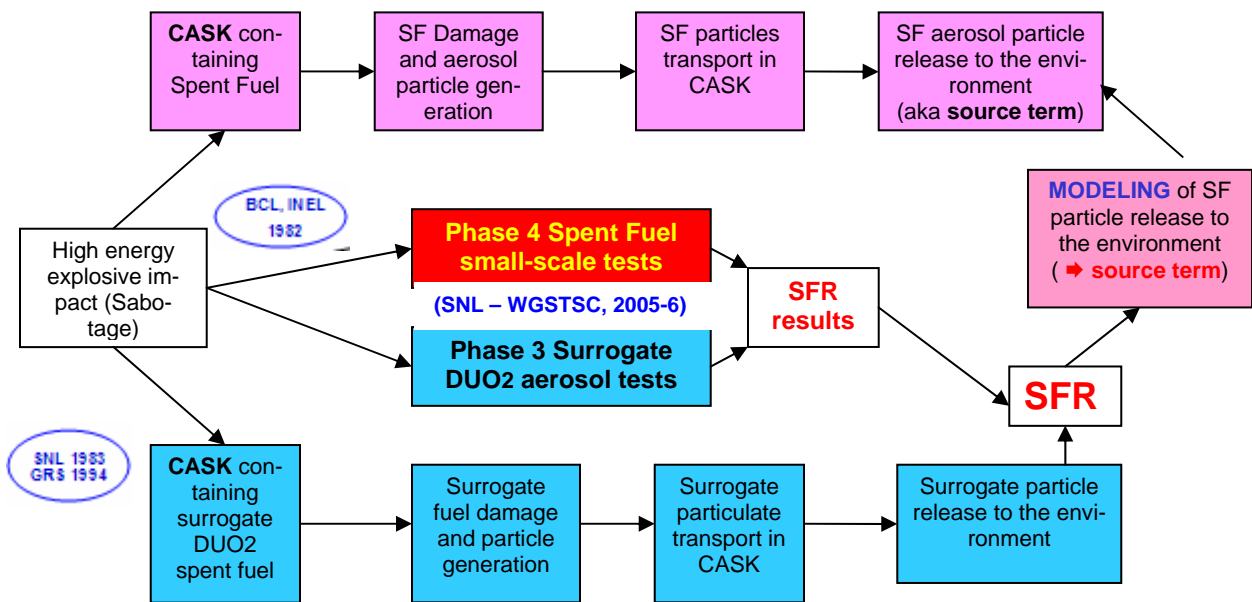


Figure 2.1 Schematic of SFR Correlations, Source-Term Estimation, and Modeling Process

### 3. TEST PROGRAM DESIGN

The overall test program plan and design was described and documented in Sandia Technical Report SAND2004-1832 [Molecke et al., 2004a]. That report identified the number and sequence of tests for the total program. It also documented test component plans and requirements as of the end of FY 2003. The following descriptions of test number, by test phase, and testing sequence, is an update and modest revision to that test plan. Changes to the original test plan were based on test observations and improvements plus programmatic decisions made during FY 2004. *This* document includes the following revised test plan and test descriptions, and is defined as the *revised* test plan.

The overall program consists of four sequential test phases, Phase 1 through Phase 4. Individual tests in each phase use the identical type of HEDD, but different test materials with similar geometries. Successive phase testing has allowed the addition and evaluation of multiple test variables and target material (pellet) response to HEDD jets, and consequent aerosol particle production. All four test phases were previously described [Molecke et al., 2004a] in detail, as of the end of FY 2003. The following details focus on modifications to Phases 2, 3, and 4.

The extensive Phase 2 tests use nonradioactive cerium oxide, CeO<sub>2</sub>, as sintered ceramic pellets contained within Zircaloy cladding tube assemblies, similar to spent fuel rods. CeO<sub>2</sub> was selected as an excellent chemical “surrogate” and a representative ceramic material for UO<sub>2</sub> fuel material for pressurized water reactor fuel rods [Molecke et al., 2004a, Molecke et al., 2004b]. Twenty four Phase 2 surrogate material tests were conducted in the 2002 - 2004 period. These tests were the necessary precursors to calibrate the equipment design prior to performance of the more difficult Phase 3 and 4 tests. The Phase 2 tests also allowed us to *anticipate* the range of results from the latter tests. The revised, final Phase 2 test matrix is listed in Table 3.1.

**Table 3.1 Phase 2 Tests: CeO<sub>2</sub> Surrogate Test Matrix**

Test Phase 2: Cerium Oxide Surrogate Pellets/Rods					
Test #	Pressure	Dopants	Variables	Date	
0	1 bar	no	top; system checkout	10/2002	
1A, 1B	1	no	top, center; Respicon samplers	10/2002	
2A, 2B	1	no	optimized for French pellet & tube size	12/2002	
3A, 3B	1	no	optimized for U.S. pellet & tube size, Respicon & Berner samplers	7/2003	
4A, 4B	1	yes	+ rev. equipment design, FP dopants	8/2003	FY 2003 ↑↑↑↑
5A – 5G	1	yes	+ vertical test chamber, instruments, Marple particle impactors.	9/03-1/04	
6A, 6B	28-38 blowdown	yes	+ equipment design modifications, Marple impactors, Large Particle Sep.	4-5/2004	
7A, 7B	1	yes	German HLW glass rod, dopants (nonradioactive)	2/2004	
8A – 8D	1	yes	particle impactors & sampling optim.	2-4/2004	FY 2004 ↑↑↑↑

The Phase 2 / Phase 3 crossover tests, Table 3.2, were separated from the remainder of the Phase 2 tests using surrogate cerium oxide test rodlets and were added in FY 2004. They are intended as the initiation to, and practice for, the following Phase 3 tests. These crossover tests use a new, more sophisticated Phase 3 explosive-aerosol test chamber plus four independently operated aerosol collection systems. Tests 2/9A, 9B, and 9C were performed in the SNL Explosive Components Facility, for new equipment handling operations and optimization testing. The final two tests, 2/9D and 9E, will be performed in the SNL GIF Test Cell 3 facility and will be handled in a “semi-remote” manner, similar to the (slightly) radioactive, Phase 3 depleted uranium oxide tests. No dopant materials will be used, in order to eliminate fission product species residual contamination concerns in subsequent DUO<sub>2</sub> tests.

**Table 3.2 Phase 2 / Phase 3 Crossover Tests: Phase 3 Chamber + CeO<sub>2</sub> Surrogate**

Test #	Pressure	Dopants	Variables	Date
9A	1 bar	no	new test chamber, 4 Marples & LPS, in ECF	8/2004
9B	1 bar N <sub>2</sub>	no	Same, with inert atmosphere, in ECF	8/2004
9C	1 bar	no	“blank” w/Zirc tube, for post-test handling operations, 4 Marples & LPS	11/2004
9D	1 bar	no	in GIF, “as if” DUO <sub>2</sub> Phase 3, 4 Marples & LPS	2005-06
9E	1 bar N <sub>2</sub>	no	in GIF, same, w/ inert atmosphere	2005-06

Phase 3 tests use unirradiated, depleted uranium oxide (DUO<sub>2</sub>) pellets in comparable, new Zircaloy cladding tube test rodlets. The overall Phase 3 aerosol-explosive test chamber is based on the similar, but less sophisticated Phase 2 chamber design(s). Six of the Phase 3 tests should be performed in 2005-06, as listed in Table 3.3. The DUO<sub>2</sub> test rodlets have been designed and fabricated by our French test partner, IRSN, and their contractor, CERCA (a subsidiary of Framatome-ANP), and will be described in detail.

**Table 3.3 Phase 3 Tests: Advanced DUO<sub>2</sub> Surrogate Test Matrix**

<b>Test Phase 3: Depleted Uranium Oxide Pellets/Rods, from IRSN</b>				
Test/Rod (order)	Pressure	Dopant	Variables	GIF Date *
3/1 (c)	1 bar	yes	air (in aerosol chamber)	2006
3/2 (a)	1	no	air	2005
3/3 (d)	1	yes	N <sub>2</sub>	2006
3/4 (e)	40 (He)	yes	air	2006
3/5 (b)	40	no	air	2005
3/6 (f)	40	yes	N <sub>2</sub>	2006

(\* estimated schedule, based on GIF availability, subject to future revision)

Note that the Phase 3 testing “order,” (a) to (f), in Table 3.3 is now different than the test/rod numbers. This was modified in order to eliminate cross-contamination from the test rodlets that contain non-radioactive fission product dopant disks. Testing with all Phase 3 test rodlets that contain no dopants will be performed first. It is projected that Phase 3 tests can be performed every two- to three-weeks. Test turn-around or cycle time is dependent on the operational and test chamber decontamination schedule times, still to be finalized.

Phase 4 tests, as listed in Table 3.4, will use radioactive spent fuel pellets in short test rodlets. Four of the Phase 4 tests will use high burnup (~ 72 GWd/MTU) spent fuel originating from the H.B. Robinson pressurized water reactor. Another four Phase 4 tests will use a low-medium burnup (~ 38 GWd/MTU) spent fuel originating from the Surry pressurized water reactor. All of the spent fuel is being characterized in detail and fabricated into test rodlets at Argonne National Laboratory. The Phase 4 HEDD-impact aerosol testing will be conducted in the Gamma Irradiation Facility, GIF, at SNL during 2006. The final calculation of the spent fuel ratio, SFR, as a function of aerosol particle size ranges, will be based on a comparison of the aerosol particle results from the Phase 4, actual spent fuel data, to the Phase 3, surrogate DUO<sub>2</sub> data. These data will be obtained from paired sets of experiments using identical test conditions and apparatus.

**Table 3.4 Phase 4 Tests: Actual Spent Fuel Test Matrix**

<b>Test Phase 4: Actual Spent Fuel (PWR) Rodlets, from ANL</b>			
<b>Test #</b>	<b>Pressure</b>	<b>Variables</b>	<b>GIF Date *</b>
4/1	~ 44 bar (rod plenum)	H.B. Robinson, high-burnup, ~72 GWd/MTU	2006
4/2	~ 44 (He)	Air (in aerosol chamber)	2006
4/3	~ 44	N <sub>2</sub>	2006
4/4	~ 44	N <sub>2</sub>	2006
4/5	~ 33 bar	Surry, low-med burnup, ~38 GWd/MTU	2006
4/6	~ 33 (He)	Air	2006
4/7	~ 33	N <sub>2</sub>	2006
4/8	~ 33	N <sub>2</sub>	2006

(\* estimated schedule, based on GIF availability, subject to future revision)

Phase 4 test conduct and test turn-around or cycle time is dependent on the operational and facility schedule times, still to be finalized. However, Phase 4 test chamber decontamination is not an issue, since each Phase 4 test chamber will be used one-time only.

## 4. TEST COMPONENT DETAILS, PHASE 2

The major components required for conduct of the surrogate and spent fuel sabotage, HEDD impact, and aerosol measurement tests include:

1. test rodlets and target pellets: The Phase 2 and Phase 2/Phase 3 cross-over test rodlets consist of Zircaloy-4 cladding tubes, plus sintered ceramic pellets of cerium oxide (with or without non-radioactive fission product dopant disks). Two tests, 2/6A and 2/6B, were internally pressurized with helium gas. Similarly, two tests, 2/7a and 2/7B, contained non-radioactive, German high-level waste (HLW) glass, with dopants, in a stainless steel cladding tube. The Phase 3 test rodlets contain depleted uranium oxide pellets, with or without non-radioactive fission product dopant disks. The Phase 4 test rodlets contain actual spent fuel pellets (high burn-up or low/medium burn-up) in their original, irradiated Zircaloy-4 cladding tubes.
2. test chamber: The test chamber consists of a vertical, two-segment, single unit, aerosol collection chamber and explosive containment chamber. The Phase 2, Phase 3, and Phase 4 test chambers will be described individually.
3. aerosol particle samplers: Marple particle impactors, large particle samplers (LPS), plus associated sampling tubes, valves, vacuum bottles, and other test equipment. (Earlier Phase 1 and Phase 2 tests used other, similar components; these will also be described).
4. conical shape charge (CSC): The HEDD. Individual tests in each phase of this program use identical precision CSCs, containing 72.5 grams of PBX-N5 explosive (95% HMX and 5% VITON A and is ~ 85 g of TNT equivalent). The CSC has an aluminum housing. Within the test chamber, the HEDD is held in place with a polyvinyl chloride (PVC) fixture-holder, and has a stand-off distance of 7.5 inches (19 cm).
5. test facilities: Non-radioactive Phase 2 and Phase 2/Phase 3 tests were performed at the Sandia Explosive Components Facility, predominantly in Sandia building 905 (tests 2/6A-6B, 2/7A-7B, 2/8A-8D, and 2/9A-9B). Additional tests were performed outside of the remote-site building 6750 (Gun Site/Terminal Ballistics Facility) (tests 2/5A through 5G). All Phase 3 (DUO<sub>2</sub>) and Phase 4 (spent fuel) explosive-aerosol tests are anticipated to be performed in the SNL Gamma Irradiation Facility (GIF), in cell 3.

Test components have been modified and upgraded as a function of time, particularly over the past year. Components used during 2002 and 2003 were described in detail in [Molecke et al., 2004a]. This section describes experimental detail for test Phase 2 test components, predominantly.

### 4.1 Surrogate Material Test Rodlets, Phase 2

The Phase 2 tests rodlets consist primarily of multiple cerium oxide surrogate, sintered ceramic pellets contained within a Zircaloy-4 cladding tube. Eight of the Phase 2 tests also incorporated non-radioactive fission product dopants. Two of the test rodlets, for tests 2/7A and 2/7B, contained non-radioactive, German high-level waste (HLW) glass, with dopants, in stainless steel cladding tubes.

#### 4.1.1 Surrogate Cerium Oxide Pellets

Cerium oxide powder has been pressed and sintered into ceramic pellets for our testing purposes, by the Ceramic Synthesis and Processing, Department 1843, at SNL. The reasons for selecting

sintered, ceramic cerium oxide (CeO<sub>2</sub>) for use as a surrogate “spent fuel” pellet material was described previously [Molecke et al., 2004a]. The cerium oxide powder (99.9 % pure, about 5 μm grain size) was mixed with about 3 wt. % organic material binder, mechanically screened, then uniaxially dry pressed in a metal die (nominally at ~200 MPa, ~29 kpsi) into “green” pellets. These were fired at about 600 °C for binder burnout, then sintered at about 1600 °C [Ewsuk and Diantonio, 2002]. Measurements of apparent pellet porosity and Archimedes density were then performed. The pellets were made to fit snugly (i.e., with minimal pellet-to-cladding gap) into the Zircaloy 4 cladding tubes. Table 4.1 lists measured cerium oxide pellet specifications.

**Table 4.1 Cerium Oxide Surrogate Pellet Specifications, as Fabricated**

Test #	Pellet Wts. ave. & (total)	Ave. Theoretical Density	Average Diameter	Average Height (total)	Pellets/ per Rod	Dopants
2/5A	3.14 g (27.933 g)	95.3% 6.80 g/cc	9.15 mm	6.98 mm (62.8 mm)	9	dopants in pellet wells
2/5E	3.15 g (28.316 g)	95.3% 6.80 g/cc	9.15 mm	7.01 mm (63.1 mm)	9	include 2 dopant disks
2/5F	3.28 g (29.533 g)	94.1% 6.71 g/cc	9.13 mm	7.47 mm (67.2 mm)	9	include 2 dopant disks
2/5G	3.24 g (29.112 g)	94.9% 6.77 g/cc	9.14 mm	7.29 mm (65.7 mm)	9	include 2 dopant disks
2/6A	3.19 g (28.741 g)	91.5% 6.53 g/cc	9.14 mm	7.46 mm (65.3 mm)	9	include 2 dopant disks
2/6B	3.20 g (28.788 g)	91.6% 6.53 g/cc	9.08 mm	7.50 mm (65.3 mm)	9	include 2 dopant disks
2/8C	3.22 g (28.982 g)	94.9% 6.77 g/cc	9.15 mm	7.26 mm (65.3 mm)	9	include 2 dopant disks
2/8D	3.16 g (28.448 g)	92.9% 6.62 g/cc	9.14 mm	7.28 mm (65.5 mm)	9	include 2 dopant disks
2/9A	3.20 g (28.765 g)	92.9% 6.62 g/cc	9.10 mm	7.42 mm (66.8 mm)	9	no dopants
2/9B	3.20 g (28.767 g)	93.4% 6.66 g/cc	9.09 mm	7.39 mm (66.5 mm)	9	no dopants

#### 4.1.2 Zircaloy 4 Cladding Tubes

The Zircaloy 4 cladding tubes used were purchased from Framatome ANP Richland, Inc. Richland, WA. This tubing was manufactured by Advanced Nuclear Fuels (ANF), GMBH, Duisburg, Germany, and was 10.6 mm outside diameter and 9.32 mm inside diameter. This tubing is the closest in diameter available (at the time) to both H.B. Robinson and Surry U.S. PWR, pressurized water reactor, spent fuel rods. All Zircaloy cladding tubes for test series 2/5 and 2/8 were 304.8 mm (12.0 inches) long. Test rodlet tubes for 2/6A and 2/6B were 254 mm (10.0 inches) long and had special end cap designed to contain internal pressurization (to be described). Zircaloy 4 consists of zirconium, with ~ 1.45 wt. % Sn, 0.11 % Cr, 0.23 % Fe, 0.34 % Fe + Cr, and 0.12 % oxygen. Some of the more significant trace impurities, at the ppm level, include: Al, C, Hf, Nb, Ni, Pb, Si, Ta, and W.

Figure 4.1 shows a typical Phase 2 test rodlet (for test 2/5G, during assembly). The Zircaloy cladding tube was 30.5 cm long, with nine cerium oxide pellets, and two fission product dopant disks; the end holder rods that hold the rod in-place within the test chamber are also shown. Fig-

ure 4.2 shows the similar test rods for tests 2/6A and 2/6B. These rodlets are different because they are internally pressurized with helium gas.

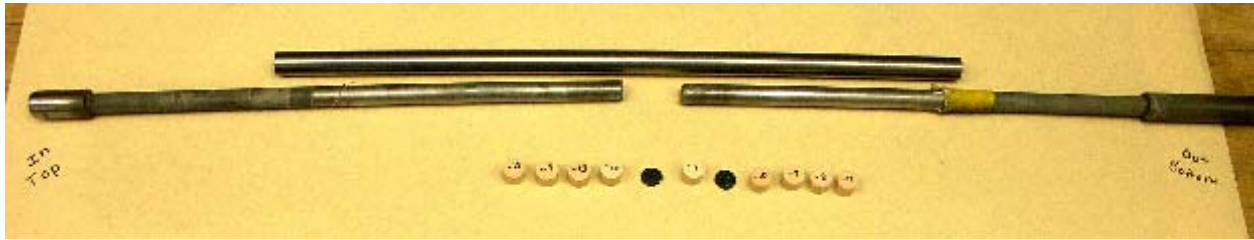


Figure 4.1 Phase 2 Test Rodlet, Pellets, Tubing, and Rod Holders, Test 2/5G



Figure 4.2 Pressurized Test Rodlets for Tests 2/6A and 2/6B

### 4.1.3 Fission Product Dopant Disks

One of the major goals of this overall experimental program is to quantify the potential enrichment of volatile fission product nuclides on respirable-size particulates produced from a spent fuel–HEDD jet impact. Volatilized species of cesium ( $^{134}\text{Cs}$ ,  $^{137}\text{Cs}$ ) and ruthenium ( $^{106}\text{Ru}$ ) have been mentioned as most significant. Cs exists in several forms in spent nuclear fuel (SNF) [Billone and Tsai, 2003, Olander, 1976], primarily as Cs vapor, plus complex oxides (e.g., cesium uranate,  $\text{Cs}_2\text{UO}_4$ , and cesium molybdenate,  $\text{Cs}_2\text{MoO}_4$ ). In colder rod regions (e.g., at fuel cladding bond, especially at crack tips), CsI vapor can condense. In general, the fission product yield of Cs is much higher than that of I, so all the iodine may be tied up as CsI, but certainly not all of the Cs. A really crude estimate for Cs based on fission yield is to assume 3%  $^{235}\text{U}$  enrichment and all fissions coming from  $^{235}\text{U}$ . If the fissions yield about 0.22 Cs/ $^{235}\text{U}$  fissioned, about 0.3 wt.% Cs would be generated. Based on isotopic measurements of  $^{137}\text{Cs}$  in PWR fuel operated to about 50 GWd/MTU, the  $^{137}\text{Cs}$  content is 0.16 wt.%. Ru exists in SNF mostly in metallic form with low vapor pressure. Therefore, it is not a volatile fission product. Ru is of radiological importance because of its high radiotoxicity.  $\text{RuO}_2$  is not stable above 1350 °C. If sufficient oxygen is present (e.g., if  $\text{UO}_2$  transforms to  $\text{U}_3\text{O}_8$ ), Ru will start to oxidize to  $\text{RuO}_3$  and  $\text{RuO}_4$ , both with very high vapor pressures (boiling point is only 108 °C for  $\text{RuO}_4$ ). Given the very short-time/high-temperature of a CSC jet, we may assume that Ru comes off in metallic form. If we dope the test rodlet/pellets with  $\text{RuO}_2$ , the produced aerosol may contain Ru.

Non-radioactive chemical forms of cesium and ruthenium have been added to the surrogate pellet test systems, starting with tests 2/4A and 2/4B [Molecke et al., 2004a] and continuing through eight more Phase 2 tests conducted in FY 2004; refer to Table 4.1. We have chosen cesium iodide, CsI [99.999%, Alfa Aesar catalog # 10992], and ruthenium oxide, RuO<sub>2</sub> [99.95%, anhydrous, Alfa Aesar catalog # 11804], for testing expediency. Strontium is another major fission product species, <sup>90</sup>Sr, but it is not easily volatilized. It has also been added to this test system as strontium oxide, SrO [99.5%, Alfa Aesar catalog # 88220], as a non-volatile “standard” fission product dopant, to be compared to the volatile Cs, Ru, and I species distribution for enrichment determinations. The boiling point, vaporization temperatures for CsI, RuO<sub>2</sub>, and SrO are 1280 °C, 1200 °C, and ~ 3000 °C, respectively. We also added europium oxide, as Eu<sub>2</sub>O<sub>3</sub> [99.99%, Alfa Aesar catalog # 11299], as another non-volatile “standard” fission product dopant.

The initial fission product dopant samples, used in tests 2/4A, 2/4B, and 2/5A, only, were prepared by inserting the solid dopant chemicals into small “wells” pre-drilled in one end (prior to sintering) into the cerium oxide pellets, one chemical per pellet; refer to Figure 4.3. Each doped pellet contained approximately 1000 ppm (0.1 wt %) of stable Cs, I, Ru, or Sr species, relative to the mass of the surrogate oxide pellet expected to be disrupted per test. The solid chemicals were held in place with a drop of super glue. Prior to HEDD impact, the dopant chemicals were not subjected to elevated temperatures so there would be no thermal volatilization.

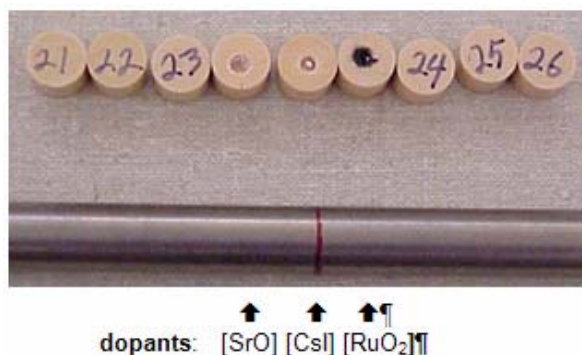


Figure 4.3 Fission product-doped cerium oxide pellets (dopant in wells), Test 2/4A



Figure 4.4 Fission Product Dopant Disks, Adjacent to Central Pellet, Test 2/5E

Starting with test 2/5E, following fabrication development time, we used a different technique for fabricating *stand-alone* fission product dopant disks, without the cerium oxide pellet “holders.” SNL (Department 6782) fabricated plastic resin-based dopant disks to slip-fit within the Zircaloy 4 tubing; these dopant disks are approximately 9.1 mm-diameter and 1 mm- thick, each, with a minimum amount of resin used, with an approximate resin/dopant mass ratio of 1.3. All of the solid fission product chemicals were mixed into the liquid resin, then solidified (cured) into a rod-shape, then cut with a diamond-blade saw into individual disks; finally, individual disks were lapped to a thickness of 1 mm. Two resin-based disks containing dopant chemicals are used per test, one on each side of the central cerium oxide pellet in the target rodlet; refer to Figure 4.4. The following amounts of dopants per test (in two disks) were requested: 2000 ppm for Cs and Iodine, 1000 ppm for Ru, 500 ppm for Sr, and 200 ppm for Eu. The weights of each fission product dopant chemical used per test is listed in Table 4.2 (both actual/calculated are specified).

A portion of a “standard” dopant disk was dissolved (wet-ashed, using sulfuric acid; this digestion technique did not retain iodine), then chemically analyzed for elemental concentrations. The measured/calculated values in weight percent for each compound were as follows: [CsI] = 18.858 wt% (calculated from [Cs]); [RuO<sub>2</sub>] = 3.539 wt% ; [SrO] = 2.718 wt%; and, [Eu<sub>2</sub>O<sub>3</sub>] = 2.866 wt%. Each dopant disk weighed 0.05 – 0.10 g. If it is assumed that two dopant disks per tests weigh 200 mg, then the calculated weights of dopant used in each test, based on the “standard disk,” are CsI: 58.4 mg = 2000 ppm; RuO<sub>2</sub>: 19.6 mg = 1000 ppm; SrO: 8.8 mg = 500 ppm; and, Eu<sub>2</sub>O<sub>3</sub>: 7.0 mg = 200 ppm. The actual weights (as calculated from chemical analysis) of each dopant species, *based on the measured dopant disks weight*, are listed in Table 4.2; the actual weights are approximately +/- 20%. Most of the actual dopant weights are appreciably less than the initially specified values.

**Table 4.2 Fission Product Dopant Chemicals, per Test**

<b>Phase 2 Test #</b>	<b>Cesium Iodide, CsI</b>	<b>Ruthenium Dioxide, RuO<sub>2</sub></b>	<b>Strontium Oxide, SrO</b>	<b>Europium Oxide Eu<sub>2</sub>O<sub>3</sub></b>	<b>Shape Factor &amp; Weight</b>
2/4A	32.6 mg	20.3 mg	18.7 mg	none	well
2/4B	30.4 mg	22.5 mg	19.2 mg	none	well
2/5A	~ 31 mg	~ 22 mg	~ 19 mg	none	well
	<b>Actual (calculated) dopant weights</b>				
2/5E	<b>22.6 mg</b>	<b>4.2 mg</b>	<b>3.3 mg</b>	<b>3.4 mg</b>	2 disks (0.12 g)
2/5G	<b>18.9 mg</b>	<b>3.5 mg</b>	<b>2.7 mg</b>	<b>2.9 mg</b>	2 disks (0.10 g)
2/6A	<b>30.2 mg</b>	<b>5.7 mg</b>	<b>4.3 mg</b>	<b>4.6 mg</b>	2 disks (0.16 g)
2/6B	<b>35.8 mg</b>	<b>6.7 mg</b>	<b>5.2 mg</b>	<b>5.4 mg</b>	2 disks (0.19 g)
2/8C	<b>33.9 mg</b>	<b>6.4 mg</b>	<b>4.9 mg</b>	<b>5.2 mg</b>	2 disks (0.18 g)
2/8D	<b>33.9 mg</b>	<b>6.4 mg</b>	<b>4.9 mg</b>	<b>5.2 mg</b>	2 disks (0.18 g)

All fission product dopant material in each test is expected to be aerosolized and possibly vaporized by the shock wave and thermal pulse from the CSC jet. As the temperature cools after the jet impact, aerosolized and/or volatilized species can sorb onto nearby particulate materials (soot, cerium oxide, copper from the CSC jet, etc.). It is postulated that the “cooled” fission product species will preferentially sorb onto the smaller aerosol particles, because the smaller particles have a higher surface area/mass ratio than larger particles. It is also possible that the cooled fission product species may also have some chemical affinity to some of the particulated particle compounds.

#### **4.1.4 Other Phase 2 Surrogate Test Rods**

With WGSTSC members cooperation, *non-radioactive* German high-level waste (HLW) glass test rods, containing multiple, non-radioactive fission product dopants, were added to, and tested in Phase 2, for tests 2/7A and 2/7B. These tests with HLW glass can be considered as an exten-

sion of prior Phase 1 tests on brittle materials, with goals parallel to those of other Phase 2 tests. The glass test rods were fabricated at the Karlsruhe Nuclear Research Center and provided to SNL for joint, cooperative testing by Fraunhofer ITEM and GRS. These glass test rods were 14 mm in diameter and 163 mm long, contained within a stainless steel cladding tube with about a 1 mm wall thickness. The glass matrix was composed of about 84 wt. %  $\text{SiO}_2$ ,  $\text{MgO}$ ,  $\text{MnO}_2$ ,  $\text{CaO}$ ,  $\text{Na}_2\text{O}$  and other glass frit material. The remaining 16 wt. % contained dopants, primarily thermally volatile  $\text{Cs}_2\text{O}$  (0.44 wt. %) and  $\text{MnO}_2$  (0.30 wt. %), plus nonvolatile  $\text{La}_2\text{O}_3$  (1.82 wt. %) and  $\text{Nd}_2\text{O}_3$  (1.04 wt. %). These surrogate HLW glass rod aerosol tests should be beneficial in providing additional data on volatile fission product enhanced sorption onto respirable particles. It is presumed that the cesium dopant was retained and not volatilized in the (molten during fabrication) glass material in silicate compounds [Peacock et al., 2002].

One of the German HLW glass test rodlets for test 2/7A, held within a SNL-fabricated rodlet end-holder assembly, is shown in Figure 4.5.



Figure 4.5 German HLW Glass Test Rodlet for Tests 2/7A

#### 4.2 Aerosol Collection/ Explosive Containment Test Chambers

The vertical, aerosol collection/ explosive containment test chamber used in Phase 2 tests 2/5A through 2/8D, is shown in Figure 4.6 (with flange cover-plates removed, not shown). The open aerosol collection chamber, with a horizontal test rodlet inserted and visible, is located in the top “aerosol collection chamber.” The “explosive containment chamber” is on the bottom. When the HEDD (CSC) installed in the bottom chamber is remotely detonated, a HEDD jet shoots upward through a small-diameter (2.5 cm) hole in the thick steel plate between the two chambers, penetrates the test rodlet (inserted horizontally; self-aligning insertion), and is stopped in the thick HEDD jet-stop block on the top of the test chamber, not visible. The explosive-aerosol test process is illustrated in Figure 4.7. The entire test chamber (body, exclusive of top-mounted aerosol apparatus and valves) is approximately 0.6 m-diameter by 1.3 m-high, and is fabricated out of thick steel to contain the explosive blast and all aerosols produced. It is a durable and demonstrated leak-tight system that has been used for approximately 24 explosive tests; as such, it was referred to as “Grandma,” prior to subsequent retirement from service. The test chamber was instrumented to measure multiple temperatures and pressures in both the top aerosol collection chamber and in the aerosol equipment shown at the top of Figure 4.6.



Figure 4.6 Phase 2 Aerosol Collection-Explosive Containment Test Chamber (open)

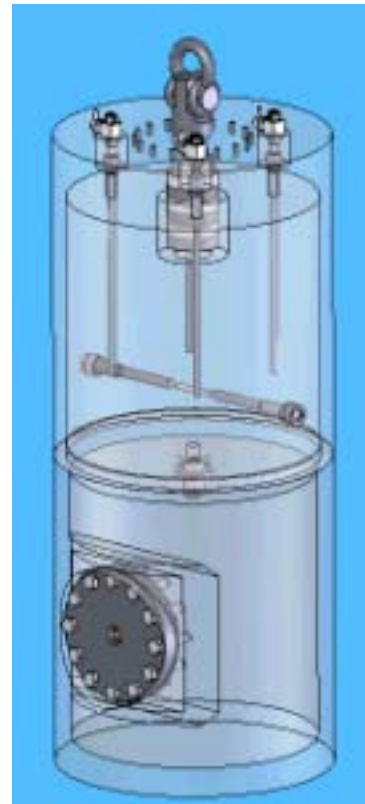


Figure 4.9 Phase 4 Test Chamber (transparent drawing)

← Figure 4.8 Phase 3 Test Chamber and Aerosol Sampling Systems

This Phase 2 vertical test chamber is representative of a “cannon-shaped” boom box. It was designed and fabricated by SNL (Department 2554) for total HEDD blast containment (pressure, fragmentation) and for total, leak-tight isolation of all particles produced. This chamber is a relatively simple, interim prototype of the Phase 3 test chamber. It is a major improvement to the even simpler “square box” aerosol chamber, external explosive test setup used for tests 2/0 through 2/4B, as described in detail earlier [Molecke et al., 2004a].

The new, more refined aerosol-explosive, vertical test chamber for all Phase 3 tests, as well as for Phase 2 / Phase 3 cross-over tests, is shown in Figure 4.8; it was initially based on the Phase 2 test chamber in Figure 4.6. The Phase 3 chamber incorporates recessed, removable flange covers for the top aerosol and bottom explosive chambers. It weighs 999 kg (2202 lbs.), without aerosol apparatus attached, and has a total interior volume of 183 L. This test chamber is quality controlled *in accordance with* the American Society of Mechanical Engineers (ASME) code for pressure vessels, Section VIII Division 1, with internal SNL documentation [Dickey, 2004, Hagan and Dickey, 2004]. It has been explosively over-tested successfully to twice the HEDD-

produced pressures expected in planned usage (peak reflected blast pressure of ~ 800 psi, 55 bar, measured). This chamber has also been modeled for stress analyses, welds have been 100% X-rayed in *accordance* with ASME code and dye-penetrant tested, and it has been hydrostatically and leak tested. SNL explosive safety personnel have concurred that this “chamber (both the Phase 3 and Phase 4 chamber iterations) is qualified for production testing and meets the requirements for a hazard classification and storage compatibility Group of 1.4S.”

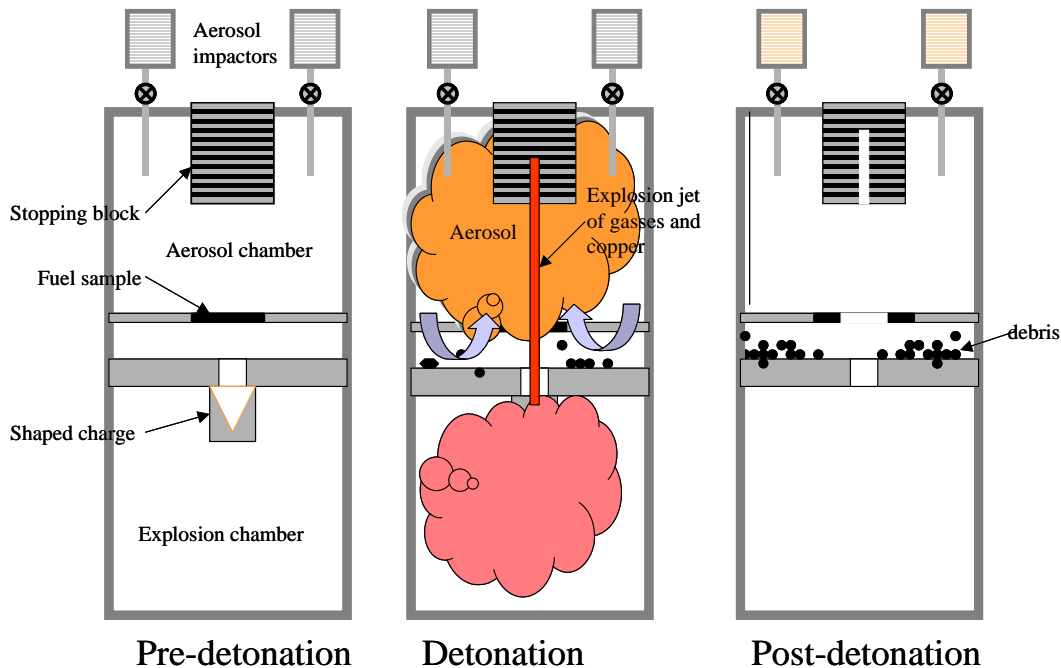


Figure 4.7 Explosive-Aerosol Test Process

The aerosol-explosive, vertical test chambers for the Phase 4 spent fuel tests have been designed and several are in the process of fabrication. These are very similar to the Phase 3 test chamber, except that there is no flanged access port to the top aerosol collection chamber. Both Phase 3 and Phase 4 test chambers have a top head plate that is 5 inches, 12.7 cm, thick, for radiation shielding. A transparent drawing of a Phase 4 explosive-aerosol test chamber is shown in Figure 4.9. The internal HEDD jet stop block, the horizontal spent fuel test rodlet, and four vertical aerosol sampling tubes are visible. Once the remotely inserted spent fuel rod has been disrupted explosively by the HEDD jet, the post-test chamber will NOT be opened, in order to prevent escape of radioactive particulates. The only particle sampling will be via the top-mounted aerosol impactor sampling devices. Each Phase 4 test chamber will be used one time only, temporarily stored at Sandia with the particulated spent fuel contained within, then shipped off-site to an approved, radioactive material storage facility prior to final disposal. The total internal volume of the Phase 4 aerosol chamber is identical to the Phase 3 aerosol chamber; compensation has been made for the lack of the internal flange support in the Phase 4 top chamber. Two of the eight required Phase 4 test chambers were being fabricated as of the end of FY 2004; the other six will be fabricated as needed.

The HEDD jet stop block is located at the top-center of the test chamber body, not quite visible in Figure 4.6 (shown in the transparent drawing, Figure 4.9). The internal components of this

stop block consist of alternating plates of mild steel and polypropylene, each 1.2 cm-thick. The purpose of these plates is to stop the very energetic HEDD explosive jet, as well as the less energetic residual metallic slug or “carrot,” within a manageable distance; this distance is appreciably less than 30 cm. The bottom-most plate (hit first by the HEDD jet) is made of steel. The polypropylene plates are critical for keeping this stopping distance to a minimum length. Multiple stop plates are replaced after each Phase 2 and Phase 3 test (but not for Phase 4 tests).

### 4.3 Aerosol Particle Sampling System

Several types of aerosol particle samplers were used during conduct of the Phase 2 tests. The Respicon™ 3-stage virtual particle impactor (two per test), and the Berner 9-stage particle impactor were used through test 2/5A, then replaced; both of these impactors were described in detail earlier [Molecke et al., 2004a].

Several 9-stage, multi-jet Marple cascade impactors (model 298) are now used per test. These are designed to operate at a nominal flow rate of 2 liter per minute. These impactors measure aerosol particle size distributions from about 0.4 - 21  $\mu\text{m}$  AED, including a final (stage 9), base stage (~ all particles < 0.4  $\mu\text{m}$ ), plus a pre-filter stage (stage #0, for larger particles). The impactor is constructed of aluminum with fiberglass substrate collection media. Sampled air enters the inlet adapter and accelerates through six radial slots in the first impactor stage. Figure 4.10 is a photograph of the Marple Impactor without the inlet adapter and an exploded view of one of the filter stages. The inlet adapter eliminates ashes and debris from the sampler. Particles larger than the cut-point of the first stage impact on the pre-cut collection substrate, stage 0. Air-stream flows through the narrower slots in the second impactor stage, smaller particles impact on the second collection substrate, and so on. The width of the radial slots is constant for each stage but are smaller for each succeeding stage. Thus, the jet velocity is higher for each succeeding stage, and smaller particles eventually acquire sufficient momentum to impact on one of the collection substrates. After the last impactor stage, remaining fine particles are collected by the built-in 34mm-diameter filter (final stage 9, in Figure 4.10).

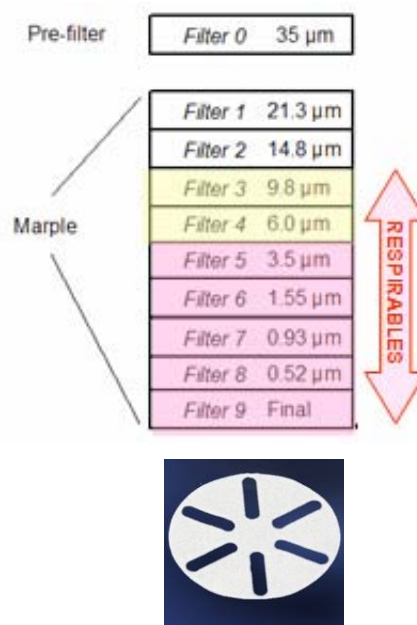


Figure 4.10 Marple Aerosol Impactor, disassembled (showing individual stages and one fiberglass substrate)

One to four of these Marples impactors were used for each Phase 2 test. Four independent Marple impactors will be used in each of the Phase 3 and Phase 4 tests. Each Marple is surrounded by an additional leak-tight cylindrical enclosure (designed, fabricated, and leak-tested at SNL); refer to Figure 4.11. Post-test, the Marple impactors are removed from the test assembly, opened, and each stage individually separated. The collected particles from each stage rest on top of an individual fiberglass substrate (one is shown in Figure 4.10), that can then be chemically dissolved for subsequent elemental analyses of the particulates.

Prior to sampling, collection substrates and back-up filters are pre-weighed, recorded and placed in the impactor. The sampling flow rate is controlled with a critical orifice which is connected to the outlet of the impactor. The sampler flow rate is measured with a Gilibrator Primary Flow Calibrator, Model # D-800268. The sampling flow rate is nominally set at 2 Lpm. The impactors are connected in-line to the explosive valves (shown in Figure 4.11), with 3/8" ball valves. The ball valves provide isolation from the initial pressure pulse from the explosive charge. After sampling, the substrates and filter are weighed. Weight increase on each substrate is the mass of particles in the size range of that impactor stage. The total weight of particles on all stages and filter is added and the percent particle mass in each size range is calculated. Respirable particle mass fraction is determined from the particle size distribution.

In addition to the Marples, a separate, in-line, large-particle separator (LPS) is used for collecting the ~30-100  $\mu\text{m}$  AED particles. The LPS is the semi-cylindrical component visible at the top of Figure 4.8. The collected particles are lodged on a thin strip of fiberglass substrate; this strip can be cut into about four separate segments for follow-on particle analyses in four distinct size ranges. The LPS collectors were jointly designed by SNL and Fraunhofer ITEM aerosol experts; the design is based on work published previously [Mädler et al., 1999]. Each Marple and LPS sampling sub-system requires a vacuum bottle to draw a calibrated, nominal 2 L/min flow rate through the samplers; a critical orifice and small HEPA filter are also used. These components are illustrated in Figure 4.11. In earlier Phase 2 tests, a vacuum pump was used instead of the vacuum bottles.

One second after the HEDD detonation, explosion proof valves (5,000 psi / 340 bar limit) on top of the chamber (visible in Figures 4.6, 4.8, and 4.11) are opened, so that aerosol produced can be collected in the top-mounted particles collectors for a period of 10 seconds. This procedure effectively samples a representative, reproducible portion of the still-suspended aerosol particles.

For tests 2/6A, 2/6B, and 2/8A-D, a separate, additional line of six sequential Gelman filter samples were incorporated, to monitor particle stratification and settling over about the 2.5 - 60 second period after HEDD detonation. The Gelman filter samples are shown in Figures 4.6 and 4.12. These are in addition to the Marple impactors and LPS. Two sampling levels in the aerosol chamber (near top and lower/at rod-target level) were used for the impactor samples with two impactors at each level. The schematic for this aerosol particle sampling scheme is illustrated in Figure 4.13. The Gelman Filter holder body and support screen are constructed of Type 316 stainless steel. Captive thrust ring and Viton<sup>®</sup> O-Rings are constructed of PTFE. The leak proof Gelman filter holder utilizes a 47mm diameter glass fiber filter. The filters were sequenced from approximately 2.5 seconds to 60 seconds after detonation of the HEDD. The filters effectively collect all aerosol particles which pass through the glass fiber media.

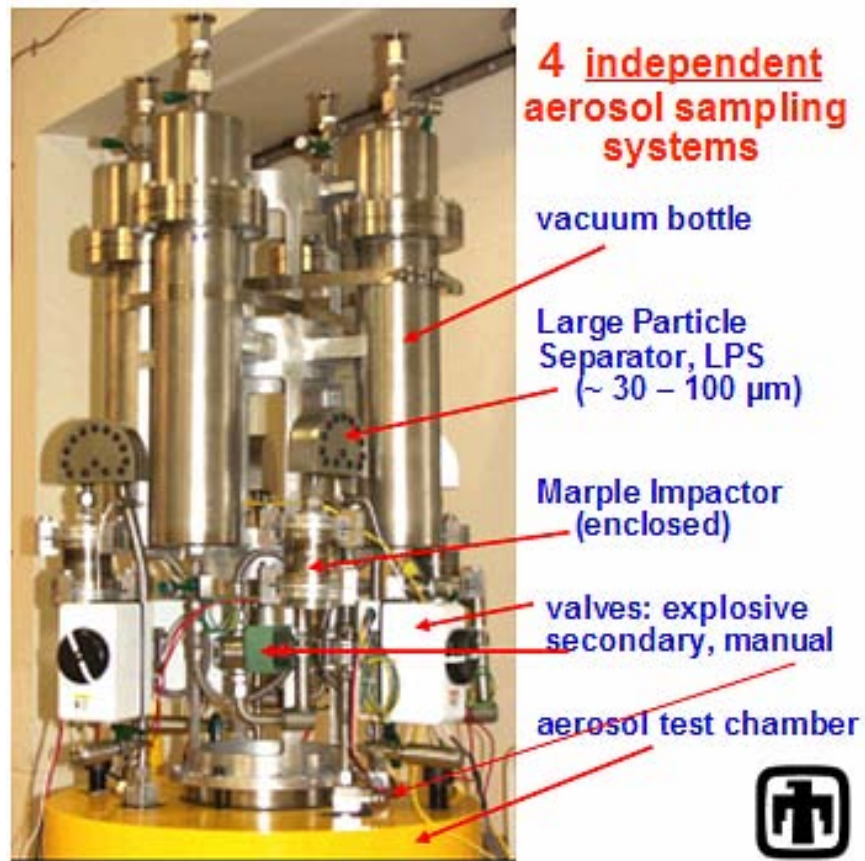


Figure 4.11 Aerosol Particle Sampling System



Figure 4.12 Gelman Filter Bank Sequential Samplers

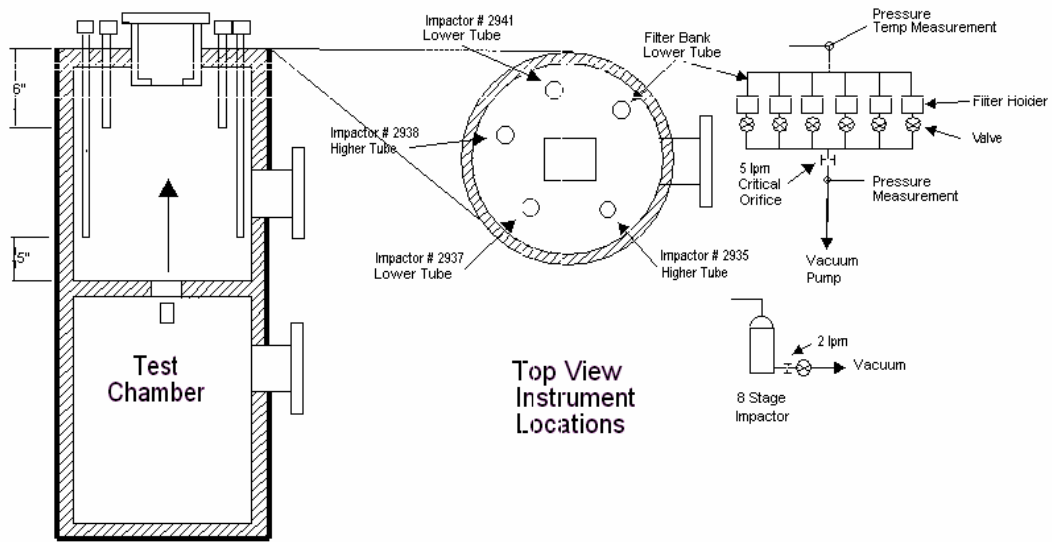


Figure 4.13 Schematic of Aerosol Sampling System, High & Low, with Gelman Filters

## 5. PHASE 3 and PHASE 4 TEST COMPONENTS

The primary difference between surrogate Phase 2 and Phase 3 and 4 test components is that the test rodlets for Phase 3 contain depleted uranium oxide pellets and are slightly radioactive, and Phase 4 test rodlets contain spent fuel and are highly radioactive. As such, these tests must be performed in a different facility, with different safety and radiological constraints. All Phase 3 and Phase 4 aerosol-explosive tests will be performed at the Sandia Gamma Irradiation Facility (GIF), Test Cell 3, using closely controlled radiological and explosive safety conditions, under both SNL and DOE-Sandia Site Office authorizations. The later tests will be performed as identically as possible to each other as possible, to minimize test variables and bias.

The Phase 3 and Phase 4 test component details and designs described in the following Sections incorporate many of the similar component plans and specified requirements in Section 6 of the earlier test program technical report, SAND2004-1832 [Molecke et al., 2004a]. Updates in design details are based on testing experience and programmatic decisions made in FY 2004.

### 5.1 Phase 3 Depleted Uranium Oxide Test Rodlets

Six, unirradiated, depleted uranium oxide pellet test rodlets are required for test Phase 3. The specific variables (internal rodlet atmosphere: air or 40 bar (4 MPa) helium within the end plenum regions of the rodlet, to simulate the approximate pressures found within spent fuel rods), inclusion of fission product dopant disks (no or yes), and aerosol test chamber atmosphere (air or nitrogen) for each rodlet were listed in Table 3.3. As part of the WGSTSC program cooperative efforts, all six of these test rodlets have been fabricated by CERCA (a Framatome-ANP, AREVA subsidiary), in Romans-Sur-Isère, France, for IRSN, for testing at SNL. Fabrication in, and shipment from, France was completed in July 2004. These rodlets were successfully received at SNL in August 2004, and have been placed in storage at the SNL GIF facility until Phase 3 testing begins. The French designation for the rodlet for test 3/1 (as listed in Table 3.3) is DUR-1, for 3/2 it is DUR-2, for 3/3 it is DUR-3, for 3/4 it is DUR-4, for 3/5 it is DUR-5, and for test 3/6 it is DUR-6.

The test rodlet design, shown schematically in Figure 5.1, was a collaborative effort by IRSN, SNL, and Argonne National Laboratory. The rodlet dimensions, except for total length, are very similar to the U.S.-origin pressurized water reactor, PWR, fuel pins. The rodlets are fabricated from Zircaloy 4 cladding tube of 10.6 mm outside diameter, 9.32 mm inside diameter, supplied to IRSN by SNL; refer to Section 4.1.2. CERCA fabricated the threaded end cap fittings (9 with no hole/left side of Figure 5.1, and 3 with a hole/right side of Figure 5.1, for pressurization with helium gas followed by laser weld sealing), with machined plenum regions, from Zircaloy 4 bar stock. Test rodlet extension holders - that screw onto the threaded ends of these test rodlets, will be fabricated at SNL. The test rodlets with end extensions will be self-aligning when inserted horizontally into the Phase 3 test chamber, Figure 4.8.

The DUO<sub>2</sub> pellets contain 0.2 wt. % of <sup>235</sup>U and were obtained from FBFC International, in Dessel, Belgium (an AREVA subsidiary). Each test rodlet contains five ~ 13.9 mm-long pellets of ~ 97% theoretical density DUO<sub>2</sub>, with dished ends, as shown in Figure 5.2. The actual, mean dimensions and specifications for the 30 DUO<sub>2</sub> pellets used are as follows:

Length = 13.9453 mm; Diameter = 9.1317 mm; Dish depth = 0.33 mm;  
Weight = 9.597 g; density = 10.639 g/cc; theoretical density = 97.073 %.

On average, *each* of these six DUO<sub>2</sub> test rodlets contains 47.99 g of uranium oxide (ceramic), 42.33 g of uranium, and 0.097 g of <sup>235</sup>U. Four of the rodlets (DUR-1, 3, 4, and -6) also contain

two of the non-radioactive fission product dopant disks (as used in the Phase 2 tests, provided by SNL; refer to Section 4.1.3) surrounding the central DUO<sub>2</sub> pellet, shown in Figure 5.1 and Figure 5.2. A photograph of all six Phase 3 test rodlets is shown in Figure 5.3. There is also an external center mark on the cladding for each rodlet, locating the center of the central pellet, for further testing (HEDD jet alignment) purposes; these marks are (barely) visible in Figure 5.3.

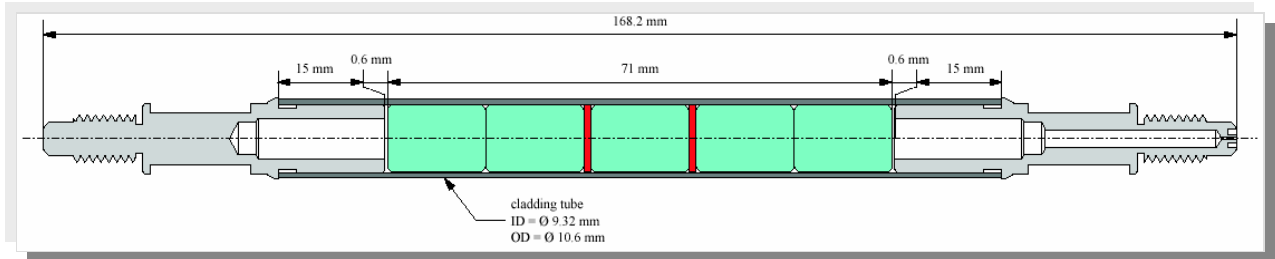


Figure 5.1 Schematic of Phase 3 DUO<sub>2</sub> Test Rodlet, DUR-4



Figure 5.2 DUO<sub>2</sub> Pellets and Dopant Disks for Test 3/1



Figure 5.3 Photograph of Phase 3 DUO<sub>2</sub> Test Rodlets

Following pellet insertion into the cladding tube(s), the end cap/plug ends were adjusted to minimize the gap between the pellet stack and the end caps. This procedure was elected rather than the alternate of installing springs at the ends of the pellet stack in the plenum region, as in real, multi-meter-long fuel rods. The use of no springs was selected for consistency with the other, short Phase 2 surrogate and Phase 4 spent fuel test rodlets. In addition, there was concern that in our short test rodlets after particulation by a HEDD jet, only a small length of pellets remain at the ends of the tubing; the potential existed that if springs were included, they might move (eject) such a small amount of residual pellet material – not desirable.

Three of the rodlets (DUR-1, DUR-2, and DUR-3) are filled with air at atmospheric pressure. The other three (DUR-4, DUR-5, and DUR-6) are internally pressurized with He at 4 MPa, similar to PWR fuel rods, within the end plenum regions of the rodlet, through the end cap hole shown in Figure 5.1 (right side). Laser end-cap and seal welding was used to fabricate the rodlets. The completed rodlets were visually inspected and dimensionally checked, He-leak tested, and then all welds were X-ray tested. CERCA and IRSN worked in cooperation with SNL to ensure that all quality control requirements were met. Internal documentation and reports were supplied to SNL for manufacturing procedures, dimensional controls, micrographic structure evaluations, leak testing, x-ray tests on weldments, pellet identification and documentation, shipping paperwork, etc.

Post-test disposal: Issues associated with the post-test disposal of the French-origin, unirradiated DUO<sub>2</sub> (residual) materials have been addressed at Sandia and resolved [Blejwas, 2003]. “Post-test depleted uranium-contaminated hardware and samples generated during ... Phase 3 testing will be managed as low-level radioactive waste in accordance with the Sandia ES&H Manual. Representatives of the test program will prepare the appropriate documentation and submit the waste to the Radioactive Waste and Nuclear Material Disposition Department. This waste will then be eligible for disposal at the Nevada Test Site as part of Sandia waste stream ALSA00000011. The Radioactive Waste and Nuclear Material Disposition Department will be responsible for transportation to the Nevada Test Site for final disposal.” Note that the post-test DUO<sub>2</sub> (residual) waste materials are not “mixed waste” or “hazardous waste.” No organic components or residual explosive compounds are present; the only post-detonation explosive residue of importance is carbon soot.

## 5.2 Phase 4 Spent Fuel Test Rodlets

Two types of pressurized water reactor (PWR) spent fuel materials will be used in this test program. Four Phase 4 test rodlets will use high-burnup fuel (72 GWd/MTU) from the H.B. Robinson reactor, and four other test rodlets will use a “lower” (medium)-burnup fuel (38 GWd/MTU) from the Surry reactor. Short lengths of spent fuel pellets contained within the original, irradiated Zircaloy 4 cladding tube will be fabricated into test rodlets very similar in geometry to the Phase 3 DUO<sub>2</sub> test rodlets. New (unirradiated) zirconium (Alloy Zr-702 bar stock) end cap fittings will be added, then circumferentially sealed with rotary tungsten inert gas (TIG) welding; refer to Figures 5.4 and 5.5.

The reason for using two different burn-up spent fuels is as follows. A hypothesis was made that high burnup spent fuels may produce appreciably more aerosol and respirable particles than lower burnup spent fuels, primarily because of more extensive micro-fracturing from extended irradiation time and thermal stresses [Einziger, 2003]. However, there is an opposite hypothesis that the release of respirable particles from *unirradiated* fuel could be measurably *greater* than the release from irradiated fuel. “Specifically, the propagation of a shock wave through the

highly fragmented pellets of irradiated fuel could lead to a substantially lower fraction of respirable material than might be expected from the shattering of solid pellets by a high explosive shock wave. If proven, this could lead to relaxed regulatory guidelines on the shipment, storage and handling of spent fuel.” [Philbin, 2002a]

All spent fuel characterization studies (non-destructive and destructive characterization of fuel material and cladding) and rodlet fabrication activities are being performed by Argonne National Laboratory in their Alpha Gamma Hot Cell (AGHC) facility. Fabrication completion is scheduled during 2005, followed by transport to SNL within a GE 100 cask, on a to-be-defined schedule. The test rodlet design for both varieties of spent fuel test rodlet is based on the design proposals and agreements between IRSN and Argonne National Laboratory, and modified as necessary in coordination with Sandia nuclear facilities personnel, for applicable remote handling capabilities at the SNL GIF.

The objectives of the pre-test characterizations for the spent fuel rods are: to verify that the rods are representative of irradiated PWR fuels; to aid the post-test evaluation of material behavior; and, to provide source-term data for follow-on release fraction analyses. The scope of pre-test characterizations included: visual inspection, axial gamma scanning (for fuel column integrity and pellet locations), optical metallography (for condition of the fuel, cladding, and evaluations of the fuel/cladding interface), measurement of the cladding hydrogen content (for potential embrittlement issues), and isotopic analyses (for radiological source term as well as burn-up credit issues). From the standpoint of source term, the following isotopes are expected to be reported:  $^{90}\text{Sr}/^{90}\text{Y}$ ,  $^{106}\text{Ru}$ ,  $^{125}\text{Sb}$ ,  $^{134, 137}\text{Cs}$ ,  $^{144}\text{Ce}$ ,  $^{154}\text{Eu}$ ,  $^{238, 239, 240, 241}\text{Pu}$ ,  $^{241, 242\text{m}, 243}\text{Am}$ ,  $^{244}\text{Cm}$ , and  $^{235-8}\text{U}$ . The content of  $^{147}\text{Pm}$  will not be reported, because of the significant extra effort involved.

### 5.2.1 High-Burnup, H.B. Robinson Spent Fuel Test Rodlets

This spent fuel material used in this program originated at the H.B. Robinson PWR, Rod R01, and is currently at Argonne National Laboratory, near Chicago. It was supplied to ANL as part of a research program sponsored jointly by NRC, DOE, and EPRI (Electric Power Research Institute). It is DOE-owned research material, not “commercial” SNF. This SNF was removed from the reactor in April 1995 and spent 5 years in wet storage. It has a peak high burnup of about 72 GWd/MTU, and an original  $^{235}\text{U}$  enrichment of about 2.90 wt. %. ANL has already conducted some characterization tests on adjacent, sibling rods from this reactor [EPRI, 2001; Tsai and Billone, 2003]. The original Rod R01 has an average burn-up of 67 GWd/MTU, with a peak burn-up (as selected for Phase 4 testing) of 72 GWd/MTU. It has Zircaloy 4 cladding that was 10.77 mm OD and 9.25 mm ID. The  $\text{UO}_2$  pellets within were 9.06 mm in diameter and 6.93 mm long, with dished ends. The initial He gas fill was 2.0 MPa (20 bars). Fission gas release was about 1.6 %. End-of-life gas pressure within, at room temperature, was about 4.4 MPa (44 bars). As such, the internal pressurization of the H.B. Robinson test rodlets will be 4.4 MPa of He. Laser welding will be used to seal the pressurization hole in the end fitting of the test rodlet.

The spent fuel test rodlets made from H.B. Robinson fuel will include eight equivalent irradiated  $\text{UO}_2$  pellets (or  $\sim 1/2 + 7$  whole +  $\sim 1/2$  pellets), each about 6.93 mm long, for a total fuel length of about 55 mm (2.2 inches). The final design of the H.B. Robinson spent fuel test rodlet is shown in Figure 5.4. The overall rodlet length is 152.4 mm (6.0 inches) and the original Zircaloy 4 cladding tube length is 86.4 mm (3.4 inches). The plenum volume is 1.13 ml. The irradiated section of the spent fuel rod will be joined with the unirradiated end plug segments, then circumferentially sealed with rotary tungsten inert gas (TIG) welding. All four of these test rodlets will

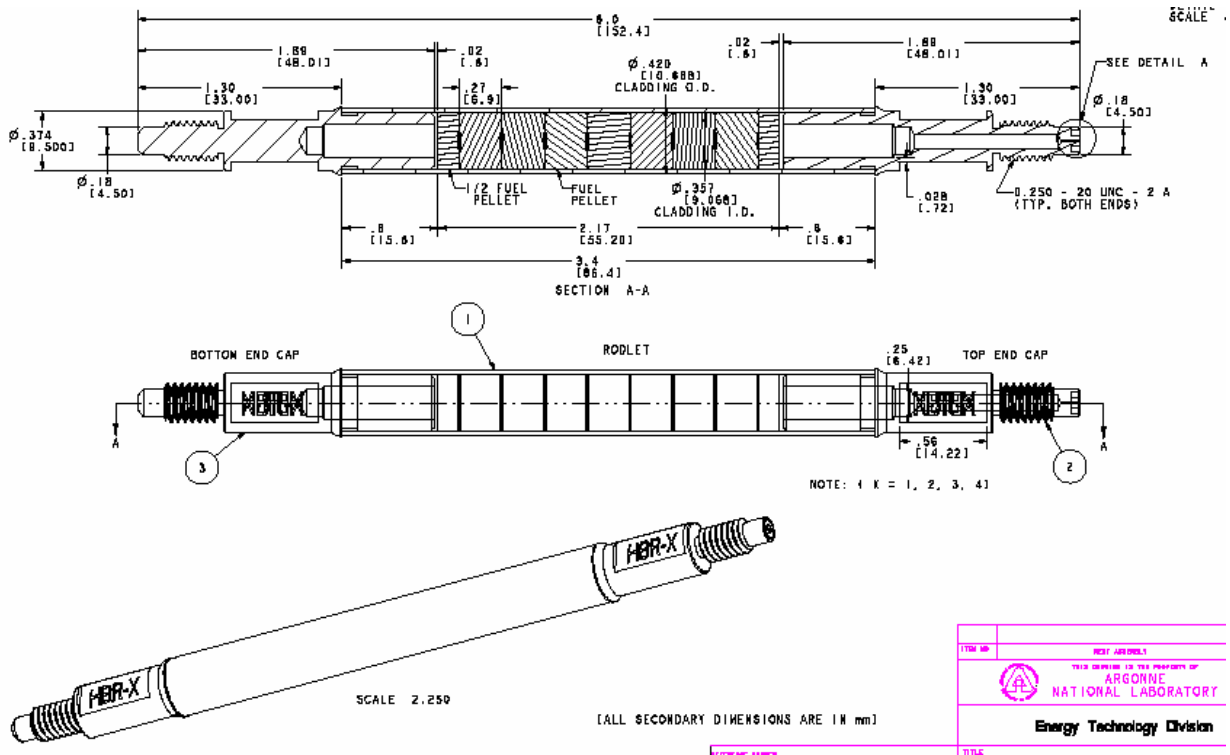


Figure 5.4 H.B. Robinson Spent Fuel Test Rodlet Design, Argonne National Laboratory

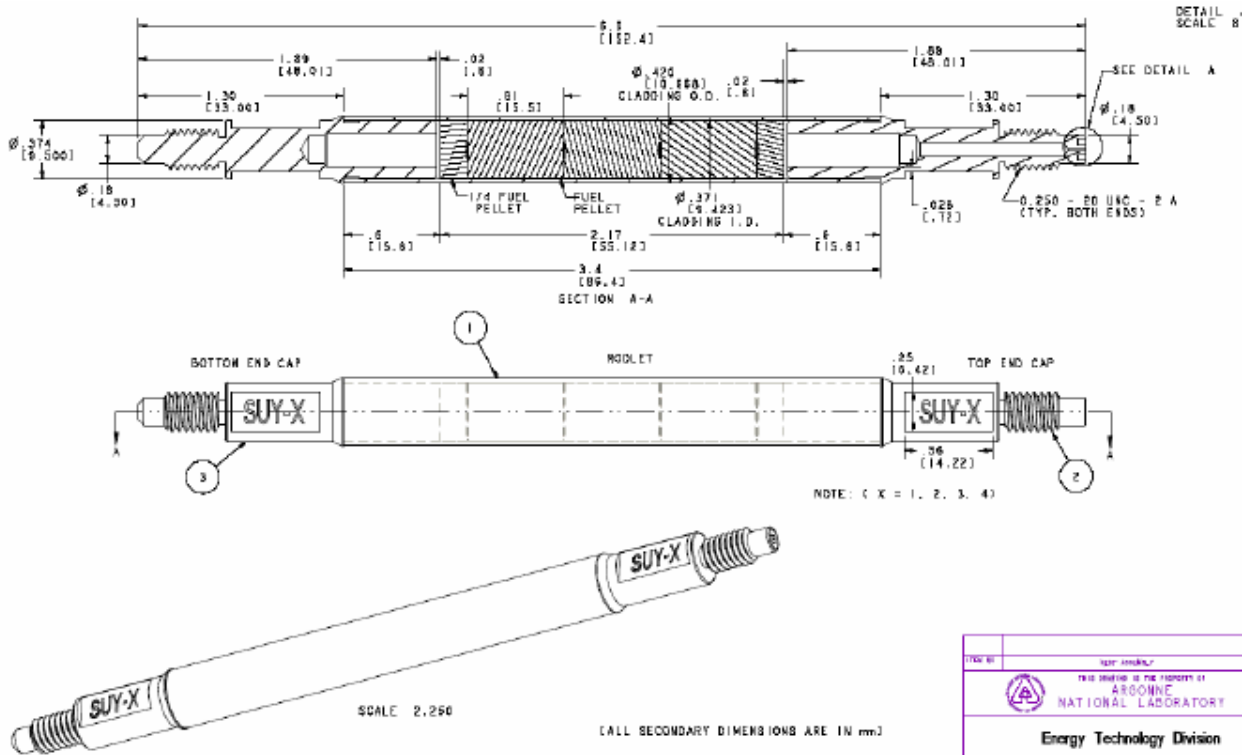


Figure 5.5 Surry Spent Fuel Test Rodlet Design, Argonne National Laboratory

be internally pressurized with He to 4.4 MPa. Laser welding will be used to seal the pressurization hole in the end fitting. ANL will complete the spent fuel rodlet fabrication, including post-welding leak testing and external contamination control, and then transport the rodlets to SNL for testing in 2006.

### **5.2.2 Lower Burnup, Surry Spent Fuel Test Rodlets**

This “lower” burnup spent fuel was irradiated in the Surry PWR reactor, discharged in 1981, spent 3.8 years in wet storage, and then was stored in a He-filled Castor V/21 cask, as part of a 15-year dry storage test. The selected Surry fuel rod, H7, peaks at about 38 GWd/MTU (as selected for the test rodlets), while the rod-average burnup is 36 GWd/MTU. Surry rod characterization results from sibling rods are documented in [Einziger et al., 2003]. This fuel rod resides at ANL and is being characterized and fabricated into test rodlets similarly to the H.B. Robinson high burnup spent fuel. The Surry fuel was supplied to ANL as part of a research program sponsored jointly by NRC, EPRI, and DOE RW. The original Surry Rod H7 had an original  $^{235}\text{U}$  enrichment of 3.11 wt. %, an average burn-up of 36 GWd/MTU, with a peak burn-up of 38 GWd/MTU. It has Zircaloy 4 cladding that was 10.72 mm OD and 9.47 mm ID. The  $\text{UO}_2$  pellets within were 9.27 mm in diameter and ~ 15.5 mm long, with dished ends. [Note: the Phase 3  $\text{DUO}_2$  pellets are, similarly, 13.9 mm long]. Because of the Surry fuel pellet length, the spent fuel test rodlets made from Surry fuel will incorporate four equivalent pellets each (or  $\sim\frac{1}{2} + 3$  whole +  $\sim\frac{1}{2}$  pellets) to achieve a comparable fuel pellet length to the H.B. Robinson test rodlet, about 55 mm (2.2 inch). The initial helium fill was 2.8 MPa (28 bars). Fission gas release was about 0.9 %. End-of-life gas pressure within, at room temperature, was about 3.3 MPa (33 bars). As such, the internal pressurization of the Surry test rodlets will be 3.3 MPa of helium. Laser welding will be used to seal the pressurization hole in the end fitting of the test rodlet. The design of the Surry spent fuel test rodlets is shown in Figure 5.5.

## 6. TEST CONDUCT AND AVAILABLE RESULTS

Four major Phase 2 test series using surrogate cerium oxide test pellets/rodlets were completed in FY 2004. There were a total of 15 Phase 2 tests performed in FY 2004 following 9 earlier Phase 2 tests in FY 2003, essentially finalizing Phase 2 of the overall test program. All of the Phase 2 tests in FY 2004 used the vertical, aerosol collection-explosive containment test chamber shown in Figure 4.6. Test series 2/5, A through G, and 2/8A and 8B were conducted to optimize the performance of the test chamber and the aerosol apparatus connected to it. In addition, pressure and temperature instruments were installed in the aerosol chamber to monitor the conditions within, during the period before and up to 60 seconds after the HEDD detonation and test rodlet particulation process. There were multiple changes made in the test apparatus and test procedures throughout series 2/5; there were also some testing problems, to be described. Test series 2/8 A-D, was similar to 2/5, but more controlled and polished. Test series 2/6 A and B followed tests 2/8A-D, used the same aerosol apparatus, adding a single large particle separator, and incorporated internally pressurized test rodlets.

Test series 2/7, A and B, were similar to series 2/5, but incorporated non-radioactive, surrogate German high-level waste glass test rodlets (refer to Section 4.1.4), in cooperation with, and jointly conducted with our German WGSTSC partners Fraunhofer ITEM and GRS. Test series 2/6, A and B, were performed last. They were similar to tests 2/8 A-D, but used internally pressurized test rodlets and the most complete collection of aerosol measurement apparatus. All of the details and differences between the Phase 2 tests performed in FY 2004, including sampling times, aerosol apparatus incorporated, and notes, are summarized in Table 6.1. This table also provides details of the two Phase 2 / Phase 3 tests, 2/9A and 2/9B, performed in FY 2004.

### 6.1 Phase 2 Tests 2/5A through 2/5G, Variables and Observations

Test 2/5A was a direct follow-on to previous tests 2/4A and 4B [Molecke et al., 2004a], but the new, vertical aerosol collection-explosive containment test chamber was added. We continued the use of the two Respicon aerosol samplers plus one large Berner aerosol impactor, as illustrated in Figure 6.1, and fission product dopants inserted into pre-drilled wells of the center



Figure 6.1 Test 2/5A Aerosol Sampling Apparatus

**Table 6.1 General Test and Aerosol Particle Sampler Information, FY 2004**

Test #	Notes: Test Modifications	Sampling Time	Aerosol samplers	Flow Rate L/min	
<b>2/5A</b> 9/30/03	new vertical test chamber, CeO <sub>2</sub> pellets, FP dopants in wells	15 sec	2 Respicons + Berner impactor, w/disconnected hose	3.13 L/min, 2.99 L/min 5.6 L/min	
<b>2/5B</b> 11/19/03	"Blank" test, w/ Zirc tube, no pellets (residual contamination)	--	P & T No aerosol, sieve only		--
<b>2/5C</b> 11/25/03	"Blank" test, no Zirc tube, no pellets, instrumented for P, T	--	P & T No aerosol, sieve only		--
<b>2/5D</b> 12/04/03					--
<b>2/5E</b> 1/21/04	vertical test chamber, CeO <sub>2</sub> pellets, 2 F.P. dopant disks	15 sec	1 Marple, 1 LPS-1	1.70 L/min	--
<b>2/5F</b> 1/22/04	safety evaluation (CSC misfire, no Jet)	--	1 Marple, 1 LPS-1	2.21 L/min	
<b>2/5G</b> 1/26/04	CeO <sub>2</sub> + FP disks (duplicate of 2/5E)	30 sec	1 Marple + LPS-1	1.70 L/min	
<b>2/6A</b> 4/30/04	CeO <sub>2</sub> + FP disks, similar to 2/8D, rodlet pressurized to 400 psi (2.76 MPa) (He)	10 sec	4 Marples, LPS, Gelman filters	1.96, 1.98 / Gelman 1.964, 2.04 Lpm / 4.39Lpm	
<b>2/6B</b> 5/05/04	CeO <sub>2</sub> + FP disks, similar to 2/6A, rodlet pressurized to 580 psi (4.0 MPa) (He)	10 sec	4 Marples, LPS, Gelman filters (complete Phase 2)	1.96, 1.98 / Gelman 1.964, 2.04 Lpm / 4.39Lpm	
<b>2/7A</b> 2/04/04	German HLW glass rodlet + F.P. simulants, non-rad.	20 sec	Marple, LPS-1, Berner, + proto-type 6-stage impactor		
<b>2/7B</b> 2/06/04	German HLW glass rodlet, similar to 2/7A, w/ 2 Marples	10 sec		2.30 L/min, Marple	
<b>2/8A</b> 2/24/04	"Blank" test, no target, soot distribution high/low	10 sec	4 Marples, Gelman filters	2.42, 1.64 / Gelman 1.64, 1.69 Lpm / 4.39Lpm	
<b>2/8B</b> 2/26/04	"Blank" test, replicate of 2/8A	10 sec	4 Marples, Gelman filters	2.42, 1.64 / Gelman 1.64, 1.69 Lpm / 4.39Lpm	
<b>2/8C</b> 3/17/04	CeO <sub>2</sub> + FP disks	10 sec	4 Marples, Gelman filters	2.42, 1.64 / Gelman 1.64, 1.69 Lpm / 4.39Lpm	
<b>2/8D</b> 4/08/04	CeO <sub>2</sub> + FP disks (replicate of 2/8C)	10 sec	4 Marples, + LPS Gelman filters	2.42, 1.64 / Gelman 1.64, 1.69 Lpm / 4.39Lpm	
<b>Phase 2 / Phase 3 Cross-Over Tests</b>					
<b>2/9A</b> 8/18/04 (at ECF)	new Phase 3 test chamber, CeO <sub>2</sub> pellets, NO F.P. dopants, air flush	10 sec	4 Marple 4 LPS	1.90, XXX 1.95, 1.98 L/min	
<b>2/9B</b> 8/26/04	Similar to 2/9A, but with N <sub>2</sub> flush, atmosphere	10 sec	4 Marple 4 LPS	1.90, 1.90 1.95, 1.98 L/min	

cerium oxide pellets. Vacuum pumps were used to draw aerosol samples into the particle collectors; they were manually turned on at + 5 sec after the HEDD detonation, and off at + 20 sec, for a total sampling time of 15 seconds. Immediately after the HEDD detonation, the hose connecting the Berner impactor to the test aerosol chamber blew off, along with the makeup air 'tee', due to the internal chamber pressure. The hose clamp holding the sampling hose was improperly tightened and did not adequately hold. The test chamber vented immediately from this open hose port; the vent plume was clearly visible and lasted about 5 seconds. No useful aerosol sample was obtained with the Berner impactor; the two Respicon samplers continued to function. The venting event was caused by the contained pressure buildup within the sealed aerosol chamber and the failure of the hose clamp used. The "make shift" plastic tubing was replaced by metal piping in all subsequent tests.

Tests 2/5B, 5C, and 5D were performed specifically to monitor pressures and temperatures within the top aerosol collection chamber, to help quantify why the sampling tube in test 2/5A disconnected. No aerosol particle samplers were used. The five sampling tubes at the top of the aerosol test chamber were capped-off to seal pressure in the vertical test apparatus. Two pressure transducers were installed on the inside surface of the aerosol chamber flange/port-cover door; one pressure gauge indicated 0 to 100 psia (6.9 bars), the other read from 0 to 2000 psia (138 bars). Two thermocouples were installed near the top of the aerosol chamber, inside of one of the aerosol internal sampling pipes. These instruments are to monitor pressure and temperature for the first 20 seconds after detonation, then again after ~ 5 minutes. Instrumentation results will be described in Section 6.5.2. In addition, all three of these tests, 2/5B, 5C, and 5D, were "blanks," with *no* cerium oxide or fission product dopant disks used. Test 2/5B did contain an empty Zircaloy tube target, tests 2/5C and 5D had no targets. Residual particle debris was collected inside the aerosol chamber for all three of these tests, then sent to the analytical chemistry laboratory for post-test mechanical sieving (from 1000  $\mu\text{m}$ , down to 25  $\mu\text{m}$  geometric diameter and residual in size) and ICP-MS (inductively coupled plasma/mass spectrometry) analyses. The chemical analyses also allowed us to evaluate how much residual contamination (cerium oxide, fission product dopant species) remained in the test chamber from the previous 2/5A test; it was determined that the chamber was not adequately cleaned-out before the succeeding tests.

Test 2/5E and 2/5G each used 9 cerium oxide pellets plus two new, resin-base fission product dopant disks; refer to Section 4.1.3. We also incorporated one 9-stage Marple impactor in series with a custom made, prototype large particle separator (designated as LPS-1, in Table 6.1), plus a solenoid-actuated, explosion-proof valve. Thermocouples were again installed in an empty sampling tube, on top of the aerosol sampling chamber. We focused one video camera on the overall test container, and a second one to visually record the opening and closing of the solenoid controlled valve, as visible by the white-line movement; refer to Figure 4.6. Test 2/5G was a replicate of 2/5E.

Test 2/5F was intended to be a replicate of 2/5E but did not function as planned. Following HEDD detonation, the test chamber was opened for examination after about one hour of wait time, per explosive safety protocol. We observed that the test rodlet was not cut in two by the HEDD jet, as expected. Instead, the test rod was deformed upwards by about 0.6 cm, into a slightly bowed shape. It was still intact, though covered with explosive soot residue. The bowed test rod was removed easily from the test chamber. Upon further post-test exam of the test rodlet, all ceramics pellets inside were visibly fractured and no longer useable, but still contained. It was also observed that the conical shape charge, HEDD, had thoroughly detonated as expected, but that the copper cone blew out downwards and sideways, as it was forming a slug;

no HEDD jet was formed. A failure test report to the CSC manufacturer and the test sponsors was written to document this event. According to the manufacturer, this is a highly unusual event, with a  $\ll 1\%$  occurrence.

There are several things that could have happened in this situation (possibly a defective copper cone or wall thickness irregularities, or an incomplete explosive loading with a void near the cone), but it would be very hard to prove that any one of these possible things was the one cause for no jet being formed. The important factor is that there were no facility or personnel safety issues involved in this test misfire. There was no un-detonated explosive material. As long as the explosive detonates and we don't have a mixed waste condition during the future radioactive Phase 4 tests, then the situation would be tolerable because the bent, damaged spent fuel test rodlet could be removed from the (Phase 4) test chamber in a safe and acceptable manner. As such, test 2/5F can be considered useful for its safety-related implications, and for providing knowledge of misfire behavior in the test chamber.

## **6.2 Phase 2 Tests 2/7A and 2/7B, Variables and Observations**

These two tests were added to the previously defined test matrix at the request of, and in cooperative testing with, our German test partners from Fraunhofer ITEM and GRS, and were jointly performed at Sandia. These two tests were performed with German glass rod targets, as described in Section 4.1.4, in the Phase 2 vertical explosive-aerosol test chamber (Figure 4.6), with one Berner impactor, two Marple impactors, one prototype Fraunhofer particle impactor, one large particle separator (prototype "LPS-1"), valves, tubing, plus associated vacuum pumps and other hardware, as shown in Figure 6.2. The aerosol-explosive test chamber (opened, post-test) is shown in Figure 6.3, along with test participants; Figure 6.4 shows two views of the post-test glass rodlet for test 2/7A. Test 2/7A used an aerosol sampling time of 20 seconds; this was shortened to 10 seconds for test 2/7B due to observed heavy particle loadings.

Three of the particle impactor samplers (the Berner, one Marple, and the German prototype design) used Mylar collection substrates, coated with paraffin; no gravimetric data was taken on these samples. The second Marple impactor used glass fiber substrates without paraffin, in parallel with the other Marple, in order to gauge the particle mass loading and to get an idea of the size distribution. Both of these tests resulted in over loaded impactors even with short (10 to 20 second) sampling times.

These observed high particle concentrations initiated some discussion between Sandia and German aerosol participants concerning the sampling strategy and the possibility that the sampling time may be dictated by the mass loading rather than desired material amounts. These conversations were very helpful and resulted in an idea and design concept for an improved large particle separator (as shown in Figure 4.11) that can eliminate the need to elutriate (vertically puff to suspend) the larger (e.g., 30 – 100  $\mu\text{m}$  AED) particulate materials in the aerosol chamber. This new LPS design (and subsequent usage) has significantly simplified the overall vertical aerosol-explosive test chamber system and associated aerosol hardware to be used in subsequent Phase 2, 3, and 4 tests – with the technical agreement of all test participants.

Following the conduct of these tests, the particle impactors were opened, the particles on each collected stage on the Mylar or fiberglass media, were visually evaluated, then packaged for shipment back to Fraunhofer ITEM for further analyses. The impact debris within the aerosol chamber was also collected by brush sweeping, packaged, and sent to Fraunhofer, along with the post-test glass rodlet residuals, as shown in Figure 6.4.

Results for the surrogate German high-level glass target rods impacted by the HEDD jet in the Phase 2 test chamber were similar to post-test observations on the cerium oxide target rodlets, although the glass test rodlets suffered somewhat more mechanical damage. About 29-44 mm of the stainless steel cladding tube was destroyed for tests 2/7A and 2/7B; there was about 37 mm of disrupted glass length, the remainder was contained in the cladding tube, shown in Figure 6.4.



Figure 6.2 Test 2/7A and 2/7B  
Aerosol Apparatus

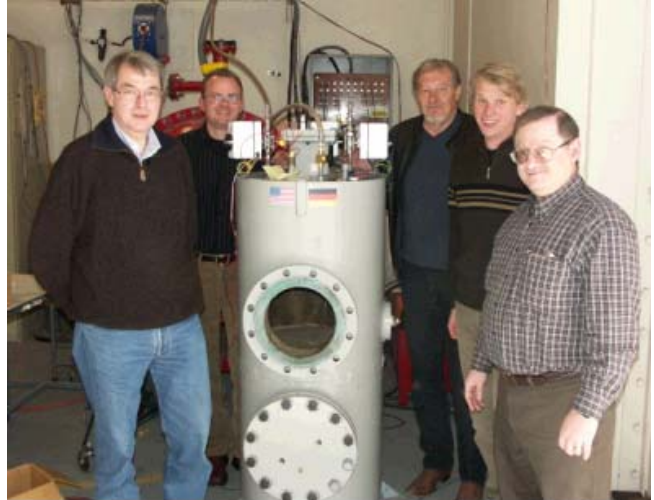


Figure 6.3 Test 2/7A Post-Test Chamber  
and Participants



Figure 6.4 Post-test Glass Target Rodlet, Test 2/7A

### 6.3 Phase 2 Tests 2/8A through 2/8D, Variables and Observations

The test series 2/8 was basically a continuation of the tests in series 2/5, but with a significant effort to advance the development, and quantity of aerosol apparatus used, and to further quantify the aerosol distributions within the aerosol chamber.

Tests 2/8A and 2/8B (replicate) The first two of these tests, 2/8A and its replicate 2/8B were “blank” tests, with no target rods; they used four Marple impactors and incorporated a separate, additional line of six sequential Gelman filter samples, to monitor particle stratification and settling, e.g., the particle/soot distribution, both high (chamber top) and low (at approximately the target rodlet height) in the aerosol chamber, over about the 2.5 - 50 second period after HEDD detonation. The Marples were sampled for the 2.5 to 12.5 second period after HEDD detonation, the Gelman filters were sampled during the 2.5 to 7.5, 7.5 to 12.5, 12.5 to 17.5, 17.5 to 27.5, 27.5 to 37.5, and 37.5 to 47.5 second periods. The Gelman filter samples are shown in Figures 4.6, 4.12, and 4.13. All aerosol analyses for these two tests were performed by weight measurements only; no ICP-MS chemical analyses were conducted. Results for the Gelman filter particle analyses are discussed in Section 6.5.3.1.

Two sampling levels were used for the particle impactor samples with two Marple impactors at each level (Marples # 2935 and # 2938 high, plus # 2937 and # 2941 low; refer to Figure 4.13). In addition, pressure and temperature measurements *within the aerosol sampling stream* (piping) were made using Druck pressure transducers (0-200 psia and 0-20 psia) upstream of the filter bank manifold and downstream of the critical orifice flow regulator (Figure 4.12), and Omega Type K thermocouples. Temperatures were also measured at the top of the aerosol chamber. The data was logged into an electronic data recorder manufactured by Omega instruments.

Tests 2/8C and 2/8D (replicate) were similar to 2/8A and 2/8B, except that target rodlets with CeO<sub>2</sub> pellets and fission product dopant disks were used. In addition, one new 4 L vacuum bottle was installed in the aerosol sampling system, rather than a vacuum pump, to draw the aerosol stream through the particle samplers. Vacuum pump connections were still used for three of the four Marple streams. Also, one new, Sandia-fabricated, large particle separator (as shown in Figure 4.11) was added in test 2/8D, in series with one of the Marple impactors. This LPS design was based on discussions between SNL and Fraunhofer aerosol experts during the 2/7A and 2/7B tests, earlier.

Of the four Marple impactor samplers used in these tests, particle stages from two impactors (# 2935, high, and # 2937, low) were submitted to analytical chemistry for standard ICP-MS elemental analyses; details and results are listed in Appendix A. The sampling stages from the other two matching impactors (# 2938, high, and # 2941, low) were submitted for neutron activation analyses, NAA, in order to evaluate the feasibility of using this analytical technique.

It appears that the fiberglass (borosilicate) filter substrates contain a significant quantity of sodium, estimated at ~ 800 ppm. Sodium is a problematic contaminant in regards to NAA work. Its high energy gammas and short-to-medium half-life precludes counting other isotopes in the sample which are masked by the Na lines. When the NAA results were received, it was obvious that NAA was not a useful technique for our purposes and will not be pursued further.

### 6.4 Phase 2 Tests 2/6A and 2/6B, Variables and Observations

The two tests, 2/6A and 2/6B, were very similar to the preceding tests 2/8C and D, except that the test rodlets, with CeO<sub>2</sub> pellets and dopant disks, were internally pressurized with He gas; re-

fer to Figure 4.2. Test rodlet 2/6A was pressurized to ~ 400 psi (27.6 bar), test rodlet 2/6B was pressurized to ~ 550 psi (37.9 bar). The intent was to be representative of Phase 3 DUO<sub>2</sub> rodlets (some pressurized with He to 40 bar) and Phase 4 spent fuel rodlets (pressurized at 33 or 44 bar), to determine if the pressure release at HEDD impact would change the amount of observed particulation, or, possibly, pressure-expel remaining pellets.

## 6.5 Phase 2 Test Results and Observations

### 6.5.1 Target Rodlet Disruptions

The observed effects of HEDD explosive jet impact on the Phase 2 test rodlets, both for CeO<sub>2</sub> pellet-containing rodlets and the empty Zircaloy cladding tube used in test 2/5B, were fairly consistent. Table 6.2 lists the measured gap (average and ranges) in the Zircaloy cladding tubes for all the Phase 2 tests performed, for completeness. This table also lists the number of cerium oxide pellets particulated, the length of particulated pellets, and the gross weight of the disrupted pellets.

**Table 6.2 Observed Post-Test Rodlet Disruptions, Phase 2 Tests**

Phase 2 Test #	Zircaloy Tube Gap mm (ave.)	# of Pellets Particulated	Pellet Length Particulated	Pellet Weight Disrupted (particles + fragments)	“Blowback” Particle Weight
2/0	27-(30)-35				
2/1A	24-(26)-28				
2/1B	20 - 32				
2/2A	27-(27.3)-28	2.3 (long)	31 mm	10.24 g	
2/2B	26-(27)-28	2.3	31 mm	10.14 g	
2/3A	21-(25)-28	4.4 (short)	31 mm	~13.4 g	1.60 g
2/3B	22-(25)-29	4.8	34 mm	~15.2 g	0.85 g
2/4A	25-(29)-33	5.2	36 mm	~16.2 g	0.22 g
2/4B	22-(25)-30	4.7	33 mm	~15.0 g	2.28 g
2/5A	23-(27)-31	(½ lost) +2.3	(½ lost) +16	--	--
2/5B	20-(27)-35	“blank test”	(no pellets)	--	--
2/5C	(no rodlet)	“blank tests”	(no pellets)	internal T & P	--
2/5D					--
2/5E	19-(22)-25	6	42.2 mm	~ 18.9 g	1.53 g
2/5F	deflection	safety eval.	--	--	--
2/5G	17-(25)-27	3.6	38 mm		1.3 g
2/6A	23-(27)-34	< 7	(pressurized, blow out; 28 bar)		
2/6B	23-(27)-30	6-7	(pressurized; 38 bar)	~21.2 g	0.67 g
2/7A	29-44	German HLW glass	~ 37 mm		
2/7B	30-41				
2/8A	(no rodlet)	“blank tests”	--	soot particulate distribution	
2/8B			--		
2/8C	20-(23)-30	5	36 mm	16.12 g	
2/8D	16-(21)-25	3.7	26 mm	11.7	
2/9A	25-(30)-35	5.8	40.8 mm	18.6 g	
2/9B	23-(26)-32				

The HEDD jet impacts the center-point of each target rodlet in  $< 90 \mu\text{sec}$ , yielding a 21-30 mm *average* gap in the Zircaloy cladding tube. The total Zircaloy tubing gaps observed varied from 16-35 mm, primarily due to jagged flaps of Zircaloy of different lengths; refer to Figures 6.5 through 6.15. Post-test rodlet damaged ends are illustrated in Figures 6.6, 6.11, 6.13, and 6.15, including views of the  $\text{CeO}_2$  pellets within. The deflected, bent rodlet from Test 2/5F is shown in Figure 6.7.



Figure 6.5 Test 2/5E Post-test Rodlet



Figure 6.6 Test 2/5E Post-test Rodlet Ends



Figure 6.7 Test 2/5F Post-test Rodlet, Bent



Figure 6.8 Test 2/5G Post-test Rodlet

#### 6.5.1.1 Pellet Disruption and Blowback Material/Rod Debris, and Impact Debris

A total of about 3.7 to 6 of the original 9  $\text{CeO}_2$  ceramic pellets in the Phase 2 rodlets, each pellet  $\sim 7$  mm-long, were fragmented/aerosolized, about a 26-42 mm length total. In most tests, the  $\text{CeO}_2$  pellets adjacent to the destroyed segment of Zircaloy tubing were firmly wedged into the tube, by “blowback” fine particles of material in the small tube-to-pellet gap, and could not easily be removed from the cladding. In some tests, this blowback material, or “rod debris” material was collected, mechanically sieved, and photographed; refer to Table 6.2 and Figures 6.18-6.20. This “rod debris” material is cerium oxide fragments, relatively uncontaminated by soot. All collected blowback, rod debris data (weight and weight percent per sieve fraction) are listed in Appendix A.



Figure 6.9 Test 2/6A Post-test Rodlet



Figure 6.10 Test 2/6A Post-test Rodlet and Test 2/6B Rodlet



Figure 6.11 Test 2/6A Post-test Rodlet Ends

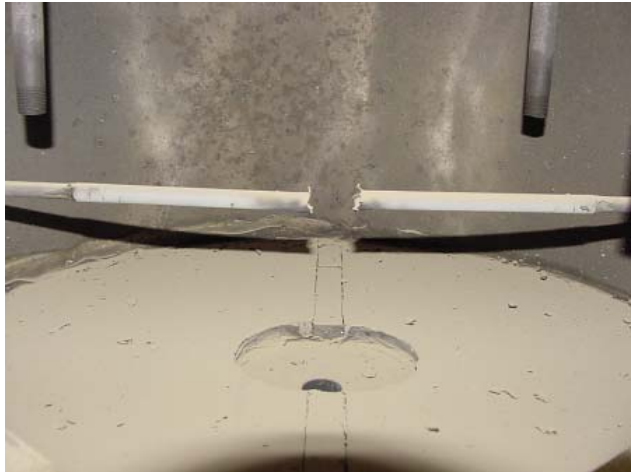


Figure 6.12 Test 2/8C Post-test Rodlet



Figure 6.13 Test 2/8D Post-test Rodlet Ends



Figure 6.14 Test 2/9A Post-test Rodlet



Figure 6.15 Test 2/9A Post-test Rodlet Ends

The remaining, captive CeO<sub>2</sub> pellets were essentially whole, with some observable external fracturing. The end-most pellets (away from the centerline) were essentially undamaged. Figure 6.13 shows that the end-most pellets in the cladding tube from pressurized rodlet 2/6A are gone. It is not clear if these pellets fell out in pieces during post-test handling operations, or if they were pushed out from the pressurized rodlet during HEDD impact and fragmentation. End-most pellets were observed in test 2/6B, a test performed at slightly greater internal pressurization.

#### **6.5.1.2 Particle Impact Debris**

Impact debris is the residual particulate material remaining in the aerosol collection chamber post-test, not sampled in the particle impactor aerosol sampling apparatus. This impact debris consists of heterogeneous fragments and particles of cerium oxide pellets, plus some plastic (debris from the HEDD holding fixture in the bottom, explosive chamber), copper from the conical shape charge cone and jet, Zircaloy metal pieces from the cladding tube, iron from the inner walls of the test chamber and/or the HEDD-jet stop block, etc.; refer to Figure 6.19 for the larger fragments and assorted debris. All of this debris was uniformly gray in color, as coated with explosive residue soot. Representative photographs of this impact debris are illustrated in Figures 6.19 through 6.21.

The collected debris was mechanically sieved using a set of 48mm-diameter sieves; 1000 μm, 500 μm, 250 μm, and 125 μm with a final catch pan. The ‘fines’ were then sieved further with disposable mesh sieves at 100 μm, 74 μm, 37 μm, and 25 μm (geometric sizes) to further differentiate the debris. The sieved impact debris materials were then chemically dissolved and elementally analyzed by ICP-MS. All data for the collected impact debris, including weights, weight percents, and elemental analyses for each sieve size range, are listed in Appendix A. Elemental analyses were performed only on debris sieve sizes 125 μm (geometric; equal to 325 μm AED for CeO<sub>2</sub>) and smaller.

#### **6.5.2 Instrumentation Results, Temperatures and Pressures**

Temperature readings in the 2/5 series of tests were taken primarily as indicators of HEDD detonation. Consequently, thermocouples were located within the aerosol chamber with survival from fragmentation as a major concern. Temperature measurements from thermocouples installed in these tests were quite dependent on their locations. The thermocouples were generally shielded within sampling tubes, and may have inadvertently touched adjacent surfaces or were contacted by hot fragments. As such, the obtained temperature readings may not reflect overall aerosol chamber conditions. For example, for test 2/5D, the observed temperature rise from a thermocouple at the top of the aerosol chamber increased about 20 °C above initial ambient conditions at 20 seconds after detonation, and peaked 5 minutes after detonation at 31 °C above initial ambient temperature. These readings are inconsistent with the measured aerosol chamber pressure and do not reflect actual chamber temperature. Efforts to make more representative aerosol chamber temperature measurements were instituted in the test series 2/8 and 2/6. The measured temperature at the top of the aerosol chamber in tests 2/8A and 2/8B peaked at about 220 °C, about 11 seconds after detonation, then decreased; refer to Figure 6.22. The measured temperature in test 2/8D peaked at about 340 °C within both the “high” and “low” sampling tubes in the aerosol chamber about 6 seconds after detonation; refer to Figure 6.23.

In both tests 2/6A and 2/6B, the measured peak temperatures were about 840 °C about 2 to 3 seconds after detonation; refer to Figure 6.24. Apparently, more of the hot explosive gas blasting out of the bottom, explosive chamber was sampled in this test.



Figure 6.16 Test 2/5G Rod Debris, 500  $\mu\text{m}$  fraction



Figure 6.19 Test 2/6A Impact Debris, 1000  $\mu\text{m}$  fraction

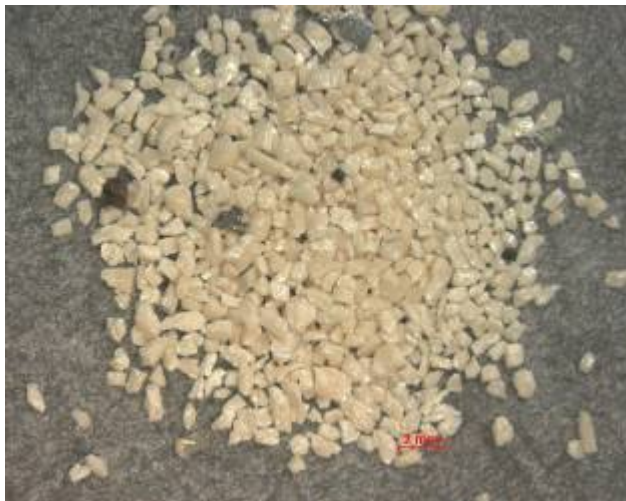


Figure 6.17 Test 2/5G Rod Debris, 250  $\mu\text{m}$  fraction



Figure 6.20 Test 2/6A Impact Debris, 250  $\mu\text{m}$  fraction



Figure 6.18 Test 2/5G Rod Debris, 100  $\mu\text{m}$  fraction



Figure 6.21 Test 2/6A Impact Debris, 74  $\mu\text{m}$  fraction

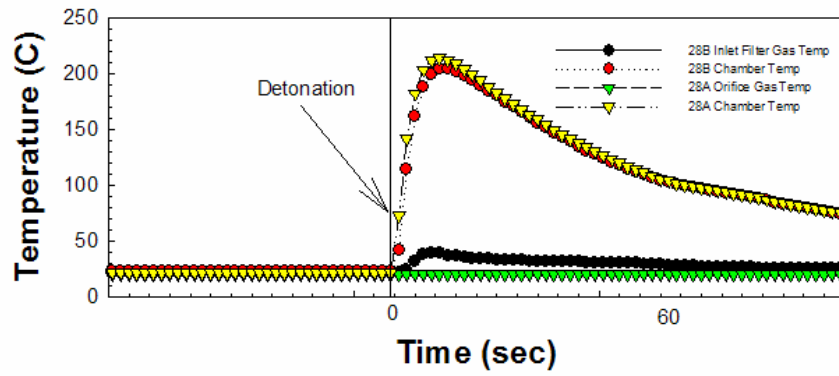


Figure 6.22 Test 2/8A and 2/8B Measured Temperatures

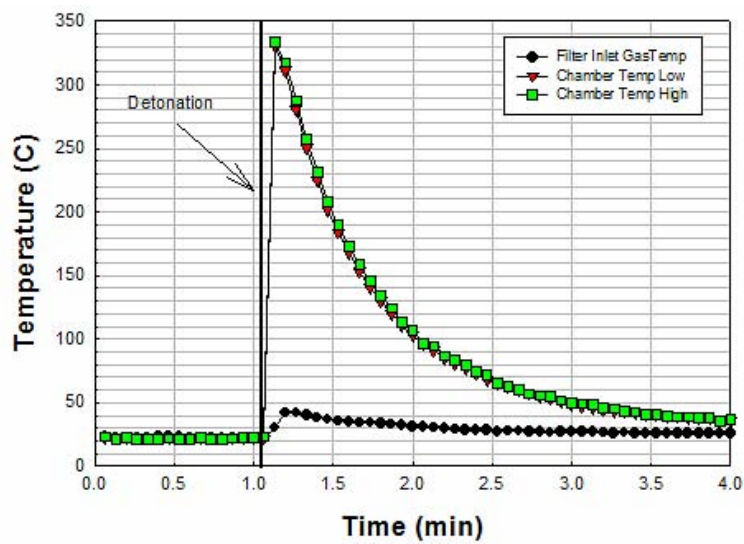


Figure 6.23 Test 2/8D Measured Temperatures

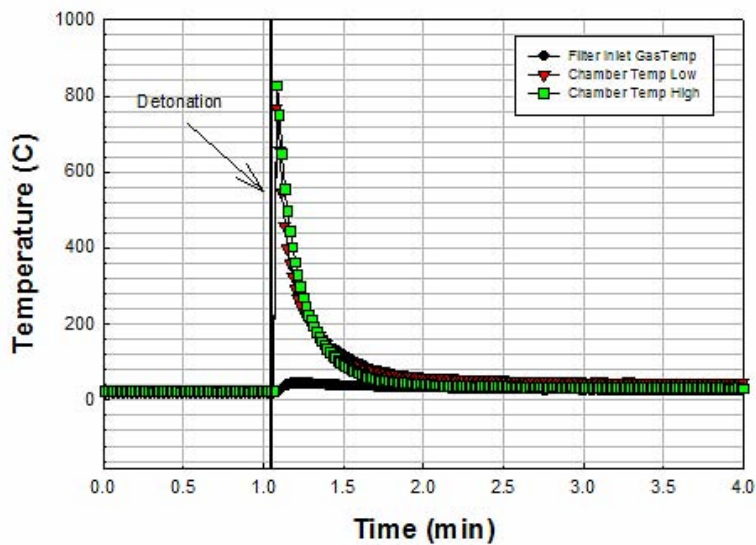


Figure 6.24 Test 2/6B Measured Temperatures

Chamber characterization with respect to temperature and pressure is necessary for adequate assessment of the sample volume collected and for estimation of aerosol behavior necessary for sample data interpretation. Pressure observations in test 2/5D (Figure 6.25) peaking at 85 psig (5.9 bars) may lead one to expect peak temperatures on the order of 1700 °C in the chamber. Use of thermocouple in measuring transients in temperature presents a problem in that the thermocouple response time is on the order of the transit time such that during the rise portion the thermocouple lags and the temperature reading is low and during the temperature fall portion, the thermocouple lag gives reading that are high. The one point at which the thermocouple reading is representative of the chamber temperature is at the peak indicated temperature.

Three supplemental tests (in the same test chamber, but with no targets or aerosol apparatus) were performed to better characterize the temperature and pressure conditions within the aerosol chamber. The first and third tests demonstrated high repeatability. Soot deposits on the thermocouples from the first test caused measured temperatures on the second test to appear low; cleaning before the third test solved the problem. The soot deposits indicate that thermophoretic deposition is occurring at a significant level. The results of these supplemental tests should form the basis of a semi-empirical model of chamber temperature based on measured chamber pressure. Chamber temperature is necessary to compute the sample flow rate into the sampling tube in the chamber; volumetric flow rate is directly proportional to chamber temperature in the sampling train. The sampling efficiency of larger particles is dependent on flow rate into the sampling tube, especially since we are sampling over the first 15 seconds after detonation during which time chamber conditions are rapidly changing.

For test 2/8D, measured peak pressures within the aerosol sampling chamber were ~ 85 psig (5.9 bars) at ~ 200 msec. after HEDD detonation, decreasing to < 1 psig (< 0.07 bar) after 5 minutes; refer to Figure 6.25. In tests 2/8A and 2/8B, pressures were measure above the test chamber, in the aerosol sampling train, both upstream of the particle impactor and after it, before the in-line critical orifice. These measurement points were isolated from the chamber by ball valves until about 2 seconds after detonation when the aerosol sampling was initiated. These pressure readings do not reflect chamber conditions until 2.5 seconds after detonation or until after the peak indicated pressure. These measured pressures, shown in Figure 6.26, never exceed ~ 40 psig (2.8 bars). Measured upstream pressures for tests 2/8D, 2/6A, and 2/6B were quite similar, peaking at 36 psig (2.5 bars). The pressures at the time of the peak temperatures of 205 °C are on the order of 20 to 22 psia. Simple ratios would suggest that the temperatures at the time of the peak pressures of nearly 40 psia would be on the order of 600 °C. More refinement of the model is necessary, but this rudimentary examination strongly suggests that sampling from the chamber takes place at somewhat extreme temperatures.

Above the aerosol test chamber, within the Marple aerosol sampling system, the measured temperatures never exceeded ~ 40 °C. The significantly higher temperatures in the test chamber at the aerosol sampling points have been reduced during the sample transit through the sampling tube; refer to Figures 4.13 and 6.9 for sampling tube locations. There remains a concern over the extent of possible thermophoretic deposition of aerosol particles in the sampling tubes and within the aerosol chamber itself. The thermal gradient along the length of an internal sampling tube, or between its outer and inner wall, may result in the thermophoretic deposition of some small aerosol particles on cooler surfaces, possibly biasing the amount of aerosol sampled in the above particle impactors. The extent of thermophoretic effects remains to be quantified with modeling and laboratory testing.

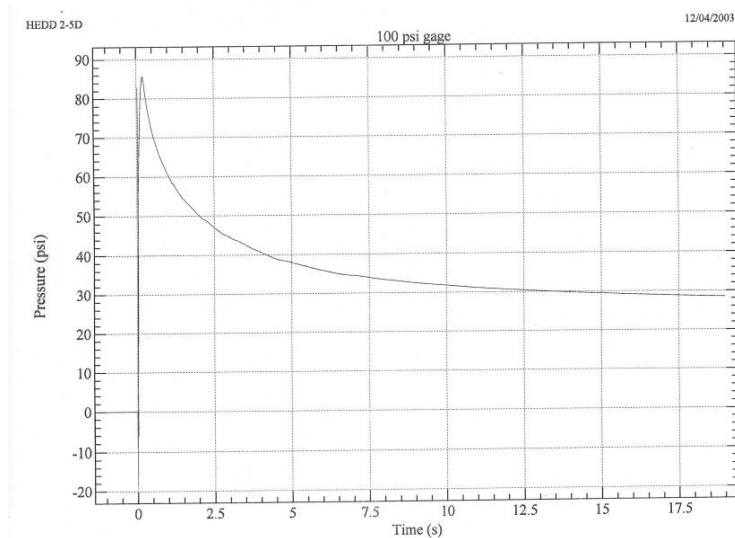


Figure 6.25 Test 2/5D Pressure Measurement, Aerosol Chamber

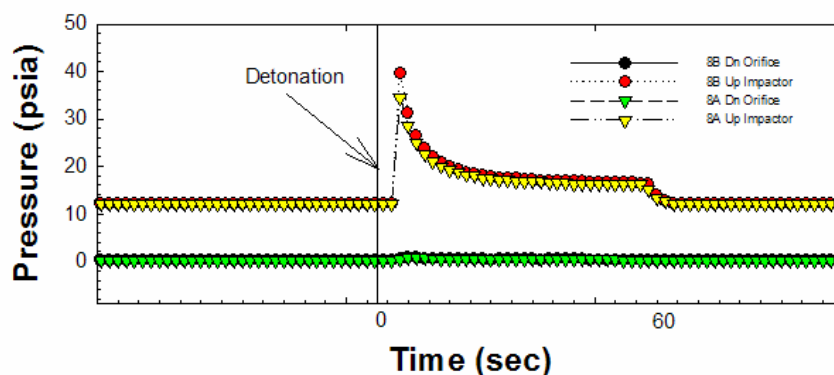


Figure 6.26 Test 2/8A and 2/8B Measured Pressures

### 6.5.3 Phase 2 Test Aerosol Particle Data

The data and analyses presented in this section are updated from (and replace) those presented at the 8th Technical Meeting of the WGSTSC [Brockmann et al., 2004], in November 2004. Newer data and input on fission product dopant quantities used (refer to Table 4.2) have been incorporated. It is also noted that the aerosol sampling data reported here are analyzed without correction for inlet sampling efficiency, chamber losses from settling and thermophoretic deposition, or gas sample volume taken at a temperature considerably higher than the volume measured at the flow orifice; such corrections will be quantified and made available in the future. The particle masses are what is measured after the test. The sample volume is taken as the flow through the orifice at the orifice temperature, which is taken as ambient temperature prior to the test.

#### 6.5.3.1 Particle Stratification Within Aerosol Sampling Chamber

Tests in series 2/8 and 2/6 used six sequential Gelman filter bank samples and four simultaneous Marple impactor samples; two sampling levels within the aerosol test chamber, high and low,

were used for the impactor samples with two impactors at each level; refer to Figures 4.6 and 4.13. A major purpose of these tests was to characterize the particle mass loading and distribution within the aerosol chamber, over the 2.5 to 12.5 second sampling period for the impactors, as well as the 2.5 to 47.5 second sampling periods for the Gelman filter bank.

Tests 2/8A and 2/8B were both blank tests (no target rodlets), so the aerosol results are relevant to soot and test debris distributions. No significant stratification between high and low sampled particulate material concentrations was observed; refer to Figures A1.8.5 and A1.8.13. Taken test by test, the means for both levels in test 2/8A and 2/8B were within the 95% confidence interval of each other and taken level by level, the means for both tests at each level were within the 95% confidence interval. Normalized data for both tests indicate a mean of 14.5 mg/liter +/- 12% (12.7 to 16.3 mg/liter) as the 95% confidence interval. The mean for test 2/8A was 13.9 mg/liter and for 2/8B was 15.1 mg/liter. The mean for the high level was 15 mg/liter and the mean for the low level was 14 mg/liter. The concentrations measured with the Gelman filter samples were significantly higher than those measured with the Marple impactors. This may be attributed to a higher flow rate for the filter samples (~ 5 L/min for the Gelman, ~ 2 L/Min for the Marples) and a higher sampling efficiency for larger particles although more analysis needs to be done. The time-sequential sampling from the Gelman filters (Figures A.1.8.6 and A.1.8.14) appear to indicate that the soot aerosols remain suspended over the 2.5 to 47.5 second sampling period.

Tests 2/8C and 2/8D were similar to 2/8A and 2/8B, but did include CeO<sub>2</sub> pellet target rodlets. Taken test by test, the means for both levels in each test were also within the 95% confidence interval of each other and, taken level by level, the means for both tests at each level were within the 95% confidence interval. Normalized data for both of these tests indicate a mean of 24.8 mg/liter +/- 14% (21.3 to 28.3 mg/liter) as the 95% confidence interval. The mean for test 2/8C was 27mg/liter and for 2/8D was 22.5 mg/liter. The mean for the high level was 23.3 mg/liter and the mean for the low level was 26.2 mg/liter. The Gelman filter measured values for 2/8C and 2/8D are about 65% higher than the blank tests, 2/8A and 2/8B, indicating a contribution of roughly 10 mg/liter from the target.

The mean aerosol concentration as measured by the impactors (with no correction for sampling efficiency, chamber loss, or sampling volume) on tests 2/8A and 2/8B is 14.5 mg/liter, and on tests 2/8C and 2/8D is 24.8 mg/liter indicating a contribution of roughly 10 mg/liter from the target.

Results for tests 2/6A and 2/6B with pressurized target rodlets were similar. The impactor samples from test 2/6 A suggest stratification with higher concentrations at the lower portion of the chamber, test 2/6 B demonstrates no stratification; refer to Figures A.1.6.5 and A.1.6.19. Taken test by test, the means for both levels in each test were within the 95% confidence interval of each other and taken level by level, the means for both tests at each level were within the 95% confidence interval. However, the concentrations grouped by level in test 2/6A lie outside the 95% confidence interval. Normalized data for both tests indicate a mean of 20.1 mg/liter +/- 11% (18.1 to 22.1 mg/liter) as the 95% confidence interval. The mean for test 2/6A was 19.9 mg/liter and for 2/6-B was 20.3 mg/liter. The mean for the high level was 18.4 mg/liter and the mean for the low level was 21.8 mg/liter.

Based on these results from these six tests, no significant stratification of particles below about 20 micrometers occurs and no appreciable aerosol particle settling is seen over the size range of particles sampled within the aerosol chamber during the 2.5 to 12.5 second sampling period after

HEDD detonation. Settling is a function of particle size and will present a greater depletion for larger particles. All subsequent tests (specifically Phase 3 and Phase 4 tests) will be sampled at only one internal aerosol chamber location level, selected as the “lower” (rodlet height) level.

### 6.5.3.2 Aerosol Results for Cerium Oxide

The *respirable fraction* produced when the HEDD jet impacts a target rodlet is the fraction of materials produced (in the rod swept volume, for particles of size  $10\ \mu\text{m}$  AED and smaller) divided by the total amount of material particulated. Respirable fractions for Ce, Zr, Cs, Ru, and Sr have been calculated from the aerosol measurements taken in all the Phase 2 tests to date (2/1A through 2/8D) based upon the measured aerosol size and concentration and the amounts of those materials dispersed into the test chamber. All relevant aerosol particle data are compiled in Appendix A of this report and Appendix A of [Molecke et al., 2004a], for tests performed in FY 2003. The aerosol particle instruments used to collect and classify the aerosol material included the Respicon, the Berner impactor, and, for all tests performed in FY 2004, the Marple impactors. Tests 2/1A through 2/4B were performed in vented, square-box aerosol collection chambers [1]; tests 2/5A through 2/8D were performed in the vertical, sealed, explosive containment-aerosol collection test chamber. The data presented for test 2/5A are somewhat *suspect*, because the test chamber did vent unintentionally, as described previously. We presume that the later tests in the closed vertical test chamber with multiple Marple impactors yielded our best quality, and largest amount of interpretable data. Based on the data collected for all Phase 2 tests, for completeness, the calculated respirable fraction results are summarized in the following tables and figures. These data were originally presented at the 8th Technical Meeting of the WGSTSC [Brockmann et al., 2004]. Table 6.3 presents results for the surrogate cerium oxide respirable fraction. The amount of  $\text{CeO}_2$  material dispersed is based on the observed gap in the target rodlet and the number of missing, fragmented pellets. Figure 6.27 illustrates the same data as in Table 6.3.

The calculated average  $\text{CeO}_2$  respirable fraction for the Marple data is appreciably lower than similar values calculate from Berner or Respicon data. The calculated surrogate respirable fraction is  $1.6 \pm 0.8\%$  of dispersed mass based on all collected data (with a 99% confidence interval); the respirable fraction average is  $0.45 \pm 0.23\%$  based on the Marple data only. This is most likely due to the use of different test chamber design (non-sealed vs. sealed). The respirable fraction data from tests 2/6A and 2/6B are significantly lower than the values from test series 2/5 and 2/8. This may be in part due to the higher amount of dispersed cerium oxide pellets in these tests. In addition, the effect of thermophoretic deposition losses of aerosol particles in the hotter, sealed test chamber (tests 2/5A and later) have not been factored in; based on present uncertainties in thermophoretic loss, the Marple calculated average respirable fraction values may be up to a factor of 2 greater.

The calculated  $\text{CeO}_2$  cumulative distributions for tests 2/4A through 2/8D are shown in Figures 6.28 through 6.36. The cerium oxide particle data collected with particle impactors matches up well with the larger impact debris particle data obtained from mechanical particle sieving. The particle sizes from the sieve data are adjusted to match up with the aerodynamic size from the impactor and all the data are normalized by the total mass of  $\text{CeO}_2$  disrupted and dispersed into the chamber. The cerium oxide cumulative fraction distributions suggest that the HEDD impact produces mechanical fragmentation without phase change; the cerium oxide surrogate material behaves as a representative brittle material.

**Table 6.3 Phase 2 Test Results for CeO<sub>2</sub> Respirable Fraction**

Test	CeO <sub>2</sub> Dispersed		Cerium Oxide Respirable Fraction (%)						Test Avg
	CeO <sub>2</sub> (mg)	Ce (mg)	Respicon 1	Respicon 2	Berner	Marple 1	Marple 2	Marple 3	
2/1A	11304	9203	0.48%	0.28%					0.38%
2/1B	11304	9203	0.53%	0.40%					0.46%
2/2A	10209	8311	4.93%	4.00%					4.46%
2/2B	10209	8311	2.81%	3.81%					3.31%
2/3A	13906	11321	2.65%		5.10%				3.88%
2/3B	15251	12416	4.53%	5.52%	4.17%				4.74%
2/4A	16149	13147	1.02%	1.56%	2.32%				1.63%
2/4B	14803	12051	1.16%	0.97%	1.72%				1.28%
2/5A	13286	10816	0.40%	0.40%					0.40%
2/5E	18869	15361				0.93%			0.93%
2/5G	16720	13612				0.54%			0.54%
2/6A	21200	17259				0.19%	0.19%	0.31%	0.23%
2/6B	21200	17259				0.20%	0.18%	0.10%	0.16%
2/8C	16017	13039				0.55%	0.70%		0.62%
2/8D	11286	9188				0.74%	0.89%		0.81%
avg all			2.09%		3.33%			0.46%	1.64%

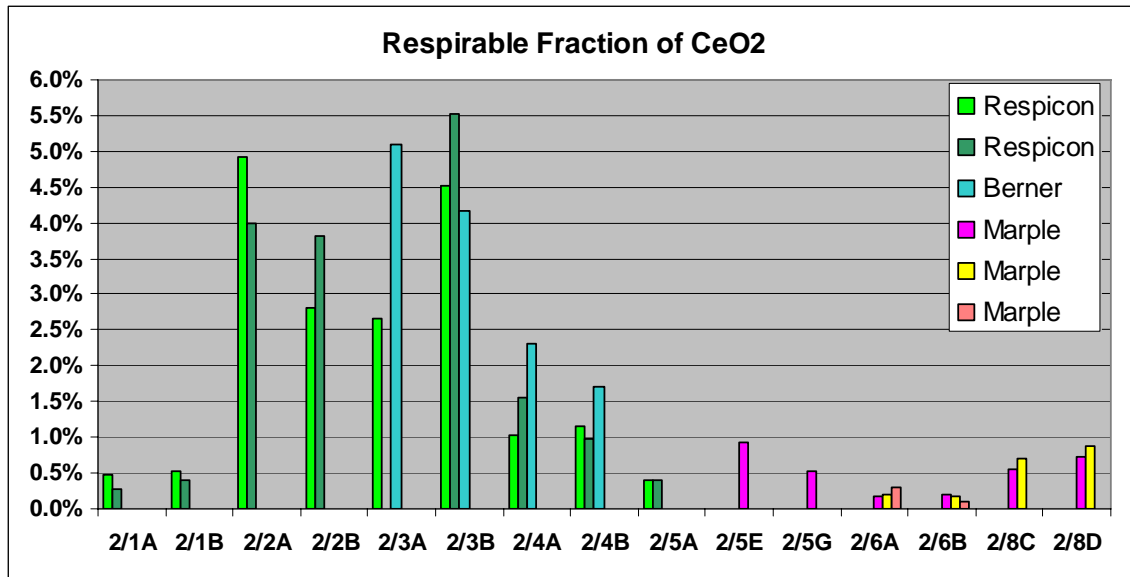


**Figure 6.27 Phase 2 Test Results for CeO<sub>2</sub> Respirable Fraction**

The data from the tests 2/4A, 2/4B, and 2/5G indicate 10% to 30% of dispersed material is less than 250 micrometer sieved size and the general trend is along a single, nearly straight line on a log-log plot. Slight mismatch between the aerosol data and the sieved debris data can be attributed to lower aerosol sampling efficiency for larger particles and how effectively debris was recovered from the chamber post test. The mismatch is greatest for tests 2/5A and 2/5E; in these

two tests, less than 5% of the dispersed  $\text{CeO}_2$  is below 250 micrometer in sieve size and this is due to a smaller fraction of the debris recovered. The data for tests 2/6A and 2/6B, with the internally pressurized test rodlets, show a higher fraction (>30%) of debris less than 250 micrometers sieve size, lower fractions of mass in the aerosol samples, and a steeper slope in the debris size distribution than the other tests. It should also be noted that less than 0.9 grams of debris was recovered in Test 2/5A, and of the more than 14.8 grams of debris recovered in Test 2/5E, less than 0.8 grams was less than 250 micrometers in sieve size.

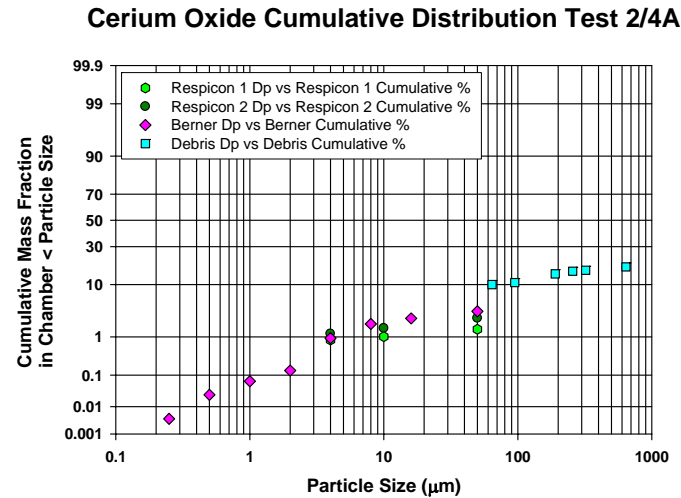


Figure 6.28 Phase 2 Test 2/4A  $\text{CeO}_2$  Cumulative Fraction

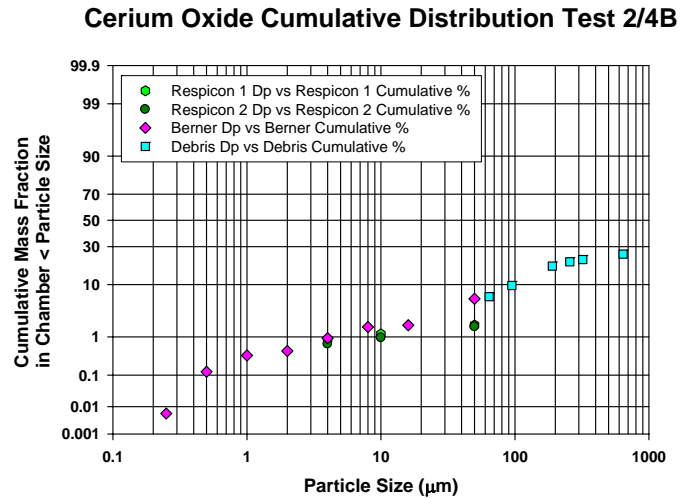


Figure 6.29 Phase 2 Test 2/4B  $\text{CeO}_2$  Cumulative Fraction

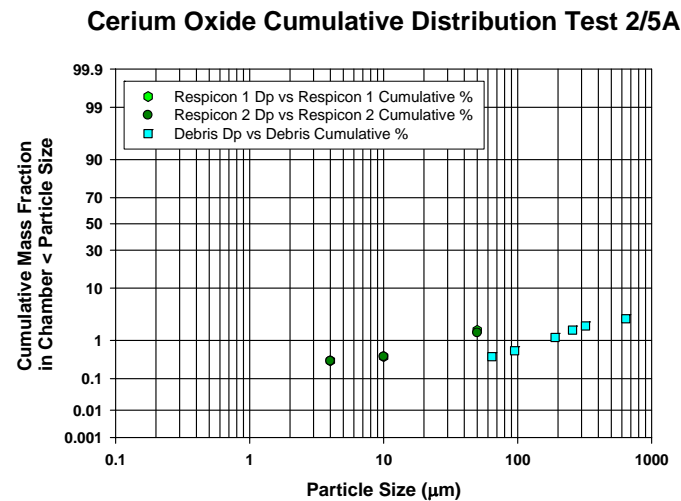


Figure 6.30 Phase 2 Test 2/5A  $\text{CeO}_2$  Cumulative Fraction

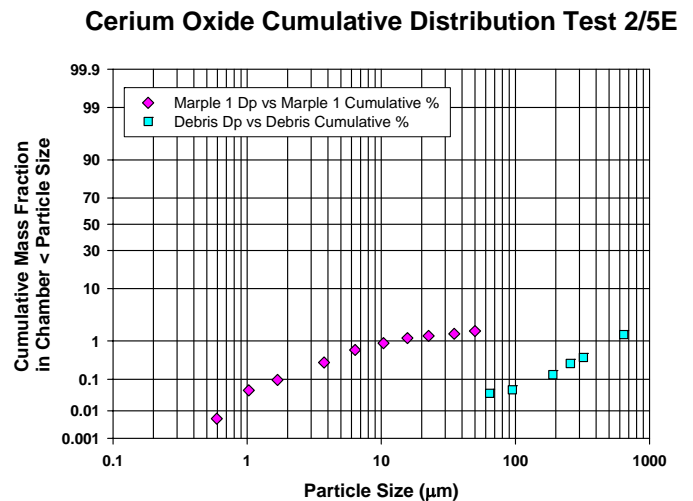


Figure 6.31 Phase 2 Test 2/5E  $\text{CeO}_2$  Cumulative Fraction

### Cerium Oxide Cumulative Distribution Test 2/5G

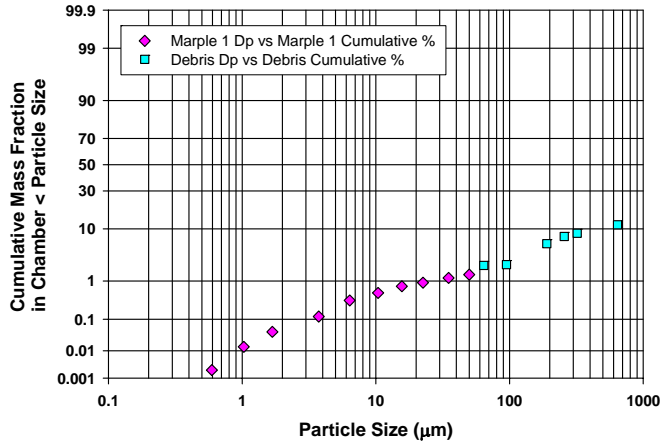


Figure 6.32 Phase 2 Test 2/5G CeO<sub>2</sub> Cumulative Fraction

### Cerium Oxide Cumulative Distribution Test 2/6A

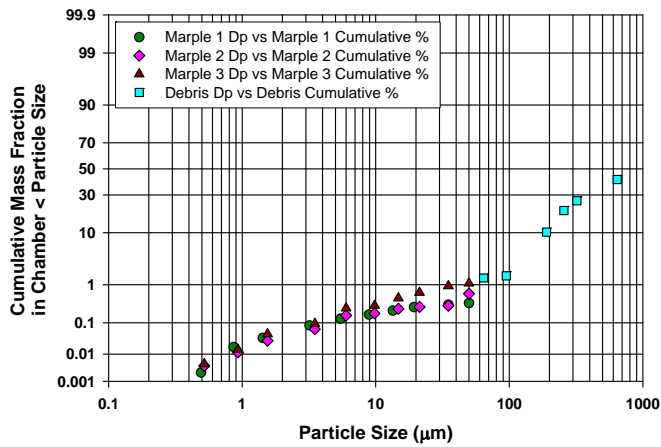


Figure 6.33 Phase 2 Test 2/6A CeO<sub>2</sub> Cumulative Fraction

### Cerium Oxide Cumulative Distribution Test 2/6B

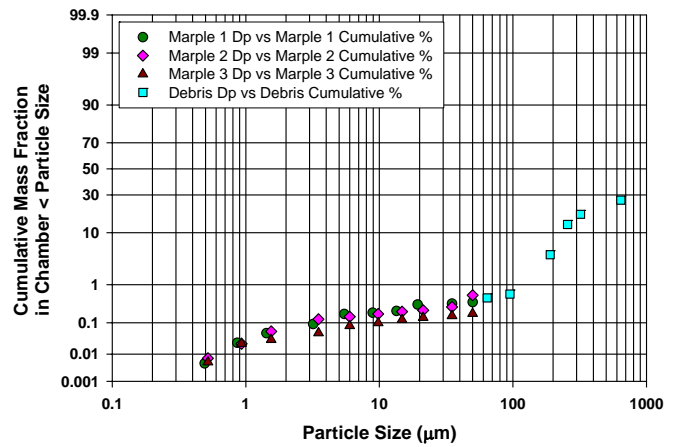


Figure 6.34 Phase 2 Test 2/6B CeO<sub>2</sub> Cumulative Fraction

### Cerium Oxide Cumulative Distribution Test 2/8C

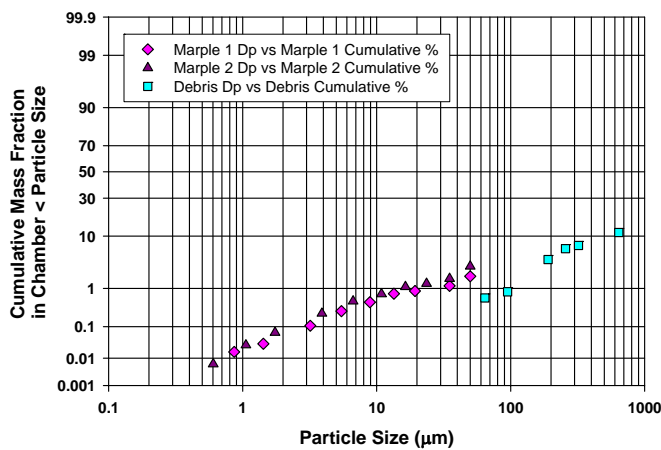


Figure 6.35 Phase 2 Test 2/8C CeO<sub>2</sub> Cumulative Fraction

### Cerium Oxide Cumulative Distribution Test 2/8D

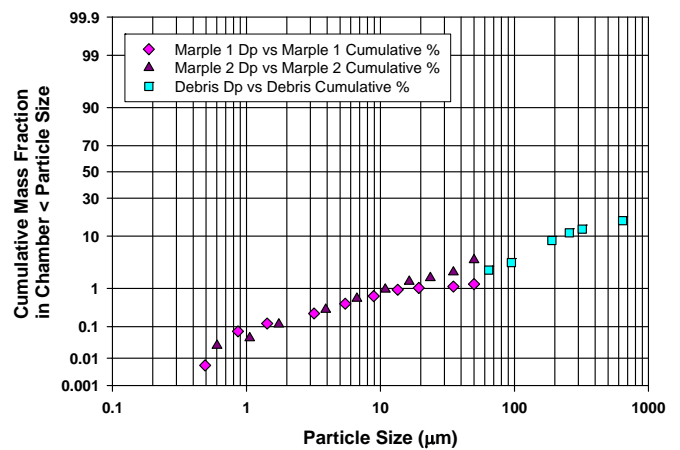


Figure 6.36 Phase 2 Test 2/8D CeO<sub>2</sub> Cumulative Fraction

From observations of the Marple impactor cerium distributions in the ~ 0 through 10  $\mu\text{m}$  AED respirable size range, and even up to ~ 35  $\mu\text{m}$ , cerium is not the most prevalent respirable material. Carbon soot from the HEDD detonation (not shown, because it is not determined by ICP-MS analysis) and copper from the HEDD jet are the dominant materials, with significant amounts of zirconium from the cladding tube and iron from the test chamber inner walls and HEDD jet stop block not far behind.

### 6.5.3.3 Aerosol Results for Zirconium

Table 6.4 presents the respirable fraction results (for particles of size  $\leq 10 \mu\text{m}$  AED) for zirconium, from the Zircaloy-4 cladding tube. The amount of zirconium material dispersed is based on the observed gap in the target rodlet. Figure 6.37 illustrates the zirconium data in Table 6.4.

The calculated zirconium respirable fraction average was 1.68 +/- 0.45 % of dispersed mass based on all collected data (with a 99% confidence interval); the respirable fraction average was 1.65 +/- 0.42 %, based on the Marple data only. These values are comparable to the cerium oxide respirable fractions measured for all data. Zirconium (Zircaloy 4 cladding) is a ductile metal, not a brittle ceramic like the  $\text{CeO}_2$  ceramic pellets. The zirconium tube was also disrupted by the HEDD jet and fragmentation may also be dominated by mechanical disruption. However, the zirconium can partially melt and oxidize as a result of the HEDD jet impact. High speed video photography was performed during tests 2/0, 2/1A, and 2/1B. Rapid oxidation (burning) of the zirconium was clearly evident, occurring within the first ~ 0.3 seconds after detonation. Zirconium oxidation is also suggested by the appreciable amount of zirconium found in the smaller, respirable impactor size ranges.

**Table 6.4 Phase 2 Test Results for Zirconium Respirable Fraction**

Test	Zr Disrupted	Zirconium Respirable Fraction (%)						Test Avg
	Zr (mg)	Respicon 1	Respicon 2	Berner	Marple 1	Marple 2	Marple 3	
2/1A	2990	0.41%	0.21%					0.31%
2/1B	2990	0.28%	0.26%					0.27%
2/2A	3035	1.85%	1.61%					1.73%
2/2B	3002	1.48%	1.94%					1.71%
2/3A	3249	1.89%		4.87%				3.38%
2/3B	3249	2.23%	2.61%	3.04%				2.63%
2/4A	3769	0.84%	1.17%	3.45%				1.82%
2/4B	3249	1.10%	0.90%	2.95%				1.65%
2/5A	3509	1.18%	1.34%					1.26%
2/5E	2859				2.92%			2.92%
2/5G	3249				1.29%			1.29%
2/6A	3510				1.12%	1.30%	1.27%	1.23%
2/6B	3510				1.24%	1.39%	1.44%	1.36%
2/8C	2989				1.32%	2.12%		1.72%
2/8D	2729				2.08%	2.35%		2.22%
avg all		1.25%		3.58%			1.65%	1.68%

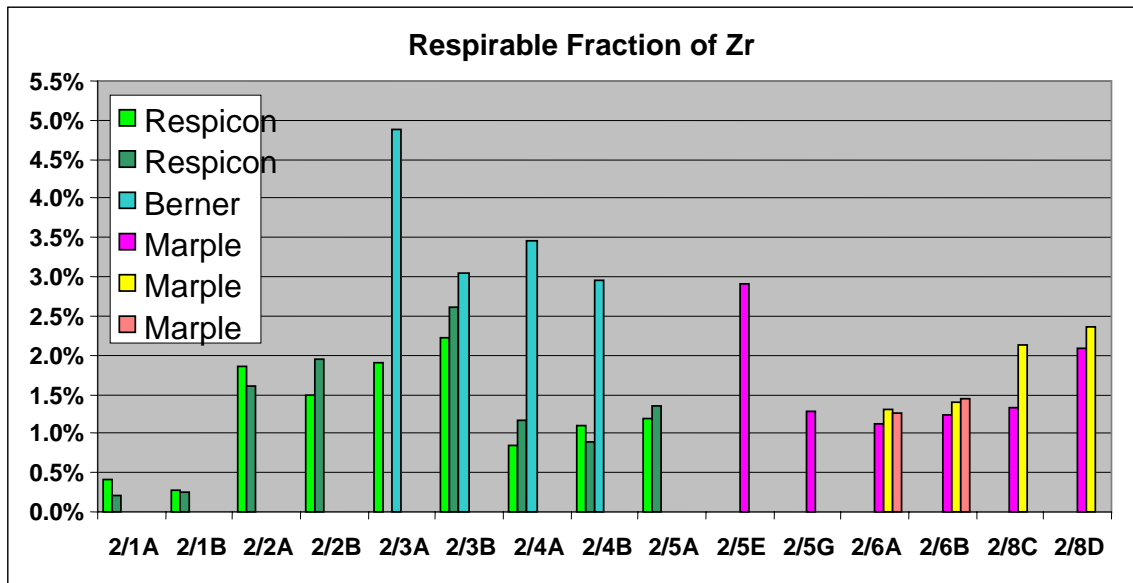


Figure 6.37 Phase 2 Test Results for Zirconium Respirable Fraction

#### 6.5.3.4 Aerosol Results for Fission Product Dopants

Later Phase 2 tests were doped with fission product simulants in the form of CsI, RuO<sub>2</sub>, SrO, and Eu<sub>2</sub>O<sub>3</sub>; refer to Table 4.2. The form of the simulants was powder material (nonradioactive chemicals) placed into drilled wells of pellets in tests 2/4A, 2/4B and 2/5A. These were also vented tests, 2/4A and 2/4B (square box aerosol chamber [Molecke et al., 2004a]) by design, and 2/5A by circumstance. The dopant disks used in the later tests, 2/5E, 2/5G, 2/6A, 2/6B, 2/8C, and 2/8D, were a thin resin base in which the dopant chemicals are imbedded. In all cases, the assumption is that the dopant materials will be dispersed (particulated or volatilized) during the HEDD jet impact. The CsI has a melting points of 899 K (626 °C) and a boiling point of 1553 K (1280 °C). The RuO<sub>2</sub> decomposes at 1473 K (1200 °C). The SrO has a melting point of 2693 K (2420 °C) and a boiling point of approximately 3270 K (2997 °C), not thermally volatile under test conditions. The SrO will not see conditions that will cause a (thermal) phase change and will be dispersed no finer than the native initial distribution of the powder. The CsI and RuO<sub>2</sub> may see conditions that will produce a phase change (volatilization), but this will depend in part on the matrix in which they are located and the specific location of that matrix with respect to the temporal and spatial energy input. Unlike the CeO<sub>2</sub> and Zr, the dopants are not uniformly distributed but they are all located in an area of the pellet stack that will be subjected to energetic disruption.

Table 6.5 presents the respirable fraction results for fission product dopant cesium, for those tests that incorporated dopants. Figure 6.38 illustrates the cesium data in Table 6.5.

The cesium measured respirable fraction average is 30 +/- 8 % based on all available data, with a 99% confidence interval; the respirable fraction average was 35.7 +/- %, based on the Marple data only. The cesium iodide used as a non-radioactive fission dopant in Phase 2 tests melts at 899 °K (626 °C) and boils at 1553 °K. It may undergo phase changes and volatilization when impacted by the HEDD jet. Based on the Marple data, cesium elemental analyses, shown in Appendix A, it is obvious that cesium is preferentially found sorbed onto respirable particles, particularly in the 0.5 to 3.5 μm AED size range. It is unclear if the cesium sorbs preferentially or is

scavenged on soot particles and/or on copper respirable particles from the HEDD jet that also peak in concentration in this size range; this will be evaluated in the future. Enhanced fission product sorption onto cerium oxide surrogate particles (or uranium oxide fuel pellets) in the respirable range may not be the most dominant mechanism.

**Table 6.5 Phase 2 Test Results for Cesium Dopant Respirable Fraction**

Test	CsI Dispersed		Cesium Respirable Fraction (%)						Test Avg
	CsI (mg)	Cs(mg)	Respicon 1	Respicon 2	Berner	Marple 1	Marple 2	Marple 3	
2/4A	32.6	16.7	24.40%	32.39%	10.34%				22.38%
2/4B	30.4	15.5	23.17%	16.91%	11.63%				17.23%
2/5A	31.0	15.9	28.50%	28.22%					28.36%
2/5E	22.6	11.6				42.44%			42.44%
2/5G	18.9	9.7				27.40%			27.40%
2/6A	30.2	15.4				17.16%	20.96%	22.26%	20.13%
2/6B	35.8	18.3				26.72%	28.12%	36.84%	30.56%
2/8C	33.9	17.3				41.88%	72.87%		57.37%
2/8D	33.9	17.3				44.86%	46.42%		45.64%
Avg all			25.60%		10.99%			35.66%	30.18%

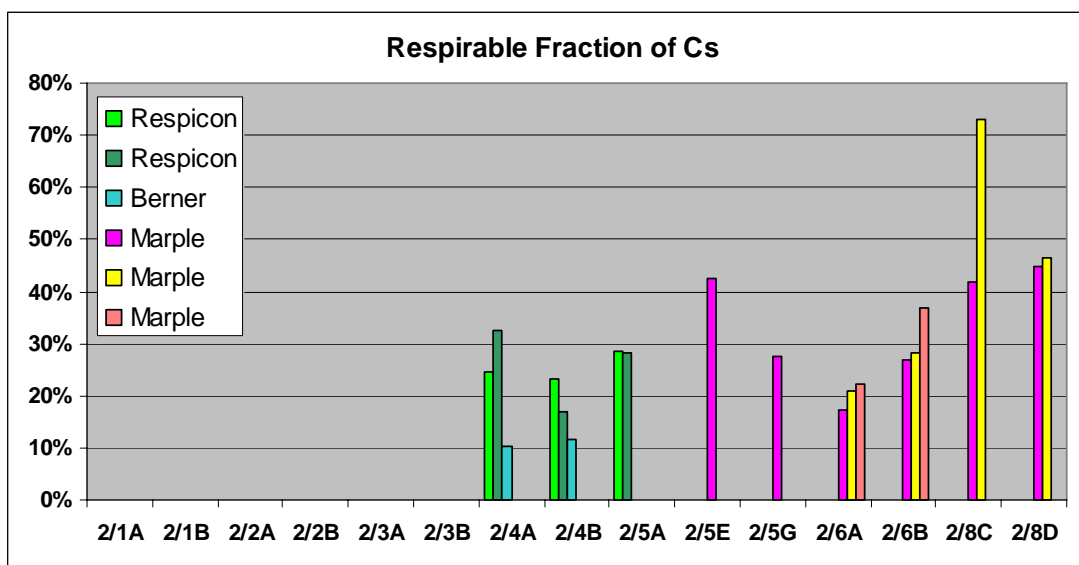


**Figure 6.38 Phase 2 Test Results for Cesium Dopant Respirable Fraction**

The higher values for cesium respirable fractions indicate that the cesium is enhanced in the smaller-sized particle range. An enhancement factor for the (cesium) respirable fraction is *defined as the ratio of cesium to cerium in the particles below 10 micrometers AED divided by the ratio of cesium to cerium dispersed into the chamber*. As defined, the enhancement factor is also equal to the respirable fraction of Cs divided by the respirable fraction of Ce. This definition can also be applied as a size dependent enhancement factor. The peak cesium concentrations were maximized in the respirable range of 0.5-1.5  $\mu\text{m}$  AED. The preliminary, calculated cesium enhancement factor ranges from x1 at 10  $\mu\text{m}$  AED climbing steeply to about a factor of more than x20 at the sizes less than 2  $\mu\text{m}$  AED. The calculated enhancement factor for cesium dopant in the German HLW glass tests (refer to Section 6.2) similarly ranged from x1 to x10 (at 0.2  $\mu\text{m}$ ).

Prior to the 8<sup>th</sup> Technical Meeting of the WGSTSC in November 2004, the German and SNL test partners both concurred that data in each of the partners respective tests exhibits cesium enrichment in the aerosol composition at a size range that is coincident with the copper distributions in the German data and the copper and soot distributions in the SNL data reported herein. SNL data exhibits more soot, and the copper and soot distributions are, for the most part, coincident with each other and with the cesium distributions with peaks on the order of one or two micrometers. The German data has considerably less soot and the copper and cesium distributions are coincident with peaks of a few tenths micrometer. At this WGSTSC meeting, a presentation [Brockmann et al., 2004] was given by the SNL partner covering data analysis for respirable fractions of cerium dioxide and cesium as well as ruthenium and strontium determined from the data. It was reported that relative enrichment of cesium with respect to cerium dioxide was observed and that the cesium distribution that tracked the soot and copper distributions.

The current status of the enhancement issue is characterized by a rather significant difference between the experiments on German surrogate HLW glass performed in Germany (by the Ernst Mach Institut (EMI)/Fraunhofer ITEM), as compared to the similar experiments, tests 2/7A and 2/7B, conducted at SNL. This is shown in Figure 6.39, where the cesium enhancement factor is plotted as a function of particle size for both experiments. The (differential) enhancement factor, EF is defined as the ratio of Cs to glass measured on the impactor stage divided by the ratio of the two compounds in the bulk glass sample. For the tests performed at SNL, a much higher cesium enhancement factor is found as compared to the German experiments.

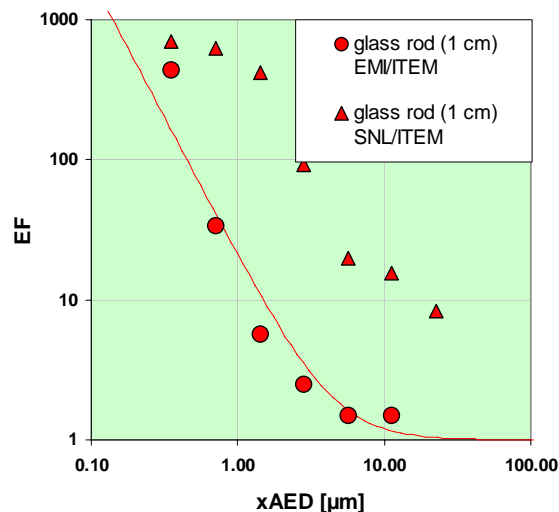


Figure 6.39 Differential Enhancement Factor for Cesium on Glass Aerosol Particles

The observed large difference in enhancement of Cs between the German (EMI/ITEM) and the Sandia (SNL/ITEM) tests may be due to different temperatures in the respective test aerosol collection chambers, with significantly higher temperatures within the SNL test chamber. This finding is neither caused by a difference in sampling technique (i.e., Berner impactor versus Marple impactor) nor possible analytical errors. In Test 2/7B, data on Cu and Cs are plotted in Figure 6.40 as they result from Berner and Marple (including Large Particle Separator) samples obtained in parallel and the analytical procedure applied at SNL, respectively at Fraunhofer. The copper and cesium size distributions match very well with a remarkably constant factor of 50 between the copper and the cesium content. This indicates again that the nucleation/condensa-

tion behavior of the two elements are identical and that copper evaporating from the HEDD jet plays a major role in the enhancement physics of volatile fission products.

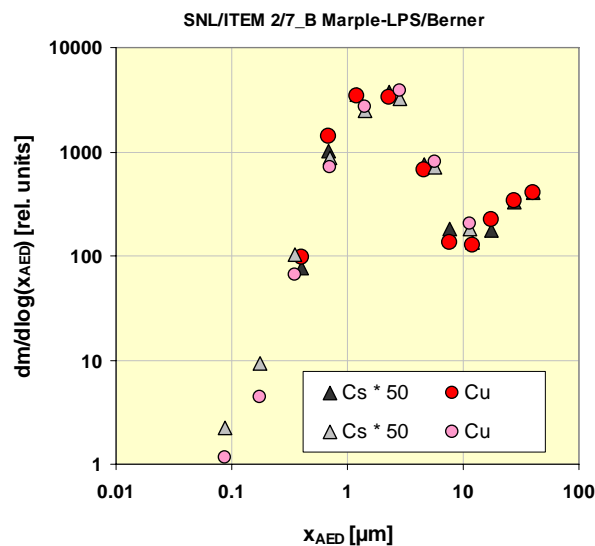


Figure 6.40 Copper and Cesium Size Distribution on HLW Glass, Test 2/7B

The dark (black, red) symbols in Figure 6.40 represent Marple aerosol samples analyzed by the SNL chemistry group. The light (gray, orange) symbols result from the Berner aerosol sample and the ITEM chemistry analysis.

Further analysis of the fission product enhancement results, and possibly future supplemental testing, will need to be made to evaluate the effects of high temperature within the aerosol collection chamber on the sampling. Tests to determine the temperature and pressure in the closed chamber tests yielded peak pressures of about 65 to 70 psia (4.5 – 5.22 bars) and peak gas temperatures on the order of 900 – 1000 °C (1200 to 1300 K) at more than 3 seconds after detonation. As discussed previously, the temperature in the vertical aerosol test chamber could be considerably higher immediately after detonation. It is possible that the higher temperatures seen in the vertical test chamber over the first couple of seconds could have caused considerable cesium vaporization. In the cooling environment, the cesium vapor would condense out either as small Cs particles or in the presence of the high aerosol surface area presented by the soot, onto pre-existing or forming or condensing soot particles. Copper may play a role in this process by also condensing out on soot particles or by participation in the formation of particles with the soot that acts to preferentially collect the cesium. In the tests reported by the German partners (ITEM/EMI), the lower temperatures may have resulted in less cesium vaporization from the glass rodlets and less soot may have been available for vapor condensation. The role of copper may be significant in this case; the copper may have formed a nucleation-condensation aerosol onto which cesium may have condensed or there may have been a binary nucleation-condensation process involving the copper and cesium.

In any case, the observed fission product enhancement of the concentration of higher vapor pressure materials in or on smaller particle sizes is a possible phenomenon that is driven by the relatively higher specific surface area of the smaller particles in a given particle distribution; the presence of soot or copper condensation aerosols would provide the necessary surface area. This phenomenon is consistent with the experimental observations. The question arises as to the form

of the volatile materials, their distributions within the fuel pellet matrix, and the energy available for vaporization. Additional tests are planned in an opened (separate, to be fabricated) aerosol chamber configuration in which the jet and target will be confined but the charge will be unconfined. These tests will address the effects of soot and temperature (less soot is expected in the chamber and lower temperatures are also expected) as well as the effects of more homogeneously distributed dopant materials.

Another possibility exists to explain some of the differences between SNL and German results on observed, enhanced cesium fission product sorption onto respirable particle. The differences may be attributable to differences in fission product *distribution within* the test target. Dopant materials that are more uniformly distributed in the matrix may behave differently than the same materials located discretely at points in or adjacent to the matrix. In the SNL test results, the fission product dopants were localized within dopant disks on either side of the central CeO<sub>2</sub> pellet in the test rodlet. In the German tests (Section 6.2), cesium dopant was evenly distributed (within silicate compounds) throughout the glass rodlet matrix -- as fission products would be in the case of actual spent nuclear fuel. In addition, the separate dopant disk design may have caused the surrogate CeO<sub>2</sub> results to be biased in a more conservative direction compared to actual spent fuel, due to enhanced mixing of the aerosolized dopant species. These potential effects and differences will be evaluated for significance with further, supplemental Phase 2 testing during FY 2005.

Based on these observations of enhanced sorption of volatile fission product (surrogate) dopant species on the smallest, respirable particles, similar results from actual spent fuel aerosol tests, in Phase 4 of this test program would not be surprising.

Other Fission Product Dopants: Test results for measured respirable fractions for ruthenium and strontium fission product dopants in Phase 2 tests were presented in [Brockmann et al., 2004]. The average measured respirable fraction for ruthenium was 1.6 +/- 0.9 % for all particle collectors, or 0.9 +/- 0.4 % from the Marple impactors only, both at the 99% confidence interval. Note that the actual Ru RF may be twice these values based on uncertainties in thermophoretic loss. Similarly, the average measured respirable fraction for strontium was 11 +/- 6 % for all particle collectors or 2.7 +/- 2.4% from the Marple impactors only, both at the 99% confidence interval. No data for the iodine dopant was measured nor reported; it is presumed that all iodine collected on aerosol particles was lost during the chemical dissolution process prior to ICP-MS analysis. Data on ruthenium were not distinct; Ru was found over the 1-16 µm particle size range. The non-volatile strontium species does not show the same sorptive behavior as volatilized cesium. Most of the strontium was collected along with larger sized particles, although a small amount was observed in the aerosol range. Again, these potential fission product dopant enhancement effects and differences will be evaluated for significance with further, supplemental Phase 2 testing during FY 2005.

The mass of collected aerosol particles below 10 µm AED diameter is dominated by far by soot and copper from the HEDD (residue and jet) which limits the sampling time for the Marple impactors to prevent overloading. The limited amount of dopant material collected (micrograms to milligrams may be close to, or below, detection limits – particularly for the small amounts of fission product dopant ruthenium and strontium. Therefore, figures and tables for the ruthenium and strontium respirable fraction measurements are not presented – they are considered too unreliable at this time.

## 6.6 Phase 2 / Phase 3 Cross-Over Tests and Results

A new series of tests, the Phase 2 / Phase 3 cross-over series, was added to the original four phase test design program in 2004, and was initiated after the completion of Phase 2 tests 2/6A and 2/6B. These Phase 2 / Phase 3 tests are intended to bridge the equipment and facility gap between Phase 2 surrogate tests (with CeO<sub>2</sub> pellets performed in the vertical aerosol collection-explosive containment chamber shown in Figure 4.6, “Grandma”) and the Phase 3 tests with DUO<sub>2</sub> test rodlets to be performed in the SNL GIF (with the new Phase 3 test chamber shown in Figure 4.8, “Tweety Bird”). The purpose of these cross-over tests is to exercise and demonstrate the full (Phase 3) test system and operational controls, to institute several new techniques, and also to collect surrogate target aerosol data, all in a non-radioactive test environment.

The first two of the Phase 2 / Phase 3 crossover tests, 2/9A and 2/9B, were performed in FY 2004 and contained cerium oxide surrogate pellets in Zircaloy 4 cladding tube test rodlets (the “Phase 2” segment) and used the new Phase 3 test chamber, Tweety Bird. We incorporated four replicate, complete, and optimized aerosol sampling subsystems, each system with an enclosed Marple impactor, a Large Particle Separator, valves, a critical orifice (~ 2 L/min), pressure and temperature gages, and a small HEPA filter preceding the 4-L vacuum bottle. The test setup for test 2/9A was illustrated in Figure 4.8. All four internal aerosol sampling tubes within the aerosol chamber are at the lower, rodlet level only. No dopant disks are used in this test series, to prevent residual cross-contaminant in subsequent Phase 3 tests using the same test chamber. These two cross-over tests were performed at the Explosive Component Facility, SNL Bldg. 905. The identical, final two Phase 2 / Phase 3 tests will be performed at the SNL GIF facility, *as if* they contained radioactive target rodlets, primarily for operational readiness, procedure check-out, and demonstration purposes.

The test 2/9A explosive-aerosol chamber was leak tested (prior to HEDD detonation) by pumping down to ~ 1 millitorr and holding. Pump-down was initiated from the bottom chamber, then finished from the top chamber; the entire pump-down procedure took less than 1 hour. The test chamber was then refilled with air. Test 2/9A was performed in 1 atmosphere air, internal.

Test 2/9B was very similar to 2/9A, but was performed with an internal atmosphere of inert nitrogen gas. This test chamber was also initially leak tested by pumping down to ~ 1 millitorr and holding. This pump-down procedure was performed using a new 4-way connector on top, right above one of the manual valves, and took < 20 minutes to pump down. Following the leak check, we used a nitrogen flushing procedure adapted from NAC International [NAC, 2002], EA790-001, Docket No. 71-9270, UMS Safety Analysis Report for the UMS Universal Transport Cask, Dec. 2002, Rev. 1, Vol 1 of 2, p. 7.1-6, steps 21-24, NAC International. This transport cask procedure was modified from a helium gas flush to a nitrogen gas flush. Basically, the air is pumped out, filled with nitrogen, pumped out, and filled with nitrogen again. This nitrogen gas internal atmosphere variable allows us to evaluate any changes in aerosol particle formation if some of the uranium (in Phase 3 and Phase 4 rodlets) is converted to higher oxidation states (from +4 to higher) by the high energy and temperature HEDD jet. The same gas flushing procedure will be used in two of the Phase 3 tests and four of the Phase 4 tests; refer to the test matrices in Tables 3.3 and 3.4.

All available aerosol particle data for tests 2/9A and 2/9B are reported and listed in Appendix A. In test 2/9A, however, aerosol sampling unit #3 inadvertently contained no flow orifice to control the aerosol sample flow through the unit. As such, significantly more particles were collected on the Marple impactor stages, seriously overloading them; refer to Figures A.1.9.3 and A.1.9.5.

The aerosol data for 2/9A Marple #3 is reported in the Appendix, but should NOT be used for further analyses. In addition, the primary valve inlet ball valve stuck partially open after the 2.5 to 12.5 sampling period ended (refer to Figure 4.8); the secondary valve did close correctly. The aerosol data from the Marple aerosol sampler #1 is also reported, but the data should be considered less accurate. Because these problems occurred in the first Phase 2 / Phase 3 cross-over test with new apparatus, new procedures have been implemented to both check for and prevent these problems from occurring in future tests.

The measured temperatures and pressures within the multiple aerosol sampling systems (NOT within the aerosol collection chamber) for tests 2/9A and 2/9B are shown in the following Figures 6.41 through 6.44.

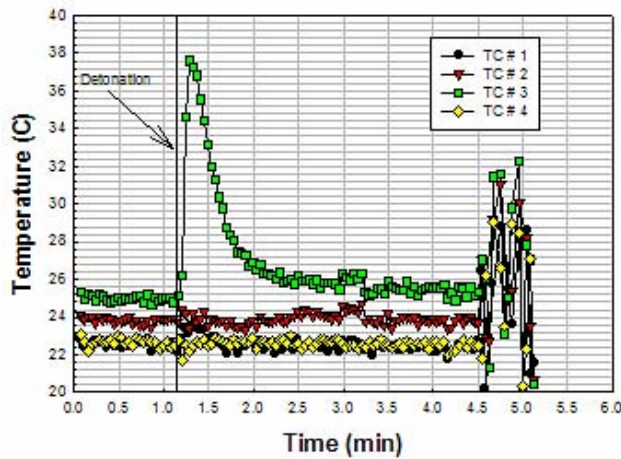


Figure 6.41 Test 2/9A Aerosol Sampler Temperatures

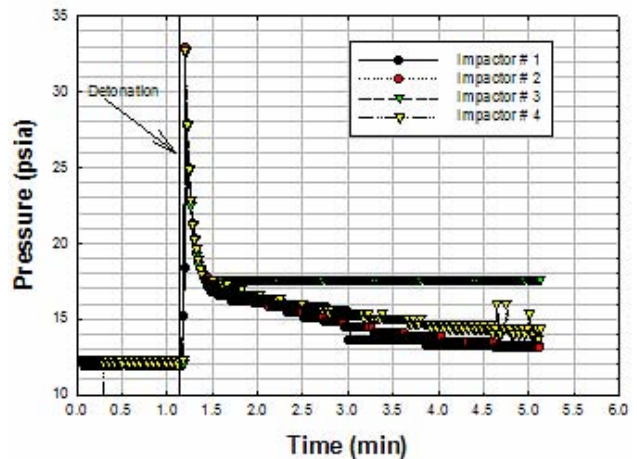


Figure 6.42 Test 2/9A Aerosol Sampler Pressures

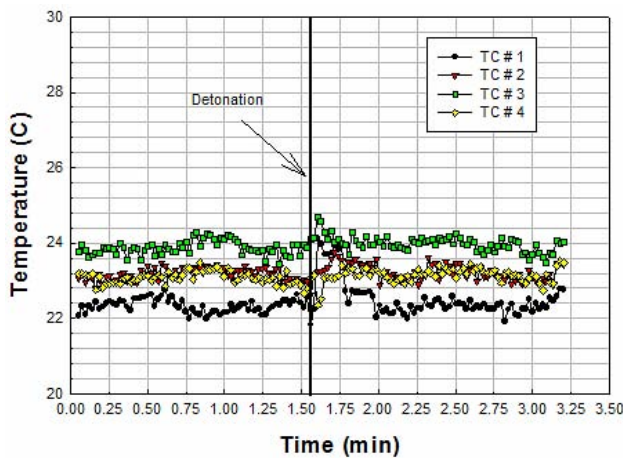


Figure 6.43 Test 2/9B Aerosol Sampler Temperatures

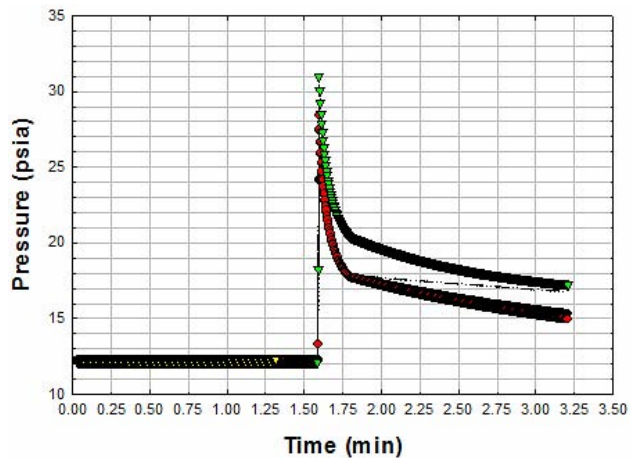


Figure 6.44 Test 2/9B Aerosol Sampler Pressures

Besides internal gas flushing procedures, another new technique was implemented during these Phase 2 / Phase 3 cross-over tests and will be used in all following Phase 3 tests with DUO<sub>2</sub>. This new technique changed the way impact debris particles remaining in the post-test aerosol

chambers are collected. Previously, we used a flat nylon artists brush to sweep up the impact debris in the aerosol chamber. Starting with test 2/9A, we used a HEPA vacuum outfitted with removable HEPA collection socks to vacuum-up the impact debris materials, inserting the vacuum wand into the opened flanged port to the top aerosol chamber. We used a commercial Euroclean WD215-H HEPA vacuum with 4 gallon (15 L) capacity, obtained from EnTech Supply (entechsupply.com), that filters 99.99% of dust particulates down to 0.3 microns. This vacuum has 5-stage filtration and includes a dust bag, pre-filter and micro-filter which collect regular to fine particulates before the HEPA filter, and exhaust filter after the motor. This HEPA vacuum has been certified and characterized in the laboratory as to collection recovery and efficiency by particle size.

Several HEPA collection socks (paper-fiber based) must be used for impact debris collection due to sock plugging from fines. They do, however, work well in collecting the debris. The pre-use and post, emptied weight of the filter socks was measured, to determine the mass of particulates collected in each sock. Impact debris from the bottom surface of the aerosol chamber was collected separately from the debris on the walls and top surface. The respective weights will give an indication of the relative importance of thermophoretic deposition. Fiberglass filter wipes of the exterior surfaces of the sampling tubes and swabs of the interior surfaces of the tubes were taken as well, to define the extent of thermophoretic deposition and its contribution to sample loss, and allow us to account for it in the spent fuel tests. (NOTE: The HEPA vacuum will NOT be used in Phase 4 tests.)

## 7. GIF FACILITY ISSUES AND REQUIREMENTS

The combination of an explosive, high energy density device and highly radioactive spent fuel test rods in Phase 4 of this program (as well as slightly radioactive, Phase 3 DUO<sub>2</sub> rodlets) gives rise to significant radiological safety testing concerns. These concerns have necessitated extensive facility environmental and safety assessment evaluations, contamination and radiation controls, plus remote handling and post-test disposal concerns. These same issues significantly increase testing expense and difficulty.

The Phase 3 testing involves a series of explosive tests planned to be performed in the Sandia Gamma Irradiation Facility, GIF, using depleted UO<sub>2</sub> (DUO<sub>2</sub>) as the surrogate material to simulate reactor fuel. These tests are a vital part of the SFR determination, but also serve for refinement of the test apparatus and processes prior to the execution of tests with the highly radioactive spent fuel samples. Introduction of DUO<sub>2</sub> samples to the testing raises only minimal additional safety and/or contamination issues. There is little threat to workers or the public, but the explosive-aerosol testing does introduce the need for careful handling and some contamination control considerations, particularly in a post-test disrupted form. Some handling components (e.g. secondary containment) and processes are required to initiate Phase 3 testing, but are considerably less than that required for Phase 4 testing with spent fuel. Post-test experiment transportation and disposal is not a significant issue since the DUO<sub>2</sub> offers only a small health or environmental hazard. Planned reuse of the test apparatus for Phase 3 tests will, however, require decontamination cleaning considerations (in process of development).

The Phase 4 tests to be performed in the GIF use small test rodlet samples of highly radioactive spent reactor fuel. These tests are a vital part of the SFR determination and the driving force for the entire spent fuel sabotage / spent fuel ratio program. Phase 4 testing involves highly radioactive materials that pose not only a direct radiation threat to associated workers, but also an inhalation threat to the workers, co-located workers, and the public, if not confined. Contamination of the GIF facility is also a significant concern, which must be protected against. The conduct of these tests will require special remote handling equipment as well as validated processes to ensure safety to the worker, co-located workers, and the public, as well as to ensure minimal impact on the facility assets. Transportation and disposal are significant issues both for the receipt of the spent fuel samples and post-test transportation and disposal of the fuel and contaminated equipment. It is required that all of these issues be resolved prior to initiation of Phase 4 testing.

Phase 3, and Phase 4 experiments will be performed in Test Cell 3 of the GIF, the layout of which is shown in Figure 8.1. An eastward looking cross-section view of the GIF is shown in Figure 8.2. In addition to a personnel passage (tortuous maze) hall, access to Cell 3 can also be provided by a normally plugged passage in the cell ceiling and by the movable south wall of the cell. An overhead crane services the ceiling access. Forklift access is afforded by moving the south cell wall. During performance of the explosive-aerosol tests, the test chamber will be positioned within the 20-foot deep, 36 inch ID (6.1 m-deep by 0.91 m diameter) storage pit in the floor of Test Cell 3, predominantly for radiation shielding purposes. The test chamber will sit on a specially designed elevator assembly within the pit that can be raised or lowered. During the tests, only the aerosol apparatus above the test chamber will be visible. The storage/test pit, shown in Figure 8.2, is aligned with the overhead access passage in the cell ceiling. Also noted in both Figure 8.1 and 8.2 is a 10 x 15 foot, by 25 foot deep (3 x 4.6 x 7.6 m deep) storage floor vault, to the north of Cell 3. Post-test spent fuel chambers will be temporarily stored in this vault until they are scheduled for off-site shipment; refer to Section 8.3. An overhead crane also services the storage vault.

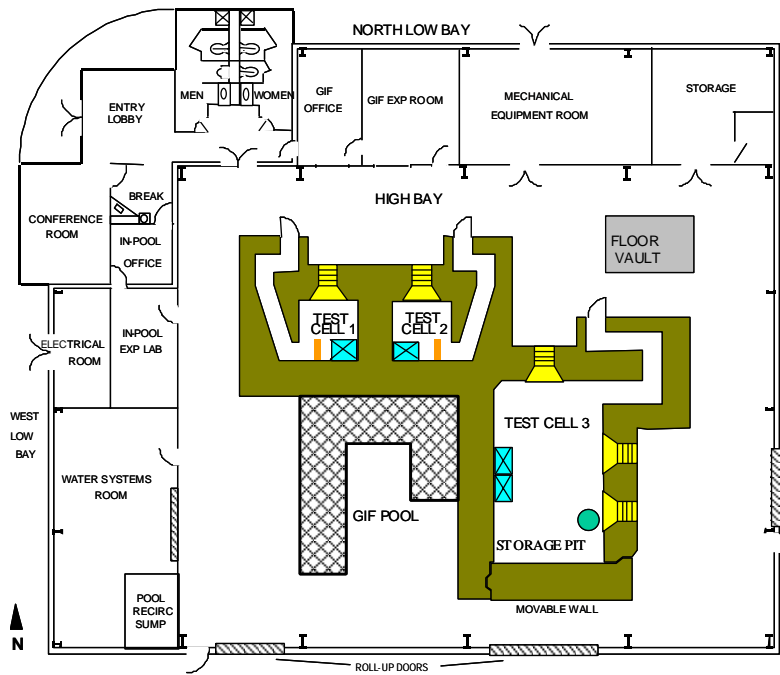


Figure 8.1 Sandia GIF Floor Plan

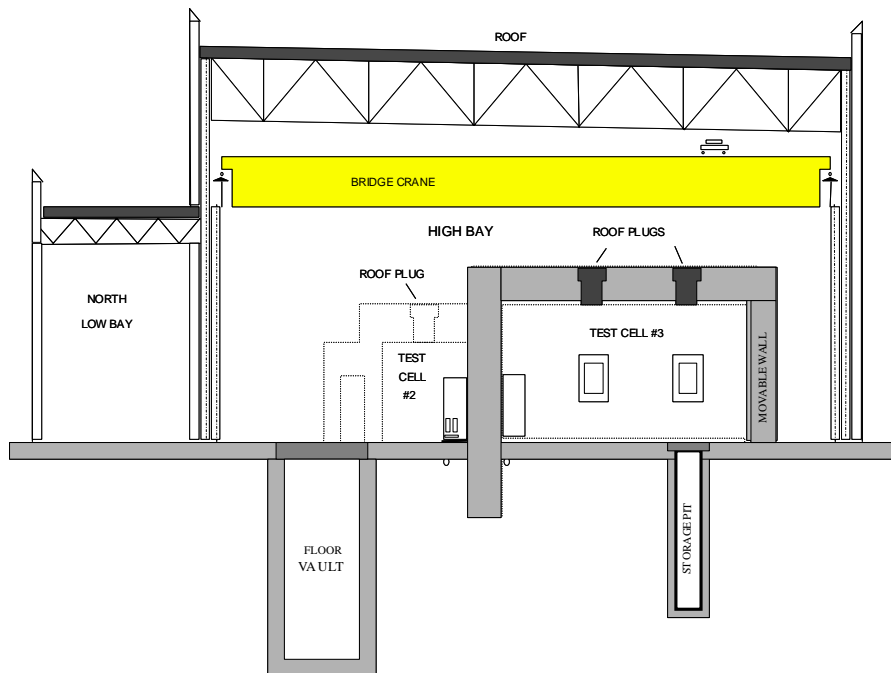


Figure 8.2 Eastward cross-sectional view of the GIF

The SNL GIF, Test Cell 3, previously has been operated as a clean facility for gamma irradiation testing only, with no radioactive contamination. The GIF is classified as a Hazard Category 3 nuclear facility with a DOE approved Documented Safety Analysis, DSA. However, the exist-

ing, previous safety basis documentation did not adequately address the use of explosives (the HEDD) and fissile materials, specifically spent fuel, due to the lack of analysis in the original DSA. The primary issue involved is the use of explosives with fissile materials in the facility and their implications for personnel safety and the potential for damage to assets. Although non-fissile material testing may fall within the current authorization basis, the revised DSA plus Technical Safety Requirements (TSR) documents are required and are being revised to explicitly accommodate these tests.

Because of the unique needs and requirements of this spent fuel sabotage explosive-aerosol test program (as described in [Molecke et al., 2004a] and this document), the current DSA has been substantially modified by Sandia to cover experiment activities in support of the Phase 3 and Phase 4 spent fuel sabotage aerosol-explosive test program. Additional modifications to the safety documentation as a whole were necessary to assure alignment with current DOE documentation requirements and interpretations of those requirements. The revised safety documentation was submitted to the Department of Energy Sandia Site Office (SSO) by the end of April, 2004 and has been under review by the DOE Sandia Site Office (SSO) since. SSO has generated a set of comments relating to issues with the documentation process, compliance, clarity, and editing. SNL is working collaboratively and iteratively with SSO to accommodate their inputs. Except for minor modifications still in negotiation, the GIF documentation is essentially complete. There are no unresolved technical, safety, or compliance issues in relation to SFR testing. Once the GIF DSA is approved by SSO, SSO will issue a Safety Evaluation Report (SER). Once the SER has been issued, Sandia will re-write procedures to address any changes made.

Staffers from the Defense Nuclear Facilities Facility Safety Board (DNFSB), which serves as a DOE oversight role for Congress, recently reviewed the SSO review and approval process for other SNL nuclear facilities. As a result of the DNFSB review, SSO is taking additional care to ensure all facility documentation, including that for the GIF, follows the prescribed documentation process [DOE-STD-3009] and satisfies the concerns and interpretations of the DNFSB. As a result, the SSO review and approval process is taking appreciably longer than anticipated, causing significant and unavoidable delays. The DOE SSO approval of the GIF DSA has become a **critical path** issue for the future scheduling and performance of Phase 3 and Phase 4 of this test program.

### 7.1 Anticipated GIF Testing Schedule

Original feedback received from DOE SSO staff indicated that the GIF Documented Safety Analysis approval would be received by late summer 2004. Based on that, we had earlier planned, in May 2004, [Molecke, Sorenson, and Gregson, 2004] to start radioactive material testing in the GIF in late 2004. By November 2004 [Molecke, 2004], the GIF test schedule was projected to slip, conservatively, by about 7 to 9 months, to start about June 2005 and finish in March 2006. This earlier schedule projection is no longer possible. Based on recent (late 2004) Sandia and DOE SSO inputs, the GIF DSA is tentatively set for approval around September-November 2005. However, there is significant uncertainty as to whether this date (month) is realistic, as large changes are being accommodated in the safety basis review process. Therefore, all postulated testing dates following are only estimates. Barring further delays, it may be possible to set up and perform the last two of the non-radioactive Phase 2/Phase 3 cross-over tests at GIF before the end 2005. We anticipate that the six Phase 3 DUO<sub>2</sub> tests may be performed at GIF over the first 18-24 weeks of 2006, followed by the eight Phase 4 spent fuel tests over the next 24-32 weeks. Optimistically, all radioactive testing could be completed by the end of calendar year 2006. Test delays may be attributed to DOE SSO deliberations with both the DNFSB and

SNL over safety authorizations for multiple Sandia nuclear facilities in Tech Area V, including the GIF. The test delays are not specific to, nor caused by, the planned explosive-aerosol testing with spent fuel test rodlets.

## 7.2 Additional Nuclear Facility Concerns

Additional nuclear facility safety and radiological concerns have been addressed and tentatively resolved, permitting us to proceed towards the performance of Phase 3 and Phase 4 testing in FY 2005-2006. These concerns include: nuclide composition in PWR spent fuel test rodlets, shielding dose calculations, contamination control (inside a leak-tight test chamber plus external secondary and, possibly, tertiary, confinement control), explosives safety and handling, testing, and identification of post-test spent fuel material disposal path. A full NEPA determination for the entire test program has also been performed and approved by SNL [Sandia NEPA, 2004]. Identification of the required test facility supporting equipment has been identified and will be tested in Phase 3 tests prior to their necessitated use in Phase 4 tests.

1. Nuclide composition in PWR spent fuel test rodlets. A study was performed on the calculated nuclide composition within the PWR spent fuel test rodlets for the Phase 4 tests [Naegele, 2004], to aid in experiment planning. The calculation methods using the ORIGEN2 and ORIGEN-ARP computer codes and the input modeling of the planned PWR spent fuel from the H. B. Robinson and the Surry nuclear power plants were discussed. The safety hazards for the calculated nuclide inventories in the spent fuel samples are characterized by the potential airborne dose and by the portion of the nuclear facility hazard category 2 and 3 thresholds that the experiment samples would present. In addition, the gamma ray photon energy source for the nuclide inventories is tabulated to facilitate subsequent calculation of the direct and shielded dose rates expected from the samples.
2. Shielding dose calculations (worker exposure to ionizing radiation). Shielding dose calculations were performed to aid in the development of the experimental plan as well as any associated administrative controls. Calculated dose results aid in the experiment conduction thought process and proved to be invaluable for the facilities. Two computer codes were used for comparison: MicroShield v. 2, a deterministic code for shielding calculations, where the results tend to be on the conservative side. MCNP, a Monte Carlo transport code used widely throughout the industry. MCNP provides an approximate dose estimate of the correct problem geometry while MicroShield calculates a dose estimate for an approximated geometry. Additional supporting calculations will be performed as needed. Due to the experiment hardware type being used, as well as its placement in the cell, decent dose estimates can be difficult to determine due to the attenuation lengths and scattering angles involved. To determine optimal placement and selection of hardware, it is often necessary to iterate on a single concept.

In addition to the ALARA concerns, contamination to the facility is also an important issue. The CeO<sub>2</sub> tests pose no threat to the facility. The DUO<sub>2</sub> tests pose a small threat to the facility; however, inhalation of heavy metals is a higher concern. For the spent fuel UO<sub>2</sub> tests, both shielding and contamination are of concern. Use of supporting hardware will be used where necessary to minimize the threat to the worker and facility. As previously identified, the use of this supporting hardware will be in place and previously checked prior to its use.

3. NEPA [Sandia NEPA, 2004]. Sandia National Laboratories completed a NEPA (National Environmental Policies Act) Checklist and sent this NEPA Action to the DOE Sandia Site

Office for review and determination. DOE/SSO completed the review and determined that the NEPA action is CX (Categorically Excluded, approved), as B 3.6 Siting/construction/ operation/ decommissioning of facilities for bench-scale research, conventional laboratory operations, small-scale research and development and pilot projects. There were no stipulations for any further actions for NEPA compliance.

In addition, the following SNL *internal* documents are required for test Phase 3 and Phase 4 testing, and are in advanced stages of development, or completed and signed off:

- (a) the Project Plan for the SNL Technical Area V, TA-V, GIF test campaign;
- (b) the Project/Experiment Quality Plan, PEQP;
- (c) the Design Requirements Document;
- (d) a specific PHS/HA (project health and safety hazard analysis) evaluation for each test phase,
- (e) a detailed Primavera test program schedule (currently on a sliding time schedule, awaiting the GIF DSA approval);
- (f) a Design Requirements Document for Spent Fuel Ratio Testing Campaign in the GIF;
- (g) a GIF Radiation Work Permit, RWP;
- (h) an Acceptance Test Plan;
- (i) a GIF experiment plan, etc.

For each of the phases of testing, a specific PHS/HA evaluation will be completed.

Further details and status of these plans, procedures, and documents will be made available in the near future.

### **7.3 Post-test Off-Site Transport of Spent Fuel Test Chambers**

Each of the spent fuel Phase 4 test chambers will be used *one time only*, temporarily stored at Sandia in the GIF floor vault, with the HEDD-disrupted, post-test spent fuel rodlet and residual particulates contained within, then shipped off-site to an approved, limited-term radioactive material (temporary) storage facility prior to final disposal, at the Yucca Mountain repository.

Sandia Radiation Sciences Center, 6700, staff and management (responsible for nuclear facilities in SNL Technical Area V, TA-V, and GIF operations) and the DOE Sandia Site Office have mandated that a spent fuel disposal pathway for these test materials must be specified and authorized before the spent fuel test rodlets can be received at, and tested at Sandia. This requirement also controls the schedule of fabrication finalizations at Argonne National Laboratory and Argonne's preparation of a formal transportation plan (from Argonne to Sandia, in an approved cask). This is an additional **critical path** requirement that mandates DOE RW support and authorizations for resolution.

Sandia personnel, with the approval of DOE RW, contacted DOE Idaho and Idaho National Laboratory, INL, staff and management (during December 2003) to determine that appropriate interim storage facilities exist in Idaho for the post-test spent fuel (containing) chambers, and to tentatively accept the transport to and interim storage of these test chambers- - pending final DOE approvals and funding. An existing, outside, in-ground facility at INL, CPP-749, was identified as being both appropriate and available for the interim storage. We identified the need for the eight Phase 4 spent fuel test chambers plus, possibly, a ninth similarly sized chamber containing associated similar PWR spent fuel and/or used experiment support equipment generated at SNL. Further SNL, DOE Sandia Site Office, DOE RW, and DOE Idaho actions are planned during the next year to resolve this critical path issue concerns: facility interfaces, DOE approvals, funding, transportation plan preparations and scheduling, transport cask rentals, etc. Due to the length of time involved in obtaining approval for the receipt and post test shipment paper-

work, the current experiment schedule allows performing  $\text{CeO}_2$  and  $\text{DUO}_2$  tests in the GIF. Delays in the approval process for the spent fuel transportation will only delay spent fuel testing.

## 8. TEST PROGRAM SUMMARY

In this technical report, we have documented a thorough overview of the FY 2004 progress, all data generated, and aerosol data interpretations for the ongoing surrogate and spent fuel sabotage – aerosol test program. The overall program involves the testing of surrogate pellet materials and actual spent fuel test rodlet sections, plus additional follow-on modeling. The test data being measured support sabotage source-term quantifications of aerosolized material particles produced from actual spent fuel and surrogate material test rods, resulting from an impact by a high energy density device, HEDD. The experimental data generated includes measurements of the spent fuel ratio and the enhanced sorption of volatile fission products onto the respirable particles. The overall program supports specified data needs of the U.S. Department of Energy, Nuclear Regulatory Commission, and the international Working Group for Sabotage Concerns of Transport and Storage Casks (WGSTSC). The aerosol-explosive testing is being performed primarily at Sandia National Laboratories, with major support, input and participation by technical experts, supplemental testing, etc., from other U.S., German, French, and British partners in the WGSTSC. This document includes the contributions from all test participants made throughout FY 2004, in support of this program.

A prime objective for this experimental program is to provide support for DOE assessments for physical protection requirements of nuclear materials in use, storage, and transport. The DOE needs this explosive-aerosol experimental program, data, and analyses relevant to a credible sabotage attack on spent fuel and nuclear materials, in transport or storage casks, plus supporting analyses and modeling of radiological consequence assessments and aerosol dispersal hazards. The information produced helps guide development of future transportation security plans, with the flexibility to modify levels of required physical protection. In addition, the overall program complements DOE efforts to build and sustain strong, collaborative relationships with our international partners to counter nuclear terrorism.

There is an agreed upon regulatory need for this experimental program. The NRC needs the explosive-aerosol experimental program and aerosol data for the generation and release of respirable particles from a credible sabotage attack on spent fuel in transport or storage casks, plus supporting analyses and modeling. The resultant source-term data generated includes measurements of the spent fuel ratio and the enhanced sorption of volatile fission products onto the respirable particles. This reliable source-term data helps validate current technical bases (based on older, less complete data) and guide appropriateness of transport regulations. It provides a defensible validation of NRC vulnerability studies; it also supports the Office of Homeland Security, in response to terrorism activities.

A substantial degree of progress and quantity of data have been generated from this program over the past two years, particularly during FY 2004. We have performed a total of 24 Phase 2 explosive-aerosol measurement tests (initiated in 2002, with 15 tests in FY 2004), essentially completing Phase 2 of the test program [Molecke et al., 2004a-d], and starting the cross-over Phase 2 / Phase 3 tests. Results and observations from all surrogate cerium oxide explosive-aerosol tests performed, as well as supplemental tests using non-radioactive German high-level waste glass rod targets, have been quite consistent. We have characterized and chemically analyzed both the aerosol particles collected by multi-staged particle impactor collection devices (Marple particle impactors, large particle separators, others), plus the residual impact debris remaining in the post-test aerosol collection chamber. We have measured and preliminarily calculated the respirable fraction (all particles up to 10  $\mu\text{m}$  AED in size) produced from the surrogate  $\text{CeO}_2$ , zirconium, and other species. We also have observed a clear indication of enhanced sorp-

tion of the volatile fission product species cesium and, to a lesser extent, ruthenium onto the smaller, respirable particles.

We have optimized the test chamber (joint aerosol collection chamber and explosive containment vessel) through multiple designs and improvements so that it is containment/leak-tight, durable, and safe for repeated use. The resultant Phase 2 vertical explosive-aerosol test chamber satisfied the aerosol vertical elutriation requirements specified by our German test partners at the Fraunhofer Institute. The optimized vertical explosive-aerosol test chamber to be used for Phase 3 DUO<sub>2</sub> tests has been fabricated, qualified, and successfully tested for use with the start of the Phase 2 / Phase 3 cross-over tests. We have almost completed fabrication for the first two, similar Phase 4 test chambers for spent fuel testing. In addition, we have designed, optimized, and assembled an aerosol sampling system that satisfies the needs of both U.S. and German aerosol experts involved with the program. Sandia, in conjunction with Fraunhofer Institute personnel, designed, fabricated, and optimized the performance of several large particle separators, LPS, for the collection of larger aerosol particles in the 30 to 100 micron AED range.

As part of the Phase 2 testing in FY 2004, we have incorporated, tested, and optimized multiple testing variables and equipment, including:

- (a) Fission product dopant disks were incorporated in some tests, with both thermally volatile and nonvolatile non-radioactive dopant species. This allowed us to quantify volatile fission product enhanced sorption onto respirable sized particle ranges.
- (b) “Blank” tests, with no CeO<sub>2</sub> pellets or no Zircaloy target rod, were used in order to evaluate behavior of soot particles and other test contaminants.
- (c) Spatial particle distributions were monitored with aerosol particle and explosive soot distributions measured spatially, at different vertical heights within the aerosol chamber, and as a function of sampling time. This information was used to evaluate particle sampling efficiencies.
- (d) Multiple modifications and optimizations were made to the test chamber aerosol containment efficiency and aerosol particle sampling apparatus, as described.
- (e) Two internally pressurized rodlet tests were performed, with 2.8 to 3.8 MPa helium gas; this pressurization simulates conditions within actual spent nuclear fuel rods. These tests were used for comparison to most tests conducted at atmospheric pressure, in air.
- (f) Temperature and pressure sensors were installed in the aerosol collection chamber and in aerosol particle sampling lines, to monitor conditions from pre-detonation to post-sampling, and to aid analyses.
- (g) Internal test chamber initial atmosphere of either air or nitrogen was used to allow the evaluation of any changes in aerosol particle formation if some of the uranium is converted to higher oxidation states (from +4 to higher) by the high energy and temperature HEDD jet. This atmosphere variable will be incorporated for use for Phase 3 DUO<sub>2</sub> tests, and the Phase 4 tests, with irradiated UO<sub>2</sub> spent fuel. This atmosphere variable was incorporated and tested in Phase 2 / Phase 3 cross-over tests, 2/9A and 2/9B.
- (h) German non-radioactive, high-level waste glass rodlets with fission product surrogate dopants were used in two tests, in a cooperative effort with our German test partners.

Respirable aerosol fractions produced from the surrogate CeO<sub>2</sub> tests for Ce, Zr, and Cs have been calculated from the aerosol measurements taken in several tests based upon the measured aerosol size and concentration and the amounts of those materials dispersed into the test chamber. The calculated respirable fraction, RF (particles up to 10 microns AED), for CeO<sub>2</sub>, in the vertical test chamber and with Marple impactor data, has ranged from 2.1 – 3.3 % average (from earlier FY 2003 data, using a less sophisticated, partially open, square aerosol chamber and Berner and

Respicon impactors), to an CeO<sub>2</sub> RF range of 0.46% (Marple impactor data average) – 1.64% (all data, average). This surrogate CeO<sub>2</sub> RF range compares to the estimate of 5% RF for UO<sub>2</sub> surrogate pellets subjected to HEDD disruption made in an earlier work [Luna et al., 1999] to support the Yucca Mountain EIS. From all of our Phase 2 tests, the calculated RF produced for Zr, from the Zircaloy cladding tube/rod, was 1.65 – 1.68 %, average. Similarly, the preliminary calculated Cs RF is 30.2 – 35.7 % average (all impactor data – Marple data); this high RF strongly suggests Cs fission product enhanced sorption on the smaller size fraction of particulates. The peak measured cesium concentrations were maximized in the respirable range of 0.5-1.5 μm AED. The preliminary, calculated cesium enhancement factor ranges from X1 at 1 μm AED up to about a factor of X20 or more at the smaller 0.4 μm AED. The calculated enhancement factor for cesium dopant in the Phase 2 German HLW glass tests similarly ranged from X1 to X10 (at 0.2 μm).

Phase 2 / Phase 3 Cross-over Test Status: Performance of the initial two Phase 2 / Phase 3 cross-over tests have basically exercised and demonstrated the full test system, with operational controls, with the collection of non-radioactive surrogate target aerosol data – at the Sandia Explosive Component Facility. Similar non-radioactive tests (with CeO<sub>2</sub> target rodlets) and demonstrated safe operation control finalizations at the SNL GIF are planned in FY 2005, to complete this test phase.

Phase 3 Test Status: Significant progress has also been made during 2004 on the plans, components, and authorizations required for the upcoming performance of radioactive Phase 3. All six Phase 3 test rodlets containing DUO<sub>2</sub> pellets were fabricated for the Institut de Radioprotection et de Surete Nucleaire, France, by their fabrication contractor CERCA, and shipped to and received by SNL in August 2004. These quality approved DUO<sub>2</sub> test rodlets were described in Section 5.1. Four of the Phase 3 rodlets each contain two of the non-radioactive fission product dopant disks (provided by SNL) surrounding the DUO<sub>2</sub> pellet in the center. Three of the rodlets are filled with air at atmospheric pressure; the other three are internally pressurized with helium at 40 atmospheres (bar), within the end plenum regions of the rodlet. Laser end-cap and seal welding was used to fabricate the rodlets. The Phase 3 and Phase 4 test rodlet design was a collaborative effort by IRSN, SNL, and ANL.

Phase 4 Test Status: The vertical aerosol-explosive test chambers for Phase 4 spent fuel tests have been designed similarly to the Phase 3 test chamber, except that there is no flanged access port to the top aerosol collection chamber. Two of these test chambers will be fabricated in the first part of FY 2005. The Phase 4 spent fuel pellets/rods, both from the high-burnup H.B. Robinson PWR reactor (~72 GWd/MTU) and the lower-burnup Surry PWR reactor (~38 GWd/MTU), have been fully characterized in the Argonne National Laboratory Alpha Gamma Hot Cell (AGHC) facility. Characterizations include: visual exams, axial gamma scanning, optical metallography, cladding hydrogen content, and isotopic analyses – for following aerosol and radiological source term material behavior evaluations. The spent fuel pellets will be contained within their original, irradiated Zircaloy cladding tubes; new Zircaloy end fittings, similar to the Phase 3 rodlet design, will be added, then circumferentially sealed with rotary tungsten inert gas welding. These spent fuel test rodlets are described in Section 5.2. Argonne will complete the spent fuel rodlet fabrication effort in FY 2005, including post-welding leak testing and external contamination control, and then transport the rodlets to SNL for testing when Sandia has received DOE authorization to accept them. This transportation is anticipated to occur in late 2005 or early 2006, but is not currently scheduled. Following preparation and approval of a transportation plan, Argonne intends to ship all eight test rodlets within either the GE-100 or T-2 trans-

port cask. Once accepted at SNL, these spent fuel rodlets will be stored at the GIF until each one is used individually in the experiment. Each Phase 4 test chamber will be used one time only, temporarily stored at Sandia with the HEDD-disrupted, post-test spent fuel rodlet and residual particulates contained within, then shipped off-site to an approved, limited-term radioactive material facility prior to final disposal. Final Phase 4 post-test clean up at the GIF and off-site spent fuel material transport will tentatively start in, and continue beyond 2006.

Safety Authorizations: The initiation of radioactive Phase 3 and Phase 4 spent fuel testing in the SNL GIF facility is awaiting finalization of the GIF Documented Safety Analysis, DSA, a formal safety authorization approval process. This is a joint SNL and DOE Sandia Site Office, SSO, operation. Sandia's safety approval processes have been funded in large part with NRC support. In conjunction with the DSA, an independent SNL review checklist plus associated supporting documentation were also required, prepared, and submitted for approvals. The SSO review and approval process is taking longer than originally anticipated, as described in Section 8. Because of this, there have been significant, unavoidable delays in authorization and initiation radioactive Phase 3 and Phase 4 tests. The DOE SSO approval of the GIF DSA has become a **critical path requirement** for the future scheduling and successful performance of the most important phases of this test program.

SNL Technical Area V (nuclear facilities) staff and management and the DOE SSO have mandated that a spent fuel disposal pathway for the spent fuel used in this program must be specified and authorized before the spent fuel test rodlets can be received at, and tested at Sandia. This issue was described in Section 8.3. This is an additional **critical path requirement** and requires additional DOE RW and DOE Idaho support and authorizations for resolution. Further SNL and DOE actions are planned during the next year to resolve these critical path issues and concerns.

Programmatic Summary: During FY 2004, SNL, Argonne National Laboratory, DOE, NRC, GRS, Fraunhofer, IRSN, and OCNS program participants participated in two technical meetings of the International Working Group for Sabotage Concerns of Transport and Storage Casks. The 6th Technical Meeting of the WGSTSC was held in Washington, DC (hosted by DOE RW), and Argonne National Laboratory, in October 2003. The 7th Technical Meeting was held in Edinburgh, Scotland, in May 2004, and hosted by the British OCNS. In early FY 2005, the 8th Technical Meeting of the WGSTSC was held in Albuquerque, NM, in November 2004, and hosted by SNL.

The overall "Spent Fuel Sabotage Aerosol Ratio Test Plan" and detailed design was previously described and formally documented in Sandia Technical Report SAND2004-1832 [Molecke et al., 2004a]. That report identified the number and sequence of tests for the total program. It also documented test component plans and requirements as of the end of FY 2003. Based on the combinations of test component optimizations, data and interpretations throughout the FY 2004 year, and periodic programmatic meetings and communications between essentially all of the WGSTSC test participants, we have slightly modified the multi-phase test program matrices and sequencing of completed as well as planned explosive-aerosol tests, as documented in Section 3 of *this* document. All test component modifications and optimizations made throughout the year were made in accordance with the specific component "requirements" as known and documented earlier (in FY 2003) [Molecke et al., 2004a – Section 6]. As such, *this current* technical report serves as both the supplement to and update of the formal "Spent Fuel Sabotage Aerosol Ratio Test Plan," at this point in time.

In summary, by the end of FY 2004, this overall spent fuel sabotage WGSTSC program was in transition from an aerosol / small-scale testing program to a testing plus follow-on modeling program, to satisfy the needs and objectives of both the U.S. and European partners. The experimental data gathered and analyses from the current program allow us to calculate the spent fuel ratio and reliable source-term information. We can extend the test results to other nuclear fuel sabotage situations through follow-on radiological consequence (including near-field aerosol dispersion, computational fluid dynamics, etc.), vulnerability modeling and assessments that are relevant to storage and transport casks. The modeling efforts are in the initial planning and conceptual design phases at the present time and will be developed further during the upcoming year, as a parallel effort (with separate, independent funding) to the testing program. The DOE and NRC, plus the other WGSTSC partners need information and results from this research to better understand potential radiological impacts from sabotage of nuclear material shipments and storage casks, and to support subsequent risk and safety assessments, modeling, and preventative measures. The current results will also be compared to, and extend, previous limited spent fuel ratio testing, explosive-aerosol testing of surrogate materials in intermediate-scale casks, and dispersion release modeling performed in the past, relevant to a credible terrorist attack scenario on nuclear fuel transport or storage casks, plus subsequent aerosolization and potential release to the environment. The continuing, successful conduct of this program provides significant technical and policy benefits for all participants. The design, status, and results of the overall program, as well as post-test analyses, follow-on modeling, and interpretations of the aerosol data, will be shared by all WGSTSC participants, under a formal multilateral agreement, currently under development.

## APPENDIX A, Aerosol and Particle Analysis Results

### A.1 Aerosol Particle Measurements, Phase 2 Tests

All available aerosol particle analyses from Phase 2 tests performed during FY 2004 are included in this Appendix, including: ICP-MS analyses from particle impactor stages of Marple and earlier Respicon and Berner aerosol apparatus used; similar data from collected and sieved impact debris particulates; plus, gravimetric soot analyses from Gelman filter stages. Table A1.1 provides a summary of particle impactor parameters used in Phase 2 tests during FY 2003, for completeness; the remainder of FY 2003 aerosol particle analyses were reported previously [1].

**Table A1.1 General Test and RESPICON Particle Sampler Information**

Test # Date	Notes: Test Modifications	Sampling Time	Respicon ID (replicates)	Flow Rate L/min	Total Filter Stages Loading
<b>2/0</b> 10/11/02	system checkout, calibration	--	(none)	--	--
<b>2/1A</b> 10/16/02	checkout, w/ 2 Respicons, 6 pellets in rodlet	60 sec	A	3.162	26.665 mg
			B	3.064	33.540 mg
<b>2/1B</b> 10/18/02	replicate of 2/1A, but w/ 5 pellets	30 sec	C	3.154	29.389 mg
			D	3.058	24.675 mg
<b>2/2A</b> 12/17/02	aerosol replicate tests, w/ 5 pellets & cladding sized to match French PWR fuel rods	30 sec	E	3.090	30.248 mg
			F	3.105	26.652 mg
<b>2/2B</b> 12/19/02	French PWR fuel rods	30 sec	G	3.090	24.834 mg
			H	3.090	26.303 mg
<b>2/3A</b> 7/29/03	aerosol replicate tests, 2 Respicons + Berner, w/ 9 pellets & cladding sized to match:	15 sec (dislodged)	I	3.111	9.165 mg
			J	none	no sample
<b>2/3B</b> 7/31/03	H.B. Robinson U.S. fuel rods; new aerosol box w/ 2 valves	15 sec	K	3.195	16.141 mg
<b>2/4A</b> 8/26/03	replicates of 2/3A & 3B, but w/ fission product dopants added.	15 sec	L	3.095	21.204 mg
			M	3.137	4.343 mg
<b>2/4B</b> 9/4/03	1 hole-closure valve	15 sec	N	2.992	9.863 mg
			O	3.111	6.925 mg
<b>2/5A</b> 9/30/03	<b>new vertical, Phase 2 test chamber</b> (+ Berner impactor, but hose disconnected)	15 sec	P	3.262	6.703 mg
			Q	3.125	14.901 mg 1.02 mg Ce
		15 sec	R	2.994	15.926 mg 0.87 mg Ce

#### A.1.1 Aerosol Fraction Analyses and Results, Tests 2/1A – 2/4B

Aerosol particle impactor and impact debris data plus associated elemental analyses collected for earlier Phase 2 tests 2/1A through 2/4B have been compiled and fully documented in Appendix A of [1], the test program status report as of the end of FY 2003.

#### A.1.5A Test 2/5A, Aerosol Fraction Analyses and Results

The Respicon fiberglass filters were digested in total using microwave assisted digestion using nitric acid and hydrogen peroxide. The digested materials were then analyzed by inductively coupled plasma – mass spectrometry, ICP/MS.

**Table A1.5.1 Test 2/5A Respicon Respirable Fraction (0-4 µm stage) Analyses**

Respicon:	Q, top	R, top	wt% detected		wt% on filter		Ce/Zr	
	mg	mg	Q	R	Q	R	Q	R
Cerium	0.1916	0.181	5.2	4.9	1.6	1.5	1.0	0.9
Copper	1.9006	1.7465	51.3	47.4	16.1	14.7		
Zirconium	0.1856	0.1944	5.0	5.3	1.6	1.6		
Iron	1.2396	1.3553	33.5	36.7	10.5	11.4		
Cesium	0.0223	0.0213	0.6	0.6	0.2	0.2		
Strontium	0.0045	0.0105	0.1	0.36	0.0	0.1		
Tin	0.0545	0.0615	1.5	1.7	0.5	0.5		
Titanium	0.0294	0.0331	0.8	0.9	0.2	0.3		
Chromium	0.0055	0.006	0.1	0.2	0.0	0.1		
Nickel	0.0000	0.0018	0.0	0.0	0.0	0.0		
Ruthenium	0.0023	0.0022	0.10	0.1	0.0	0.0		
Hafnium	0.0003	0.0003	0.0	0.0	0.0	0.0		
Molybdenum	0.0004	0.0004	0.0	0.0	0.0	0.0		
Terbium	0.0000	0.0001	0.0	0.0	0.0	0.0		
Lead	0.0038	0.0044	0.1	0.1	0.0	0.0		
Manganese	0.0628	0.0694	1.7	1.9	0.5	0.6		
mg, Metals Detected	<b>3.7032</b>	<b>3.6882</b>	<b>100.0</b>	<b>100.0</b>	<b>31.5</b>	<b>31.1</b>	<b>%sums</b>	
mg, Filter Loading	<b>11.7700</b>	<b>11.856</b>						

(yellow shading indicates most significant elements and data)

**Table A1.5.2 Test 2/5A Respicon Thoracic Fraction (4-10 µm stage) Analyses**

Respicon:	Q, mid	R, mid	wt% detected		wt% on filter		Ce/Zr	
	mg	mg	Q	R	Q	R	Q	R
Cerium	0.0530	0.0541	9.02	8.6	3.5	3.4	1.1	0.9
Copper	0.2646	0.2668	44.7	42.6	17.3	16.7		
Zirconium	0.0473	0.0590	8.0	9.4	3.1	3.7		
Iron	0.1901	0.2077	32.1	33.2	12.4	13.0		
Cesium	0.0031	0.0028	0.5	0.4	0.2	0.2		
Strontium	0.0124	0.0125	2.1	2.0	0.8	0.8		
Tin	0.0080	0.0093	1.4	1.5	0.5	0.6		
Titanium	0.0016	0.0019	0.3	0.3	0.1	0.1		
Chromium	0.0025	0.0024	0.4	0.4	0.2	0.2		
Nickel	0.0002	0.0002	0.0	0.0	0.0	0.0		
Ruthenium	0.0003	0.0002	0.1	0.0	0.0	0.0		
Hafnium	0.0003	0.0004	0.1	0.1	0.0	0.0		
Molybdenum	0.0000	0.0000	0.0	0.0	0.0	0.0		
Terbium	0.0001	0.0001	0.0	0.0	0.0	0.0		
Lead	0.0000	0.0000	0.0	0.0	0.0	0.0		
Manganese	0.0078	0.00864	1.3	1.4	0.5	0.5		
mg, Metals Detected	<b>0.5913</b>	<b>0.6260</b>	<b>100.0</b>	<b>100.0</b>	<b>38.6</b>	<b>39.1</b>	<b>%sums</b>	
mg, Filter Loading	<b>1.533</b>	<b>1.600</b>						

**Table A1.5.3 Test 2/5A Respicon Inhalable Fraction (10-100 µm stage) Analyses**

Respicon:	Q, bot	R, bot	wt% detected		wt% on filter		Ce/Zr	
	mg	mg	Q	R	Q	R	Q	R
Cerium	0.7762	0.6356	48.6	38.7	31.2	25.7	4.8	2.6
Copper	0.2913	0.3558	18.2	21.7	11.7	14.4		
Zirconium	0.1608	0.2414	10.1	14.7	6.5	9.8		
Iron	0.3336	0.3705	20.9	22.6	13.4	15.0		
Cesium	0.0019	0.00158	0.1	0.1	0.1	0.1		
Strontium	0.0104	0.0112	0.7	0.7	0.4	0.5		
Tin	0.0051	0.0063	0.3	0.4	0.2	0.3		
Titanium	0.0061	0.0064	0.4	0.4	0.2	0.3		
Chromium	0.0036	0.0035	0.2	0.2	0.1	0.1		
Nickel	0.0006	0.0006	0.0	0.0	0.0	0.0		
Ruthenium	0.0002	0.0002	0.0	0.0	0.0	0.0		
Hafnium	0.0004	0.0004	0.0	0.0	0.0	0.0		
Molybdenum	0.0000	0.0000	0.0	0.0	0.0	0.0		
Terbium	0.0002	0.0001	0.0	0.0	0.0	0.0		
Lead	0.0000	0.0000	0.0	0.0	0.0	0.0		
Manganese	0.0073	0.0084	0.5	0.5	0.3	0.3		
mg, Metals Detected	<b>1.5977</b>	<b>1.6419</b>	<b>100.0</b>	<b>100.0</b>	<b>64.3</b>	<b>66.5</b>	<b>%sums</b>	
mg, Filter Loading	<b>2.4850</b>	<b>2.4700</b>						

**Table A1.5.4 Test 2/5A Distribution of Fission Product Dopants on Respicon Filters**

	Respirable	Thoracic	Inhalable	
	<i>Top</i>	<i>Middle</i>	<i>Bottom</i>	Total
	<b>milligrams</b>	<b>CESIUM</b>		
Q	0.0223	0.0031	0.0019	0.0273
R	0.0213	0.0028	0.0015	0.0256
	<b>wt%</b>			
Q	81.7	11.4	7.0	
R	83.2	10.9	5.9	
	<b>milligrams</b>	<b>RUTHENIUM</b>		
Q	0.0023	0.0003	0.0002	0.0028
R	0.0022	0.0002	0.0002	0.0026
	<b>wt%</b>			
Q	82.1	10.7	7.1	
R	84.6	7.7	7.7	
	<b>milligrams</b>	<b>STRONTIUM</b>		
Q	0.0045	0.0124	0.0104	0.0273
R	0.0105	0.0125	0.0112	0.0342
	<b>wt%</b>			
Q	16.5	45.4	38.1	
R	30.7	36.5	32.7	
	<b>milligrams</b>	<b>IODINE</b>		
Q	(not detected)			
R	(not detected)			
	<b>wt%</b>			
Q	(not detected)			
R	(not detected)			

**Table A1.5.5 Test 2/5A Distribution of Cerium on Respicon Filters**

	Respirable	Thoracic	Inhalable	
	<i>Top</i>	<i>Middle</i>	<i>Bottom</i>	Total
	milligrams			
Q	0.1916	0.053	0.7762	1.0208
R	0.181	0.0541	0.6356	0.8707
	wt%			
Q	18.8	5.2	76.8	
R	20.8	6.2	73.0	

**Test 2/5A Impact Debris Particle Sampling and Results**

After the aerosol particle samplers were removed from the test chamber, the aerosol collection, top chamber was opened and all remaining particulated debris on the internal surfaces of the chamber was swept into a small collection pile using a flat nylon brush. This impact debris was composed of heterogeneous fragments, some plastic (from the HEDD holding fixture in the bottom, explosive chamber), copper and Zircaloy metal pieces, etc. All of this debris was uniformly gray in color, as coated with explosive residue soot. The collected debris was mechanically sieved using a set of 48mm sieves; 1000  $\mu\text{m}$ , 500  $\mu\text{m}$ , 250  $\mu\text{m}$ , and 125  $\mu\text{m}$  with a final catch pan. The ‘fines’ were then sieved further with disposable mesh sieves at 100  $\mu\text{m}$ , 74  $\mu\text{m}$ , 37  $\mu\text{m}$ , and 25  $\mu\text{m}$  (geometric sizes) to further differentiate the debris. The weights of the sieved impact debris particles are listed in the following Table A1.5.6. However, since much of the smaller particulated debris was visibly vented out of the disconnected sampling hose to the Berner impactor, no chemical analyses of these particles, or further interpretations, are reported.

**Table A1.5.6 Test 2/5A, Weight Distribution of Remaining Impact Debris**

Sieve Fraction	Weight, g	%
1000 $\mu\text{m}$	0.0046	0.5
500 $\mu\text{m}$	0.0321	3.7
250 $\mu\text{m}$	0.0837	9.6
125 $\mu\text{m}$	0.2251	25.7
100 $\mu\text{m}$	0.0923	10.5
74 $\mu\text{m}$	0.1298	14.8
37 $\mu\text{m}$	0.1575	18.0
25 $\mu\text{m}$	0.0405	4.6
<25 $\mu\text{m}$	0.1105	12.6
<b>Total</b>	<b>0.8761 g</b>	<b>100.0 (incomplete)</b>

**Test 2/5A Rod Debris Particle Sampling and Results**

The rod debris is the material that was poured out of the test rod after impact that is not intact ceria pellets, i.e., it is fragmented cerium oxide pellet material. The rod debris material was sieved similarly to the impact debris, and examined using a Zeiss optical microscope. The rod debris material had no soot coating. Table A1.5.7 lists the rod debris sieved weight distribution.

**Table A1.5.7 Test 2/5A, Weight Distribution of Ceria Rod Debris**

Sieve Fraction	Weight, g	%
1000 µm	21.0219	65.7
500 µm	3.7613	11.8
250 µm	2.7038	8.4
125 µm	1.794	5.6
100 µm	0.6484	2.0
74 µm	0.9133	2.9
37 µm	0.8486	2.7
25 µm	0.0918	0.3
<25 µm	0.2187	0.7
<b>Total</b>	<b>32.0018 g</b>	<b>100.0</b>

#### **A.1.5B Test 2/5B Analyses and Results**

This was a test “**blank.**” The target was an empty Zircaloy tube, with NO ceria pellets. There were no particle impactors installed, and, as such, no aerosol data. One of the goals of this test was to collect and analyze the particulate impact debris residue, consisting of the soot, Zircaloy, and other particulates, to establish a particulate ‘background’ for these tests. All debris on the internal surfaces of the aerosol collection chamber was swept into small collection piles and removed. The impact debris was composed of heterogeneous fragments and metal pieces with a mostly chocolate-brown color with some light rose-colored pieces (cerium oxide) distributed in the sample.

**Table A1.5.8 Test 2/5B, Weight Distribution of Impact Debris**

Sieve Fraction	Weight, g	%
1000 µm	10.7902	65.68
500 µm	2.5240	15.36
250 µm	1.3086	7.97
125 µm	0.9463	5.76
100 µm	0.1994	1.21
74 µm	0.3648	2.22
37 µm	0.1950	1.19
25 µm	0.0609	0.37
<25 µm	0.0399	0.24
<b>Total</b>	<b>16.4291 g</b>	<b>100.0</b>

#### **Test 2/5B Elemental Analysis of Impact Debris**

The sieved fractions of interest were homogenized by grinding with a mortar and pestle. An approximately 0.05 gram portion of the ground fraction was digested in a Teflon beaker using 10

mL of concentrated nitric acid (HNO<sub>3</sub>) and refluxing for 30 minutes. After cooling, 4 mL of concentrated hydrofluoric acid (HF) was added, and the mixture heated for an additional 30 minutes. After cooling a second time, and additional 5.0 mL of 30% hydrogen peroxide was added, and this mixture was heated to reduce the solution volume to < 1 mL. The reduced preparation was cooled, and 10 mL of conc. HNO<sub>3</sub> was added. This sample was heated for 30 minutes, cooled, and then 5 mL of 30% hydrogen peroxide (H<sub>2</sub>O<sub>2</sub>) was added and allowed to react. This mixture was heated for 30 minutes, and then cooled. This digestate was then diluted to 100 grams with DI water and analyzed by inductively coupled plasma/mass spectrometry (ICP/MS). The elemental analysis results and residue weighings as weight percent of metal are summarized in Table A1.5.9.

**Table A1.5.9 Test 2/5B, Elemental Analysis wt% of Sieved Impact Debris**

Test 2/5B Sieve Fraction	125 µm	100 µm	74 µm	37 µm	25 µm	<25 µm
Cerium *	16.170	20.550	19.890	17.860	7.130	5.013
Iron	43.610	36.370	37.970	34.590	35.230	32.120
Copper	5.540	5.933	6.413	7.614	12.390	14.160
Zirconium	2.432	2.888	3.361	4.202	7.223	8.548
Aluminum	2.679	3.608	4.341	4.638	6.620	6.467
Manganese	0.917	0.734	0.684	0.631	0.614	0.517
Tin	0.050	0.060	0.067	0.076	0.136	0.153
Chromium	0.051	0.043	0.040	0.040	0.045	0.045
Magnesium	0.118	0.130	0.138	0.152	0.209	0.185
Nickel	0.051	0.040	0.038	0.032	0.030	0.025
Titanium	1.253	0.870	0.783	0.638	0.561	0.453
Molybdenum	0.015	0.013	0.013	0.014	0.030	0.026
Strontium *	0.010	0.013	0.012	0.012	0.008	0.006
Cesium *	0.001	0.001	0.001	0.001	0.004	0.003
Ruthenium *	0.000	0.000	0.000	0.000	0.000	0.000
Terbium	0.002	0.003	0.003	0.002	0.001	0.001
Lead	0.005	0.005	0.006	0.008	0.019	0.017
Barium	0.055	0.053	0.061	0.063	0.069	0.047
Hafnium	0.002	0.001	0.001	0.003	0.001	0.001
<b>Total</b>	<b>72.961</b>	<b>71.315</b>	<b>73.822</b>	<b>70.576</b>	<b>70.320</b>	<b>67.787</b>

\* “pink” colored rows indicate residual chamber contamination debris from the prior test, 2/5A

The unaccounted for weight percentages in the above table are likely due to unanalyzed carbon and oxygen content, predominantly.

The weight percent distribution of metals in the impact sieved fractions for test 2/5B is shown in Figure A1.5.1.

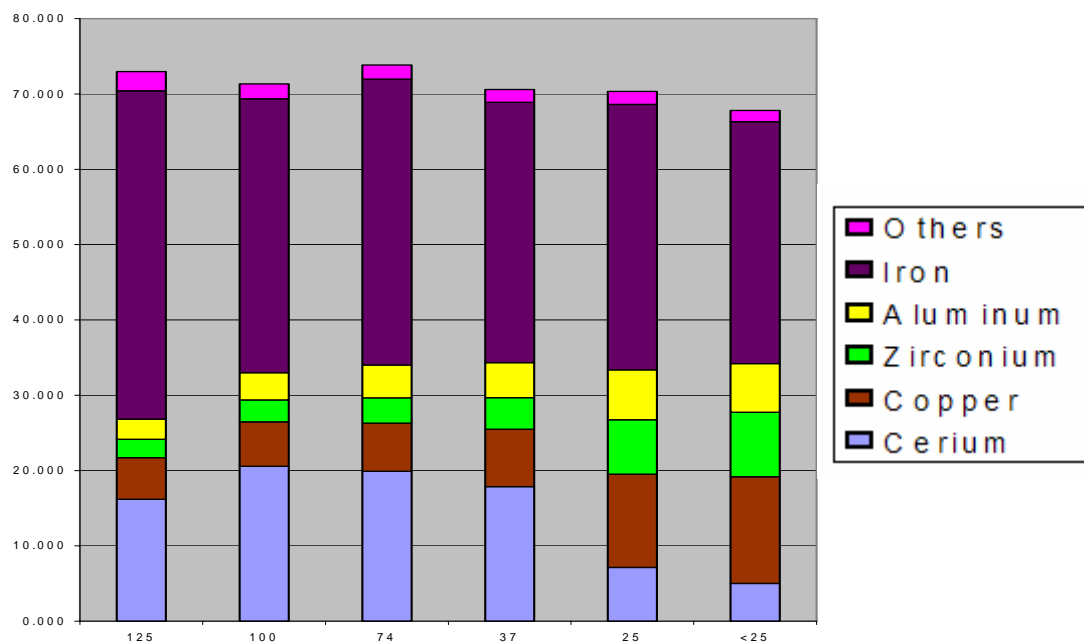


Figure A1.5.1 Test 2/5B, Weight Percent Distribution of Metals in Impact Sieved Fractions

### A.1.5C Test 2/5C Analyses and Results

This test was also a “blank,” to optimize instrumentation (thermocouples, pressure transducers). There was NO target, no Zircaloy tube, and no pellets. There were no particle impactors installed, and, as such, no aerosol data. All debris on the internal surfaces of the aerosol collection chamber was swept into a small collection pile and removed. The impact fraction sieved debris weights and elemental analysis weight percentages are summarized in Tables A1.5.10 and A1.5.11. The analyzed impact debris metal elemental analysis results are shown in Figure A1.5.2.

Table A1.5.10 Test 2/5C, Weight Distribution of Impact Debris

Sieve Fraction	Weight, g	%
1000 $\mu\text{m}$	3.8767	69.37
500 $\mu\text{m}$	0.7498	13.42
250 $\mu\text{m}$	0.4128	7.39
125 $\mu\text{m}$	0.2604	4.66
100 $\mu\text{m}$	0.0710	1.27
74 $\mu\text{m}$	0.0633	1.13
37 $\mu\text{m}$	0.1120	2.00
25 $\mu\text{m}$	0.0180	0.32
<25 $\mu\text{m}$	0.0243	0.43
<b>Total</b>	<b>5.5883 g</b>	<b>100.0</b>

**Table A1.5.11 Test 2/5C, Elemental Analysis wt% of Sieved Impact Debris**

Test 2/5C Sieve Fraction		125 µm	100 µm	74 µm	37 µm	25 µm	<25 µm
Cerium *		4.957	7.401	8.604	6.033	2.131	1.058
Iron		44.760	38.270	37.520	34.920	24.210	16.820
Copper		5.090	5.608	6.309	6.994	6.197	4.894
Zirconium		1.984	2.711	3.260	3.762	3.609	3.008
Aluminum		4.417	6.439	6.786	5.827	3.001	2.023
Manganese		0.877	0.713	0.640	0.472	0.260	0.157
Tin		0.037	0.050	0.060	0.070	0.053	0.045
Chromium		0.049	0.045	0.047	0.040	0.031	0.021
Magnesium		0.153	0.190	0.199	0.170	0.104	0.066
Nickel		0.041	0.036	0.033	0.024	0.015	0.009
Titanium		1.170	0.877	0.754	0.469	0.216	0.109
Molybdenum		0.021	0.023	0.025	0.026	0.019	0.015
Strontium *		0.006	0.007	0.007	0.005	0.002	0.001
Cesium *		0.000	0.000	0.000	0.000	0.000	0.000
Ruthenium *		0.000	0.000	0.000	0.000	0.000	0.000
Terbium		0.001	0.001	0.002	0.001	0.000	0.000
Lead		0.004	0.005	0.006	0.007	0.006	0.005
Barium		0.035	0.083	0.082	0.082	0.080	0.059
Hafnium		0.002	0.006	0.001	0.001	ND	ND
<b>Total</b>		<b>63.604</b>	<b>62.465</b>	<b>64.335</b>	<b>58.903</b>	<b>39.934</b>	<b>28.290</b>

\* “pink” colored rows indicate residual contamination debris from the prior tests, 2/5A and 2/5B

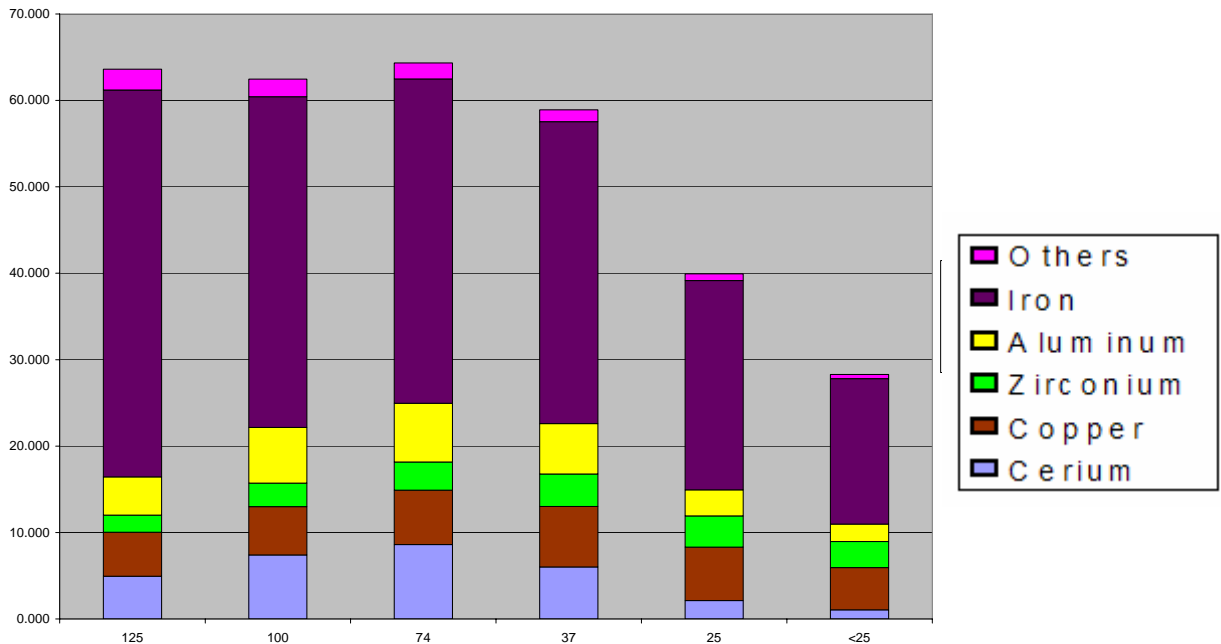


**Figure A1.5.2 Test 2/5C, Weight Percent Distribution of Metals in Impact Sieved Fractions**

### A.1.5D Test 2/5D Analyses and Results

Test 2/5D was a replicate of 2/5C, and also a “blank,” to optimize instrumentation (thermocouples, pressure transducers). There was no collection of impact debris nor chemical analyses.

### A.1.5E Test 2/5E Analyses and Results

Test 2/5E used a test rodlet with 9 CeO<sub>2</sub> pellets plus 2 fission product dopant disks, on either side of the center pellet. It used one Marple impactor and one large particle separator. Aerosol sampling time was 15 seconds. The metals analyses from each particulate stage of the Marple impactor used are summarized in Tables A1.5.12 through A1.5.14. The cerium and fission product distributions analyzed on each stage of the Marple impactor, by size, are listed in Table A1.5.15, and shown in Figures A1.5.3 and A1.5.4. No iodine was detected on any of the particle size stages.

**Table A1.5.12 Test 2/5E, Marple Particle Elemental Analyses, Stages 0-3**

2/5E	STAGE 0			STAGE 1			STAGE 2			STAGE 3		
	Particle size 35 µm			Particle size 21.3 µm			Particle size 14.8 µm			Particle size 9.8 µm		
	mg	% detected	% loading	mg	% detected	% loading	mg	% detected	% loading	mg	% detected	% loading
<b>Ce</b>	0.1063	47.7	30.3	0.0735	51.0	28.5	0.0711	57.0	30.0	0.1385	51.1	28.5
<b>Cu</b>	0.0101	4.5	2.9	0.0130	9.0	5.0	0.0114	9.1	4.8	0.0266	9.8	5.5
<b>Zr</b>	0.0150	6.7	4.3	0.0152	10.5	5.9	0.0134	10.7	5.7	0.0311	11.5	6.4
<b>Fe</b>	0.0812	36.5	23.1	0.0383	26.6	14.8	0.0282	22.6	11.9	0.0720	26.6	14.8
<b>Mg</b>	0.0052	2.3	1.5	0.0000	0.0	0.0	0.0000	0.0	0.0	0.0000	0.0	0.0
<b>Cr</b>	0.0007	0.3	0.2	0.0009	0.6	0.3	0.0000	0.0	0.0	0.0000	0.0	0.0
<b>Ni</b>	0.0000	0.0	0.0	0.0005	0.3	0.2	0.0000	0.0	0.0	0.0000	0.0	0.0
<b>Mn</b>	0.0015	0.7	0.4	0.0006	0.4	0.2	0.0004	0.3	0.2	0.0010	0.4	0.2
<b>Sn</b>	0.0000	0.0	0.0	0.0006	0.4	0.2	0.0003	0.2	0.1	0.0011	0.4	0.2
<b>Mo</b>	0.0000	0.0	0.0	0.0000	0.0	0.0	0.0000	0.0	0.0	0.0000	0.0	0.0
<b>Ti</b>	0.0007	0.3	0.2	0.0003	0.2	0.1	0.0000	0.0	0.0	0.0006	0.2	0.1
<b>Hf</b>	0.0000	0.0	0.0	0.0013	0.9	0.5	0.0000	0.0	0.0	0.0000	0.0	0.0
<b>Pb</b>	0.0015	0.7	0.4	0.0000	0.0	0.0	0.0000	0.0	0.0	0.0000	0.0	0.0
<b>Cs</b>	0.0000	0.0	0.0	0.0000	0.0	0.0	0.0000	0.0	0.0	0.0002	0.1	0.0
<b>Sr</b>	0.0008	0.4	0.2	0.0000	0.0	0.0	0.0000	0.0	0.0	0.0000	0.0	0.0
<b>Ru</b>	0.0000	0.0	0.0	0.0000	0.0	0.0	0.0000	0.0	0.0	0.0000	0.0	0.0
<b>mg, Metals Found</b>	<b>0.2227</b>	<b>100.0</b>	<b>63.4</b>	<b>0.1442</b>	<b>100.0</b>	<b>55.9</b>	<b>0.1248</b>	<b>100.0</b>	<b>52.7</b>	<b>0.2711</b>	<b>100.0</b>	<b>55.8</b>
<b>mg, Filter Loading</b>	<b>0.3510</b>			<b>0.2580</b>			<b>0.2370</b>			<b>0.4860</b>		

**Table A1.5.13 Test 2/5E, Marple Particle Elemental Analyses, Stages 4-7**

2/5E	STAGE 4			STAGE 5			STAGE 6			STAGE 7		
	Particle size 6.0 µm			Particle size 3.5 µm			Particle size 1.55 µm			Particle size 0.93 µm		
	mg	% detected	% loading	mg	% detected	% loading	mg	% detected	% loading	mg	% detected	% loading
Ce	0.1397	47.3	26.9	0.1604	33.5	17.3	0.0992	8.7	3.2	0.0247	4.2	1.4
Cu	0.0374	12.7	7.2	0.1149	24.0	12.4	0.6043	52.9	19.7	0.3349	57.6	19.2
Zr	0.0371	12.6	7.1	0.0600	12.5	6.5	0.0792	6.9	2.6	0.0360	6.2	2.1
Fe	0.0782	26.5	15.1	0.1317	27.5	14.2	0.3217	28.2	10.5	0.1632	28.1	9.3
Mg	0.0000	0.0	0.0	0.0000	0.0	0.0	0.0008	0.1	0.0	0.0000	0.0	0.0
Cr	0.0000	0.0	0.0	0.0011	0.2	0.1	0.0009	0.1	0.0	0.0004	0.1	0.0
Ni	0.0000	0.0	0.0	0.0002	0.0	0.0	0.0029	0.3	0.1	0.0003	0.1	0.0
Mn	0.0012	0.4	0.2	0.0024	0.5	0.3	0.0070	0.6	0.2	0.0043	0.7	0.2
Sn	0.0012	0.4	0.2	0.0042	0.9	0.5	0.0157	1.4	0.5	0.0103	1.8	0.6
Mo	0.0000	0.0	0.0	0.0000	0.0	0.0	0.0005	0.0	0.0	0.0003	0.1	0.0
Ti	0.0005	0.2	0.1	0.0019	0.4	0.2	0.0027	0.2	0.1	0.0007	0.1	0.0
Hf	0.0000	0.0	0.0	0.0000	0.0	0.0	0.0000	0.0	0.0	0.0016	0.3	0.1
Pb	0.0000	0.0	0.0	0.0000	0.0	0.0	0.0010	0.1	0.0	0.0007	0.1	0.0
Cs	0.0003	0.1	0.1	0.0011	0.2	0.1	0.0057	0.5	0.2	0.0039	0.7	0.2
Sr	0.0000	0.0	0.0	0.0002	0.0	0.0	0.0000	0.0	0.0	0.0000	0.0	0.0
Ru	0.0000	0.0	0.0	0.0000	0.0	0.0	0.0000	0.0	0.0	0.0004	0.1	0.0
mg, Metals Found	<b>0.2956</b>	<b>100.0</b>	<b>57.0</b>	<b>0.4781</b>	<b>100.0</b>	<b>51.7</b>	<b>1.1416</b>	<b>100.0</b>	<b>37.3</b>	<b>0.5817</b>	<b>100.0</b>	<b>33.3</b>
mg, Filter Loading	<b>0.5190</b>			<b>0.9250</b>			<b>3.0630</b>			<b>1.7480</b>		

**Table A1.5.14 Test 2/5E, Marple Particle Elemental Analyses, Stages 8-9**

2/5E	STAGE 8			STAGE 9								
	Particle size 0.52 µm			Particle size final, >0.5 µm								
	mg	% detected	% loading	mg	% detected	% loading						
Ce	0.0208	4.4	1.5	0.0027	3.8	0.9						
Cu	0.2114	44.6	14.8	0.0165	23.4	5.5						
Zr	0.0380	8.0	2.7	0.0073	10.4	2.4						
Fe	0.1811	38.2	12.7	0.0326	46.2	10.9						
Mg	0.0000	0.0	0.0	0.0068	9.6	2.3						
Cr	0.0004	0.1	0.0	0.0000	0.0	0.0						
Ni	0.0003	0.1	0.0	0.0000	0.0	0.0						
Mn	0.0044	0.9	0.3	0.0007	1.0	0.2						
Sn	0.0114	2.4	0.8	0.0017	2.4	0.6						
Mo	0.0004	0.1	0.0	0.0000	0.0	0.0						
Ti	0.0008	0.2	0.1	0.0009	1.3	0.3						
Hf	0.0000	0.0	0.0	0.0000	0.0	0.0						
Pb	0.0007	0.1	0.0	0.0000	0.0	0.0						
Cs	0.0040	0.8	0.3	0.0005	0.7	0.2						
Sr	0.0000	0.0	0.0	0.0008	1.1	0.3						
Ru	0.0000	0.0	0.0	0.0000	0.0	0.0						
mg, Metals Found	<b>0.4737</b>	<b>100.0</b>	<b>33.2</b>	<b>0.0705</b>	<b>100.0</b>	<b>23.6</b>						
mg, Filter Loading	<b>1.4250</b>			<b>0.2990</b>								

**Table A1.5.15 Test 2/5E, Marple Particle Cerium and Fission Product Distributions**

2/5E Particle Size	Cerium		Cesium		Strontium		Ruthenium	
	mg	wt%	mg	wt%	mg	wt%	mg	wt%
35µm and >	0.1063	12.7	0.0000	0.0	0.0008	44.4	0.0000	0.0
21.3µm	0.0735	8.8	0.0000	0.0	0.0000	0.0	0.0000	0.0
14.8µm	0.0711	8.5	0.0000	0.0	0.0000	0.0	0.0000	0.0
9.8µm	0.1385	16.5	0.0002	1.3	0.0000	0.0	0.0000	0.0
6.0µm	0.1397	16.7	0.0003	1.9	0.0000	0.0	0.0000	0.0
3.5µm	0.1604	19.2	0.0011	7.0	0.0002	11.1	0.0000	0.0
1.55µm	0.0992	11.9	0.0057	36.3	0.0000	0.0	0.0000	0.0
0.93µm	0.0247	3.0	0.0039	24.8	0.0000	0.0	0.0004	100.0
0.52µm	0.0208	2.5	0.0040	25.5	0.0000	0.0	0.0000	0.0
Final filter	0.0027	0.3	0.0005	3.2	0.0008	44.4	0.0000	0.0
<b>Sum</b>	<b>0.8369</b>		<b>0.0157</b>		<b>0.0018</b>		<b>0.0004</b>	

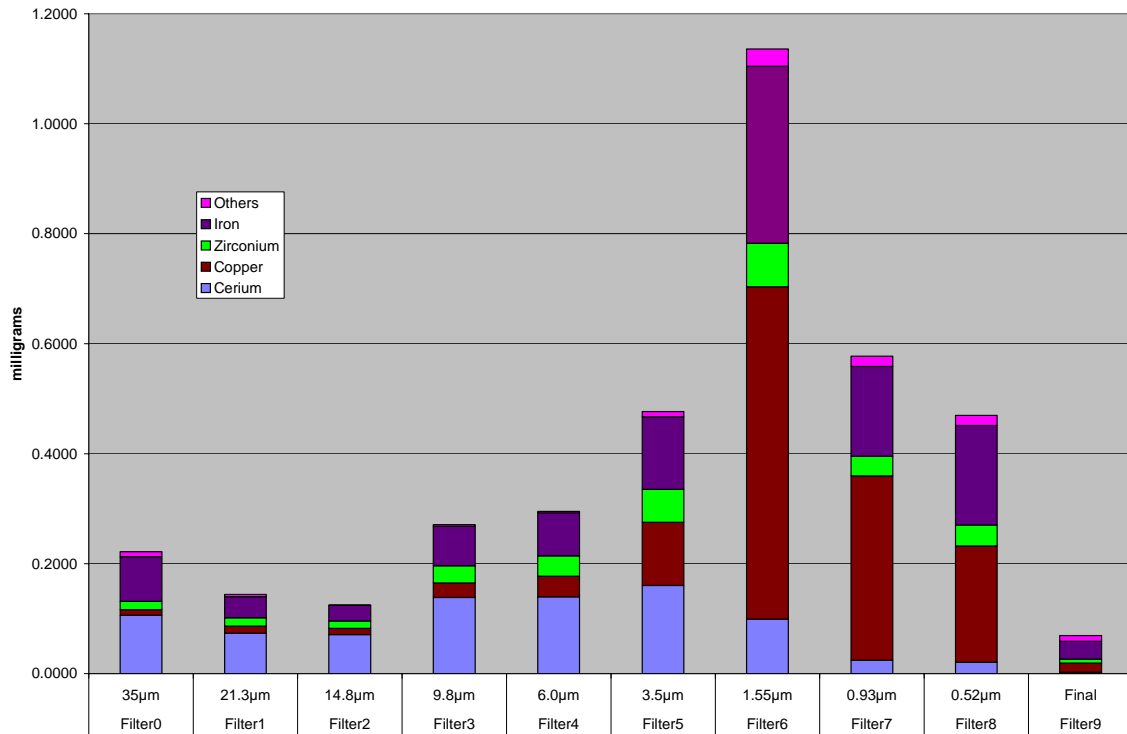


**Figure A1.5.3 Test 2/5E Marple Metals Analysis Distribution, milligrams**

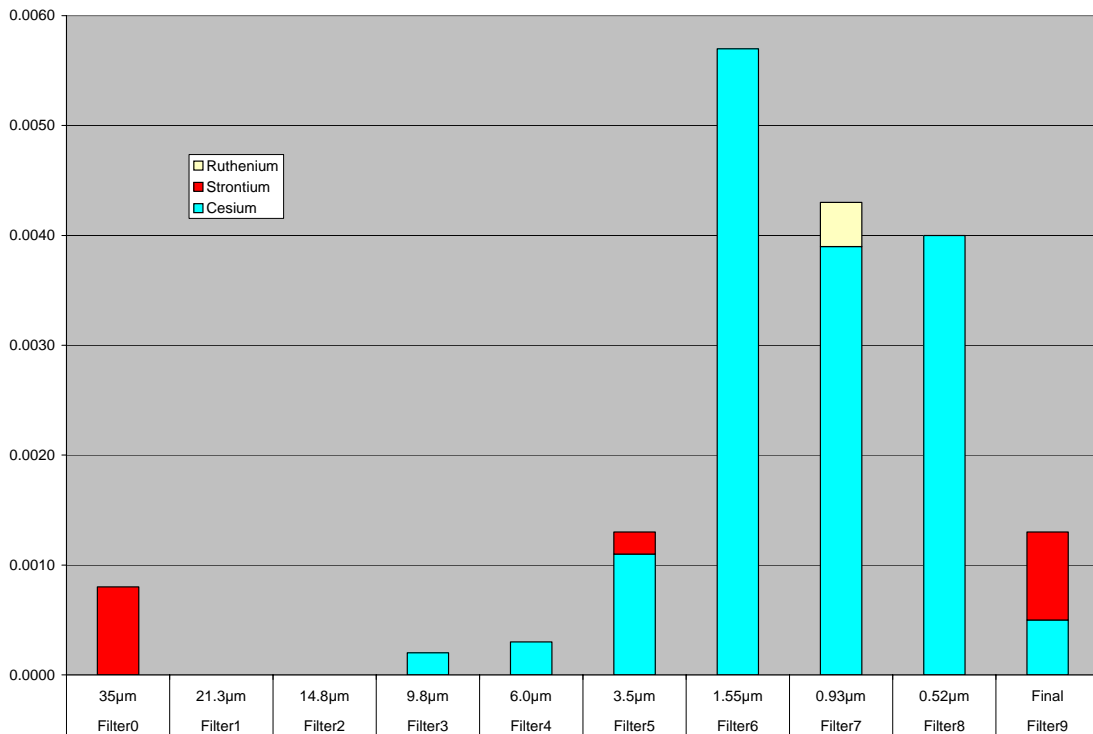


Figure A1.5.4 Test 2/5E Marple Fission Product Dopant Analysis Distribution, milligrams

### Test 2/5E Elemental Analysis of Impact Debris

All impact debris materials on the internal surfaces of the aerosol collection chamber were swept into a small collection pile and removed. The impact fraction sieved debris weights and elemental analysis weight percentages are summarized in Table A1.5.16 and A1.5.17. The analyzed impact debris metal and fission product dopant species elemental analysis results are shown in Figures A1.5.5 and A1.5.6, respectively.

**Table A1.5.16 Test 2/5E, Weight Distribution of Impact Debris**

Sieve Fraction	Weight, g	%
1000 µm	11.5193	77.76
500 µm	1.5836	10.69
250 µm	0.9351	6.31
125 µm	0.5442	3.67
100 µm	0.0600	0.41
74 µm	0.0764	0.52
37 µm	0.0613	0.41
25 µm	0.0065	0.04
<25 µm	0.0271	0.18
<b>Total</b>	<b>14.8135</b>	<b>100.00</b>

**Table A1.5.17 Test 2/5E, Elemental Analysis Wt% of Sieved Impact Debris**

Test 2/5E Sieve Fraction	125 µm	100 µm	74 µm	37 µm	25 µm	<25 µm
Cerium	28.060	31.140	28.200	21.950	25.040	21.450
Iron	26.870	24.570	26.400	27.180	21.730	24.980
Copper	3.452	3.268	3.870	4.878	7.775	5.888
Zirconium	1.287	1.289	1.437	1.642	2.377	1.918
Aluminum	3.894	4.055	4.766	4.938	4.674	5.295
Manganese	0.422	0.406	0.382	0.406	0.312	0.351
Tin	0.045	0.045	0.051	0.074	0.107	0.079
Chromium	0.029	0.027	0.027	0.030	0.026	0.028
Magnesium	0.128	0.142	0.154	0.180	0.172	0.181
Nickel	0.020	0.020	0.020	0.023	0.019	0.022
Titanium	0.457	0.418	0.388	0.448	0.351	0.331
Molybdenum	0.007	0.007	0.007	0.007	0.007	0.007
Strontium	0.004	0.005	0.005	0.008	0.010	0.008
Cesium	0.007	0.008	0.006	0.011	0.016	0.013
Ruthenium	0.000	0.000	0.001	0.002	0.004	0.000
Terbium	0.005	0.006	0.005	0.004	0.005	0.004
Lead	0.003	0.006	0.006	0.011	0.017	0.011
Barium	0.046	0.000	0.000	0.000	0.000	0.000
Hafnium	0.000	0.000	0.000	0.000	0.000	0.000
<b>Total</b>	<b>64.736</b>	<b>65.412</b>	<b>65.725</b>	<b>61.792</b>	<b>62.642</b>	<b>60.566</b>

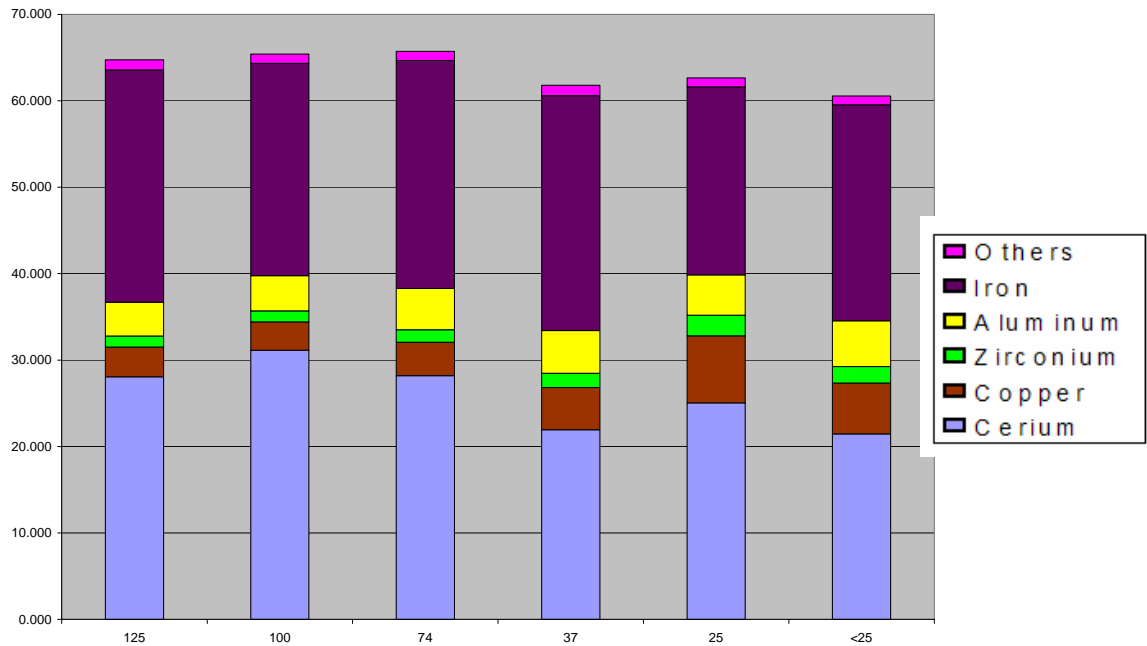


**Figure A1.5.5 Test 2/5E, Weight Percent Distribution of Metals in Impact Sieved Fractions**

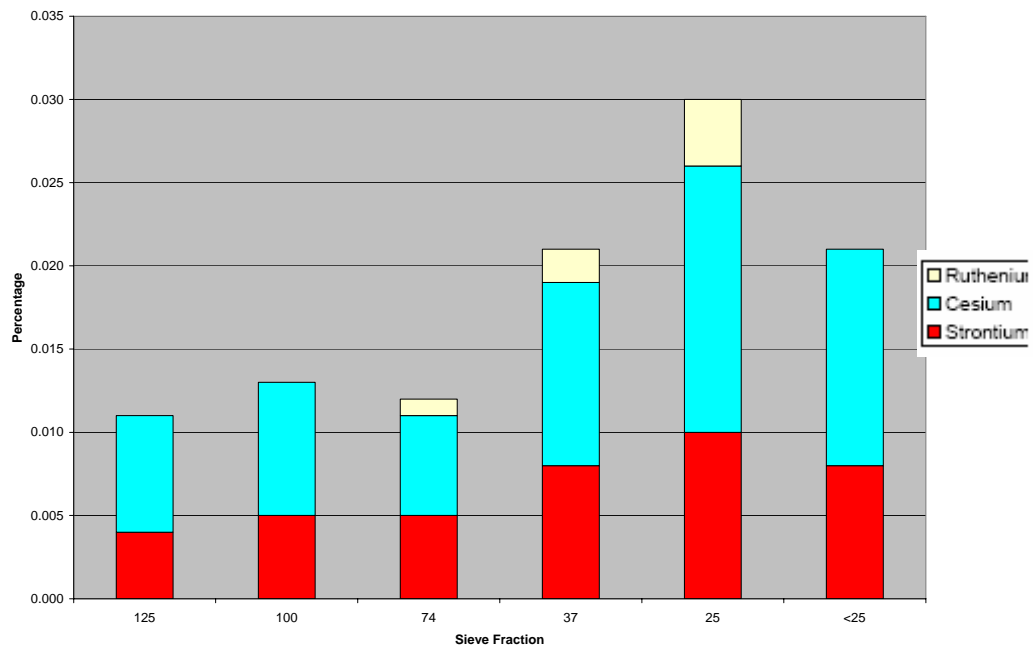


Figure A1.5.6 Test 2/5E, Weight % Distribution of Fission Product Dopants, Sieved Impact Debris

#### A.1.5F Test 2/5F Analyses and Results

There was no collection of impact debris or chemical analyses from test 2/5F.

#### A.1.5G Test 2/5G Analyses and Results

Test 2/5G used a test rodlet with 9 CeO<sub>2</sub> pellets plus 2 fission product dopant disks, on either side of the center pellet. This test used one Marple impactor and one large particle separator. Aerosol sampling time was 30 seconds. The metals analyses from each particulate stage of the Marple impactor used are summarized in Tables A1.5.16 through A1.5.18. The cerium and fission product distributions analyzed on each stage of the Marple impactor, by size, are listed in Table A1.5.19, and shown in Figures A1.5.7 and A1.5.8. No iodine was detected on any of the particle size stages.

**Table A1.5.18 Test 2/5G, Marple Particle Elemental Analyses, Stages 0-3**

2/5G	STAGE 0			STAGE 1			STAGE 2			STAGE 3		
	Particle size 35 µm			Particle size 21.3 µm			Particle size 14.8 µm			Particle size 9.8 µm		
	mg	% detected	% loading	mg	% detected	% loading	mg	% detected	% loading	mg	% detected	% loading
Ce	0.1973	63.5	21.0	0.2336	60.7	31.3	0.1432	60.6	33.0	0.2127	60.7	34.0
Cu	0.0104	3.3	1.1	0.0472	12.3	6.3	0.0243	10.3	5.6	0.0301	8.6	4.8
Zr	0.0222	7.1	2.4	0.0421	10.9	5.6	0.0286	12.1	6.6	0.0459	13.1	7.3
Fe	0.0667	21.5	7.1	0.0579	15.0	7.8	0.0386	16.3	8.9	0.0589	16.8	9.4
Mg	0.0019	0.6	0.2	0.0000	0.0	0.0	0.0000	0.0	0.0	0.0000	0.0	0.0
Cr	0.0055	1.8	0.6	0.0002	0.1	0.0	0.0000	0.0	0.0	0.0000	0.0	0.0
Ni	0.0028	0.9	0.3	0.0003	0.1	0.0	0.0000	0.0	0.0	0.0000	0.0	0.0
Mn	0.0014	0.5	0.1	0.0010	0.3	0.1	0.0005	0.2	0.1	0.0007	0.2	0.1
Sn	0.0009	0.3	0.1	0.0019	0.5	0.3	0.0008	0.3	0.2	0.0016	0.5	0.3
Mo	0.0000	0.0	0.0	0.0000	0.0	0.0	0.0000	0.0	0.0	0.0000	0.0	0.0
Ti	0.0015	0.5	0.2	0.0004	0.1	0.1	0.0000	0.0	0.0	0.0005	0.1	0.1
Hf	0.0000	0.0	0.0	0.0000	0.0	0.0	0.0000	0.0	0.0	0.0000	0.0	0.0
Pb	0.0003	0.1	0.0	0.0000	0.0	0.0	0.0000	0.0	0.0	0.0000	0.0	0.0
Cs	0.0000	0.0	0.0	0.0004	0.1	0.1	0.0002	0.1	0.0	0.0002	0.1	0.0
Sr	0.0000	0.0	0.0	0.0000	0.0	0.0	0.0000	0.0	0.0	0.0000	0.0	0.0
Ru	0.0000	0.0	0.0	0.0000	0.0	0.0	0.0000	0.0	0.0	0.0000	0.0	0.0
mg, Metals Found	0.3109	100.0	33.1	0.3850	100.0	51.5	0.2362	100.0	54.4	0.3506	100.0	56.0
mg, Filter Loading	0.9380			0.7470			0.4340			0.6260		

**Table A1.5.19 Test 2/5G, Marple Particle Elemental Analyses, Stages 4-7**

2/5G	STAGE 4			STAGE 5			STAGE 6			STAGE 7		
	Particle size 6.0 µm			Particle size 3.5 µm			Particle size 1.55 µm			Particle size 0.93 µm		
	mg	% detected	% loading	mg	% detected	% loading	mg	% detected	% loading	mg	% detected	% loading
Ce	0.1647	57.4	26.7	0.1898	32.9	14.6	0.0699	6.5	2.7	0.0250	4.7	1.5
Cu	0.0355	12.4	5.8	0.1798	31.2	13.9	0.6608	61.7	25.9	0.3266	61.0	19.4
Zr	0.0405	14.1	6.6	0.0826	14.3	6.4	0.0726	6.8	2.8	0.0412	7.7	2.4
Fe	0.0422	14.7	6.9	0.1104	19.1	8.5	0.2262	21.1	8.9	0.1235	23.1	7.3
Mg	0.0000	0.0	0.0	0.0000	0.0	0.0	0.0000	0.0	0.0	0.0000	0.0	0.0
Cr	0.0000	0.0	0.0	0.0004	0.1	0.0	0.0014	0.1	0.1	0.0004	0.1	0.0
Ni	0.0000	0.0	0.0	0.0003	0.1	0.0	0.0033	0.3	0.1	0.0004	0.1	0.0
Mn	0.0006	0.2	0.1	0.0022	0.4	0.2	0.0066	0.6	0.3	0.0033	0.6	0.2
Sn	0.0013	0.5	0.2	0.0063	1.1	0.5	0.0166	1.6	0.7	0.0094	1.8	0.6
Mo	0.0000	0.0	0.0	0.0002	0.0	0.0	0.0006	0.1	0.0	0.0003	0.1	0.0
Ti	0.0000	0.0	0.0	0.0025	0.4	0.2	0.0023	0.2	0.1	0.0009	0.2	0.1
Hf	0.0000	0.0	0.0	0.0000	0.0	0.0	0.0000	0.0	0.0	0.0000	0.0	0.0
Pb	0.0000	0.0	0.0	0.0004	0.1	0.0	0.0019	0.2	0.1	0.0008	0.1	0.0
Cs	0.0021	0.7	0.3	0.0015	0.3	0.1	0.0079	0.7	0.3	0.0034	0.6	0.2
Sr	0.0000	0.0	0.0	0.0003	0.1	0.0	0.0000	0.0	0.0	0.0000	0.0	0.0
Ru	0.0000	0.0	0.0	0.0000	0.0	0.0	0.0003	0.0	0.0	0.0002	0.0	0.0
mg, Metals Found	0.2869	100.0	46.6	0.5767	100.0	44.5	1.0704	100.0	42.0	0.5354	100.0	31.8
mg, Filter Loading	0.6160			1.2970			2.5510			1.6840		

**Table A1.5.20 Test 2/5G, Marple Particle Elemental Analyses, Stages 8-9**

2/5G	STAGE 8			STAGE 9								
	Particle size 0.52 µm			Particle size final, >0.5 µm								
	mg	% detected	% loading	mg	% detected	% loading						
Ce	0.0103	6.0	1.6	0.0018	7.8	1.8						
Cu	0.0808	47.3	12.5	0.0089	38.7	9.0						
Zr	0.0193	11.3	3.0	0.0030	13.0	3.0						
Fe	0.0524	30.6	8.1	0.0073	31.7	7.4						
Mg	0.0000	0.0	0.0	0.0009	3.9	0.9						
Cr	0.0000	0.0	0.0	0.0000	0.0	0.0						
Ni	0.0000	0.0	0.0	0.0000	0.0	0.0						
Mn	0.0015	0.9	0.2	0.0002	0.9	0.2						
Sn	0.0047	2.7	0.7	0.0007	3.0	0.7						
Mo	0.0000	0.0	0.0	0.0000	0.0	0.0						
Ti	0.0000	0.0	0.0	0.0000	0.0	0.0						
Hf	0.0000	0.0	0.0	0.0000	0.0	0.0						
Pb	0.0003	0.2	0.0	0.0000	0.0	0.0						
Cs	0.0015	0.9	0.2	0.0002	0.9	0.2						
Sr	0.0002	0.1	0.0	0.0000	0.0	0.0						
Ru	0.0000	0.0	0.0	0.0000	0.0	0.0						
mg, Metals Found	0.1710	100.0	26.5	0.0230	100.0	23.2						
mg, Filter Loading	0.6450			0.0990								

**Table A1.5.21 Test 2/5G, Marple Particle Cerium and Fission Product Distributions**

2/5G	Cerium		Cesium		Strontium		Ruthenium	
	mg	wt%	mg	wt%	mg	wt%	mg	wt%
35µm and >	0.1973	15.8	0.0000	0.0	0.0000	0.0	0.0000	0.0
21.3µm	0.2336	18.7	0.0004	2.3	0.0000	0.0	0.0000	0.0
14.8µm	0.1432	11.5	0.0002	1.1	0.0000	0.0	0.0000	0.0
9.8µm	0.2127	17.0	0.0002	1.1	0.0000	0.0	0.0000	0.0
6.0µm	0.1647	13.2	0.0021	12.1	0.0000	0.0	0.0000	0.0
3.5µm	0.1898	15.2	0.0015	8.6	0.0003	60.0	0.0000	0.0
1.55µm	0.0699	5.6	0.0079	45.4	0.0000	0.0	0.0003	60.0
0.93µm	0.0250	2.0	0.0034	19.5	0.0000	0.0	0.0002	40.0
0.52µm	0.0103	0.8	0.0015	8.6	0.0002	40.0	0.0000	0.0
Final filter	0.0018	0.1	0.0002	1.1	0.0000	0.0	0.0000	0.0
<b>Sum</b>	<b>1.2483</b>		<b>0.0174</b>		<b>0.0005</b>		<b>0.0005</b>	

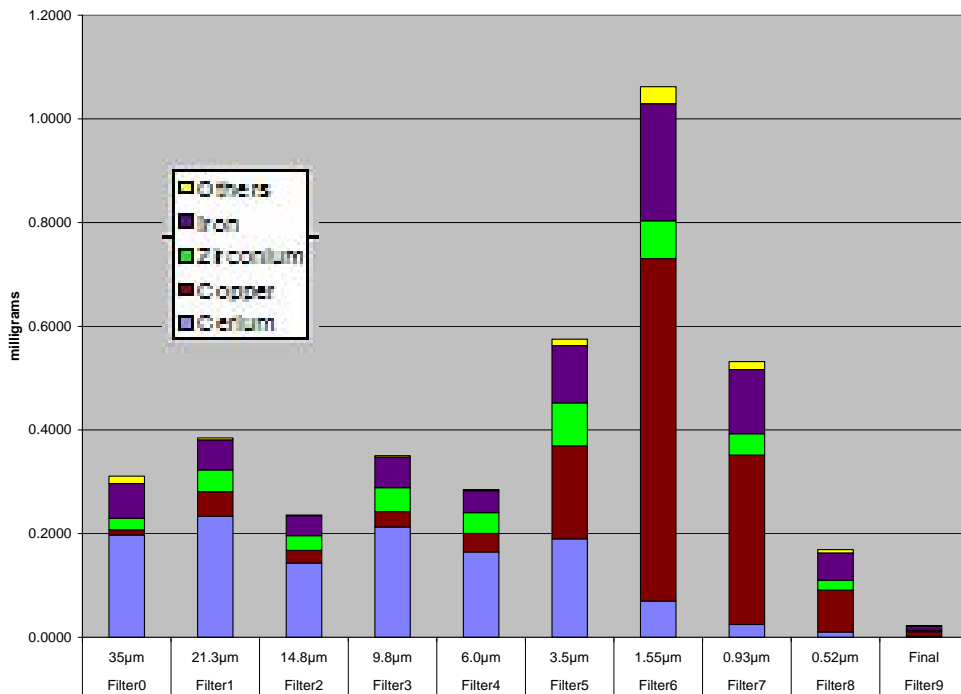


Figure A1.5.7 Test 2/5G Marple Metals Analysis Distribution, milligrams

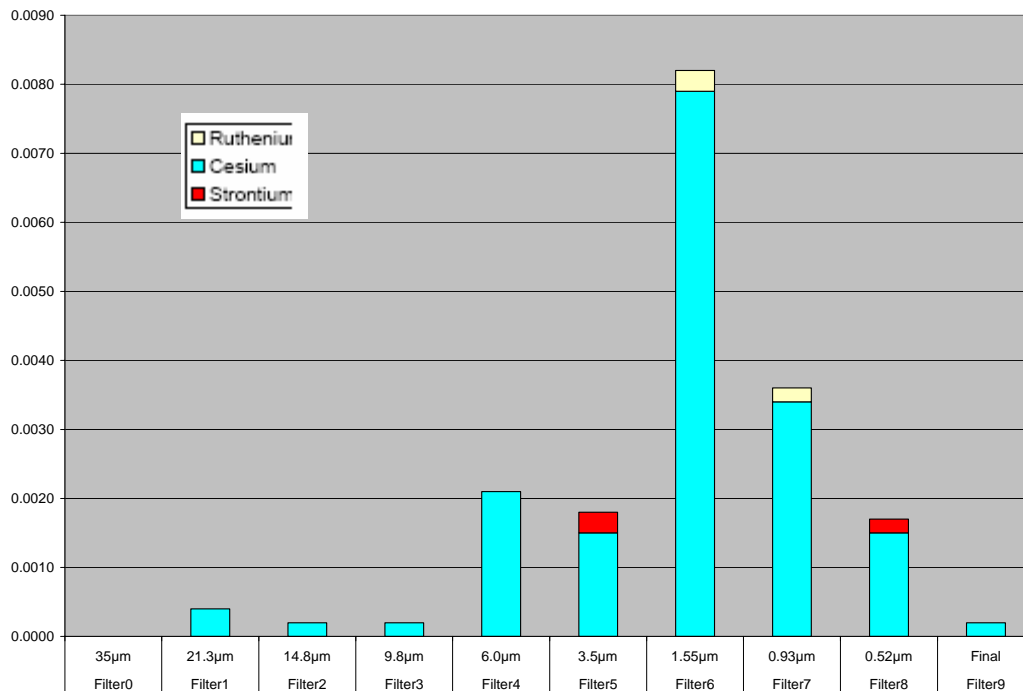


Figure A1.5.8 Test 2/5G Marple Fission Product Dopant Analysis Distribution, milligrams

## Test 2/5G Elemental Analysis of Impact Debris

The impact fraction sieved debris weights and elemental analysis weight percentages are summarized in Tables A1.5.20 and A1.5.21. The analyzed impact debris metal and fission product dopant species elemental analysis results are shown in Figures A1.5.9 and A1.5.10, respectively.

**Table A1.5.22 Test 2/5G, Weight Distribution of Impact Debris**

Sieve Fraction	Weight, g	%
1000 $\mu\text{m}$	4.7005	47.88
500 $\mu\text{m}$	0.6478	6.60
250 $\mu\text{m}$	0.8243	8.40
125 $\mu\text{m}$	0.8832	9.00
100 $\mu\text{m}$	0.2991	3.05
74 $\mu\text{m}$	0.5872	5.98
37 $\mu\text{m}$	1.1430	11.64
25 $\mu\text{m}$	0.0294	0.30
<25 $\mu\text{m}$	0.7035	7.17
<b>Total</b>	<b>9.818</b>	<b>100.00</b>

**Table A1.5.23 Test 2/5G, Elemental Analysis. Wt% of Sieved Impact Debris**

Test 2/5G Sieve Fraction	125 $\mu\text{m}$	100 $\mu\text{m}$	74 $\mu\text{m}$	37 $\mu\text{m}$	25 $\mu\text{m}$	<25 $\mu\text{m}$
Cerium	45.560	43.480	42.830	41.070	42.320	42.500
Iron	17.650	15.070	15.740	14.420	12.270	10.750
Copper	2.932	2.120	2.150	2.094	1.979	2.459
Zirconium	1.306	1.491	1.685	2.476	3.367	4.164
Aluminum	3.696	4.977	6.420	4.792	5.793	4.187
Manganese	0.308	0.279	0.263	0.218	0.210	0.150
Tin	0.027	0.031	0.042	0.065	0.096	0.117
Chromium	0.028	0.029	0.034	0.040	0.050	0.045
Magnesium	0.105	0.146	0.172	0.182	0.196	0.152
Nickel	0.017	0.017	0.018	0.018	0.023	0.018
Titanium	0.507	0.440	0.366	0.309	0.274	0.210
Molybdenum	0.004	0.004	0.004	0.003	0.003	0.002
Strontium *	0.002	0.003	0.004	0.007	0.010	0.011
Cesium *	0.004	0.003	0.004	0.006	0.007	0.011
Ruthenium *	0.000	0.000	0.000	0.000	0.001	0.001
Terbium	0.006	0.007	0.006	0.006	0.007	0.006
Lead	0.002	0.002	0.002	0.002	0.003	0.004
Barium	0.047	0.024	0.080	0.072	0.181	0.030
<b>Total</b>	<b>72.201</b>	<b>68.123</b>	<b>69.820</b>	<b>65.780</b>	<b>66.790</b>	<b>64.817</b>

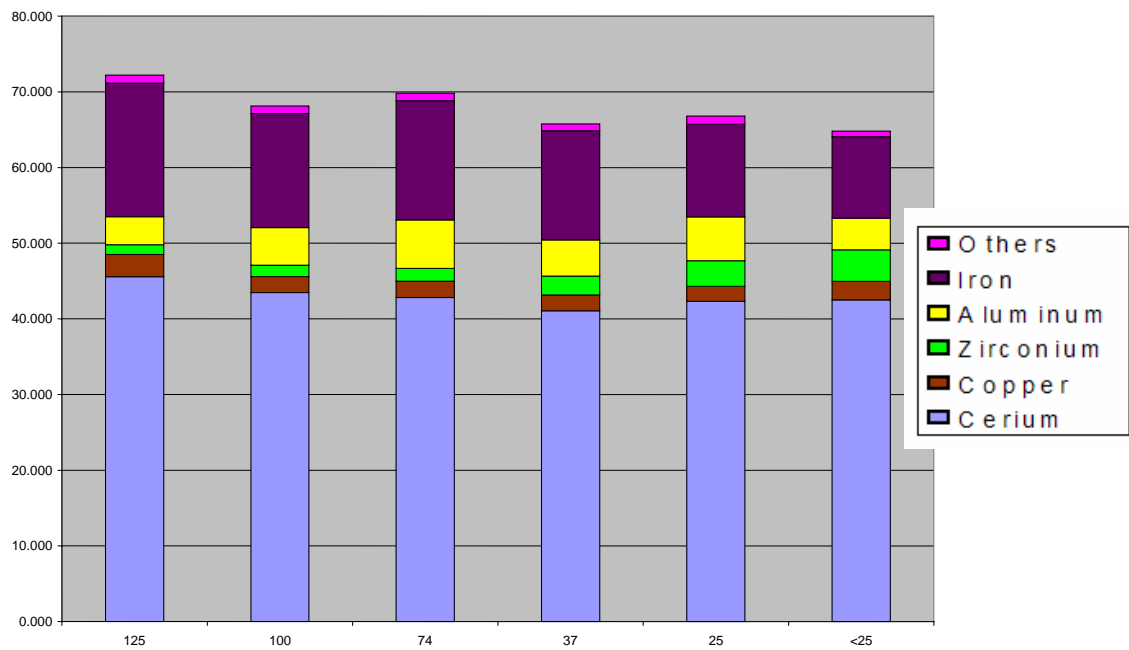


Figure A1.5.9 Test 2/5G, Weight Percent Distribution of Metals in Impact Sieved Fractions

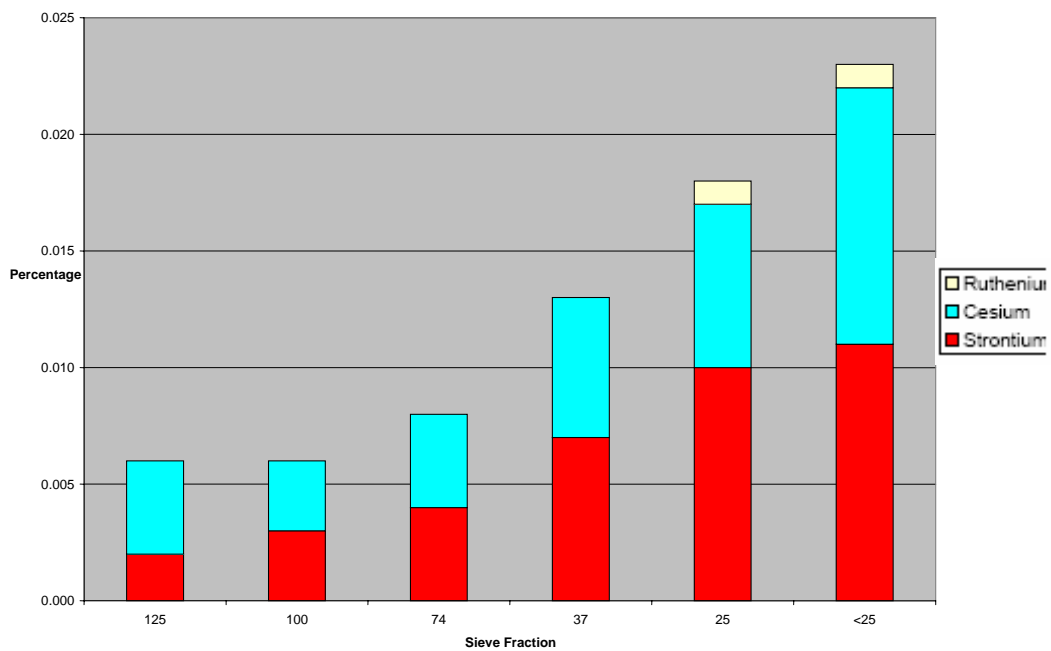


Figure A1.5.10 Test 2/5G, Weight % Distribution of Fission Product Dopants, Sieved Impact Debris

### A.1.6A Test 2/6A Analyses and Results

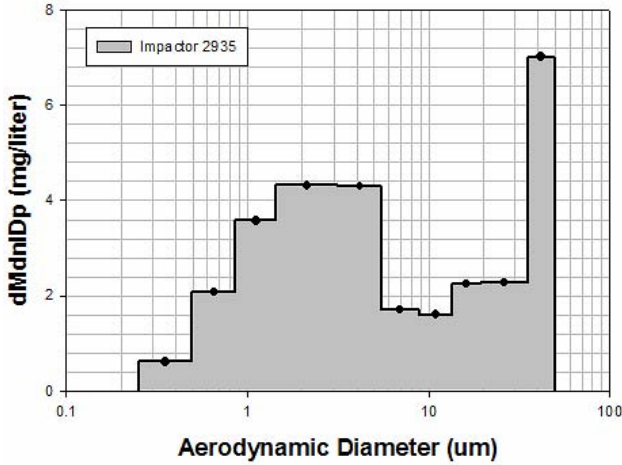


Figure A1.6.1 Test 2/6A Marple 2935 (high) Particle Size Distribution

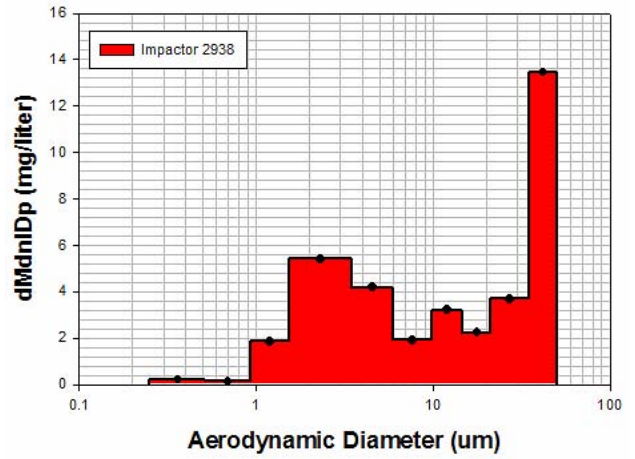


Figure A1.6.2 Test 2/6A Marple 2938 (high) Particle Size Distribution

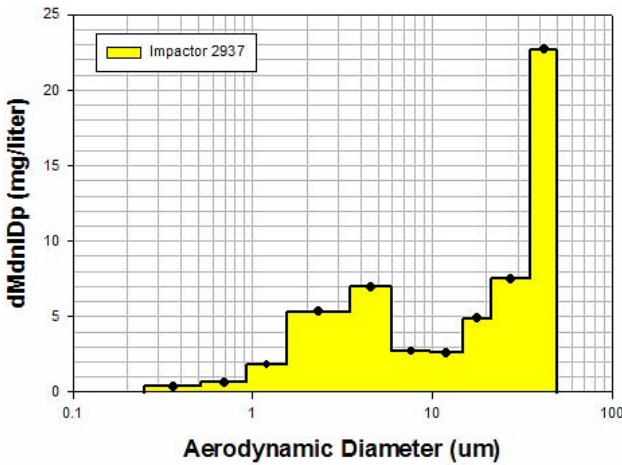


Figure A1.6.3 Test 2/6A Marple 2937 (low) Particle Size Distribution

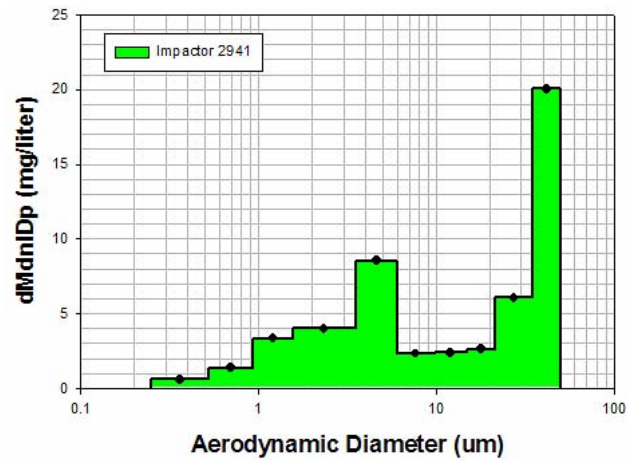


Figure A1.6.4 Test 2/6A Marple 2941 (low) Particle Size Distribution

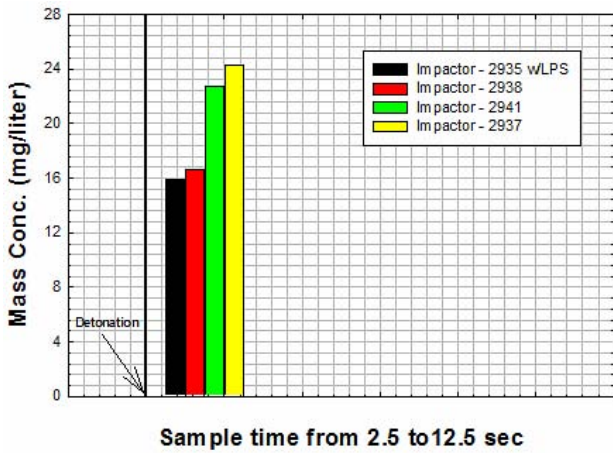


Figure A1.6.5 Test 2/6A Marple Impactors Mass Concentration

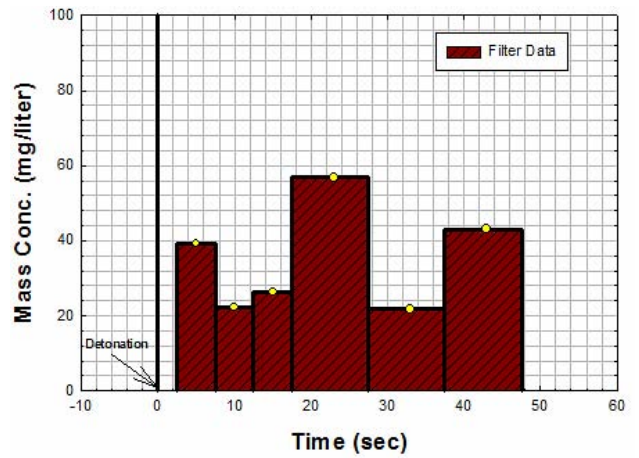


Figure A1.6.6 Test 2/6A Gelman Filters Mass Concentration

**Table A1.6.1 Test 2/6A, Marple #2935 (high) Elemental Analyses, Stages 0-3**

2/6A	STAGE 0			STAGE 1			STAGE 2			STAGE 3		
#2935	Particle size 35 µm			Particle size 21.3 µm			Particle size 14.8 µm			Particle size 9.8 µm		
	mg	% detected	% loading	mg	% detected	% loading	mg	% detected	% loading	mg	% detected	% loading
Ce	0.0115	5.7	2.2	0.0160	12.0	3.6	0.0204	33.7	7.7	0.0182	13.7	8.5
Cu	0.0829	41.0	15.9	0.0402	30.2	9.1	0.0116	19.1	4.4	0.0175	13.2	8.2
Zr	0.0214	10.6	4.1	0.0119	8.9	2.7	0.0060	9.9	2.3	0.0144	10.9	6.7
Fe	0.0780	38.6	15.0	0.0541	40.7	12.3	0.0207	34.2	7.8	0.0356	26.9	16.6
Al	0.0000	0.0	0.0	0.0000	0.0	0.0	0.0000	0.0	0.0	0.0422	31.8	19.7
Mg	0.0000	0.0	0.0	0.0038	2.9	0.9	0.0000	0.0	0.0	0.0022	1.7	1.0
Cr	0.0026	1.3	0.5	0.0027	2.0	0.6	0.0007	1.2	0.3	0.0003	0.2	0.1
Ni	0.0018	0.9	0.3	0.0017	1.3	0.4	0.0005	0.8	0.2	0.0003	0.2	0.1
Mn	0.0011	0.5	0.2	0.0007	0.5	0.2	0.0002	0.3	0.1	0.0004	0.3	0.2
Sn	0.0006	0.3	0.1	0.0000	0.0	0.0	0.0000	0.0	0.0	0.0000	0.0	0.0
Mo	0.0004	0.2	0.1	0.0003	0.2	0.1	0.0000	0.0	0.0	0.0000	0.0	0.0
Ti	0.0008	0.4	0.2	0.0010	0.8	0.2	0.0004	0.7	0.2	0.0013	1.0	0.6
Sb	0.0000	0.0	0.0	0.0000	0.0	0.0	0.0000	0.0	0.0	0.0000	0.0	0.0
Pb	0.0003	0.1	0.1	0.0002	0.2	0.0	0.0000	0.0	0.0	0.0000	0.0	0.0
Cs	0.0008	0.4	0.2	0.0004	0.3	0.1	0.0001	0.2	0.0	0.0001	0.1	0.0
Sr	0.0000	0.0	0.0	0.0000	0.0	0.0	0.0000	0.0	0.0	0.0000	0.0	0.0
Ru	0.0000	0.0	0.0	0.0000	0.0	0.0	0.0000	0.0	0.0	0.0000	0.0	0.0
Eu	0.0000	0.0	0.0	0.0000	0.0	0.0	0.0000	0.0	0.0	0.0000	0.0	0.0
mg, Metals Found	<b>0.2022</b>	<b>100.0</b>	<b>38.9</b>	<b>0.1330</b>	<b>100.0</b>	<b>30.2</b>	<b>0.0606</b>	<b>100.0</b>	<b>22.8</b>	<b>0.1325</b>	<b>100.0</b>	<b>61.9</b>
mg, Filter Loading	<b>0.5200</b>			<b>0.4400</b>			<b>0.2660</b>			<b>0.2140</b>		

**Table A1.6.2 Test 2/6A, Marple #2935 (high) Elemental Analyses, Stages 4-7**

2/6A	STAGE 4			STAGE 5			STAGE 6			STAGE 7		
#2935	Particle size 6.0 µm			Particle size 3.5 µm			Particle size 1.55 µm			Particle size 0.93 µm		
	mg	% detected	% loading	mg	% detected	% loading	mg	% detected	% loading	mg	% detected	% loading
Ce	0.0150	10.3	5.5	0.0176	3.0	2.3	0.0181	4.1	1.6	0.0062	2.3	1.1
Cu	0.0257	17.7	9.4	0.1731	29.3	23.0	0.2034	46.3	17.9	0.0846	31.1	14.4
Zr	0.0161	11.1	5.9	0.0311	5.3	4.1	0.0222	5.1	2.0	0.0090	3.3	1.5
Fe	0.0304	20.9	11.2	0.0714	12.1	9.5	0.0854	19.5	7.5	0.0284	10.4	4.8
Mg	0.0566	38.9	20.8	0.2866	48.5	38.2	0.0968	22.1	8.5	0.1375	50.6	23.5
Al	0.0000	0.0	0.0	0.0043	0.7	0.6	0.0027	0.6	0.2	0.0000	0.0	0.0
Cr	0.0001	0.1	0.0	0.0003	0.1	0.0	0.0002	0.0	0.0	0.0000	0.0	0.0
Ni	0.0000	0.0	0.0	0.0002	0.0	0.0	0.0002	0.0	0.0	0.0000	0.0	0.0
Mn	0.0004	0.3	0.1	0.0010	0.2	0.1	0.0015	0.3	0.1	0.0006	0.2	0.1
Sn	0.0000	0.0	0.0	0.0015	0.3	0.2	0.0034	0.8	0.3	0.0034	1.3	0.6
Mo	0.0000	0.0	0.0	0.0000	0.0	0.0	0.0002	0.0	0.0	0.0000	0.0	0.0
Ti	0.0010	0.7	0.4	0.0014	0.2	0.2	0.0011	0.3	0.1	0.0006	0.2	0.1
Sb	0.0000	0.0	0.0	0.0000	0.0	0.0	0.0001	0.0	0.0	0.0000	0.0	0.0
Pb	0.0000	0.0	0.0	0.0005	0.1	0.1	0.0008	0.2	0.1	0.0003	0.1	0.1
Cs	0.0002	0.1	0.1	0.0013	0.2	0.2	0.0026	0.6	0.2	0.0010	0.4	0.2
Sr	0.0000	0.0	0.0	0.0001	0.0	0.0	0.0000	0.0	0.0	0.0002	0.1	0.0
Ru	0.0000	0.0	0.0	0.0001	0.0	0.0	0.0002	0.0	0.0	0.0000	0.0	0.0
Eu	0.0000	0.0	0.0	0.0000	0.0	0.0	0.0000	0.0	0.0	0.0000	0.0	0.0
mg, Metals Found	<b>0.1455</b>	<b>100.0</b>	<b>53.5</b>	<b>0.5905</b>	<b>100.0</b>	<b>78.6</b>	<b>0.4389</b>	<b>100.0</b>	<b>38.7</b>	<b>0.2718</b>	<b>100.0</b>	<b>46.4</b>
mg, Filter Loading	<b>0.2720</b>			<b>0.7510</b>			<b>1.1350</b>			<b>0.5860</b>		

**Table A1.6.3 Test 2/6A, Marple #2935 (high) Elemental Analyses, Stages 8-9**

2/6A	STAGE 8			STAGE 9								
#2935	Particle size 0.52 µm			Particle size final, >0.5 µm								
	mg	% detected	% loading	mg	% detected	% loading						
Ce	0.0056	3.0	1.5	0.0008	5.4	0.6						
Cu	0.0644	34.8	16.9	0.0107	72.3	7.9						
Zr	0.0089	4.8	2.3	0.0013	8.8	1.0						
Fe	0.0314	17.0	8.2	0.0018	12.2	1.3						
Mg	0.0716	38.7	18.8	0.0000	0.0	0.0						
Al	0.0000	0.0	0.0	0.0000	0.0	0.0						
Cr	0.0000	0.0	0.0	0.0000	0.0	0.0						
Ni	0.0002	0.1	0.1	0.0000	0.0	0.0						
Mn	0.0005	0.3	0.1	0.0000	0.0	0.0						
Sn	0.0004	0.2	0.1	0.0000	0.0	0.0						
Mo	0.0000	0.0	0.0	0.0000	0.0	0.0						
Ti	0.0006	0.3	0.2	0.0000	0.0	0.0						
Sb	0.0000	0.0	0.0	0.0000	0.0	0.0						
Pb	0.0003	0.2	0.1	0.0000	0.0	0.0						
Cs	0.0009	0.5	0.2	0.0002	1.4	0.1						
Sr	0.0000	0.0	0.0	0.0000	0.0	0.0						
Ru	0.0000	0.0	0.0	0.0000	0.0	0.0						
Eu	0.0000	0.0	0.0	0.0000	0.0	0.0						
mg, Metals Found	<b>0.1848</b>	<b>100.0</b>	<b>48.5</b>	<b>0.0148</b>	<b>100.0</b>	<b>11.0</b>						
mg, Filter Loading	<b>0.3810</b>			<b>0.1350</b>								

**Table A1.6.4 Test 2/6A, Marple #2935 Particle Cerium and Fission Product Distributions**

2/6A #2935 high	Cerium		Cesium		Strontium		Ruthenium		Europium	
	mg	wt%	mg	wt%	mg	wt%	mg	wt%	mg	wt%
35µm and >	0.0115	8.9	0.0008	10.5	0.0000	0.0	0.0000	0.0	0.0000	0.0
21.3µm	0.0160	12.4	0.0004	5.3	0.0000	0.0	0.0000	0.0	0.0000	0.0
14.8µm	0.0204	15.8	0.0001	1.3	0.0000	0.0	0.0000	0.0	0.0000	0.0
9.8µm	0.0182	14.1	0.0001	1.3	0.0000	0.0	0.0000	0.0	0.0000	0.0
6.0µm	0.0150	11.6	0.0002	2.6	0.0000	0.0	0.0000	0.0	0.0000	0.0
3.5µm	0.0176	13.6	0.0013	17.1	0.0001	33.3	0.0001	33.3	0.0000	0.0
1.55µm	0.0181	14.0	0.0026	34.2	0.0000	0.0	0.0002	66.7	0.0000	0.0
0.93µm	0.0062	4.8	0.0010	13.2	0.0002	66.7	0.0000	0.0	0.0000	0.0
0.52µm	0.0056	4.3	0.0009	11.8	0.0000	0.0	0.0000	0.0	0.0000	0.0
Final filter	0.0008	0.6	0.0002	2.6	0.0000	0.0	0.0000	0.0		
<b>Sum</b>	<b>0.1294</b>		<b>0.0076</b>		<b>0.0003</b>		<b>0.0003</b>		<b>0.0000</b>	

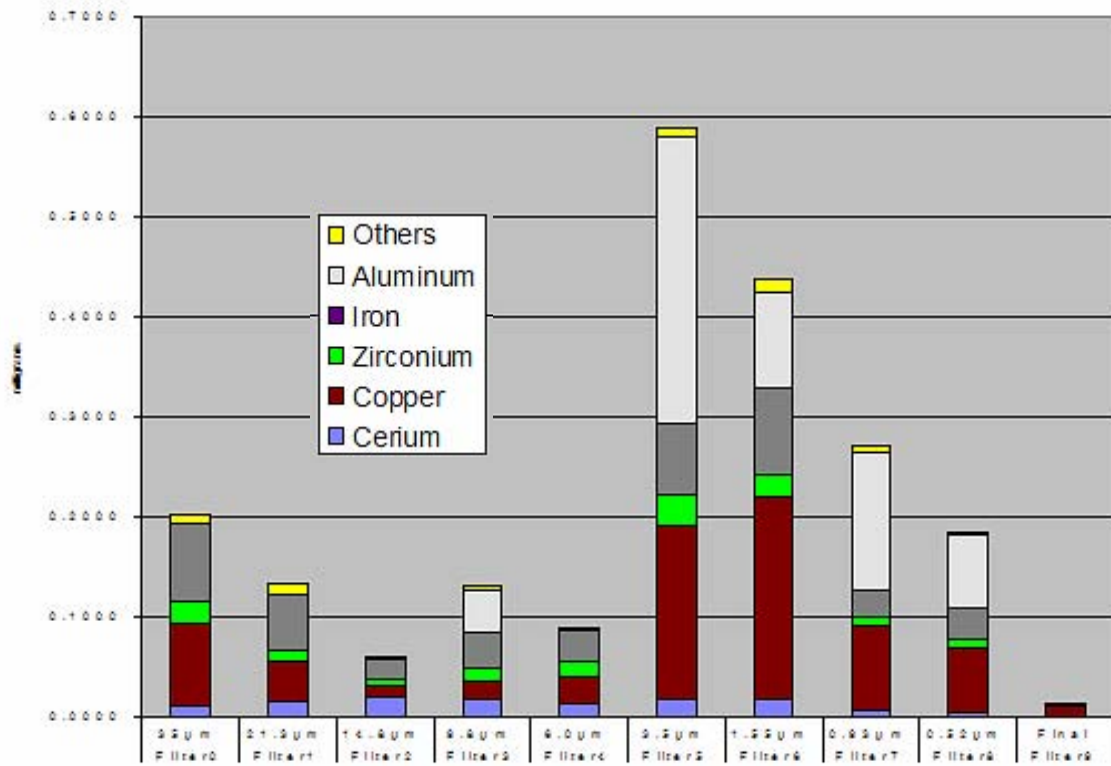


Figure A1.6.7 Test 2/6A, Marple #2935 (high) Metals Analysis Distribution, milligrams

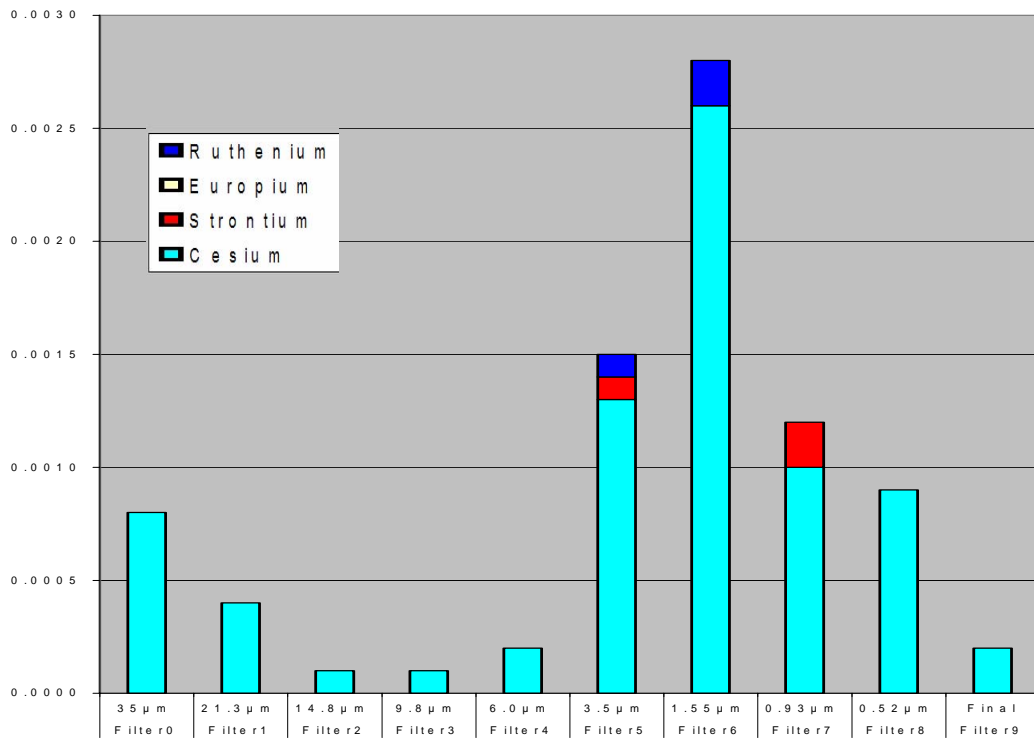


Figure A1.6.8 Test 2/6A, Marple #2935 (high) Fission Product Dopant Analysis Distrib., mg

**Table A1.6.5 Test 2/6A, Marple #2937 (low) Elemental Analyses, Stages 0-3**

2/6A	STAGE 0			STAGE 1			STAGE 2			STAGE 3		
#2937	Particle size 35 µm			Particle size 21.3 µm			Particle size 14.8 µm			Particle size 9.8 µm		
	mg	% detect	% loading	mg	% detect	% loading	mg	% detect	% loading	mg	% detect	% loading
Ce	0.1136	17.0	5.2	0.0082	2.2	0.7	0.0114	8.3	2.0	0.0231	17.5	6.6
Cu	0.1191	17.8	5.5	0.0650	17.1	5.3	0.0242	17.6	4.2	0.0250	19.0	7.1
Zr	0.0489	7.3	2.2	0.0187	4.9	1.5	0.0096	7.0	1.7	0.0182	13.8	5.2
Fe	0.2836	42.5	13.0	0.1640	43.1	13.5	0.0694	50.4	11.9	0.0581	44.1	16.6
Al	0.0343	5.1	1.6	0.0780	20.5	6.4	0.0069	5.0	1.2	0.0000	0.0	0.0
Mg	0.0005	0.1	0.0	0.0017	0.4	0.1	0.0006	0.4	0.1	0.0000	0.0	0.0
Cr	0.0371	5.6	1.7	0.0252	6.6	2.1	0.0086	6.2	1.5	0.0035	2.7	1.0
Ni	0.0165	2.5	0.8	0.0116	3.0	1.0	0.0038	2.8	0.7	0.0016	1.2	0.5
Mn	0.0038	0.6	0.2	0.0024	0.6	0.2	0.0009	0.7	0.2	0.0006	0.5	0.2
Sn	0.0019	0.3	0.1	0.0005	0.1	0.0	0.0000	0.0	0.0	0.0000	0.0	0.0
Mo	0.0049	0.7	0.2	0.0033	0.9	0.3	0.0011	0.8	0.2	0.0004	0.3	0.1
Ti	0.0020	0.3	0.1	0.0012	0.3	0.1	0.0009	0.7	0.2	0.0009	0.7	0.3
Li	0.0002	0.0	0.0	0.0002	0.1	0.0	0.0000	0.0	0.0	0.0000	0.0	0.0
Sb	0.0000	0.0	0.0	0.0000	0.0	0.0	0.0000	0.0	0.0	0.0000	0.0	0.0
Pb	0.0004	0.1	0.0	0.0002	0.1	0.0	0.0001	0.1	0.0	0.0002	0.2	0.1
Cs	0.0011	0.2	0.1	0.0007	0.2	0.1	0.0002	0.1	0.0	0.0002	0.2	0.1
Sr	0.0000	0.0	0.0	0.0000	0.0	0.0	0.0000	0.0	0.0	0.0000	0.0	0.0
Ru	0.0000	0.0	0.0	0.0000	0.0	0.0	0.0000	0.0	0.0	0.0000	0.0	0.0
Eu	0.0000	0.0	0.0	0.0000	0.0	0.0	0.0000	0.0	0.0	0.0000	0.0	0.0
mg, Metals Found	<b>0.6679</b>	<b>100.0</b>	<b>30.6</b>	<b>0.3809</b>	<b>100.0</b>	<b>31.3</b>	<b>0.1377</b>	<b>100.0</b>	<b>23.7</b>	<b>0.1318</b>	<b>100.0</b>	<b>37.5</b>
mg, Filter Loading	<b>2.184</b>			<b>1.2160</b>			<b>0.5810</b>			<b>0.3510</b>		

**Table A1.6.6 Test 2/6A, Marple #2937 (low) Elemental Analyses, Stages 4-7**

2/6A	STAGE 4			STAGE 5			STAGE 6			STAGE 7		
#2937	Particle size 6.0 µm			Particle size 3.5 µm			Particle size 1.55 µm			Particle size 0.93 µm		
	mg	% detect	% loading	mg	% detect	% loading	mg	% detect	% loading	mg	% detect	% loading
Ce	0.0085	7.0	2.0	0.0358	6.4	2.9	0.0134	2.4	3.2			
Cu	0.0335	27.4	7.7	0.2901	51.5	23.7	0.2323	41.4	56.0	0.0061	3.5	2.0
Zr	0.0215	17.6	5.0	0.0424	7.5	3.5	0.0274	4.9	6.6	0.0630	36.2	20.8
Fe	0.0508	41.6	11.7	0.1432	25.4	11.7	0.0942	16.8	22.7	0.0078	4.5	2.6
Mg	0.0000	0.0	0.0	0.0342	6.1	2.8	0.1727	30.8	41.6	0.0264	15.2	8.7
Al	0.0000	0.0	0.0	0.0013	0.2	0.1	0.0060	1.1	1.4	0.0654	37.6	21.6
Cr	0.0033	2.7	0.8	0.0032	0.6	0.3	0.0016	0.3	0.4	0.0015	0.9	0.5
Ni	0.0016	1.3	0.4	0.0015	0.3	0.1	0.0007	0.1	0.2	0.0006	0.3	0.2
Mn	0.0006	0.5	0.1	0.0018	0.3	0.1	0.0017	0.3	0.4	0.0002	0.1	0.1
Sn	0.0000	0.0	0.0	0.0036	0.6	0.3	0.0042	0.7	1.0	0.0004	0.2	0.1
Mo	0.0004	0.3	0.1	0.0005	0.1	0.0	0.0004	0.1	0.1	0.0003	0.2	0.1
Ti	0.0013	1.1	0.3	0.0023	0.4	0.2	0.0016	0.3	0.4	0.0000	0.0	0.0
Li	0.0000	0.0	0.0	0.0000	0.0	0.0	0.0000	0.0	0.0	0.0008	0.5	0.3
Sb	0.0000	0.0	0.0	0.0002	0.0	0.0	0.0002	0.0	0.0	0.0000	0.0	0.0
Pb	0.0002	0.2	0.0	0.0007	0.1	0.1	0.0008	0.1	0.2	0.0000	0.0	0.0
Cs	0.0003	0.2	0.1	0.0024	0.4	0.2	0.0032	0.6	0.8	0.0009	0.5	0.3
Sr	0.0001	0.1	0.0	0.0000	0.0	0.0	0.0000	0.0	0.0	0.0004	0.2	0.1
Ru	0.0000	0.0	0.0	0.0002	0.0	0.0	0.0001	0.0	0.0	0.0000	0.0	0.0
Eu	0.0000	0.0	0.0	0.0000	0.0	0.0	0.0000	0.0	0.0	0.0000	0.0	0.0
mg, Metals Found	<b>0.1221</b>	<b>100.0</b>	<b>28.1</b>	<b>0.5634</b>	<b>100.0</b>	<b>46.0</b>	<b>0.5605</b>	<b>100.0</b>	<b>135.1</b>	<b>0.1741</b>	<b>100.0</b>	<b>57.5</b>
mg, Filter Loading	<b>0.4340</b>			<b>1.2240</b>			<b>0.4150</b>			<b>0.3030</b>		

**Table A1.6.7 Test 2/6A, Marple #2937 (low) Elemental Analyses, Stages 8-9**

2/6A #2937	STAGE 8			STAGE 9								
	Particle size 0.52 µm			Particle size final, >0.5 µm								
	mg	% detect	% loading	mg	% detect	% loading						
Ce	0.0028	3.0	2.3	0.0014	4.0	1.5						
Cu	0.0304	32.5	24.7	0.0167	47.7	18.2						
Zr	0.0047	5.0	3.8	0.0025	7.1	2.7						
Fe	0.0129	13.8	10.5	0.0128	36.6	13.9						
Mg	0.0369	39.5	30.0	0.0000	0.0	0.0						
Al	0.0038	4.1	3.1	0.0000	0.0	0.0						
Cr	0.0002	0.2	0.2	0.0005	1.4	0.5						
Ni	0.0000	0.0	0.0	0.0002	0.6	0.2						
Mn	0.0002	0.2	0.2	0.0002	0.6	0.2						
Sn	0.0000	0.0	0.0	0.0000	0.0	0.0						
Mo	0.0000	0.0	0.0	0.0000	0.0	0.0						
Ti	0.0007	0.7	0.6	0.0003	0.9	0.3						
Sb	0.0000	0.0	0.0	0.0000	0.0	0.0						
Li	0.0000	0.0	0.0	0.0000	0.0	0.0						
Pb	0.0002	0.2	0.2	0.0001	0.3	0.1						
Cs	0.0005	0.5	0.4	0.0003	0.9	0.3						
Sr	0.0002	0.2	0.2	0.0000	0.0	0.0						
Ru	0.0000	0.0	0.0	0.0000	0.0	0.0						
Eu	0.0000	0.0	0.0	0.0000	0.0	0.0						
mg, Metals Found	<b>0.0935</b>	<b>100.0</b>	<b>76.0</b>	<b>0.0350</b>	<b>100.0</b>	<b>38.0</b>						
mg, Filter Loading	<b>0.1230</b>			<b>0.0920</b>								

**Table A1.6.8 Test 2/6A, Marple #2937 Particle Cerium and Fission Product Distributions**

2/6A #2937 low	Cerium		Cesium		Strontium		Ruthenium		Europium	
	mg	wt%	mg	wt%	mg	wt%	mg	wt%	mg	wt%
35µm and >	0.1136	50.6	0.0011	11.2	0.0000	0.0	0.0000	0.0	0.0000	0.0
21.3µm	0.0082	3.7	0.0007	7.1	0.0000	0.0	0.0000	0.0	0.0000	0.0
14.8µm	0.0114	5.1	0.0002	2.0	0.0000	0.0	0.0000	0.0	0.0000	0.0
9.8µm	0.0231	10.3	0.0002	2.0	0.0000	0.0	0.0000	0.0	0.0000	0.0
6.0µm	0.0085	3.8	0.0003	3.1	0.0001	14.3	0.0000	0.0	0.0000	0.0
3.5µm	0.0358	16.0	0.0024	24.5	0.0000	0.0	0.0002	66.7	0.0000	0.0
1.55µm	0.0134	6.0	0.0032	32.7	0.0000	0.0	0.0001	33.3	0.0000	0.0
0.93µm	0.0061	2.7	0.0009	9.2	0.0004	57.1	0.0000	0.0	0.0000	0.0
0.52µm	0.0028	1.2	0.0005	5.1	0.0002	28.6	0.0000	0.0	0.0000	0.0
Final filter	0.0014	0.6	0.0003	3.1	0.0000	0.0	0.0000	0.0	0.0000	0.0
<b>Sum</b>	<b>0.2243</b>		<b>0.0098</b>		<b>0.0007</b>		<b>0.0003</b>		<b>0.0000</b>	

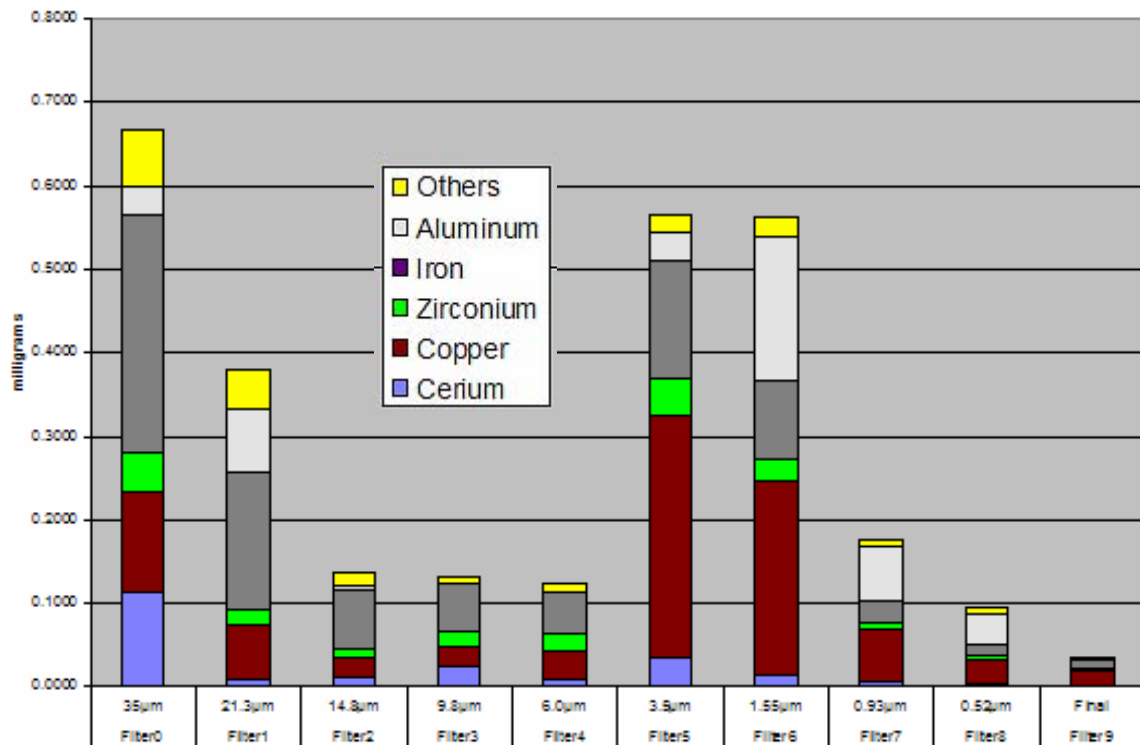


Figure A1.6.9 Test 2/6A, Marple #2937 (low) Metals Analysis Distribution, milligrams

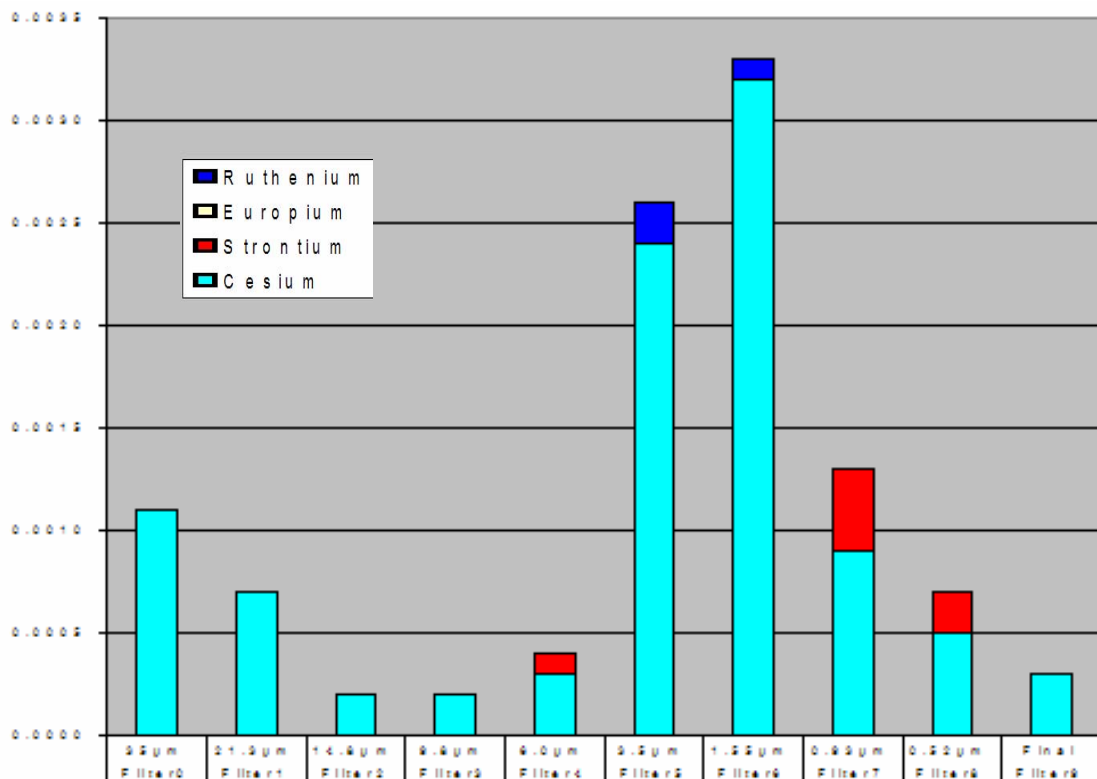


Figure A1.6.10 Test 2/6A, Marple #2937 (low) Fission Product Dopant Analysis Distrib, mg

**Table A1.6.9 Test 2/6A, Marple #2941 (low) Elemental Analyses, Stages 0-3**

2/6A	STAGE 0			STAGE 1			STAGE 2			STAGE 3		
#2941	Particle size 35 µm			Particle size 21.3 µm			Particle size 14.8 µm			Particle size 9.8 µm		
	mg	% detect	% loading	mg	% detect	% loading	mg	% detect	% loading	mg	% detect	% loading
Ce	0.0556	13.3	2.8	0.1082	30.9	10.6	0.0684	40.3	21.1	0.0643	39.3	19.3
Cu	0.1083	26.0	5.4	0.0643	18.4	6.3	0.0242	14.3	7.5	0.0242	14.8	7.2
Zr	0.0451	10.8	2.3	0.0243	6.9	2.4	0.0133	7.8	4.1	0.0196	12.0	5.9
Fe	0.1906	45.7	9.5	0.1379	39.4	13.5	0.0572	33.7	17.7	0.0518	31.6	15.5
Al	0.0000	0.0	0.0	0.0000	0.0	0.0	0.0000	0.0	0.0	0.0000	0.0	0.0
Mg	0.0000	0.0	0.0	0.0000	0.0	0.0	0.0000	0.0	0.0	0.0000	0.0	0.0
Cr	0.0065	1.6	0.3	0.0068	1.9	0.7	0.0031	1.8	1.0	0.0013	0.8	0.4
Ni	0.0036	0.9	0.2	0.0039	1.1	0.4	0.0016	0.9	0.5	0.0008	0.5	0.2
Mn	0.0021	0.5	0.1	0.0016	0.5	0.2	0.0006	0.4	0.2	0.0005	0.3	0.1
Sn	0.0016	0.4	0.1	0.0004	0.1	0.0	0.0000	0.0	0.0	0.0000	0.0	0.0
Mo	0.0006	0.1	0.0	0.0006	0.2	0.1	0.0003	0.2	0.1	0.0001	0.1	0.0
Ti	0.0018	0.4	0.1	0.0011	0.3	0.1	0.0009	0.5	0.3	0.0009	0.5	0.3
Li	0.0000	0.0	0.0	0.0000	0.0	0.0	0.0000	0.0	0.0	0.0000	0.0	0.0
Sb	0.0000	0.0	0.0	0.0000	0.0	0.0	0.0000	0.0	0.0	0.0000	0.0	0.0
Pb	0.0003	0.1	0.0	0.0002	0.1	0.0	0.0000	0.0	0.0	0.0001	0.1	0.0
Cs	0.0009	0.2	0.0	0.0005	0.1	0.0	0.0002	0.1	0.1	0.0002	0.1	0.1
Sr	0.0000	0.0	0.0	0.0000	0.0	0.0	0.0000	0.0	0.0	0.0000	0.0	0.0
Ru	0.0000	0.0	0.0	0.0000	0.0	0.0	0.0000	0.0	0.0	0.0000	0.0	0.0
Eu	0.0000	0.0	0.0	0.0000	0.0	0.0	0.0000	0.0	0.0	0.0000	0.0	0.0
mg, Metals Found	<b>0.4170</b>	<b>100.0</b>	<b>20.8</b>	<b>0.3498</b>	<b>100.0</b>	<b>34.3</b>	<b>0.1698</b>	<b>100.0</b>	<b>52.4</b>	<b>0.1638</b>	<b>100.0</b>	<b>49.0</b>
mg, Filter Loading	<b>2.0020</b>			<b>1.0210</b>			<b>0.3240</b>			<b>0.3340</b>		

**Table A1.6.10 Test 2/6A, Marple #2941 (low) Elemental Analyses, Stages 4-7**

2/6A	STAGE 4			STAGE 5			STAGE 6			STAGE 7		
#2941	Particle size 6.0 µm			Particle size 3.5 µm			Particle size 1.55 µm			Particle size 0.93 µm		
	mg	% detect	% loading	mg	% detect	% loading	mg	% detect	% loading	mg	% detect	% loading
Ce	0.0174	14.9	4.5	0.0628	10.0	4.0	0.0183	6.0	1.7	0.0120	6.0	2.1
Cu	0.0304	26.1	7.9	0.3564	56.8	22.8	0.1833	59.9	16.7	0.1169	58.3	20.3
Zr	0.0198	17.0	5.1	0.0477	7.6	3.1	0.0191	6.2	1.7	0.0131	6.5	2.3
Fe	0.0452	38.8	11.7	0.1426	22.7	9.1	0.0754	24.6	6.9	0.0523	26.1	9.1
Mg	0.0000	0.0	0.0	0.0000	0.0	0.0	0.0000	0.0	0.0	0.0000	0.0	0.0
Al	0.0000	0.0	0.0	0.0000	0.0	0.0	0.0000	0.0	0.0	0.0000	0.0	0.0
Cr	0.0012	1.0	0.3	0.0014	0.2	0.1	0.0005	0.2	0.0	0.0003	0.1	0.1
Ni	0.0009	0.8	0.2	0.0014	0.2	0.1	0.0006	0.2	0.1	0.0003	0.1	0.1
Mn	0.0005	0.4	0.1	0.0022	0.4	0.1	0.0012	0.4	0.1	0.0008	0.4	0.1
Sn	0.0000	0.0	0.0	0.0050	0.8	0.3	0.0031	1.0	0.3	0.0018	0.9	0.3
Mo	0.0000	0.0	0.0	0.0003	0.0	0.0	0.0002	0.1	0.0	0.0001	0.0	0.0
Ti	0.0008	0.7	0.2	0.0026	0.4	0.2	0.0008	0.3	0.1	0.0008	0.4	0.1
Li	0.0000	0.0	0.0	0.0000	0.0	0.0	0.0000	0.0	0.0	0.0000	0.0	0.0
Sb	0.0000	0.0	0.0	0.0002	0.0	0.0	0.0002	0.1	0.0	0.0000	0.0	0.0
Pb	0.0000	0.0	0.0	0.0009	0.1	0.1	0.0007	0.2	0.1	0.0004	0.2	0.1
Cs	0.0002	0.2	0.1	0.0030	0.5	0.2	0.0026	0.8	0.2	0.0017	0.8	0.3
Sr	0.0000	0.0	0.0	0.0000	0.0	0.0	0.0000	0.0	0.0	0.0000	0.0	0.0
Ru	0.0000	0.0	0.0	0.0004	0.1	0.0	0.0000	0.0	0.0	0.0000	0.0	0.0
Eu	0.0000	0.0	0.0	0.0001	0.0	0.0	0.0000	0.0	0.0	0.0000	0.0	0.0
mg, Metals Found	<b>0.1164</b>	<b>100.0</b>	<b>30.2</b>	<b>0.6270</b>	<b>100.0</b>	<b>40.2</b>	<b>0.3060</b>	<b>100.0</b>	<b>27.9</b>	<b>0.2005</b>	<b>100.0</b>	<b>34.9</b>
mg, Filter Loading	<b>0.3860</b>			<b>1.5600</b>			<b>1.0980</b>			<b>0.5750</b>		

**Table A1.6.11 Test 2/6A, Marple #2941 (low) Elemental Analyses, Stages 8-9**

<b>2/6A</b>	<b>STAGE 8</b>			<b>STAGE 9</b>								
<b>#2941</b>	Particle size 0.52 µm			Particle size final, >0.5 µm								
	mg	% detect	% loading	mg	% detect	% loading						
Ce	0.0038	6.1	1.4	0.0017	6.4	1.2						
Cu	0.0331	53.0	12.5	0.0102	38.6	7.2						
Zr	0.0055	8.8	2.1	0.0028	10.6	2.0						
Fe	0.0180	28.8	6.8	0.0106	40.2	7.5						
Mg	0.0000	0.0	0.0	0.0000	0.0	0.0						
Al	0.0000	0.0	0.0	0.0000	0.0	0.0						
Cr	0.0001	0.2	0.0	0.0000	0.0	0.0						
Ni	0.0003	0.5	0.1	0.0001	0.4	0.1						
Mn	0.0003	0.5	0.1	0.0000	0.0	0.0						
Sn	0.0000	0.0	0.0	0.0000	0.0	0.0						
Mo	0.0000	0.0	0.0	0.0000	0.0	0.0						
Ti	0.0005	0.8	0.2	0.0007	2.7	0.5						
Sb	0.0000	0.0	0.0	0.0000	0.0	0.0						
Li	0.0000	0.0	0.0	0.0000	0.0	0.0						
Pb	0.0002	0.3	0.1	0.0000	0.0	0.0						
Cs	0.0006	1.0	0.2	0.0003	1.1	0.2						
Sr	0.0000	0.0	0.0	0.0000	0.0	0.0						
Ru	0.0000	0.0	0.0	0.0000	0.0	0.0						
Eu	0.0000	0.0	0.0	0.0000	0.0	0.0						
mg, Metals Found	<b>0.0624</b>	<b>100.0</b>	<b>23.5</b>	<b>0.0264</b>	<b>100.0</b>	<b>18.6</b>						
mg, Filter Loading	<b>0.2650</b>			<b>0.1420</b>								

**Table A1.6.12 Test 2/6A, Marple #2941 Particle Cerium and Fission Product Distributions**

<b>2/6A #2941 low</b>	<b>Cerium</b>		<b>Cesium</b>		<b>Strontium</b>		<b>Ruthenium</b>		<b>Europium</b>	
<b>Particle Size</b>	mg	wt%	mg	wt%	mg	wt%	mg	wt%	mg	wt%
35µm and >	0.0556	13.5	0.0009	8.8	0.0000	0.0	0.0000	0.0	0.0000	0.0
21.3µm	0.1082	26.2	0.0005	4.9	0.0000	0.0	0.0000	0.0	0.0000	0.0
14.8µm	0.0684	16.6	0.0002	2.0	0.0000	0.0	0.0000	0.0	0.0000	0.0
9.8µm	0.0643	15.6	0.0002	2.0	0.0000	0.0	0.0000	0.0	0.0000	0.0
6.0µm	0.0174	4.2	0.0002	2.0	0.0000	0.0	0.0000	0.0	0.0000	0.0
3.5µm	0.0628	15.2	0.0030	29.4	0.0000	0.0	0.0004	100.0	0.0001	100.0
1.55µm	0.0183	4.4	0.0026	25.5	0.0000	0.0	0.0000	0.0	0.0000	0.0
0.93µm	0.0120	2.9	0.0017	16.7	0.0000	0.0	0.0000	0.0	0.0000	0.0
0.52µm	0.0038	0.9	0.0006	5.9	0.0000	0.0	0.0000	0.0	0.0000	0.0
Final filter	0.0017	0.4	0.0003	2.9	0.0000	0.0	0.0000	0.0	0.0000	0.0
<b>Sum</b>	<b>0.4125</b>		<b>0.0102</b>		<b>0.0000</b>		<b>0.0004</b>		<b>0.0001</b>	

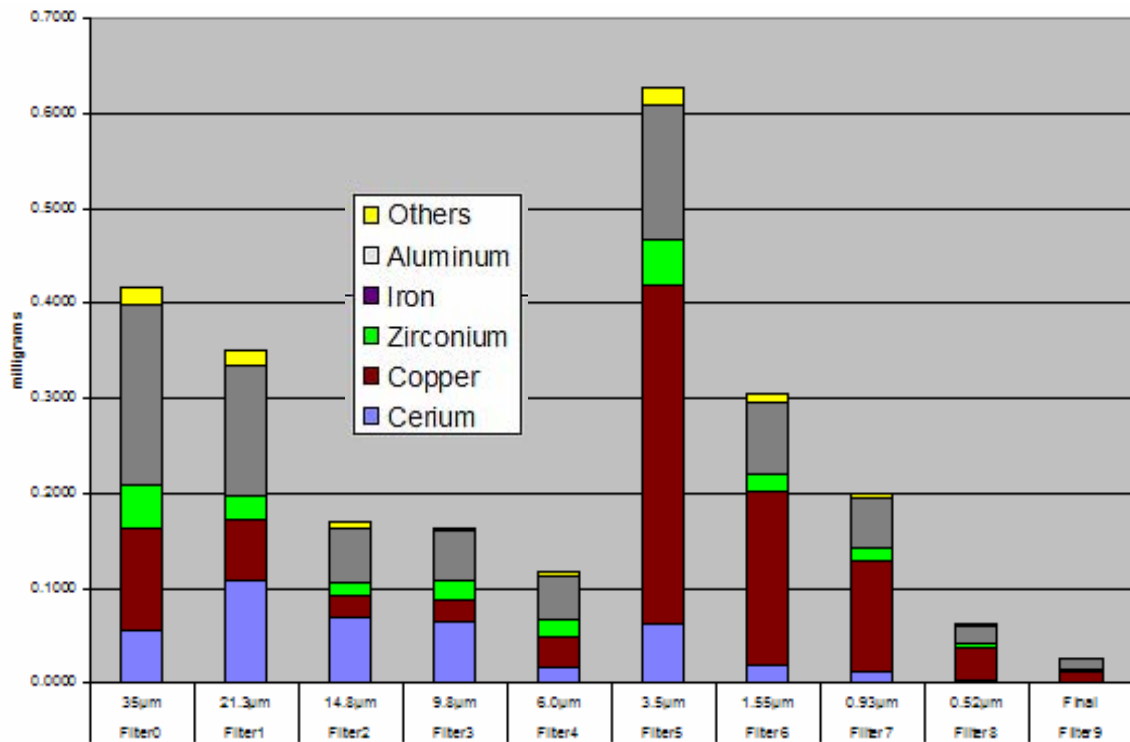


Figure A1.6.11 Test 2/6A, Marple #2941 (low) Metals Analysis Distribution, milligrams

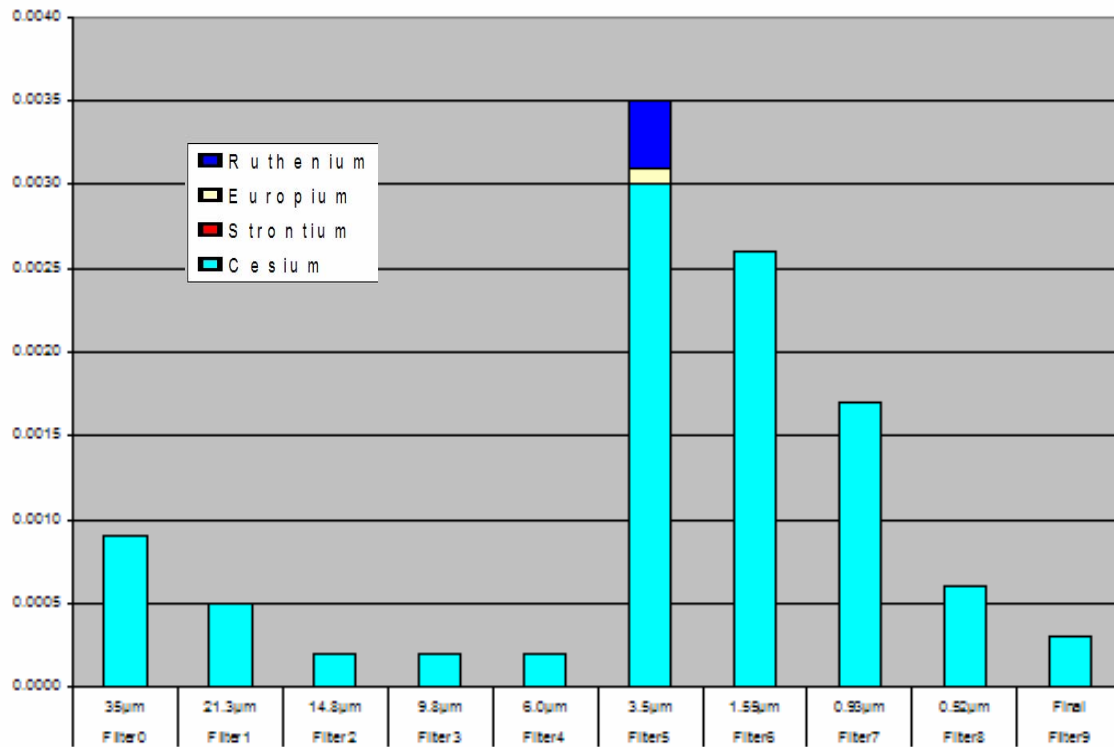


Figure A1.6.12 Test 2/6A, Marple #2941 (low) Fission Product Dopant Analysis Distrib, mg

**Table A1.6.13 Test 2/6A, Weight Distribution of Impact Debris**

Sieve Fraction	Weight, g	%
1000 µm	11.719	38.93
500 µm	2.5133	8.35
250 µm	3.4927	11.60
125 µm	4.3627	14.49
100 µm	1.7077	5.67
74 µm	2.9571	9.82
37 µm	2.7977	9.29
25 µm	0.0583	0.19
<25 µm	0.4971	1.65
<b>Total</b>	<b>30.1056</b>	<b>100.00</b>

**Table A1.6.14 Test 2/6A, Elemental Analysis. Wt% of Sieved Impact Debris**

Test 2/6A Sieve Fraction	125 µm	100 µm	74 µm	37 µm	25 µm	<25 µm
Cerium	55.230	54.240	52.450	47.900	44.090	44.770
Iron	12.970	12.470	12.240	12.250	13.360	12.570
Copper	3.623	3.089	3.471	4.227	4.579	4.709
Zirconium	1.209	1.454	1.871	2.759	3.387	3.763
Aluminum	1.524	1.967	2.715	3.421	4.245	4.547
Manganese	0.105	0.096	0.096	0.098	0.127	0.108
Tin	0.021	0.028	0.040	0.062	0.091	0.095
Chromium	0.025	0.020	0.021	0.023	0.029	0.026
Magnesium	0.023	0.026	0.035	0.044	0.062	0.055
Boron	0.003	0.002	0.001	0.002	0.012	0.004
Lithium	0.001	0.000	0.000	0.000	0.000	0.000
Nickel	0.013	0.011	0.011	0.011	0.015	0.012
Titanium	0.081	0.080	0.097	0.113	0.134	0.120
Molybdenum	0.003	0.002	0.002	0.002	0.002	0.002
Lead	0.001	0.002	0.002	0.004	0.004	0.005
Barium	0.005	0.004	0.004	0.005	0.007	0.006
Antimony	0.000	0.000	0.001	0.002	0.002	0.002
Strontium	0.003	0.003	0.004	0.006	0.010	0.010
Cesium	0.003	0.003	0.004	0.006	0.008	0.009
Ruthenium	0.000	0.000	0.000	0.001	0.000	0.002
<b>Total *</b>	<b>74.859</b>	<b>73.512</b>	<b>73.080</b>	<b>70.952</b>	<b>70.185</b>	<b>70.835</b>
Lanthanum	0.002	0.002	0.001	0.001	0.001	0.001
Praseodymium	0.001	0.001	0.001	0.001	0.001	0.001
Neodymium	0.002	0.001	0.001	0.001	0.001	0.001
Samarium	0.000	0.000	0.000	0.000	0.000	0.000
Europium	0.003	0.004	0.005	0.007	0.011	0.011
Terbium	0.008	0.007	0.007	0.006	0.007	0.006

\* includes "minor" lanthanides shown in Table

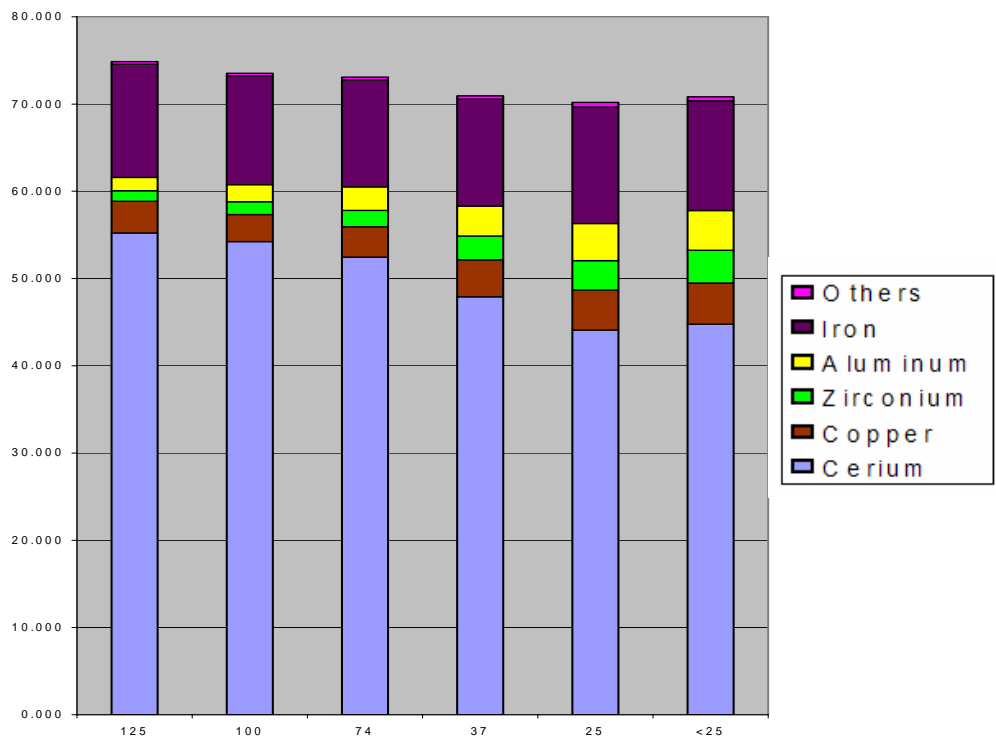


Figure A1.6.13 Test 2/6A Weight % Distribution of Metals in Impact Debris

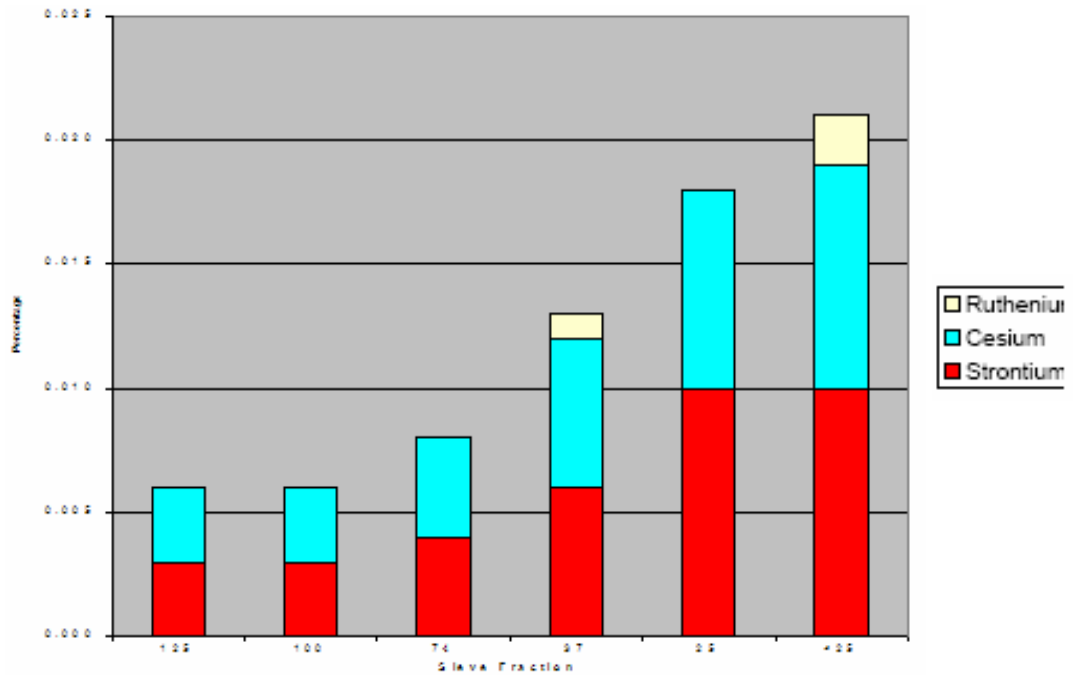


Figure A1.6.14 Test 2/6A Weight % Distribution of Fission Products in Impact Debris

### A.1.6B Test 2/6B Analyses and Results

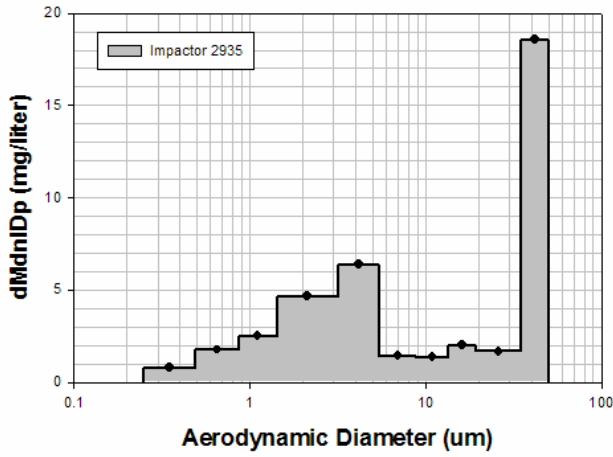


Figure A1.6.15 Test 2/6B Marple 2935 (high) Particle Size Distribution

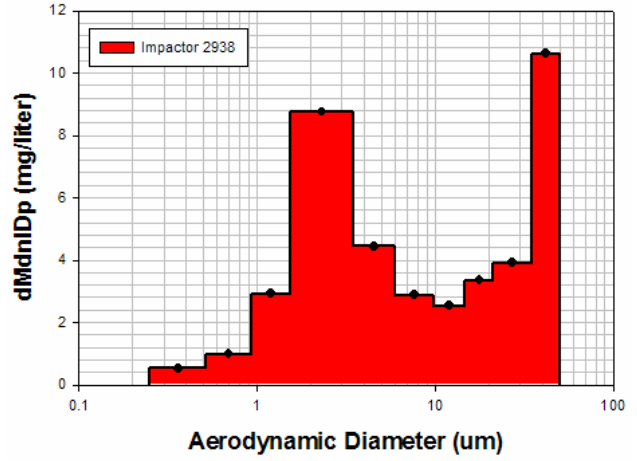


Figure A1.6.16 Test 2/6B Marple 2938 (high) Particle Size Distribution

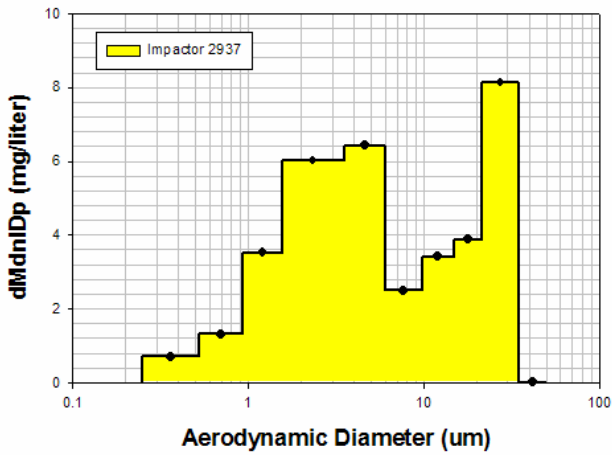


Figure A1.6.17 Test 2/6B Marple 2937 (low) Particle Size Distribution

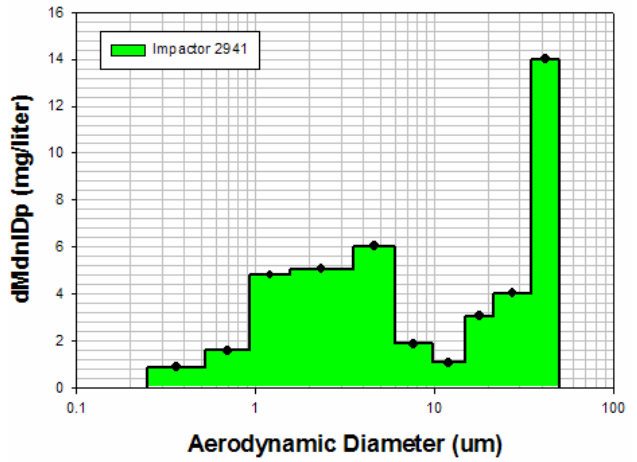


Figure A1.6.18 Test 2/6B Marple 2941 (low) Particle Size Distribution

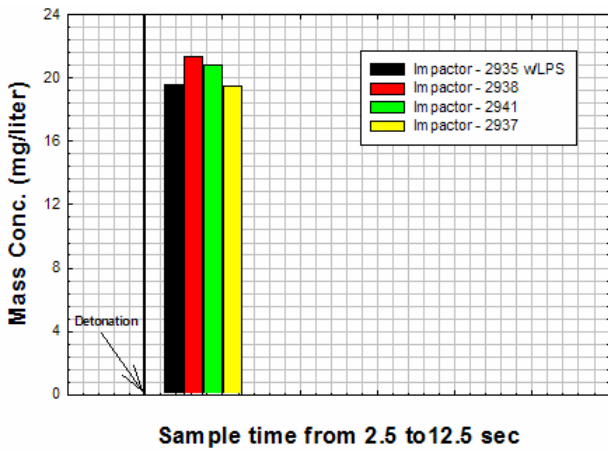


Figure A1.6.19 Test 2/6B Marple Impactors Mass Concentration

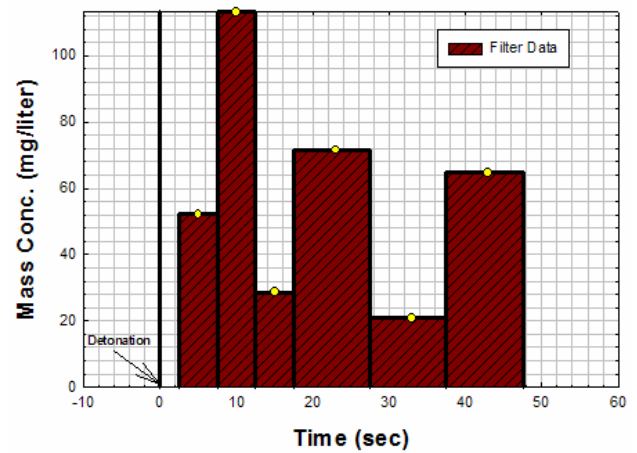


Figure A1.6.20 Test 2/6B Gelman Filters Mass Concentration

**Table A1.6.15 Test 2/6B, Marple #2935 (high) Elemental Analyses, Stages 0-3**

2/6B	STAGE 0			STAGE 1			STAGE 2			STAGE 3		
#2935	Particle size 35 µm			Particle size 21.3 µm			Particle size 14.8 µm			Particle size 9.8 µm		
	mg	% detect	% loading	mg	% detect	% loading	mg	% detect	% loading	mg	% detect	% loading
Ce	0.0117	4.2	1.5	0.0083	5.9	2.6	0.0430	12.2	3.8	0.0091	11.2	5.1
Cu	0.0959	34.3	12.1	0.0450	31.7	14.1	0.0149	4.2	1.3	0.0218	26.8	12.2
Zr	0.0193	6.9	2.4	0.0105	7.4	3.3	0.0072	2.0	0.6	0.0164	20.1	9.2
Fe	0.0924	33.1	11.6	0.0513	36.2	16.0	0.1763	49.9	15.5	0.0322	39.6	18.0
Al	0.0503	18.0	6.3	0.0172	12.1	5.4	0.0000	0.0	0.0	0.0000	0.0	0.0
Mg	0.0000	0.0	0.0	0.0037	2.6	1.2	0.0026	0.7	0.2	0.0003	0.4	0.2
Cr	0.0031	1.1	0.4	0.0021	1.5	0.7	0.0010	0.3	0.1	0.0003	0.4	0.2
Ni	0.0018	0.6	0.2	0.0011	0.8	0.3	0.0007	0.2	0.1	0.0000	0.0	0.0
Mn	0.0012	0.4	0.2	0.0007	0.5	0.2	0.0010	0.3	0.1	0.0004	0.5	0.2
Sn	0.0010	0.4	0.1	0.0000	0.0	0.0	0.0000	0.0	0.0	0.0000	0.0	0.0
Mo	0.0003	0.1	0.0	0.0003	0.2	0.1	0.0001	0.0	0.0	0.0000	0.0	0.0
Ti	0.0010	0.4	0.1	0.0008	0.6	0.3	0.1061	30.0	9.3	0.0007	0.9	0.4
Li	0.0000	0.0	0.0	0.0000	0.0	0.0	0.0000	0.0	0.0	0.0000	0.0	0.0
Sb	0.0000	0.0	0.0	0.0000	0.0	0.0	0.0000	0.0	0.0	0.0000	0.0	0.0
Pb	0.0003	0.1	0.1	0.0002	0.1	0.1	0.0001	0.0	0.0	0.0000	0.0	0.0
Cs	0.0012	0.4	0.2	0.0006	0.4	0.2	0.0002	0.1	0.0	0.0002	0.2	0.1
Sr	0.0000	0.0	0.0	0.0000	0.0	0.0	0.0000	0.0	0.0	0.0000	0.0	0.0
Ru	0.0000	0.0	0.0	0.0000	0.0	0.0	0.0000	0.0	0.0	0.0000	0.0	0.0
Eu	0.0000	0.0	0.0	0.0000	0.0	0.0	0.0000	0.0	0.0	0.0000	0.0	0.0
mg, Metals Found	<b>0.2795</b>	<b>100.0</b>	<b>35.2</b>	<b>0.1418</b>	<b>100.0</b>	<b>44.3</b>	<b>0.3532</b>	<b>100.0</b>	<b>31.0</b>	<b>0.0814</b>	<b>100.0</b>	<b>45.5</b>
mg, Filter Loading	<b>0.7950</b>			<b>0.3200</b>			<b>1.1380</b>			<b>0.1790</b>		

**Table A1.6.16 Test 2/6B, Marple #2935 (high) Elemental Analyses, Stages 4-7**

2/6B	STAGE 4			STAGE 5			STAGE 6			STAGE 7		
#2935	Particle size 6.0 µm			Particle size 3.5 µm			Particle size 1.55 µm			Particle size 0.93 µm		
	mg	% detect	% loading	mg	% detect	% loading	mg	% detect	% loading	mg	% detect	% loading
Ce	0.0066	6.9	2.9	0.0353	8.3	3.2	0.0176	3.1	1.4	0.0099	3.3	2.4
Cu	0.0359	37.6	16.0	0.2839	66.5	25.7	0.3043	53.2	24.9	0.1214	40.4	29.8
Zr	0.0176	18.4	7.8	0.0299	7.0	2.7	0.0274	4.8	2.2	0.0110	3.7	2.7
Fe	0.0335	35.1	14.9	0.0693	16.2	6.3	0.1056	18.4	8.6	0.0490	16.3	12.0
Mg	0.0000	0.0	0.0	0.0000	0.0	0.0	0.1017	17.8	8.3	0.1036	34.5	25.4
Al	0.0000	0.0	0.0	0.0000	0.0	0.0	0.0007	0.1	0.1	0.0004	0.1	0.1
Cr	0.0002	0.2	0.1	0.0002	0.0	0.0	0.0004	0.1	0.0	0.0002	0.1	0.0
Ni	0.0000	0.0	0.0	0.0001	0.0	0.0	0.0002	0.0	0.0	0.0000	0.0	0.0
Mn	0.0004	0.4	0.2	0.0012	0.3	0.1	0.0019	0.3	0.2	0.0009	0.3	0.2
Sn	0.0000	0.0	0.0	0.0025	0.6	0.2	0.0050	0.9	0.4	0.0014	0.5	0.3
Mo	0.0000	0.0	0.0	0.0001	0.0	0.0	0.0002	0.0	0.0	0.0000	0.0	0.0
Ti	0.0008	0.8	0.4	0.0016	0.4	0.1	0.0016	0.3	0.1	0.0004	0.1	0.1
Li	0.0000	0.0	0.0	0.0000	0.0	0.0	0.0000	0.0	0.0	0.0000	0.0	0.0
Sb	0.0000	0.0	0.0	0.0001	0.0	0.0	0.0002	0.0	0.0	0.0000	0.0	0.0
Pb	0.0000	0.0	0.0	0.0002	0.0	0.0	0.0009	0.2	0.1	0.0004	0.1	0.1
Cs	0.0004	0.4	0.2	0.0026	0.6	0.2	0.0048	0.8	0.4	0.0019	0.6	0.5
Sr	0.0000	0.0	0.0	0.0000	0.0	0.0	0.0000	0.0	0.0	0.0000	0.0	0.0
Ru	0.0000	0.0	0.0	0.0000	0.0	0.0	0.0000	0.0	0.0	0.0000	0.0	0.0
Eu	0.0000	0.0	0.0	0.0000	0.0	0.0	0.0000	0.0	0.0	0.0000	0.0	0.0
mg, Metals Found	<b>0.0954</b>	<b>100.0</b>	<b>42.4</b>	<b>0.4270</b>	<b>100.0</b>	<b>38.7</b>	<b>0.5725</b>	<b>100.0</b>	<b>46.9</b>	<b>0.3005</b>	<b>100.0</b>	<b>73.7</b>
mg, Filter Loading	<b>0.2250</b>			<b>1.1040</b>			<b>1.2210</b>			<b>0.4080</b>		

**Table A1.6.17 Test 2/6B, Marple #2935 (high) Elemental Analyses, Stages 8-9**

2/6B #2935	STAGE 8			STAGE 9								
	Particle size 0.52 µm			Particle size final, >0.5 µm								
	mg	% detect	% loading	mg	% detect	% loading						
Ce	0.0078	3.4	2.4	0.0019	5.7	1.1						
Cu	0.0734	31.9	22.7	0.0175	52.4	10.4						
Zr	0.0090	3.9	2.8	0.0028	8.4	1.7						
Fe	0.0341	14.8	10.5	0.0099	29.6	5.9						
Mg	0.0978	42.5	30.2	0.0000	0.0	0.0						
Al	0.0034	1.5	1.0	0.0000	0.0	0.0						
Cr	0.0002	0.1	0.1	0.0000	0.0	0.0						
Ni	0.0000	0.0	0.0	0.0000	0.0	0.0						
Mn	0.0006	0.3	0.2	0.0002	0.6	0.1						
Sn	0.0009	0.4	0.3	0.0000	0.0	0.0						
Mo	0.0000	0.0	0.0	0.0000	0.0	0.0						
Ti	0.0008	0.3	0.2	0.0007	2.1	0.4						
Li	0.0000	0.0	0.0	0.0000	0.0	0.0						
Sb	0.0000	0.0	0.0	0.0000	0.0	0.0						
Pb	0.0003	0.1	0.1	0.0000	0.0	0.0						
Cs	0.0013	0.6	0.4	0.0004	1.2	0.2						
Sr	0.0003	0.1	0.1	0.0000	0.0	0.0						
Ru	0.0000	0.0	0.0	0.0000	0.0	0.0						
Eu	0.0000	0.0	0.0	0.0000	0.0	0.0						
mg, Metals Found	<b>0.2299</b>	<b>100.0</b>	<b>71.0</b>	<b>0.0334</b>	<b>100.0</b>	<b>19.9</b>						
mg, Filter Loading	<b>0.3240</b>			<b>0.1680</b>								

**Table A1.6.18 Test 2/6B, Marple #2935 Particle Cerium and Fission Product Distributions**

2/6B #2935 high	Cerium		Cesium		Strontium		Ruthenium		Europium	
	mg	wt%	mg	wt%	mg	wt%	mg	wt%	mg	wt%
35µm and >	0.0117	7.7	0.0012	8.8	0.0000	0.0	0.0000	0.0	0.0000	0.0
21.3µm	0.0083	5.5	0.0006	4.4	0.0000	0.0	0.0000	0.0	0.0000	0.0
14.8µm	0.0430	28.4	0.0002	1.5	0.0000	0.0	0.0000	0.0	0.0000	0.0
9.8µm	0.0091	6.0	0.0002	1.5	0.0000	0.0	0.0000	0.0	0.0000	0.0
6.0µm	0.0066	4.4	0.0004	2.9	0.0000	0.0	0.0000	0.0	0.0000	0.0
3.5µm	0.0353	23.3	0.0026	19.1	0.0000	0.0	0.0001	33.3	0.0000	0.0
1.55µm	0.0176	11.6	0.0048	35.3	0.0000	0.0	0.0002	66.7	0.0000	0.0
0.93µm	0.0099	6.5	0.0019	14.0	0.0000	0.0	0.0000	0.0	0.0000	0.0
0.52µm	0.0078	5.2	0.0013	9.6	0.0003	100.0	0.0000	0.0	0.0000	0.0
Final filter	0.0019	1.3	0.0004	2.9	0.0000	0.0	0.0000	0.0	0.0000	0.0
Sum	<b>0.1512</b>		<b>0.0136</b>		<b>0.0003</b>		<b>0.0003</b>		<b>0.0000</b>	

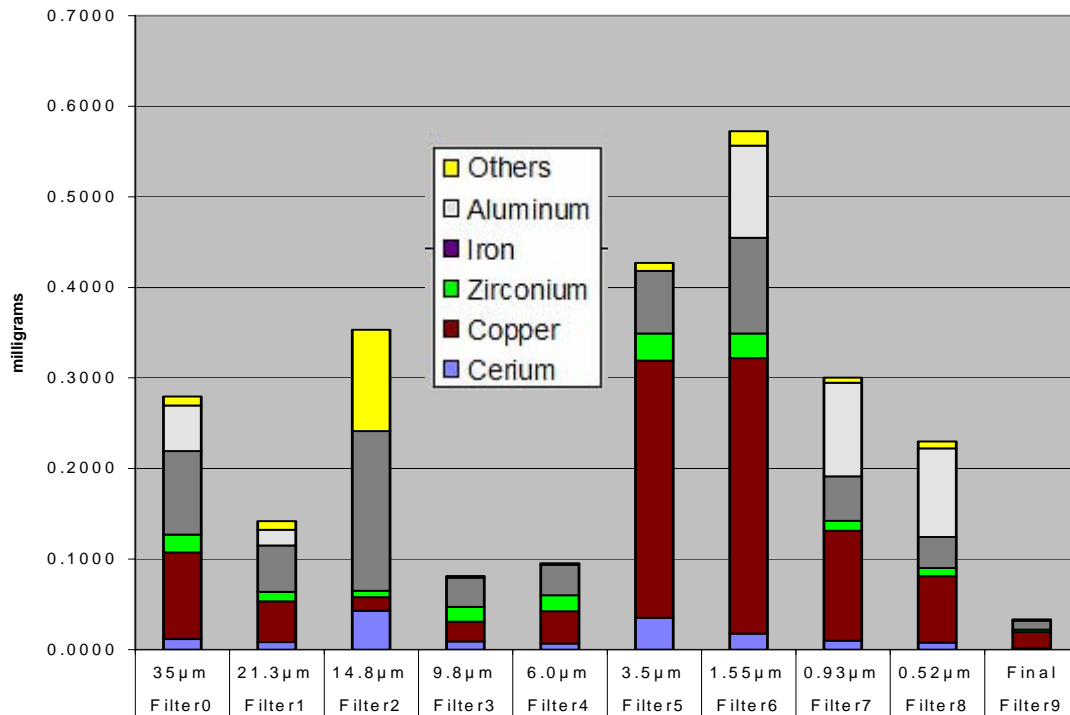


Figure A1.6.21 Test 2/6B, Marple #2935 (high) Metals Analysis Distribution, milligrams

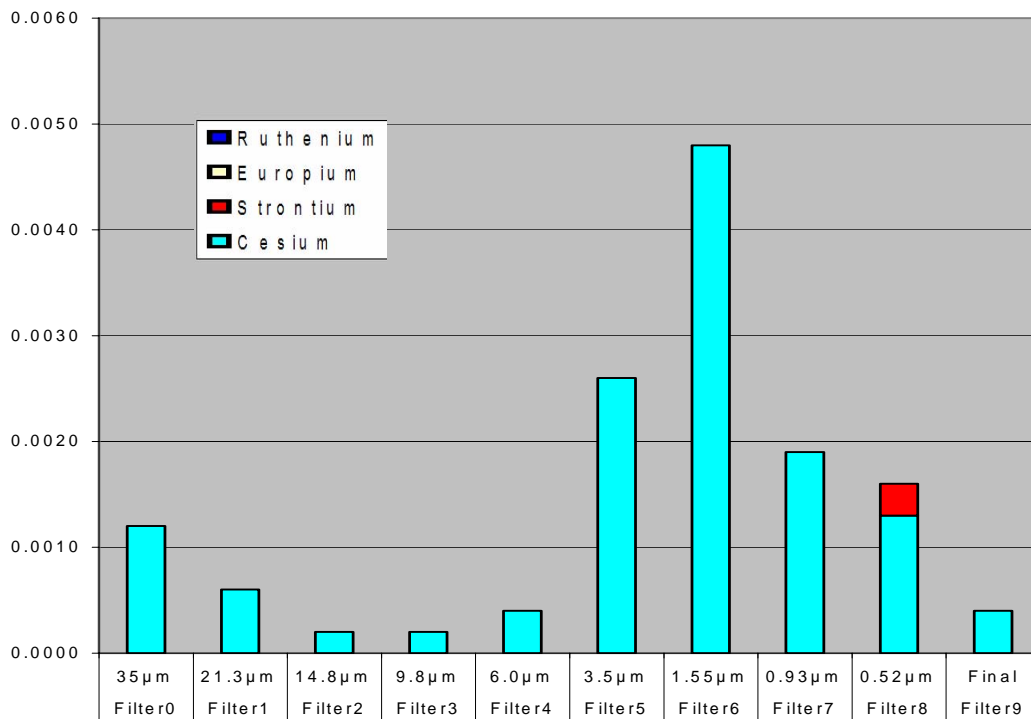


Figure A1.6.22 Test 2/6B, Marple #2935 (high) Fission Product Dopant Analysis Distrib, mg

**Table A1.6.19 Test 2/6B, Marple #2937 (low) Elemental Analyses, Stages 0-3**

2/6B	STAGE 0			STAGE 1			STAGE 2			STAGE 3		
#2937	Particle size 35 µm			Particle size 21.3 µm			Particle size 14.8 µm			Particle size 9.8 µm		
	mg	% detect	% loading	mg	% detect	% loading	mg	% detect	% loading	mg	% detect	% loading
Ce				0.0214	6.2	1.6	0.0074	4.9	1.6	0.0115	5.1	2.5
Cu				0.0735	21.4	5.6	0.0299	19.8	6.5	0.0331	14.6	7.2
Zr				0.0253	7.4	1.9	0.0102	6.8	2.2	0.0237	10.5	5.2
Fe				0.1864	54.3	14.2	0.0696	46.1	15.1	0.0669	29.6	14.6
Al				0.0000	0.0	0.0	0.0189	12.5	4.1	0.0620	27.4	13.5
Mg				0.0000	0.0	0.0	0.0014	0.9	0.3	0.0078	3.4	1.7
Cr				0.0202	5.9	1.5	0.0074	4.9	1.6	0.0051	2.3	1.1
Ni				0.0087	2.5	0.7	0.0031	2.1	0.7	0.0022	1.0	0.5
Mn				0.0024	0.7	0.2	0.0009	0.6	0.2	0.0009	0.4	0.2
Sn				0.0004	0.1	0.0	0.0000	0.0	0.0	0.0000	0.0	0.0
Mo				0.0025	0.7	0.2	0.0009	0.6	0.2	0.0006	0.3	0.1
Ti				0.0014	0.4	0.1	0.0007	0.5	0.2	0.0112	5.0	2.4
Li				0.0002	0.1	0.0	0.0001	0.1	0.0	0.0001	0.0	0.0
Sb				0.0000	0.0	0.0	0.0000	0.0	0.0	0.0000	0.0	0.0
Pb				0.0002	0.1	0.0	0.0001	0.1	0.0	0.0001	0.0	0.0
Cs				0.0008	0.2	0.1	0.0004	0.3	0.1	0.0004	0.2	0.1
Sr				0.0000	0.0	0.0	0.0000	0.0	0.0	0.0005	0.2	0.1
Ru				0.0000	0.0	0.0	0.0000	0.0	0.0	0.0000	0.0	0.0
Eu				0.0000	0.0	0.0	0.0000	0.0	0.0	0.0000	0.0	0.0
mg, Metals Found				<b>0.3434</b>	<b>100.0</b>	<b>26.1</b>	<b>0.1510</b>	<b>100.0</b>	<b>32.8</b>	<b>0.2261</b>	<b>100.0</b>	<b>49.4</b>
mg, Filter Loading	<b>(no stage 0)</b>			<b>1.3160</b>			<b>0.4600</b>			<b>0.4580</b>		

**Table A1.6.20 Test 2/6B, Marple #2937 (low) Elemental Analyses, Stages 4-7**

2/6B	STAGE 4			STAGE 5			STAGE 6			STAGE 7		
#2937	Particle size 6.0 µm			Particle size 3.5 µm			Particle size 1.55 µm			Particle size 0.93 µm		
	mg	% detect	% loading	mg	% detect	% loading	mg	% detect	% loading	mg	% detect	% loading
Ce	0.0122	4.8	3.0	0.0089	1.6	0.8	0.0292	6.8	1.8	0.0133	5.8	2.3
Cu	0.0344	13.5	8.4	0.2818	49.5	25.0	0.2600	60.2	16.3	0.1434	62.4	24.5
Zr	0.0224	8.8	5.5	0.0407	7.2	3.6	0.0264	6.1	1.7	0.0145	6.3	2.5
Fe	0.0532	20.8	13.0	0.1116	19.6	9.9	0.1013	23.4	6.3	0.0499	21.7	8.5
Mg	0.1145	44.8	28.0	0.1056	18.6	9.4	0.0000	0.0	0.0	0.0000	0.0	0.0
Al	0.0105	4.1	2.6	0.0046	0.8	0.4	0.0000	0.0	0.0	0.0000	0.0	0.0
Cr	0.0032	1.3	0.8	0.0025	0.4	0.2	0.0012	0.3	0.1	0.0010	0.4	0.2
Ni	0.0014	0.5	0.3	0.0011	0.2	0.1	0.0005	0.1	0.0	0.0005	0.2	0.1
Mn	0.0008	0.3	0.2	0.0018	0.3	0.2	0.0018	0.4	0.1	0.0009	0.4	0.2
Sn	0.0000	0.0	0.0	0.0038	0.7	0.3	0.0044	1.0	0.3	0.0020	0.9	0.3
Mo	0.0004	0.2	0.1	0.0004	0.1	0.0	0.0003	0.1	0.0	0.0002	0.1	0.0
Ti	0.0014	0.5	0.3	0.0025	0.4	0.2	0.0013	0.3	0.1	0.0008	0.3	0.1
Li	0.0001	0.0	0.0	0.0000	0.0	0.0	0.0000	0.0	0.0	0.0000	0.0	0.0
Sb	0.0000	0.0	0.0	0.0001	0.0	0.0	0.0002	0.0	0.0	0.0000	0.0	0.0
Pb	0.0001	0.0	0.0	0.0006	0.1	0.1	0.0008	0.2	0.1	0.0004	0.2	0.1
Cs	0.0004	0.2	0.1	0.0030	0.5	0.3	0.0044	1.0	0.3	0.0026	1.1	0.4
Sr	0.0006	0.2	0.1	0.0001	0.0	0.0	0.0000	0.0	0.0	0.0000	0.0	0.0
Ru	0.0000	0.0	0.0	0.0000	0.0	0.0	0.0004	0.1	0.0	0.0002	0.1	0.0
Eu	0.0000	0.0	0.0	0.0000	0.0	0.0	0.0000	0.0	0.0	0.0000	0.0	0.0
mg, Metals Found	<b>0.2556</b>	<b>100.0</b>	<b>62.5</b>	<b>0.5691</b>	<b>100.0</b>	<b>50.5</b>	<b>0.4322</b>	<b>100.0</b>	<b>27.1</b>	<b>0.2297</b>	<b>100.0</b>	<b>39.2</b>
mg, Filter Loading	<b>0.4090</b>			<b>1.1280</b>			<b>1.5960</b>			<b>0.5860</b>		

**Table A1.6.21 Test 2/6B, Marple #2937 (low) Elemental Analyses, Stages 8-9**

<b>2/6B</b>	<b>STAGE 8</b>			<b>STAGE 9</b>								
<b>#2937</b>	Particle size 0.52 µm			Particle size final, >0.5 µm								
	<b>mg</b>	<b>% detect</b>	<b>% loading</b>	<b>mg</b>	<b>% detect</b>	<b>% loading</b>						
Ce	0.0061	6.6	2.4	0.0029	7.0	1.7						
Cu	0.0549	59.0	22.0	0.0214	51.7	12.7						
Zr	0.0062	6.7	2.5	0.0034	8.2	2.0						
Fe	0.0228	24.5	9.2	0.0093	22.5	5.5						
Mg	0.0000	0.0	0.0	0.0000	0.0	0.0						
Al	0.0000	0.0	0.0	0.0018	4.3	1.1						
Cr	0.0003	0.3	0.1	0.0005	1.2	0.3						
Ni	0.0001	0.1	0.0	0.0001	0.2	0.1						
Mn	0.0004	0.4	0.2	0.0002	0.5	0.1						
Sn	0.0004	0.4	0.2	0.0000	0.0	0.0						
Mo	0.0000	0.0	0.0	0.0000	0.0	0.0						
Ti	0.0004	0.4	0.2	0.0006	1.4	0.4						
Li	0.0000	0.0	0.0	0.0000	0.0	0.0						
Sb	0.0000	0.0	0.0	0.0000	0.0	0.0						
Pb	0.0002	0.2	0.1	0.0001	0.2	0.1						
Cs	0.0012	1.3	0.5	0.0005	1.2	0.3						
Sr	0.0000	0.0	0.0	0.0006	1.4	0.4						
Ru	0.0001	0.1	0.0	0.0000	0.0	0.0						
Eu	0.0000	0.0	0.0	0.0000	0.0	0.0						
mg, Metals Found	<b>0.0931</b>	<b>100.0</b>	<b>37.4</b>	<b>0.0414</b>	<b>100.0</b>	<b>24.6</b>						
mg, Filter Loading	<b>0.2490</b>			<b>0.1680</b>								

**Table A1.6.22 Test 2/6B, Marple #2937 Particle Cerium and Fission Product Distributions**

<b>2/6B #2937 low</b>	<b>Cerium</b>		<b>Cesium</b>		<b>Strontium</b>		<b>Ruthenium</b>		<b>Europium</b>	
<b>Particle Size</b>	<b>mg</b>	<b>wt%</b>	<b>mg</b>	<b>wt%</b>	<b>mg</b>	<b>wt%</b>	<b>mg</b>	<b>wt%</b>	<b>mg</b>	<b>wt%</b>
35µm and >	0.0000	0.0	0.0000	0.0	0.0000	0.0	0.0000	0.0	0.0000	0.0
21.3µm	0.0214	19.0	0.0008	5.8	0.0000	0.0	0.0000	0.0	0.0000	0.0
14.8µm	0.0074	6.6	0.0004	2.9	0.0000	0.0	0.0000	0.0	0.0000	0.0
9.8µm	0.0115	10.2	0.0004	2.9	0.0005	27.8	0.0000	0.0	0.0000	0.0
6.0µm	0.0122	10.8	0.0004	2.9	0.0006	33.3	0.0000	0.0	0.0000	0.0
3.5µm	0.0089	7.9	0.0030	21.9	0.0001	5.6	0.0000	0.0	0.0000	0.0
1.55µm	0.0292	25.9	0.0044	32.1	0.0000	0.0	0.0004	57.1	0.0000	0.0
0.93µm	0.0133	11.8	0.0026	19.0	0.0000	0.0	0.0002	28.6	0.0000	0.0
0.52µm	0.0061	5.4	0.0012	8.8	0.0000	0.0	0.0001	14.3	0.0000	0.0
Final filter	0.0029	2.6	0.0005	3.6	0.0006	33.3	0.0000	0.0	0.0000	0.0
<b>Sum</b>	<b>0.1129</b>		<b>0.0137</b>		<b>0.0018</b>		<b>0.0007</b>		<b>0.0000</b>	

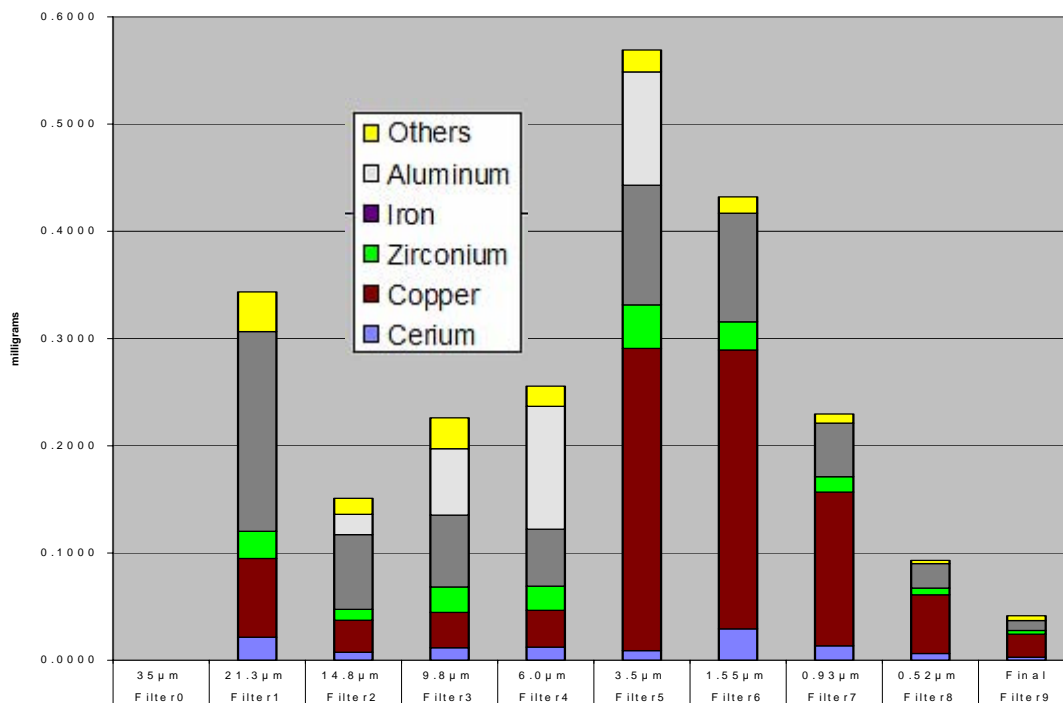


Figure A1.6.23 Test 2/6B, Marple #2937 (low) Metals Analysis Distribution, milligrams

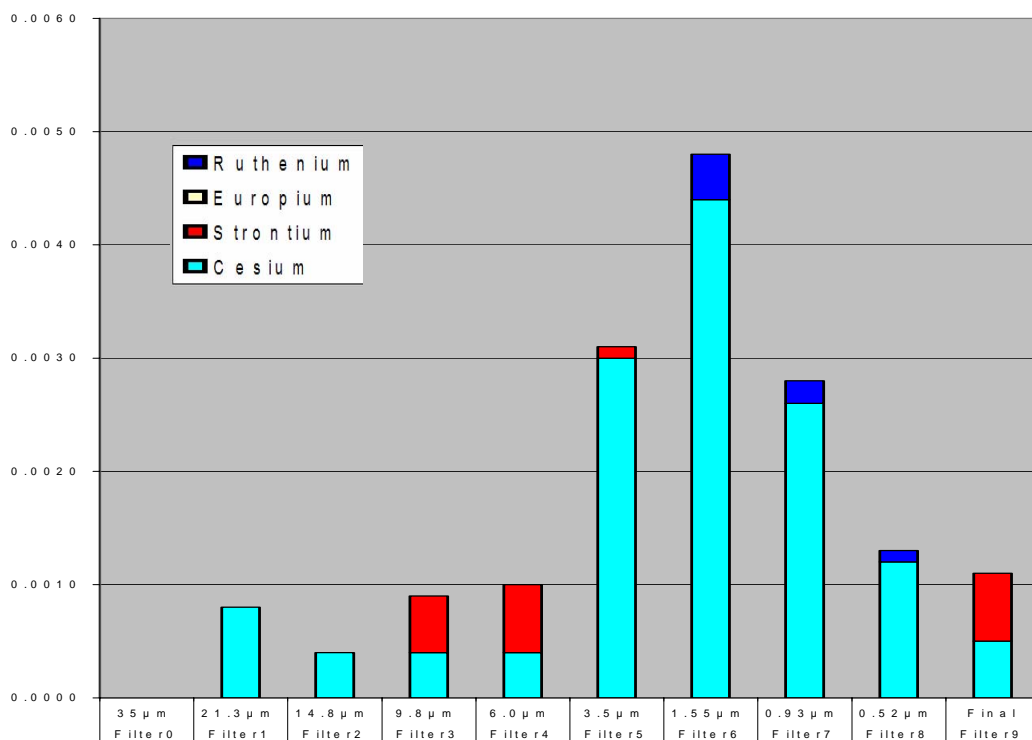


Figure A1.6.24 Test 2/6B, Marple #2937 (low) Fission Product Dopant Analysis Distrib, mg

**Table A1.6.23 Test 2/6B, Marple #2941 (low) Elemental Analyses, Stages 0-3**

2/6B	STAGE 0			STAGE 1			STAGE 2			STAGE 3		
#2941	Particle size 35 µm			Particle size 21.3 µm			Particle size 14.8 µm			Particle size 9.8 µm		
	mg	% detect	% loading	mg	% detect	% loading	mg	% detect	% loading	mg	% detect	% loading
Ce	0.0105	3.2	0.6	0.0070	3.6	1.0	0.0081	7.5	2.2	0.0098	9.4	6.5
Cu	0.1054	32.4	6.2	0.0666	34.5	9.9	0.0362	33.6	9.6	0.0252	24.1	16.8
Zr	0.0472	14.5	2.8	0.0236	12.2	3.5	0.0131	12.2	3.5	0.0204	19.5	13.6
Fe	0.1466	45.1	8.6	0.0825	42.7	12.2	0.0406	37.7	10.8	0.0395	37.7	26.3
Al	0.0000	0.0	0.0	0.0000	0.0	0.0	0.0000	0.0	0.0	0.0000	0.0	0.0
Mg	0.0000	0.0	0.0	0.0022	1.1	0.3	0.0046	4.3	1.2	0.0056	5.3	3.7
Cr	0.0060	1.8	0.4	0.0042	2.2	0.6	0.0020	1.9	0.5	0.0013	1.2	0.9
Ni	0.0024	0.7	0.1	0.0019	1.0	0.3	0.0008	0.7	0.2	0.0005	0.5	0.3
Mn	0.0018	0.6	0.1	0.0011	0.6	0.2	0.0006	0.6	0.2	0.0005	0.5	0.3
Sn	0.0016	0.5	0.1	0.0002	0.1	0.0	0.0000	0.0	0.0	0.0000	0.0	0.0
Mo	0.0008	0.2	0.0	0.0004	0.2	0.1	0.0002	0.2	0.1	0.0002	0.2	0.1
Ti	0.0016	0.5	0.1	0.0023	1.2	0.3	0.0008	0.7	0.2	0.0012	1.1	0.8
Li	0.0000	0.0	0.0	0.0000	0.0	0.0	0.0000	0.0	0.0	0.0000	0.0	0.0
Sb	0.0000	0.0	0.0	0.0000	0.0	0.0	0.0000	0.0	0.0	0.0000	0.0	0.0
Pb	0.0002	0.1	0.0	0.0002	0.1	0.0	0.0001	0.1	0.0	0.0000	0.0	0.0
Cs	0.0012	0.4	0.1	0.0008	0.4	0.1	0.0004	0.4	0.1	0.0003	0.3	0.2
Sr	0.0000	0.0	0.0	0.0000	0.0	0.0	0.0002	0.2	0.1	0.0002	0.2	0.1
Ru	0.0000	0.0	0.0	0.0000	0.0	0.0	0.0000	0.0	0.0	0.0000	0.0	0.0
Eu	0.0000	0.0	0.0	0.0000	0.0	0.0	0.0000	0.0	0.0	0.0000	0.0	0.0
mg, Metals Found	<b>0.3253</b>	<b>100.0</b>	<b>19.2</b>	<b>0.1930</b>	<b>100.0</b>	<b>28.6</b>	<b>0.1077</b>	<b>100.0</b>	<b>28.6</b>	<b>0.1047</b>	<b>100.0</b>	<b>69.8</b>
mg, Filter Loading	<b>1.6980</b>			<b>0.6760</b>			<b>0.3760</b>			<b>0.1500</b>		

**Table A1.6.24 Test 2/6B, Marple #2941 (low) Elemental Analyses, Stages 4-7**

2/6B	STAGE 4			STAGE 5			STAGE 6			STAGE 7		
#2941	Particle size 6.0 µm			Particle size 3.5 µm			Particle size 1.55 µm			Particle size 0.93 µm		
	mg	% detect	% loading	mg	% detect	% loading	mg	% detect	% loading	mg	% detect	% loading
Ce	0.0074	6.8	2.4	0.0135	3.0	1.2	0.0080	2.0	0.6	0.0032	1.1	0.4
Cu	0.0350	32.1	11.3	0.2976	66.4	26.9	0.2258	56.4	16.2	0.2016	67.1	24.2
Zr	0.0242	22.2	7.8	0.0417	9.3	3.8	0.0230	5.7	1.6	0.0217	7.2	2.6
Fe	0.0386	35.4	12.4	0.0810	18.1	7.3	0.0677	16.9	4.8	0.0635	21.1	7.6
Mg	0.0000	0.0	0.0	0.0000	0.0	0.0	0.0555	13.9	4.0	0.0000	0.0	0.0
Al	0.0009	0.8	0.3	0.0014	0.3	0.1	0.0048	1.2	0.3	0.0000	0.0	0.0
Cr	0.0007	0.6	0.2	0.0008	0.2	0.1	0.0005	0.1	0.0	0.0002	0.1	0.0
Ni	0.0004	0.4	0.1	0.0007	0.2	0.1	0.0003	0.1	0.0	0.0001	0.0	0.0
Mn	0.0005	0.5	0.2	0.0020	0.4	0.2	0.0014	0.3	0.1	0.0012	0.4	0.1
Sn	0.0000	0.0	0.0	0.0031	0.7	0.3	0.0030	0.7	0.2	0.0036	1.2	0.4
Mo	0.0000	0.0	0.0	0.0002	0.0	0.0	0.0001	0.0	0.0	0.0001	0.0	0.0
Ti	0.0010	0.9	0.3	0.0025	0.6	0.2	0.0022	0.5	0.2	0.0007	0.2	0.1
Li	0.0000	0.0	0.0	0.0000	0.0	0.0	0.0000	0.0	0.0	0.0000	0.0	0.0
Sb	0.0000	0.0	0.0	0.0001	0.0	0.0	0.0001	0.0	0.0	0.0002	0.1	0.0
Pb	0.0000	0.0	0.0	0.0006	0.1	0.1	0.0006	0.1	0.0	0.0005	0.2	0.1
Cs	0.0004	0.4	0.1	0.0031	0.7	0.3	0.0072	1.8	0.5	0.0038	1.3	0.5
Sr	0.0000	0.0	0.0	0.0001	0.0	0.0	0.0002	0.0	0.0	0.0000	0.0	0.0
Ru	0.0000	0.0	0.0	0.0001	0.0	0.0	0.0000	0.0	0.0	0.0000	0.0	0.0
Eu	0.0000	0.0	0.0	0.0000	0.0	0.0	0.0000	0.0	0.0	0.0000	0.0	0.0
mg, Metals Found	<b>0.1091</b>	<b>100.0</b>	<b>35.1</b>	<b>0.4485</b>	<b>100.0</b>	<b>40.6</b>	<b>0.4004</b>	<b>100.0</b>	<b>28.7</b>	<b>0.3004</b>	<b>100.0</b>	<b>36.0</b>
mg, Filter Loading	<b>0.3110</b>			<b>1.1050</b>			<b>1.3960</b>			<b>0.8340</b>		

**Table A1.6.25 Test 2/6B, Marple #2941 (low) Elemental Analyses, Stages 8-9**

2/6B #2941	STAGE 8			STAGE 9								
	Particle size 0.52 µm			Particle size final, >0.5 µm								
	mg	% detect	% loading	mg	% detect	% loading						
Ce	0.0073	6.4	2.3	0.0022	8.6	2.2						
Cu	0.0652	57.6	20.9	0.0139	54.3	13.9						
Zr	0.0098	8.7	3.1	0.0022	8.6	2.2						
Fe	0.0250	22.1	8.0	0.0062	24.2	6.2						
Mg	0.0000	0.0	0.0	0.0000	0.0	0.0						
Al	0.0015	1.3	0.5	0.0000	0.0	0.0						
Cr	0.0003	0.3	0.1	0.0002	0.8	0.2						
Ni	0.0000	0.0	0.0	0.0000	0.0	0.0						
Mn	0.0006	0.5	0.2	0.0000	0.0	0.0						
Sn	0.0005	0.4	0.2	0.0000	0.0	0.0						
Mo	0.0000	0.0	0.0	0.0000	0.0	0.0						
Ti	0.0008	0.7	0.3	0.0003	1.2	0.3						
Sb	0.0000	0.0	0.0	0.0000	0.0	0.0						
Li	0.0000	0.0	0.0	0.0000	0.0	0.0						
Pb	0.0002	0.2	0.1	0.0000	0.0	0.0						
Cs	0.0015	1.3	0.5	0.0005	2.0	0.5						
Sr	0.0004	0.4	0.1	0.0000	0.0	0.0						
Ru	0.0001	0.1	0.0	0.0000	0.0	0.0						
Eu	0.0000	0.0	0.0	0.0000	0.0	0.0						
mg, Metals Found	<b>0.1132</b>	<b>100.0</b>	<b>36.3</b>	<b>0.0256</b>	<b>100.0</b>	<b>25.6</b>						
mg, Filter Loading	<b>0.3120</b>			<b>0.1000</b>								

**Table A1.6.26 Test 2/6B, Marple #2941 Particle Cerium and Fission Product Distributions**

2/6B #2941 low	Cerium		Cesium		Strontium		Ruthenium		Europium	
	mg	wt%	mg	wt%	mg	wt%	mg	wt%	mg	wt%
35µm and >	0.0105	13.6	0.0012	6.3	0.0000	0.0	0.0000	0.0	0.0000	0.0
21.3µm	0.0070	9.1	0.0008	4.2	0.0000	0.0	0.0000	0.0	0.0000	0.0
14.8µm	0.0081	10.5	0.0004	2.1	0.0002	18.2	0.0000	0.0	0.0000	0.0
9.8µm	0.0098	12.7	0.0003	1.6	0.0002	18.2	0.0000	0.0	0.0000	0.0
6.0µm	0.0074	9.6	0.0004	2.1	0.0000	0.0	0.0000	0.0	0.0000	0.0
3.5µm	0.0135	17.5	0.0031	16.1	0.0001	9.1	0.0001	50.0	0.0000	0.0
1.55µm	0.0080	10.4	0.0072	37.5	0.0002	18.2	0.0000	0.0	0.0000	0.0
0.93µm	0.0032	4.2	0.0038	19.8	0.0000	0.0	0.0000	0.0	0.0000	0.0
0.52µm	0.0073	9.5	0.0015	7.8	0.0004	36.4	0.0001	50.0	0.0000	0.0
Final filter	0.0022	2.9	0.0005	2.6	0.0000	0.0	0.0000	0.0	0.0000	0.0
<b>Sum</b>	<b>0.0770</b>		<b>0.0192</b>		<b>0.0011</b>		<b>0.0002</b>		<b>0.0000</b>	

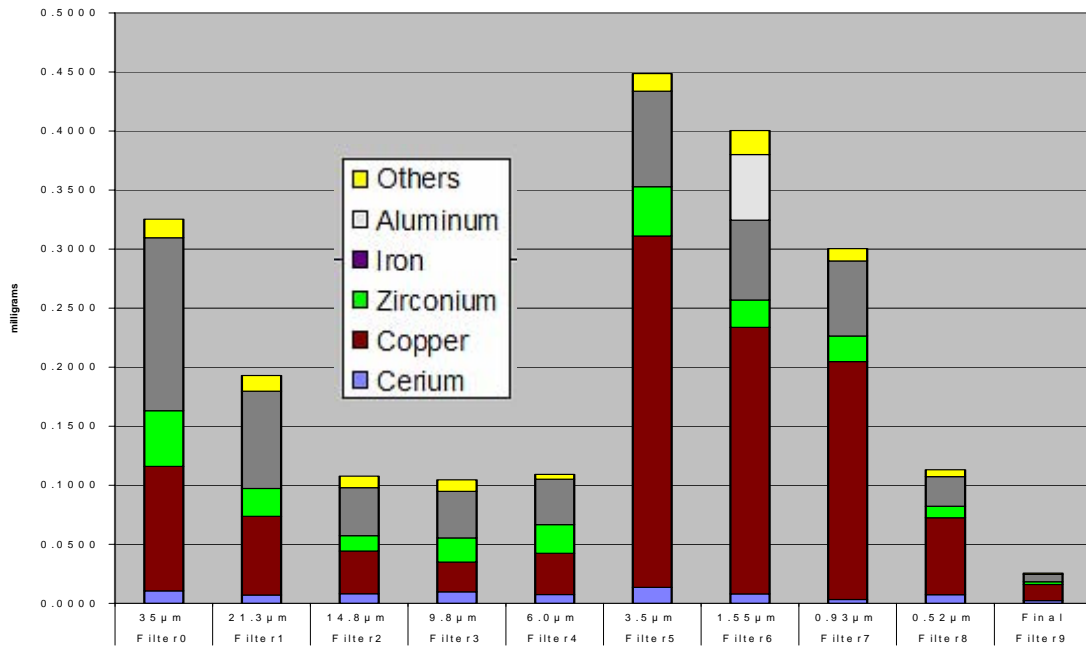


Figure A1.6.25 Test 2/6B, Marple #2941 (low) Metals Analysis Distribution, milligrams

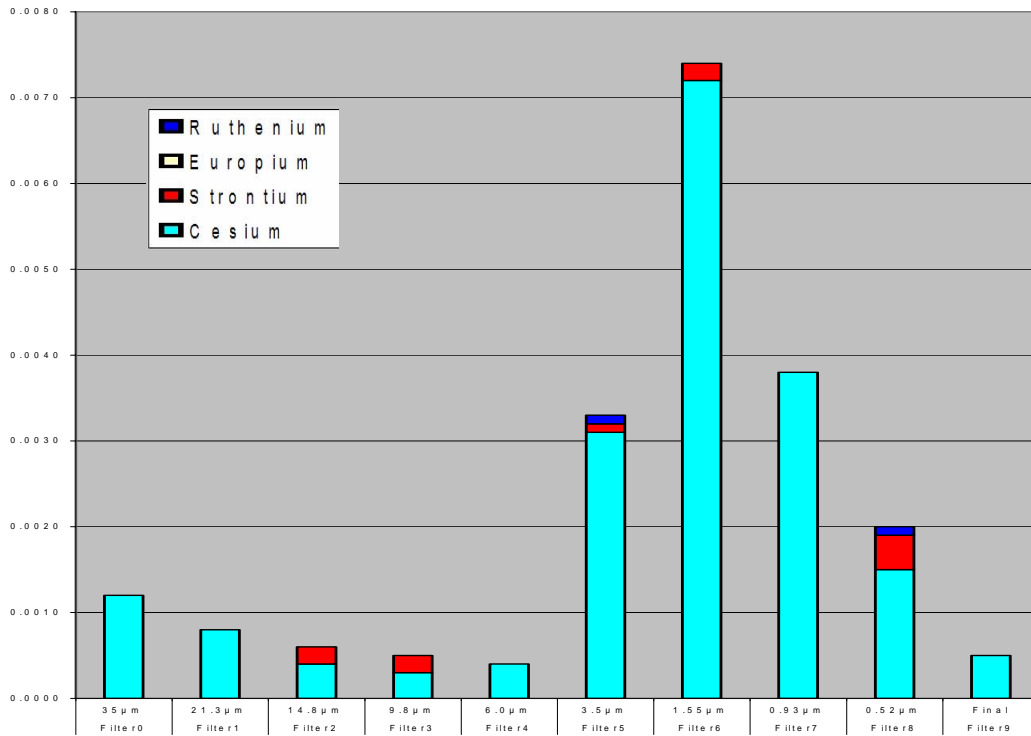


Figure A1.6.26 Test 2/6B, Marple #2941 (low) Fission Product Dopant Analysis Distrib, mg

**Table A1.6.27 Test 2/6B, Weight Distribution of Impact Debris**

Sieve Fraction	Weight, g	%
1000 µm	19.7833	57.33
500 µm	1.9123	5.54
250 µm	2.8771	8.34
125 µm	3.4107	9.88
100 µm	1.7452	5.06
74 µm	3.2097	9.30
37 µm	1.3492	3.91
25 µm	0.0436	0.13
<25 µm	0.1745	0.51
<b>Total</b>	<b>34.5056</b>	<b>100.00</b>

**Table A1.6.28 Test 2/6B, Elemental Analysis. Wt% of Sieved Impact Debris**

Test 2/6A Sieve Fraction	125 µm	100 µm	74 µm	37 µm	25 µm	<25 µm
Cerium	42.360	48.020	48.020	46.600	46.600	47.230
Iron	16.950	12.980	11.190	11.300	11.390	11.460
Copper	4.063	3.543	3.540	3.814	3.744	3.785
Zirconium	2.005	2.140	2.590	3.319	3.657	3.968
Aluminum	4.346	3.951	4.036	4.521	4.550	4.489
Manganese	0.149	0.096	0.075	0.086	0.090	0.086
Tin	0.038	0.047	0.057	0.073	0.086	0.091
Chromium	0.023	0.016	0.015	0.016	0.017	0.017
Magnesium	0.049	0.040	0.041	0.043	0.043	0.043
Boron	0.002	0.002	0.001	0.001	0.006	0.004
Lithium	0.000	0.000	0.000	0.000	0.000	0.000
Nickel	0.016	0.010	0.009	0.009	0.009	0.009
Titanium	0.115	0.096	0.100	0.107	0.091	0.091
Molybdenum	0.003	0.002	0.001	0.002	0.001	0.001
Lead	0.003	0.004	0.004	0.005	0.004	0.006
Barium	0.007	0.006	0.006	0.006	0.006	0.006
Bismuth	0.000	0.000	0.000	0.000	0.003	0.000
Strontium	0.005	0.005	0.006	0.008	0.009	0.010
Cesium	0.007	0.009	0.010	0.012	0.010	0.012
Ruthenium	0.000	0.001	0.002	0.002	0.004	0.003
<b>Total *</b>	<b>70.157</b>	<b>70.984</b>	<b>69.721</b>	<b>69.944</b>	<b>70.345</b>	<b>71.334</b>
Lanthanum	0.002	0.002	0.002	0.001	0.002	0.001
Praeseodymium	0.001	0.001	0.001	0.001	0.002	0.001
Neodymium	0.002	0.001	0.001	0.001	0.001	0.001
Samarium	0.000	0.000	0.000	0.000	0.000	0.000
Europium	0.005	0.006	0.008	0.010	0.013	0.013
Terbium	0.005	0.005	0.005	0.005	0.005	0.005

\* includes "minor" lanthanides shown in Table

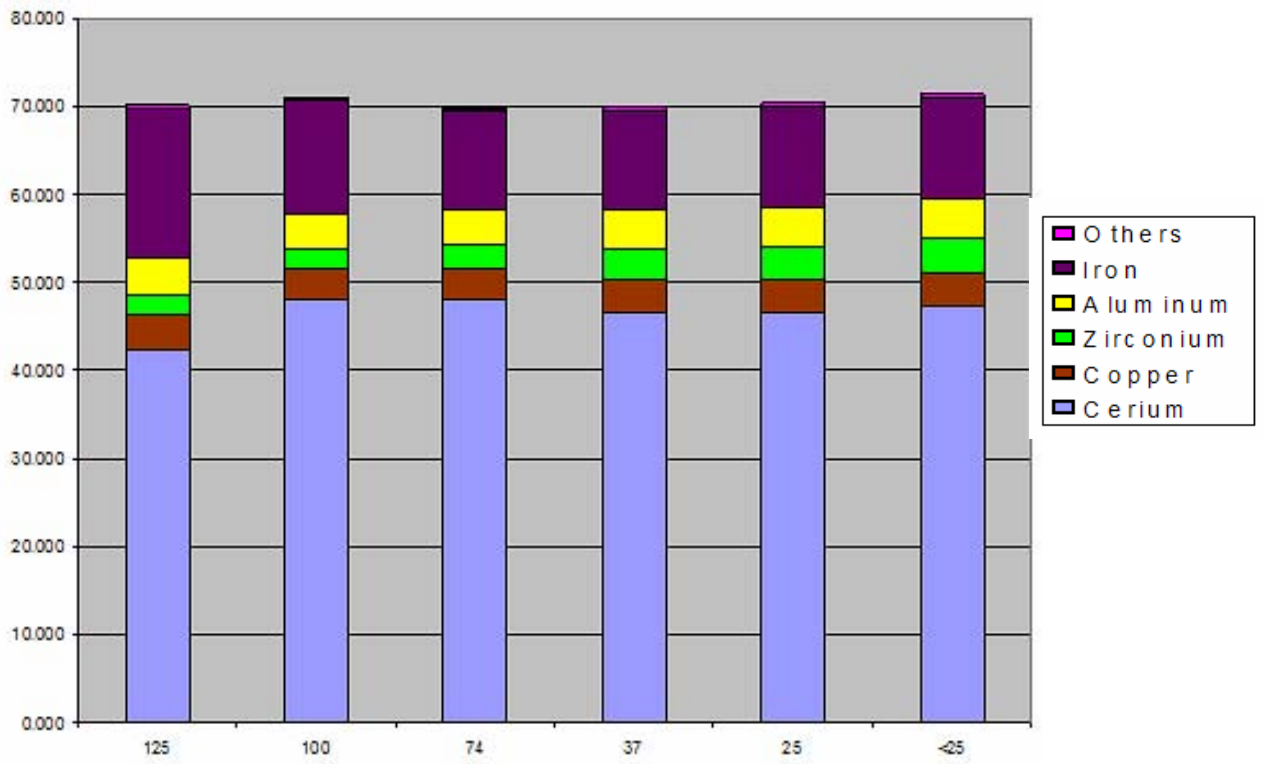


Figure A1.6.27 Test 2/6B Weight % Distribution of Metals in Impact Debris

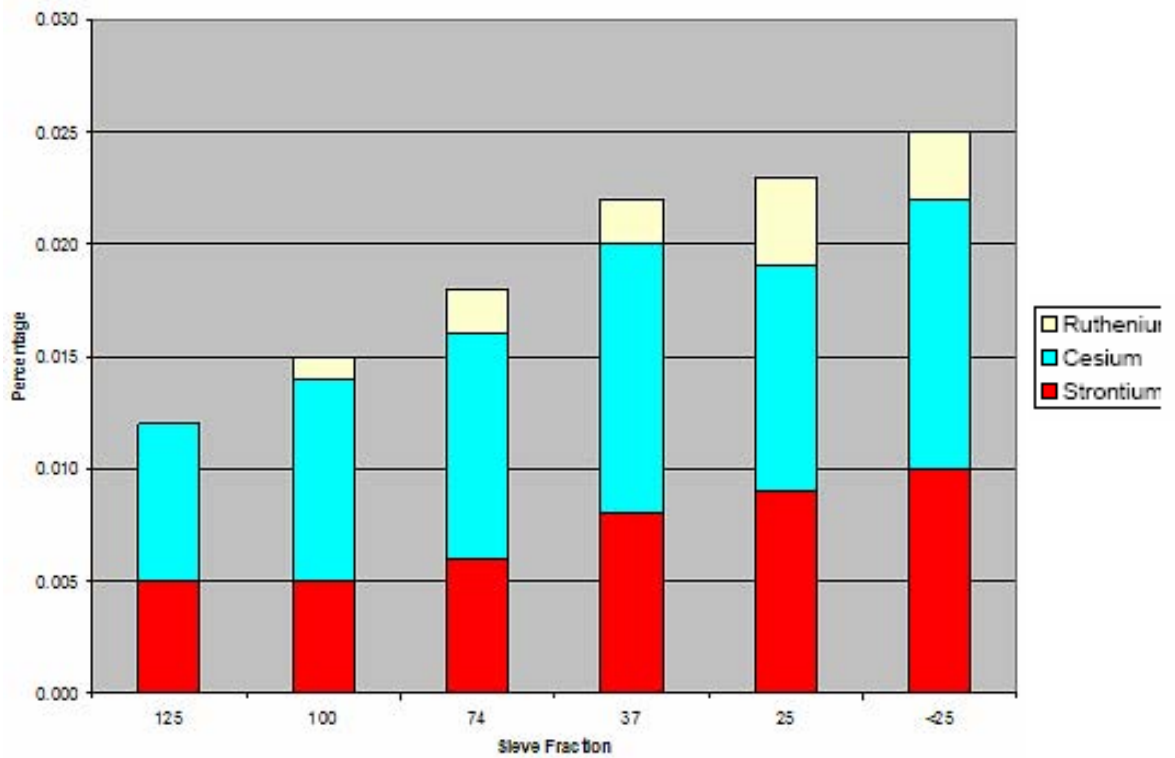


Figure A1.6.28 Test 2/6B Weight % Distribution of Fission Products in Impact Debris

### A.1.7B Test 2/7B Analyses and Results

Most particle samples were returned to Fraunhofer ITEM for post-test analyses, including all samples for tests 2/7A. For test 2/7N, one Marple impactor, # 2941 (low), with fiberglass stage/filter media, was analyzed at SNL for particle elemental analyses, as listed in Table A1.7.11.

**Table A1.7.1 Test 2/7B, Marple #2941 (low) Elemental Analyses, mg**

Stage	0	1	2	3	4	5	6	7	8	9	
Particle Size	35 µm	21.3 µm	14.8 µm	9.8 µm	6.0 µm	3.5 µm	1.55 µm	0.93 µm	0.52 µm	< 0.5 µm	
Al	0.1389	0.1628		0.1176	0.1491	0.2613	0.2391	0.2498			
Cu	0.0710	0.0390	0.0201	0.0159	0.0205	0.0798	0.3271	0.3252	0.1032	0.0078	
Fe	0.0647	0.0289	0.0123	0.0200	0.0328	0.0709	0.1620	0.1621	0.0663	0.0074	
Cr	0.0041	0.0008	0.0003	0.0006	0.0010	0.0024	0.0037	0.0039	0.0015		
Mg	0.0037	0.0061		0.0041	0.0035	0.0099	0.0088	0.0082		0.0002	
Ni	0.0021	0.0004	0.0002	0.0003	0.0004	0.0010	0.0019	0.0020	0.0008	0.0002	
Ti	0.0015	0.0012	0.0002	0.0010	0.0010	0.0050	0.0030	0.0027	0.0008	0.0004	
Cs	0.0014	0.0008	0.0005	0.0003	0.0003	0.0014	0.0059	0.0064	0.0028	0.0002	
Ce	0.0014	0.0005	0.0002	0.0012	0.0023	0.0022	0.0006				
Mn	0.0013	0.0006	0.0002	0.0003	0.0005	0.0014	0.0036	0.0036	0.0013	0.0002	
Sn	0.0012					0.0012	0.0063	0.0069	0.0020		
Mo	0.0004	0.0002	0.0001		0.0001	0.0004	0.0014	0.0016	0.0007		
Pb	0.0003	0.0002				0.0004	0.0009	0.0009	0.0003		
Zr	0.0002	0.0003		0.0004	0.0004	0.0014	0.0003				
La	0.0001			0.0001	0.0002	0.0003	0.0001				
Sr				0.0002		0.0002					
Nd					0.0001	0.0002					
Sb						0.0001	0.0003	0.0003	0.0001		
mg, Total	<b>0.2923</b>	<b>0.2418</b>	<b>0.0494</b>	<b>0.1620</b>	<b>0.2122</b>	<b>0.4397</b>	<b>0.7650</b>	<b>0.7736</b>	<b>0.7472</b>	<b>0.0164</b>	

### A.1.8A Test 2/8A Analyses and Results

Test 2/8A was a “blank” tests, with no target rod, with four Marple impactors, two high (chamber top, Marples # 2935 and # 2938) and low (at approximately the target rodlet height, Marples # 2937 and # 2941) in the aerosol chamber, to monitor particle stratification and settling, e.g., the particle/soot distribution. There also was a separate, additional line of six sequential Gelman filter samples, all sampling at the “high” level. Measured particle size distributions and mass concentration distribution data are shown in the following Figures A1.8.1 through A1.8.6.

The impact debris from this “blank” test was also collected, mechanically sieved, and analyzed by ICP-MS (total\* includes expanded list of “minor” lanthanides). The weight distribution and chemical analyses for this impact debris are listed in Tables A1.8.1 and A1.8.2, respectively. Figure A1.8.7 and A1.8.8 show distributions of metals and fission products in the impact debris.

**Table A1.8.1 Test 2/8A, Weight Distribution of Impact Debris**

Sieve Fraction	Weight, g	%
1000 µm	3.1345	40.37
500 µm	1.4261	18.37
250 µm	1.4387	18.53
125 µm	0.9761	12.57
100 µm	0.2355	3.03
74 µm	0.2739	3.53
37 µm	0.1982	2.55
25 µm	0.0321	0.41
<25 µm	0.0498	0.64
<b>Total</b>	<b>7.7649</b>	<b>100.00</b>

**Table A1.8.2 Test 2/8A, Elemental Analysis. Wt% of Sieved Impact Debris**

Test 2/8A Sieve Fraction	125 µm	100 µm	74 µm	37 µm	25 µm	<25 µm
Cerium	3.328	3.214	3.369	4.107	4.509	7.441
Iron	39.150	38.670	39.080	38.270	36.720	33.780
Copper	9.062	8.659	8.513	8.861	9.570	10.480
Zirconium	0.390	0.338	0.348	0.368	0.420	0.502
Aluminum	6.637	7.545	7.958	8.354	8.738	9.513
Manganese	0.507	0.464	0.478	0.435	0.445	0.378
Tin	0.045	0.045	0.044	0.047	0.067	0.094
Chromium	0.224	0.173	0.165	0.135	0.137	0.110
Magnesium	0.343	0.313	0.314	0.279	0.297	0.280
Boron	0.335	0.208	0.179	0.100	0.067	0.054
Lithium	0.138	0.091	0.075	0.046	0.043	0.029
Nickel	0.132	0.098	0.096	0.077	0.081	0.063
Titanium	0.371	0.323	0.309	0.262	0.260	0.201
Molybdenum	0.049	0.040	0.036	0.030	0.037	0.043
Lead	0.005	0.007	0.004	0.006	0.008	0.012
Barium	0.054	0.040	0.033	0.027	0.031	0.019
Bismuth	0.002	0.004	0.000	0.003	0.002	0.003
Strontium	0.018	0.013	0.011	0.008	0.008	0.004
Cesium	0.022	0.014	0.011	0.007	0.009	0.011
Ruthenium	0.000	0.000	0.000	0.000	0.000	0.000
<b>Total *</b>	<b>61.109</b>	<b>60.456</b>	<b>61.192</b>	<b>61.530</b>	<b>61.545</b>	<b>63.074</b>
Lanthanum	0.150	0.103	0.086	0.056	0.050	0.037
Praeseodymium	0.025	0.017	0.014	0.009	0.008	0.004
Neodymium	0.098	0.061	0.056	0.034	0.030	0.012
Samarium	0.020	0.014	0.011	0.007	0.006	0.003
Europium	0.003	0.002	0.002	0.002	0.002	0.001
Terbium	0.001	0.000	0.000	0.000	0.000	0.000

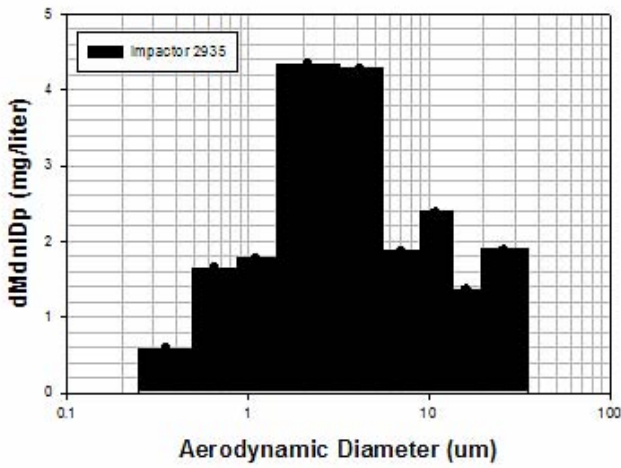


Figure A1.8.1 Test 2/8A Marple 2935 (high) Particle Size Distribution

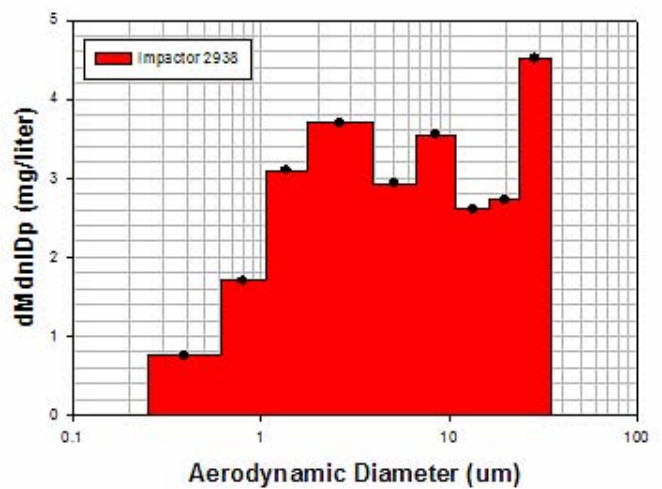


Figure A1.8.2 Test 2/8A Marple 2938 (high) Particle Size Distribution

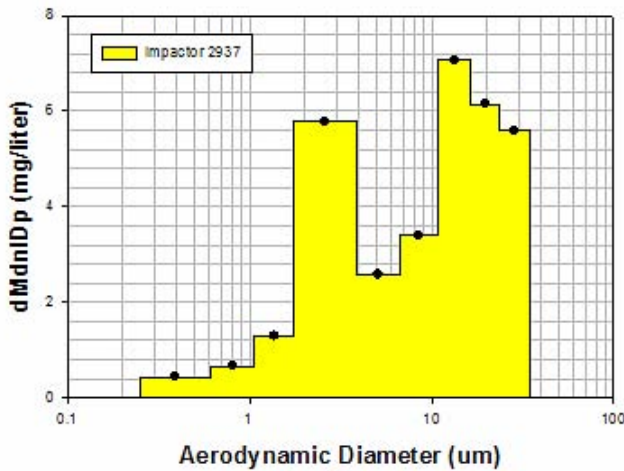


Figure A1.8.3 Test 2/8A Marple 2937 (low) Particle Size Distribution

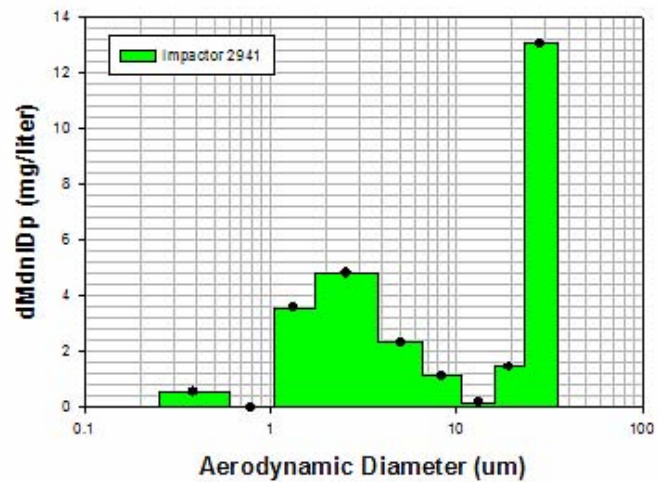


Figure A1.8.4 Test 2/8A Marple 2941 (low) Particle Size Distribution

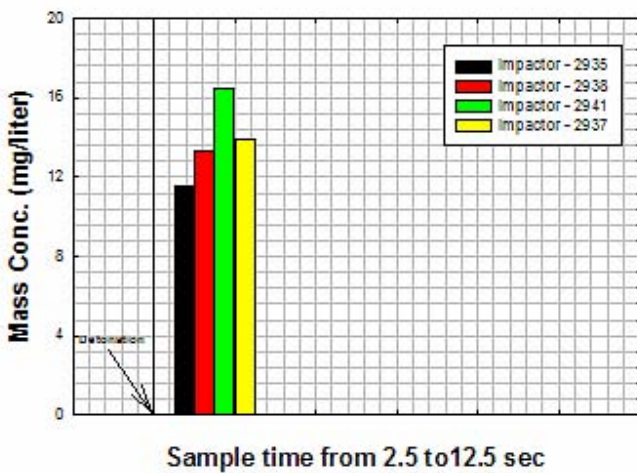


Figure A1.8.5 Test 2/8A Marple Impactors Mass Concentration

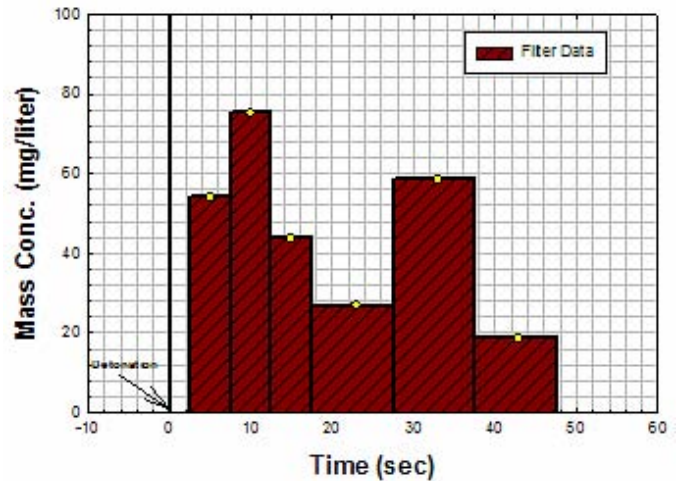


Figure A1.8.6 Test 2/8A Gelman Filters Mass Concentration

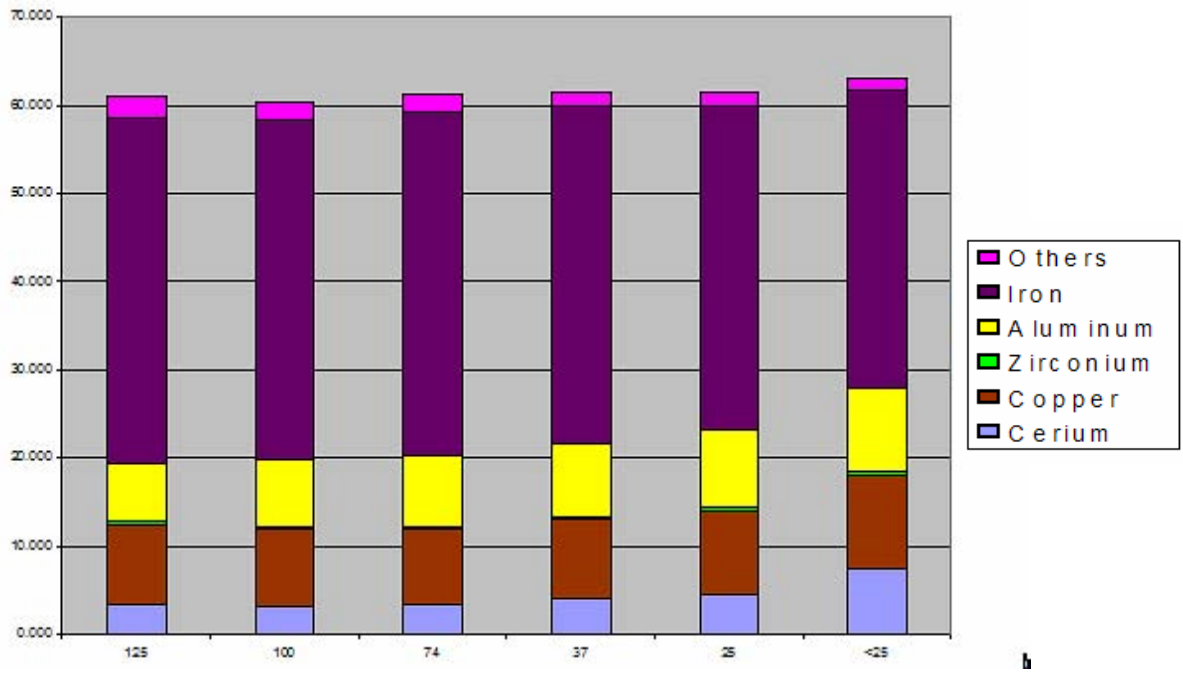


Figure A1.8.7 Test 2/8A Weight % Distribution of Metals in Impact Debris

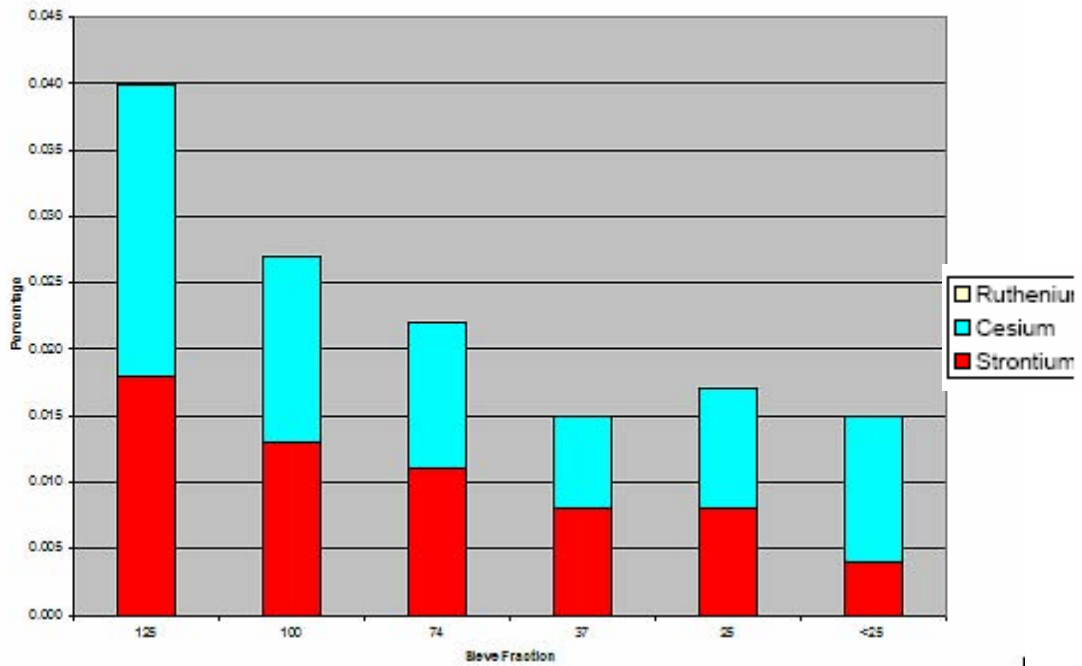


Figure A1.8.8 Test 2/8A Weight % Distribution of Fission Products in Impact Debris

### A.1.8B Test 2/8B Analyses and Results

Test 2/8B was a replicate of 2/8A, with identical aerosol sampler configuration. The following tables and figures parallel those for test 2/8A.

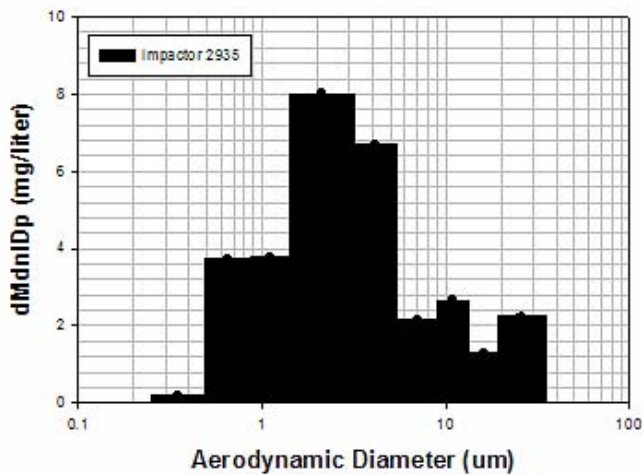


Figure A1.8.9 Test 2/8B Marple 2935 (high) Particle Size Distribution

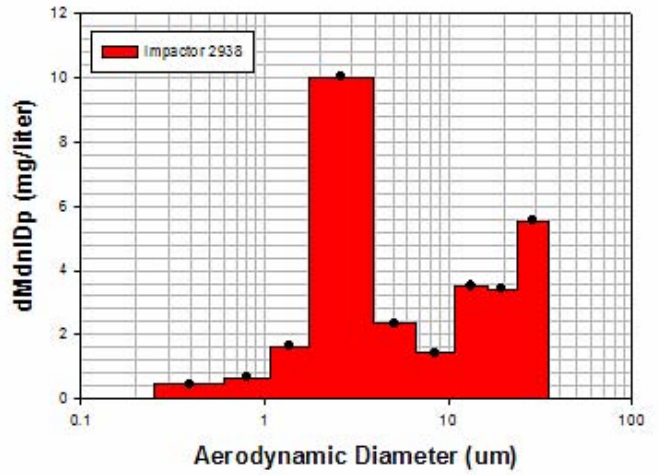


Figure A1.8.10 Test 2/8B Marple 2938 (high) Particle Size Distribution

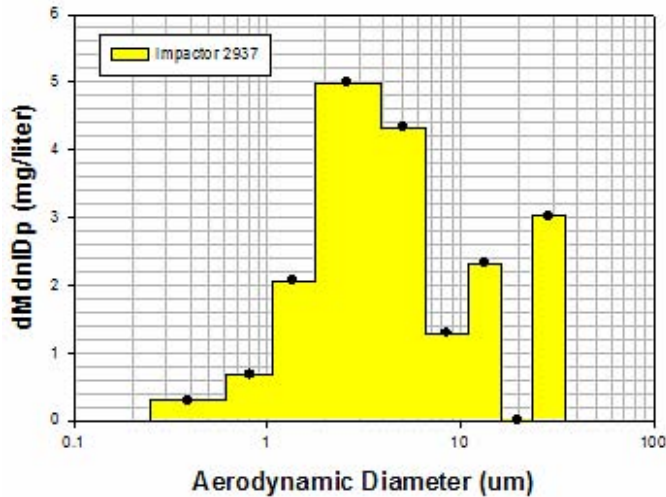


Figure A1.8.11 Test 2/8B Marple 2937 (low) Particle Size Distribution

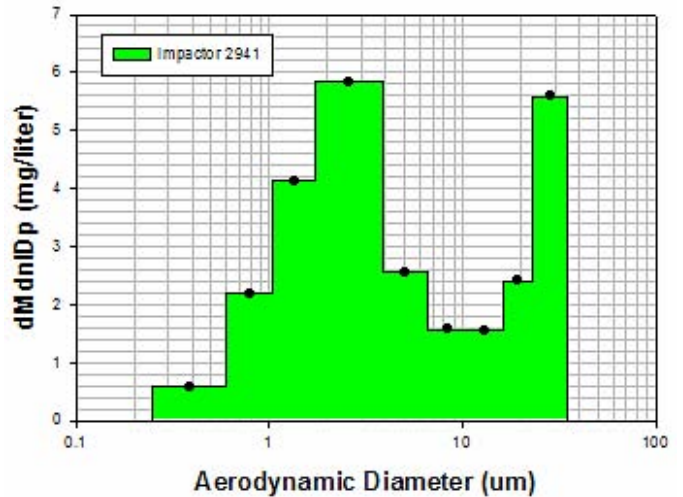


Figure A1.8.12 Test 2/8B Marple 2941 (low) Particle Size Distribution

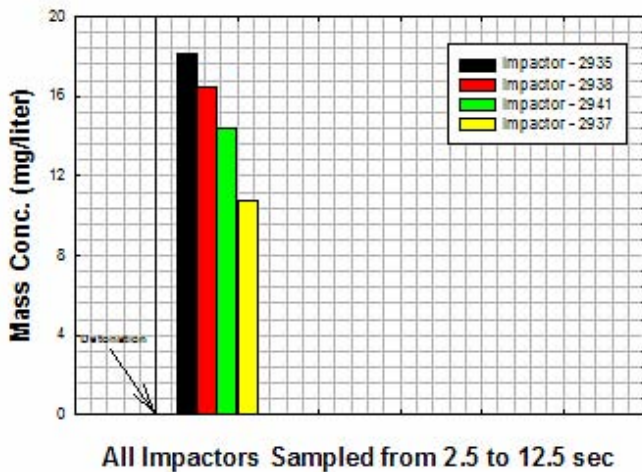


Figure A1.8.13 Test 2/8B Marple Impactors Mass Concentration

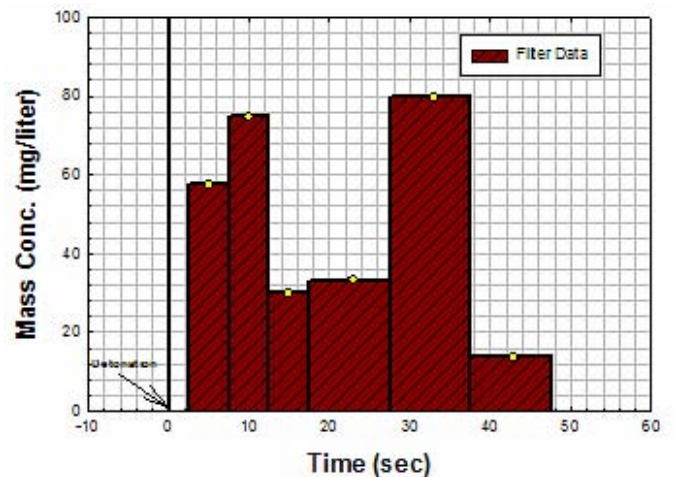


Figure A1.8.14 Test 2/8B Gelman Filters Mass Concentration

**Table A1.8.3 Test 2/8B, Weight Distribution of Impact Debris**

Sieve Fraction	Weight, g	%
1000 µm	3.3190	63.75
500 µm	0.2931	5.63
250 µm	0.7372	14.16
125 µm	0.4702	9.03
100 µm	0.1103	2.12
74 µm	0.1023	1.97
37 µm	0.1163	2.23
25 µm	0.0119	0.23
<25 µm	0.0458	0.88
<b>Total</b>	<b>5.2061</b>	<b>100.00</b>

**Table A1.8.4 Test 2/8B, Elemental Analysis. Wt% of Sieved Impact Debris**

Test 2/8B Sieve Fraction		125 µm	100 µm	74 µm	37 µm	25 µm	<25 µm
Cerium		2.654	2.839	3.117	3.785	4.483	6.147
Iron		37.580	39.580	39.620	38.690	38.470	34.490
Copper		9.445	9.221	8.598	8.206	8.184	10.080
Zirconium		0.362	0.324	0.325	0.352	0.401	0.378
Aluminum		8.389	8.956	8.891	10.350	10.570	11.180
Manganese		0.425	0.422	0.416	0.402	0.399	0.352
Tin		0.096	0.088	0.085	0.080	0.086	0.149
Chromium		0.138	0.118	0.111	0.095	0.094	0.081
Magnesium		0.318	0.296	0.303	0.294	0.299	0.317
Boron		0.155	0.109	0.080	0.046	0.043	0.026
Lithium		0.072	0.045	0.036	0.022	0.020	0.019
Nickel		0.087	0.075	0.068	0.058	0.063	0.048
Titanium		0.338	0.282	0.283	0.270	0.258	0.276
Molybdenum		0.035	0.025	0.022	0.016	0.015	0.017
Lead		0.008	0.007	0.006	0.005	0.004	0.012
Barium		0.031	0.024	0.021	0.016	0.017	0.011
Strontium		0.010	0.007	0.006	0.004	0.004	0.003
Cesium		0.012	0.007	0.005	0.003	0.003	0.006
Ruthenium		0.000	0.000	0.000	0.000	0.000	0.000
<b>Total *</b>		<b>60.301</b>	<b>62.527</b>	<b>62.077</b>	<b>62.748</b>	<b>63.467</b>	<b>63.616</b>
Lanthanum		0.076	0.053	0.044	0.028	0.028	0.012
Praeseodymium		0.012	0.009	0.007	0.005	0.005	0.002
Neodymium		0.046	0.032	0.026	0.016	0.016	0.007
Samarium		0.010	0.007	0.006	0.004	0.004	0.002
Europium		0.002	0.001	0.001	0.001	0.001	0.001

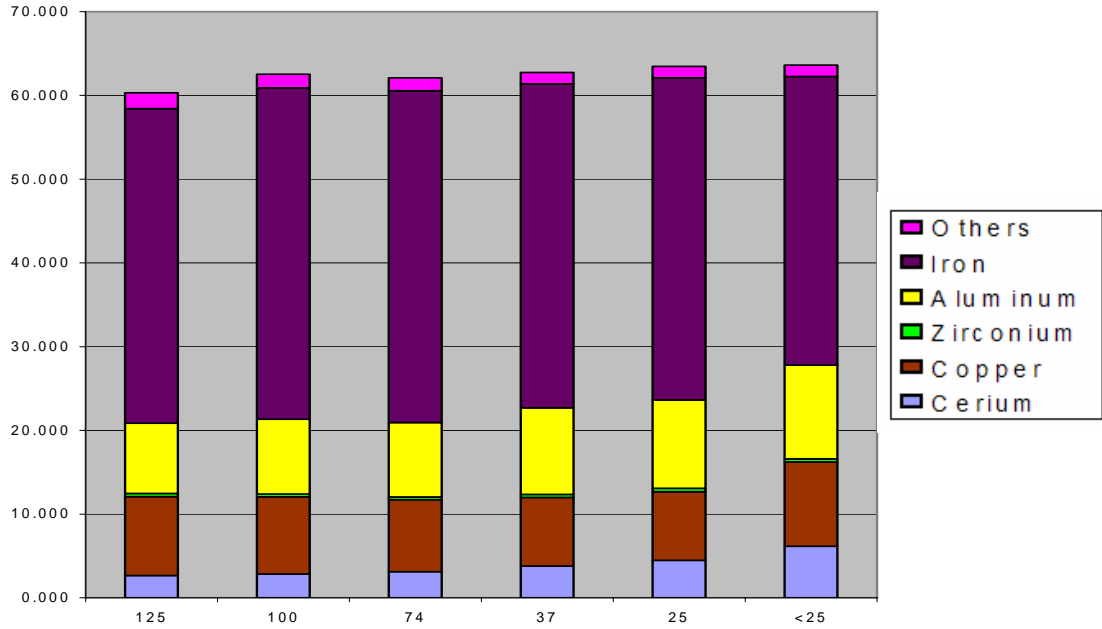


Figure A1.8.15 Test 2/8B Weight % Distribution of Metals in Impact Debris

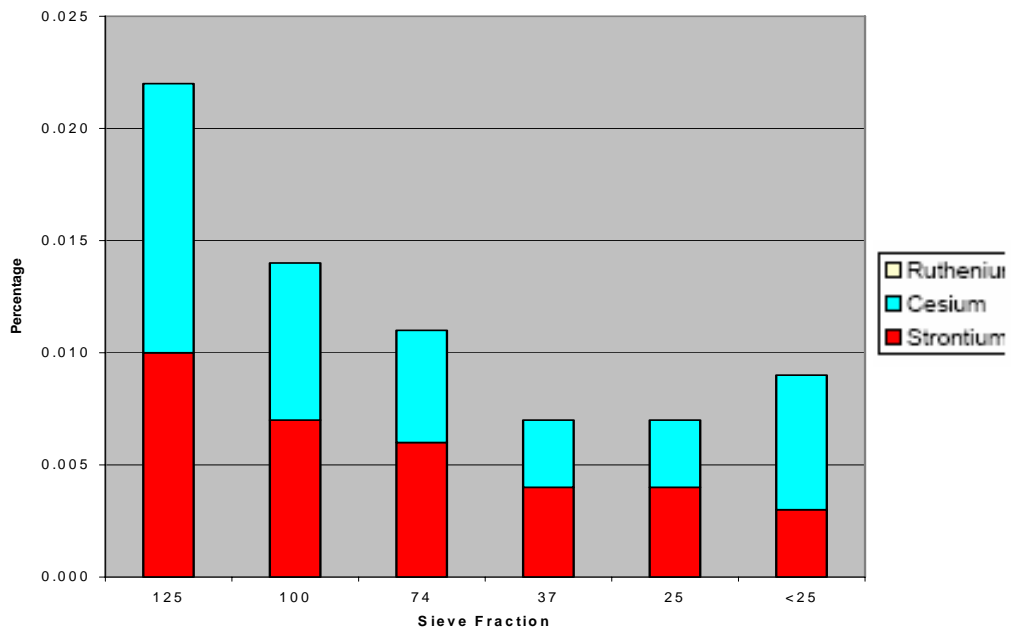


Figure A1.8.16 Test 2/8B Weight % Distribution of Fission Products in Impact Debris

### A.1.8C Test 2/8C Analyses and Results

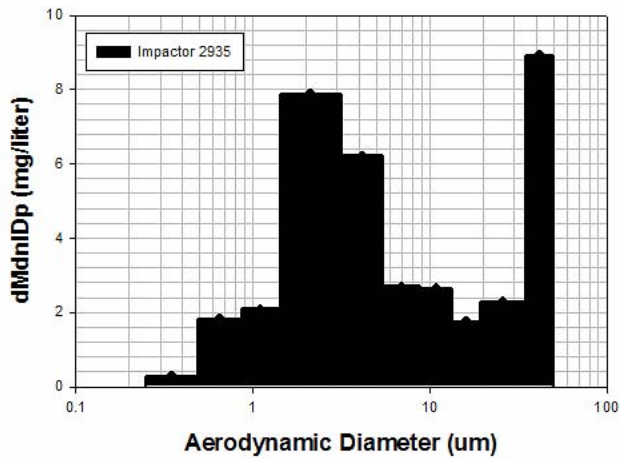


Figure A1.8.17 Test 2/8C Marple 2935 (high) Particle Size Distribution

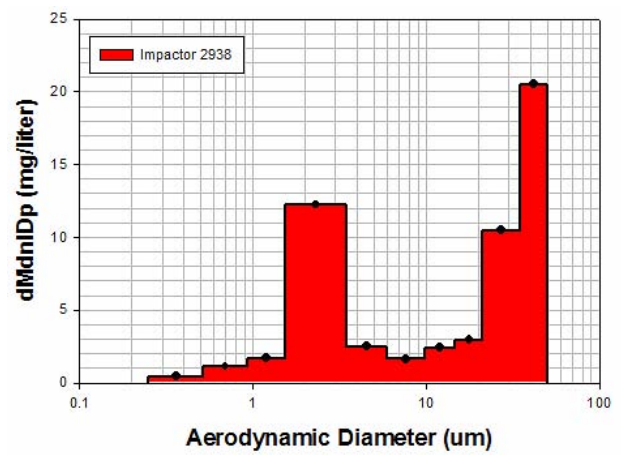


Figure A1.8.18 Test 2/8C Marple 2938 (high) Particle Size Distribution

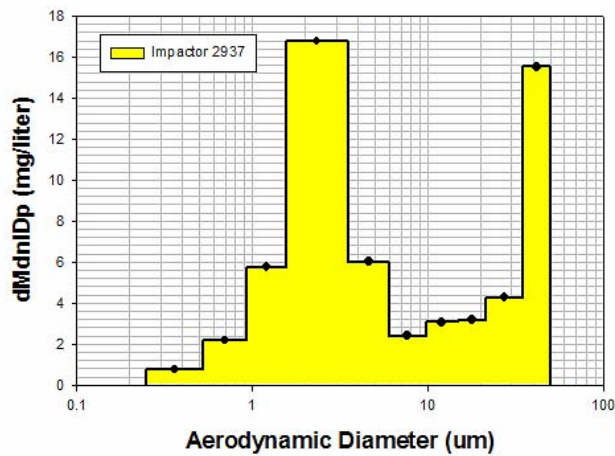


Figure A1.8.19 Test 2/8C Marple 2937 (low) Particle Size Distribution

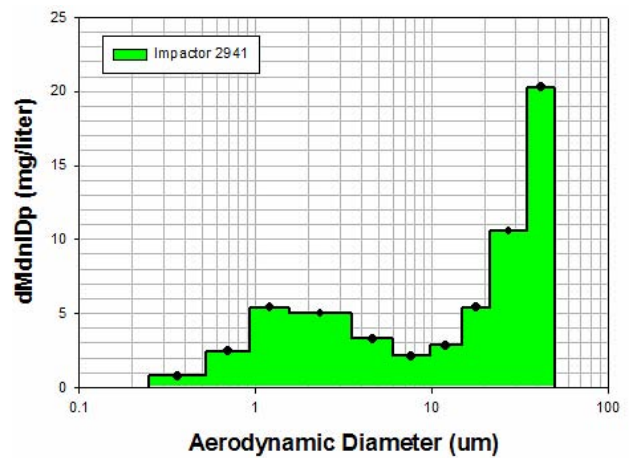


Figure A1.8.20 Test 2/8C Marple 2941 (low) Particle Size Distribution

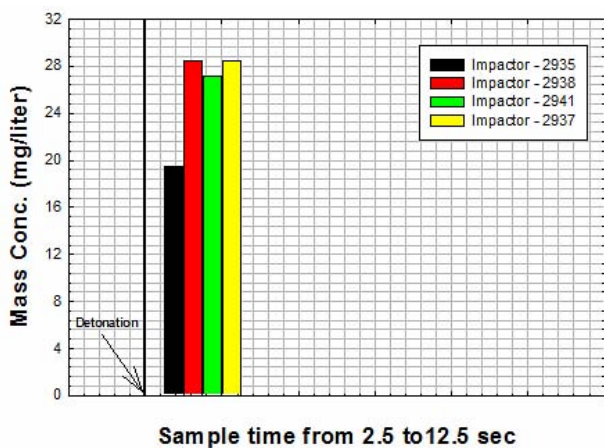


Figure A1.8.21 Test 2/8C Marple Impactors Mass Concentration

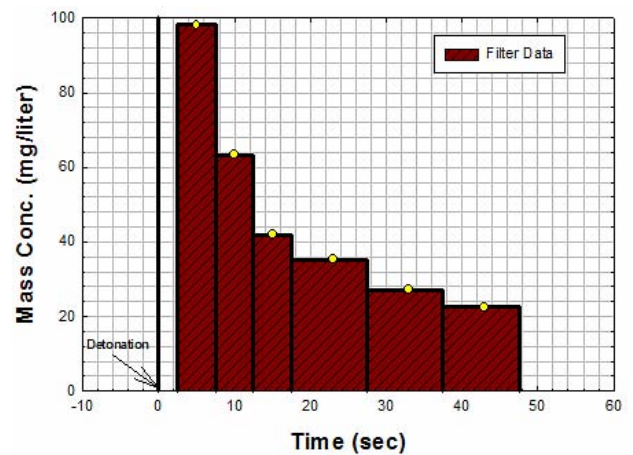


Figure A1.8.22 Test 2/8C Gelman Filters Mass Concentration

**Table A1.8.5 Test 2/8C, Marple #2935 (high) Elemental Analyses, Stages 0-3**

<b>2/8C</b>	<b>STAGE 0</b>			<b>STAGE 1</b>			<b>STAGE 2</b>			<b>STAGE 3</b>		
<b>#2935</b>	Particle size 35 µm			Particle size 21.3 µm			Particle size 14.8 µm			Particle size 9.8 µm		
	mg	% detected	% loading	mg	% detected	% loading	mg	% detected	% loading	mg	% detected	% loading
Ce	0.2702	41.6	21.2	0.1035	32.9	18.9	0.0457	38.7	17.8	0.1088	46.0	24.7
Cu	0.1403	21.6	11.0	0.0824	26.2	15.0	0.0327	27.7	12.7	0.0395	16.7	9.0
Zr	0.0486	7.5	3.8	0.0226	7.2	4.1	0.0091	7.7	3.5	0.0241	10.2	5.5
Fe	0.1556	23.9	12.2	0.0710	22.6	13.0	0.0286	24.2	11.1	0.0606	25.6	13.8
Al	0.0225	3.5	1.8	0.0263	8.4	4.8	0.0000	0.0	0.0	0.0000	0.0	0.0
Mg	0.0000	0.0	0.0	0.0019	0.6	0.3	0.0000	0.0	0.0	0.0000	0.0	0.0
Cr	0.0008	0.1	0.1	0.0005	0.2	0.1	0.0000	0.0	0.0	0.0002	0.1	0.0
Ni	0.0005	0.1	0.0	0.0004	0.1	0.1	0.0000	0.0	0.0	0.0000	0.0	0.0
Mn	0.0026	0.4	0.2	0.0013	0.4	0.2	0.0005	0.4	0.2	0.0010	0.4	0.2
Sn	0.0041	0.6	0.3	0.0022	0.7	0.4	0.0009	0.8	0.3	0.0014	0.6	0.3
Mo	0.0003	0.0	0.0	0.0002	0.1	0.0	0.0000	0.0	0.0	0.0000	0.0	0.0
Ti	0.0017	0.3	0.1	0.0007	0.2	0.1	0.0000	0.0	0.0	0.0005	0.2	0.1
Li	0.0000	0.0	0.0	0.0000	0.0	0.0	0.0000	0.0	0.0	0.0000	0.0	0.0
Pb	0.0004	0.1	0.0	0.0003	0.1	0.1	0.0000	0.0	0.0	0.0000	0.0	0.0
Cs	0.0021	0.3	0.2	0.0012	0.4	0.2	0.0005	0.4	0.2	0.0006	0.3	0.1
Sr	0.0000	0.0	0.0	0.0000	0.0	0.0	0.0000	0.0	0.0	0.0000	0.0	0.0
Ru	0.0000	0.0	0.0	0.0000	0.0	0.0	0.0000	0.0	0.0	0.0000	0.0	0.0
mg, Metals Found	<b>0.6497</b>	<b>100.0</b>	<b>51.0</b>	<b>0.3145</b>	<b>100.0</b>	<b>57.4</b>	<b>0.1180</b>	<b>100.0</b>	<b>45.8</b>	<b>0.2367</b>	<b>100.0</b>	<b>53.7</b>
mg, Filter Loading	<b>1.2734</b>			<b>0.5480</b>			<b>0.2574</b>			<b>0.4405</b>		

**Table A1.8.6 Test 2/8C, Marple #2935 (high) Elemental Analyses, Stages 4-7**

<b>2/8C</b>	<b>STAGE 4</b>			<b>STAGE 5</b>			<b>STAGE 6</b>			<b>STAGE 7</b>		
<b>#2935</b>	Particle size 6.0 µm			Particle size 3.5 µm			Particle size 1.55 µm			Particle size 0.93 µm		
	mg	% detected	% loading	mg	% detected	% loading	mg	% detected	% loading	mg	% detected	% loading
Ce	0.0734	34.5	13.7	0.0629	10.0	4.7	0.0290	2.6	1.1	0.0052	2.5	1.2
Cu	0.0558	26.2	10.4	0.3395	53.9	25.3	0.5952	53.4	23.2	0.1360	65.4	32.2
Zr	0.0223	10.5	4.2	0.0340	5.4	2.5	0.0362	3.2	1.4	0.0071	3.4	1.7
Fe	0.0566	26.6	10.6	0.1379	21.9	10.3	0.2032	18.2	7.9	0.0422	20.3	10.0
Mg	0.0000	0.0	0.0	0.0399	6.3	3.0	0.2176	19.5	8.5	0.0112	5.4	2.6
Al	0.0000	0.0	0.0	0.0000	0.0	0.0	0.0000	0.0	0.0	0.0000	0.0	0.0
Cr	0.0000	0.0	0.0	0.0003	0.0	0.0	0.0005	0.0	0.0	0.0000	0.0	0.0
Ni	0.0000	0.0	0.0	0.0003	0.0	0.0	0.0009	0.1	0.0	0.0000	0.0	0.0
Mn	0.0009	0.4	0.2	0.0029	0.5	0.2	0.0051	0.5	0.2	0.0011	0.5	0.3
Sn	0.0015	0.7	0.3	0.0048	0.8	0.4	0.0096	0.9	0.4	0.0024	1.2	0.6
Mo	0.0000	0.0	0.0	0.0005	0.1	0.0	0.0012	0.1	0.0	0.0002	0.1	0.0
Ti	0.0014	0.7	0.3	0.0016	0.3	0.1	0.0018	0.2	0.1	0.0000	0.0	0.0
Li	0.0000	0.0	0.0	0.0003	0.0	0.0	0.0006	0.1	0.0	0.0000	0.0	0.0
Pb	0.0000	0.0	0.0	0.0008	0.1	0.1	0.0018	0.2	0.1	0.0004	0.2	0.1
Cs	0.0008	0.4	0.1	0.0047	0.7	0.3	0.0115	1.0	0.4	0.0022	1.1	0.5
Sr	0.0000	0.0	0.0	0.0000	0.0	0.0	0.0000	0.0	0.0	0.0000	0.0	0.0
Ru	0.0000	0.0	0.0	0.0000	0.0	0.0	0.0000	0.0	0.0	0.0000	0.0	0.0
mg, Metals Found	<b>0.2127</b>	<b>100.0</b>	<b>39.8</b>	<b>0.6304</b>	<b>100.0</b>	<b>46.9</b>	<b>1.1142</b>	<b>100.0</b>	<b>43.4</b>	<b>0.2080</b>	<b>100.0</b>	<b>49.2</b>
mg, Filter Loading	<b>0.5346</b>			<b>1.3443</b>			<b>2.5683</b>			<b>0.4227</b>		

**Table A1.8.7 Test 2/8C, Marple #2935 (high) Elemental Analyses, Stages 8-9**

<b>2/8C</b>	<b>STAGE 8</b>			<b>STAGE 9</b>								
<b>#2935</b>	Particle size 0.52 µm			Particle size final, >0.5 µm								
	<b>mg</b>	<b>% detected</b>	<b>% loading</b>	<b>mg</b>	<b>% detected</b>	<b>% loading</b>						
Ce	0.0062	3.4	1.5	0.0000	0.0	0.0						
Cu	0.1141	62.8	27.5	0.0057	73.1	7.3						
Zr	0.0091	5.0	2.2	0.0000	0.0	0.0						
Fe	0.0466	25.6	11.2	0.0015	19.2	1.9						
Mg	0.0000	0.0	0.0	0.0000	0.0	0.0						
Al	0.0000	0.0	0.0	0.0000	0.0	0.0						
Cr	0.0000	0.0	0.0	0.0000	0.0	0.0						
Ni	0.0000	0.0	0.0	0.0000	0.0	0.0						
Mn	0.0011	0.6	0.3	0.0000	0.0	0.0						
Sn	0.0024	1.3	0.6	0.0006	7.7	0.8						
Mo	0.0003	0.2	0.1	0.0000	0.0	0.0						
Ti	0.0000	0.0	0.0	0.0000	0.0	0.0						
Li	0.0000	0.0	0.0	0.0000	0.0	0.0						
Pb	0.0003	0.2	0.1	0.0000	0.0	0.0						
Cs	0.0017	0.9	0.4	0.0000	0.0	0.0						
Sr	0.0000	0.0	0.0	0.0000	0.0	0.0						
Ru	0.0000	0.0	0.0	0.0000	0.0	0.0						
mg, Metals Found	<b>0.1818</b>	<b>100.0</b>	<b>43.8</b>	<b>0.0078</b>	<b>100.0</b>	<b>10.1</b>						
mg, Filter Loading	<b>0.4153</b>			<b>0.0776</b>								

**Table A1.8.8 Test 2/8C, Marple #2935 Particle Cerium and Fission Product Distributions**

<b>2/8C #2935 high</b>	<b>Cerium</b>		<b>Cesium</b>		<b>Strontium</b>		<b>Ruthenium</b>	
	<b>mg</b>	<b>wt%</b>	<b>mg</b>	<b>wt%</b>	<b>mg</b>	<b>wt%</b>	<b>mg</b>	<b>wt%</b>
35µm and >	0.2702	38.3	0.0021	8.3	0.0000	0.0	0.0000	0.0
21.3µm	0.1035	14.7	0.0012	4.7	0.0000	0.0	0.0000	0.0
14.8µm	0.0457	6.5	0.0005	2.0	0.0000	0.0	0.0000	0.0
9.8µm	0.1088	15.4	0.0006	2.4	0.0000	0.0	0.0000	0.0
6.0µm	0.0734	10.4	0.0008	3.2	0.0000	0.0	0.0000	0.0
3.5µm	0.0629	8.9	0.0047	18.6	0.0000	0.0	0.0000	0.0
1.55µm	0.0290	4.1	0.0115	45.5	0.0000	0.0	0.0004	100.0
0.93µm	0.0052	0.7	0.0022	8.7	0.0000	0.0	0.0000	0.0
0.52µm	0.0062	0.9	0.0017	6.7	0.0000	0.0	0.0000	0.0
Final filter	0.0000	0.0	0.0000	0.0	0.0000	0.0	0.0000	0.0
<b>Sum</b>	<b>0.7049</b>		<b>0.0253</b>		<b>0.0000</b>		<b>0.0004</b>	

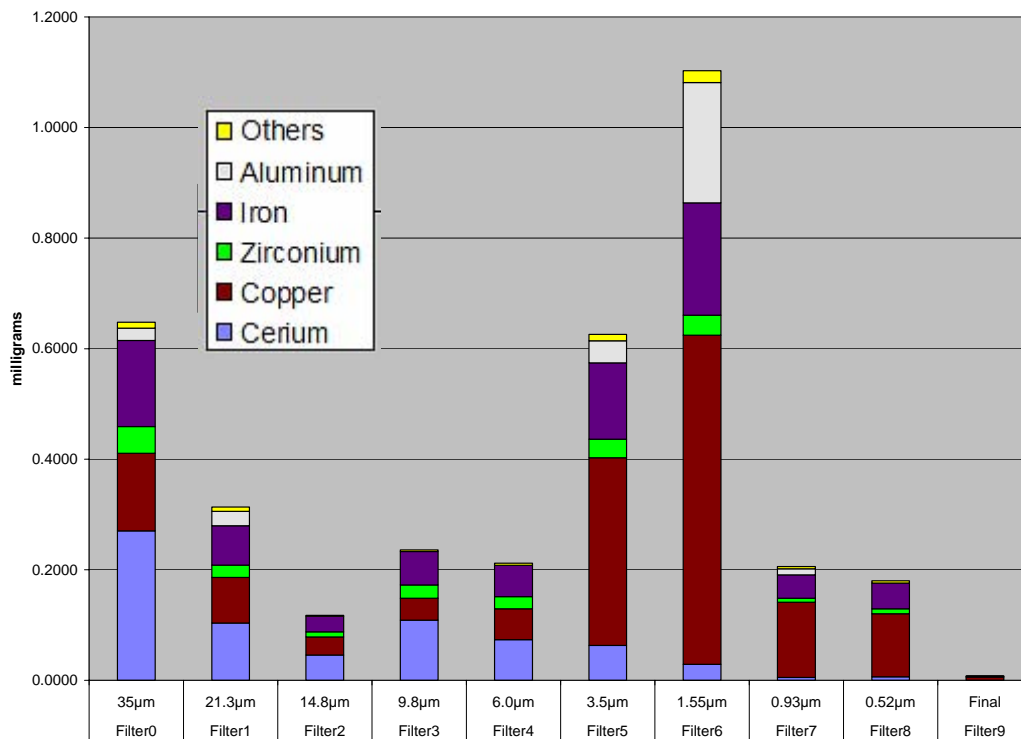


Figure A1.8.23 Test 2/8C, Marple #2935 (high) Metals Analysis Distribution, milligrams

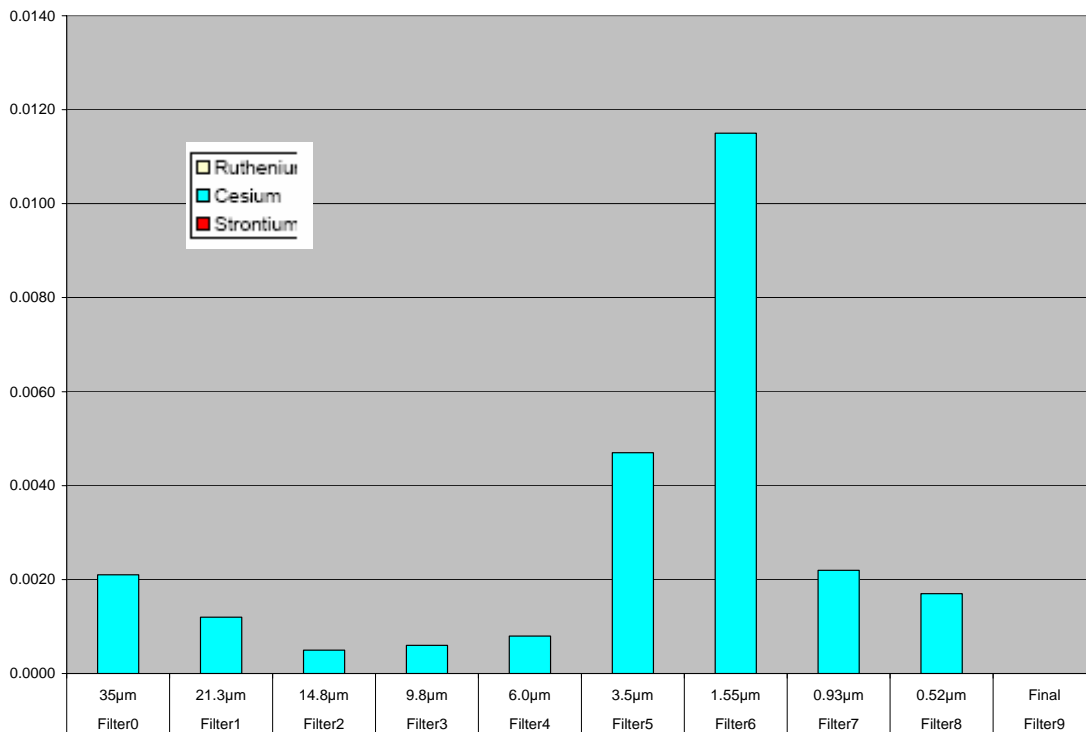


Figure A1.8.24 Test 2/8C, Marple #2935 (high) Fission Product Dopant Analysis Distrib, mg

**Table A1.8.9 Test 2/8C, Marple #2937 (low) Elemental Analyses, Stages 0-3**

<b>2/8C</b>	<b>STAGE 0</b>			<b>STAGE 1</b>			<b>STAGE 2</b>			<b>STAGE 3</b>		
<b>#2937</b>	Particle size 35 µm			Particle size 21.3 µm			Particle size 14.8 µm			Particle size 9.8 µm		
	mg	% detected	% loading	mg	% detected	% loading	mg	% detected	% loading	mg	% detected	% loading
Ce	0.3360	39.4	22.5	0.0944	34.6	16.3	0.0514	27.7	13.3	0.0901	36.1	23.3
Cu	0.1598	18.7	10.7	0.0795	29.2	13.7	0.0355	19.1	9.2	0.0328	13.1	8.5
Zr	0.0595	7.0	4.0	0.0199	7.3	3.4	0.0104	5.6	2.7	0.0197	7.9	5.1
Fe	0.2086	24.4	14.0	0.0713	26.1	12.3	0.0395	21.3	10.2	0.0543	21.7	14.0
Al	0.0730	8.6	4.9	0.0000	0.0	0.0	0.0434	23.4	11.2	0.0488	19.5	12.6
Mg	0.0008	0.1	0.1	0.0000	0.0	0.0	0.0017	0.9	0.4	0.0008	0.3	0.2
Cr	0.0025	0.3	0.2	0.0017	0.6	0.3	0.0009	0.5	0.2	0.0004	0.2	0.1
Ni	0.0015	0.2	0.1	0.0010	0.4	0.2	0.0006	0.3	0.2	0.0002	0.1	0.1
Mn	0.0032	0.4	0.2	0.0013	0.5	0.2	0.0007	0.4	0.2	0.0009	0.4	0.2
Sn	0.0037	0.4	0.2	0.0017	0.6	0.3	0.0010	0.5	0.3	0.0011	0.4	0.3
Mo	0.0005	0.1	0.0	0.0004	0.1	0.1	0.0000	0.0	0.0	0.0000	0.0	0.0
Ti	0.0018	0.2	0.1	0.0003	0.1	0.1	0.0000	0.0	0.0	0.0003	0.1	0.1
Li	0.0000	0.0	0.0	0.0000	0.0	0.0	0.0000	0.0	0.0	0.0000	0.0	0.0
Pb	0.0004	0.0	0.0	0.0000	0.0	0.0	0.0000	0.0	0.0	0.0000	0.0	0.0
Cs	0.0022	0.3	0.1	0.0012	0.4	0.2	0.0005	0.3	0.1	0.0004	0.2	0.1
Sr	0.0000	0.0	0.0	0.0000	0.0	0.0	0.0000	0.0	0.0	0.0000	0.0	0.0
Ru	0.0000	0.0	0.0	0.0000	0.0	0.0	0.0000	0.0	0.0	0.0000	0.0	0.0
mg, Metals Found	<b>0.8535</b>	<b>100.0</b>	<b>57.1</b>	<b>0.2727</b>	<b>100.0</b>	<b>47.1</b>	<b>0.1856</b>	<b>100.0</b>	<b>48.0</b>	<b>0.2498</b>	<b>100.0</b>	<b>64.6</b>
mg, Filter Loading	<b>1.4944</b>			<b>0.5792</b>			<b>0.3865</b>			<b>0.3865</b>		

**Table A1.8.10 Test 2/8C, Marple #2937 (low) Elemental Analyses, Stages 4-7**

<b>2/8C</b>	<b>STAGE 4</b>			<b>STAGE 5</b>			<b>STAGE 6</b>			<b>STAGE 7</b>		
<b>#2937</b>	Particle size 6.0 µm			Particle size 3.5 µm			Particle size 1.55 µm			Particle size 0.93 µm		
	mg	% detected	% loading	mg	% detected	% loading	mg	% detected	% loading	mg	% detected	% loading
Ce	0.0637	41.5	19.9	0.0654	14.1	7.4	0.0435	2.6	1.2	0.0102	2.5	1.3
Cu	0.0324	21.1	10.1	0.2090	45.0	23.6	0.8156	48.6	21.9	0.2519	60.7	31.4
Zr	0.0175	11.4	5.5	0.0329	7.1	3.7	0.0512	3.1	1.4	0.0145	3.5	1.8
Fe	0.0372	24.2	11.6	0.0959	20.7	10.8	0.2420	14.4	6.5	0.0808	19.5	10.1
Mg	0.0000	0.0	0.0	0.0488	10.5	5.5	0.4799	28.6	12.9	0.0451	10.9	5.6
Al	0.0000	0.0	0.0	0.0000	0.0	0.0	0.0034	0.2	0.1	0.0000	0.0	0.0
Cr	0.0003	0.2	0.1	0.0004	0.1	0.0	0.0010	0.1	0.0	0.0004	0.1	0.0
Ni	0.0002	0.1	0.1	0.0004	0.1	0.0	0.0014	0.1	0.0	0.0005	0.1	0.1
Mn	0.0007	0.5	0.2	0.0020	0.4	0.2	0.0064	0.4	0.2	0.0019	0.5	0.2
Sn	0.0009	0.6	0.3	0.0038	0.8	0.4	0.0115	0.7	0.3	0.0039	0.9	0.5
Mo	0.0000	0.0	0.0	0.0004	0.1	0.0	0.0016	0.1	0.0	0.0004	0.1	0.0
Ti	0.0002	0.1	0.1	0.0012	0.3	0.1	0.0023	0.1	0.1	0.0003	0.1	0.0
Li	0.0000	0.0	0.0	0.0002	0.0	0.0	0.0009	0.1	0.0	0.0004	0.1	0.0
Pb	0.0000	0.0	0.0	0.0005	0.1	0.1	0.0023	0.1	0.1	0.0006	0.1	0.1
Cs	0.0005	0.3	0.2	0.0032	0.7	0.4	0.0148	0.9	0.4	0.0041	1.0	0.5
Sr	0.0000	0.0	0.0	0.0000	0.0	0.0	0.0000	0.0	0.0	0.0000	0.0	0.0
Ru	0.0000	0.0	0.0	0.0000	0.0	0.0	0.0004	0.0	0.0	0.0000	0.0	0.0
mg, Metals Found	<b>0.1536</b>	<b>100.0</b>	<b>47.9</b>	<b>0.4641</b>	<b>100.0</b>	<b>52.4</b>	<b>1.6782</b>	<b>100.0</b>	<b>45.0</b>	<b>0.4150</b>	<b>100.0</b>	<b>51.7</b>
mg, Filter Loading	<b>0.3209</b>			<b>0.8850</b>			<b>3.7280</b>			<b>0.8031</b>		

**Table A1.8.11 Test 2/8C, Marple #2937 (low) Elemental Analyses, Stages 8-9**

<b>2/8C</b>	<b>STAGE 8</b>			<b>STAGE 9</b>								
<b>#2937</b>	Particle size 0.52 µm			Particle size final, >0.5 µm								
	<b>mg</b>	<b>% detected</b>	<b>% loading</b>	<b>mg</b>	<b>% detected</b>	<b>% loading</b>						
Ce	0.0054	3.5	1.6	0.0016	4.5	1.1						
Cu	0.0927	60.1	26.8	0.0212	59.9	13.9						
Zr	0.0091	5.9	2.6	0.0022	6.2	1.4						
Fe	0.0350	22.7	10.1	0.0088	24.9	5.8						
Mg	0.0060	3.9	1.7	0.0000	0.0	0.0						
Al	0.0005	0.3	0.1	0.0000	0.0	0.0						
Cr	0.0000	0.0	0.0	0.0000	0.0	0.0						
Ni	0.0000	0.0	0.0	0.0000	0.0	0.0						
Mn	0.0009	0.6	0.3	0.0003	0.8	0.2						
Sn	0.0022	1.4	0.6	0.0008	2.3	0.5						
Mo	0.0002	0.1	0.1	0.0000	0.0	0.0						
Ti	0.0003	0.2	0.1	0.0000	0.0	0.0						
Li	0.0000	0.0	0.0	0.0000	0.0	0.0						
Pb	0.0002	0.1	0.1	0.0000	0.0	0.0						
Cs	0.0018	1.2	0.5	0.0005	1.4	0.3						
Sr	0.0000	0.0	0.0	0.0000	0.0	0.0						
Ru	0.0000	0.0	0.0	0.0000	0.0	0.0						
mg, Metals Found	<b>0.1543</b>	<b>100.0</b>	<b>44.6</b>	<b>0.0354</b>	<b>100.0</b>	<b>23.3</b>						
mg, Filter Loading	<b>0.3462</b>			<b>0.1521</b>								

**Table A1.8.12 Test 2/8C, Marple #2937 Particle Cerium and Fission Product Distributions**

<b>2/8C #2937 low</b>	<b>Cerium</b>		<b>Cesium</b>		<b>Strontium</b>		<b>Ruthenium</b>	
	<b>mg</b>	<b>wt%</b>	<b>mg</b>	<b>wt%</b>	<b>mg</b>	<b>wt%</b>	<b>mg</b>	<b>wt%</b>
35µm and >	0.3360	44.1	0.0022	7.5	0.0000	0.0	0.0000	0.0
21.3µm	0.0944	12.4	0.0012	4.1	0.0000	0.0	0.0000	0.0
14.8µm	0.0514	6.7	0.0005	1.7	0.0000	0.0	0.0000	0.0
9.8µm	0.0901	11.8	0.0004	1.4	0.0000	0.0	0.0000	0.0
6.0µm	0.0637	8.4	0.0005	1.7	0.0000	0.0	0.0000	0.0
3.5µm	0.0654	8.6	0.0032	11.0	0.0000	0.0	0.0000	0.0
1.55µm	0.0435	5.7	0.0148	50.7	0.0000	0.0	0.0000	0.0
0.93µm	0.0102	1.3	0.0041	14.0	0.0000	0.0	0.0000	0.0
0.52µm	0.0054	0.7	0.0018	6.2	0.0000	0.0	0.0000	0.0
Final filter	0.0016	0.2	0.0005	1.7	0.0000	0.0	0.0000	0.0
<b>Sum</b>	<b>0.7617</b>		<b>0.0292</b>		<b>0.0000</b>		<b>0.0004</b>	

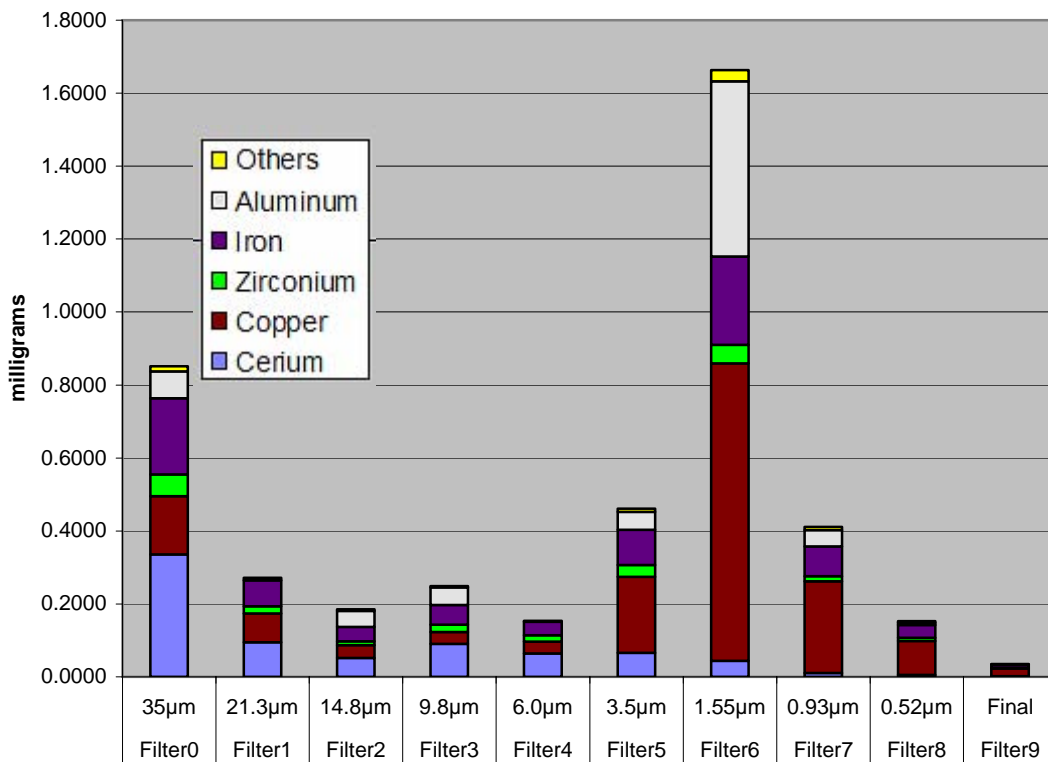


Figure A1.8.25 Test 2/8C, Marple #2937 (low) Metals Analysis Distribution, milligrams

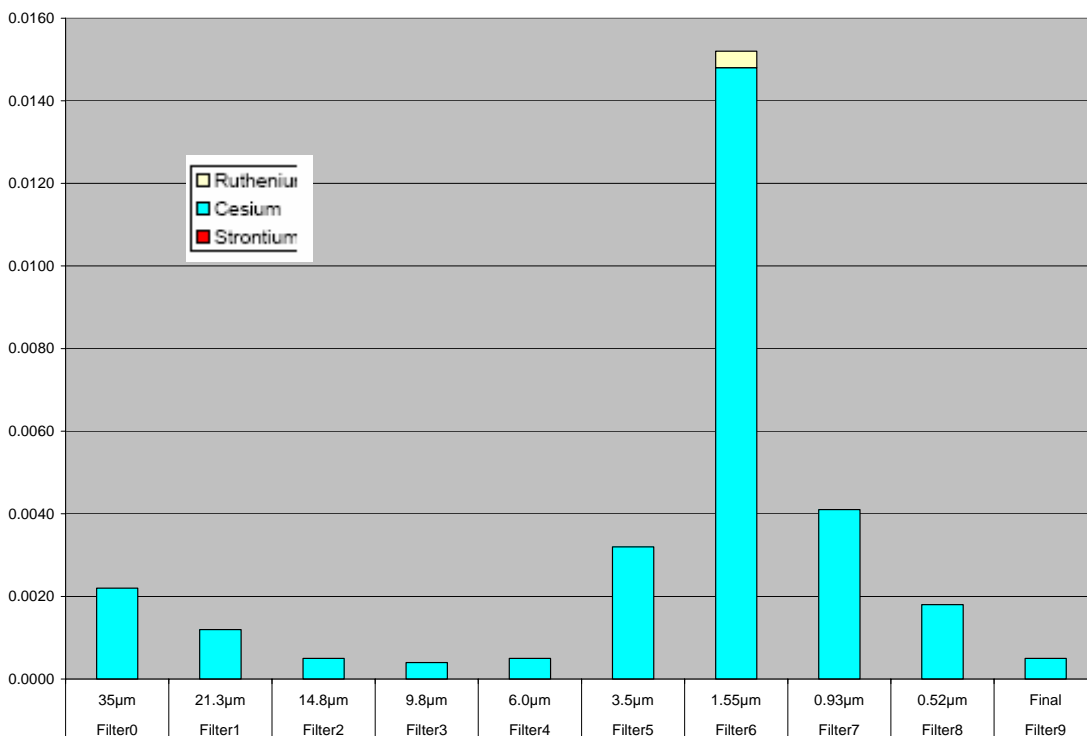


Figure A1.8.26 Test 2/8C, Marple #2937 (low) Fission Product Dopant Analysis Distrib, mg

**Table A1.8.13 Test 2/8C, Weight Distribution of Impact Debris**

Sieve Fraction	Weight, g	%
1000 µm	5.7877	35.2
500 µm	1.8197	11.1
250 µm	2.9997	18.2
125 µm	2.7018	16.4
100 µm	0.4635	2.8
74 µm	1.1219	6.8
37 µm	1.2708	7.7
25 µm	0.0867	0.5
<25 µm	0.1998	1.2
<b>Total</b>	<b>16.4516</b>	<b>100.0</b>

**Table A1.8.14 Test 2/8C, Elemental Analysis. Wt% of Sieved Impact Debris**

Test 2/8C Sieve Fraction		125 µm	100 µm	74 µm	37 µm	25 µm	<25 µm
Cerium		20.220	23.370	26.420	32.530	36.650	38.610
Iron		30.470	25.890	25.680	21.320	18.600	16.160
Copper		6.090	6.208	5.410	4.767	4.079	4.354
Zirconium		1.423	1.694	1.758	2.484	3.063	3.481
Aluminum		6.011	5.195	6.629	6.027	6.214	5.308
Manganese		0.356	0.301	0.298	0.249	0.222	0.193
Tin		0.082	0.092	0.079	0.090	0.100	0.106
Chromium		0.096	0.074	0.069	0.053	0.047	0.039
Magnesium		0.185	0.173	0.172	0.149	0.139	0.117
Boron		0.086	0.041	0.033	0.013	0.007	0.007
Lithium		0.035	0.023	0.018	0.009	0.007	0.007
Nickel		0.056	0.044	0.039	0.028	0.025	0.019
Titanium		0.244	0.211	0.199	0.163	0.149	0.128
Molybdenum		0.020	0.016	0.012	0.008	0.006	0.006
Lead		0.008	0.010	0.007	0.006	0.004	0.005
Barium		0.029	0.020	0.014	0.008	0.011	0.010
Strontium		0.011	0.011	0.010	0.011	0.013	0.014
Cesium		0.040	0.046	0.033	0.026	0.020	0.025
Ruthenium		0.002	0.002	0.002	0.002	0.002	0.001
<b>Total *</b>		<b>65.550</b>	<b>63.482</b>	<b>66.933</b>	<b>67.975</b>	<b>69.386</b>	<b>68.616</b>
Lanthanum		0.041	0.027	0.022	0.011	0.007	0.005
Praeseodymium		0.007	0.005	0.004	0.002	0.002	0.003
Neodymium		0.025	0.017	0.013	0.007	0.005	0.003
Samarium		0.006	0.004	0.003	0.001	0.000	0.000
Europium		0.004	0.004	0.005	0.006	0.008	0.009
Terbium		0.003	0.004	0.004	0.005	0.006	0.006

\* includes "minor" lanthanides shown in Table

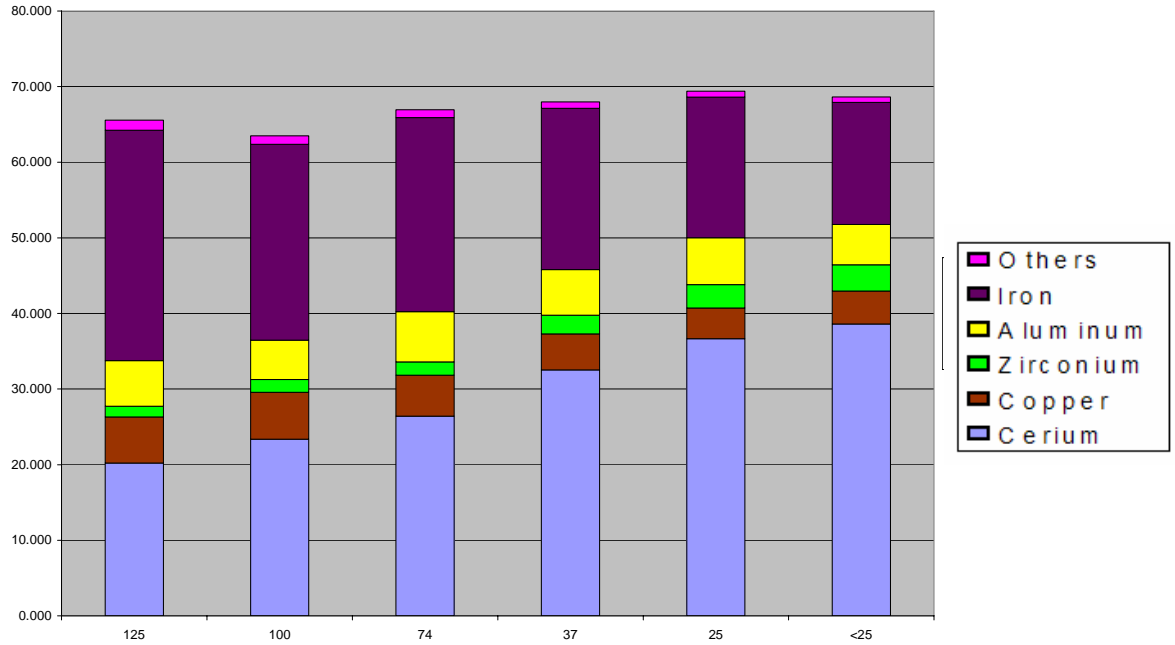


Figure A1.8.27 Test 2/8C Weight % Distribution of Metals in Impact Debris

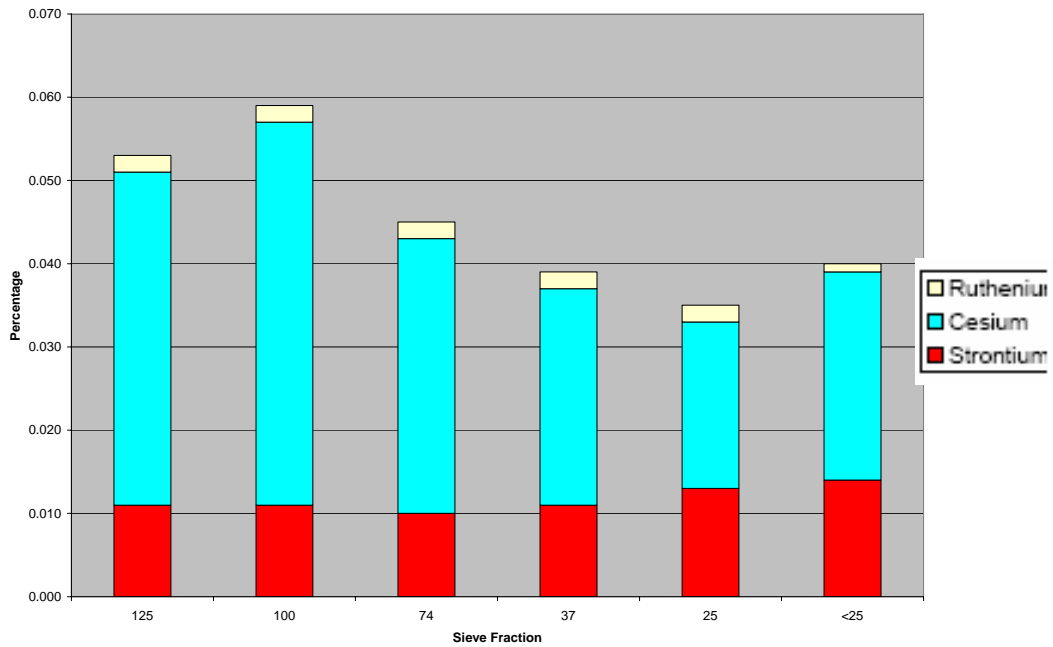


Figure A1.8.28 Test 2/8C Weight % Distribution of Fission Products in Impact Debris

### A.1.8D Test 2/8D Analyses and Results

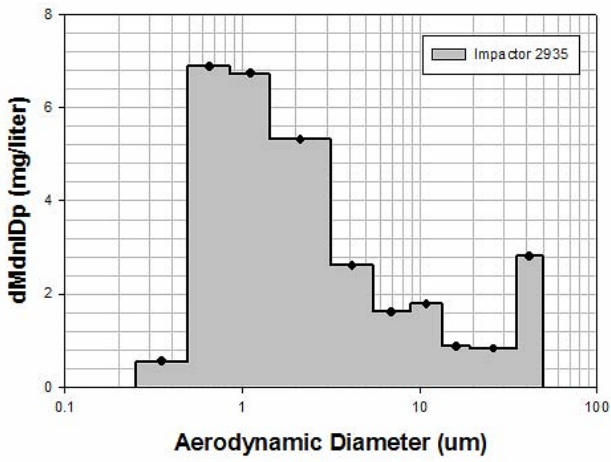


Figure A1.8.29 Test 2/8D Marple 2935 (high) Particle Size Distribution

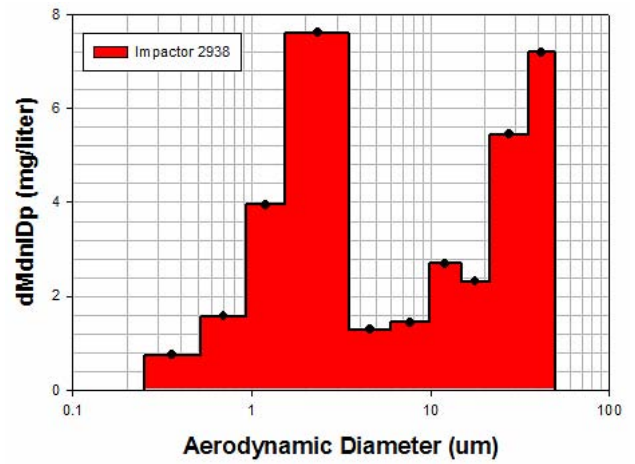


Figure A1.8.30 Test 2/8D Marple 2938 (high) Particle Size Distribution

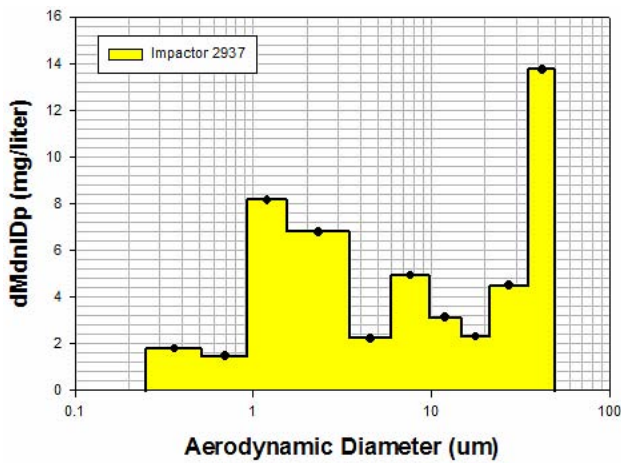


Figure A1.8.31 Test 2/8D Marple 2937 (low) Particle Size Distribution

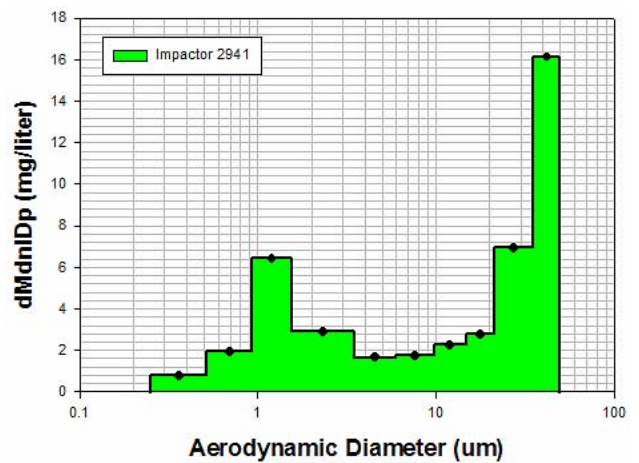


Figure A1.8.32 Test 2/8D Marple 2941 (low) Particle Size Distribution

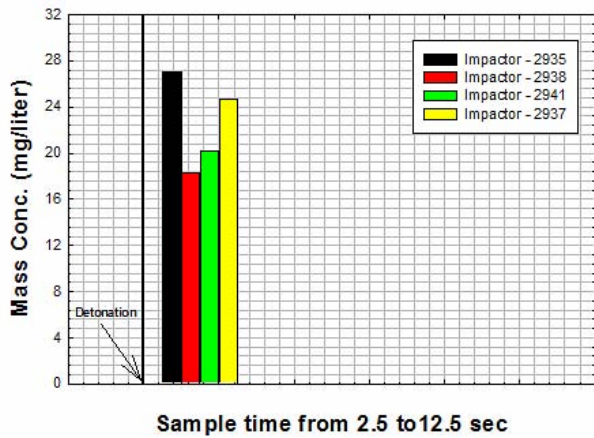


Figure A1.8.33 Test 2/8D Marple Impactors Mass Concentration

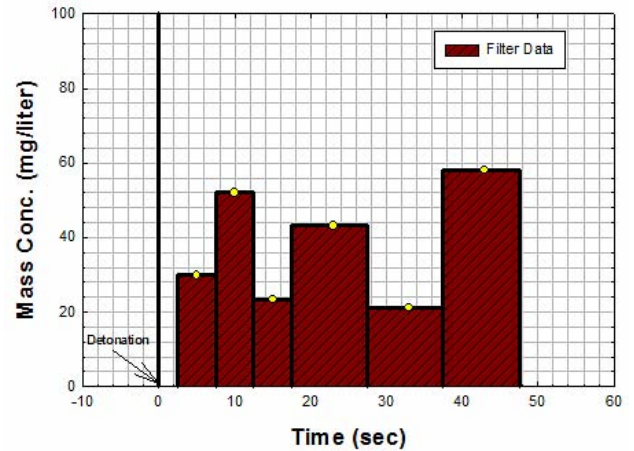


Figure A1.8.34 Test 2/8D Gelman Filters Mass Concentration

**Table A1.8.15 Test 2/8D, Marple #2935 (high) Elemental Analyses, Stages 0-3**

<b>2/8D</b>	<b>STAGE 0</b>			<b>STAGE 1</b>			<b>STAGE 2</b>			<b>STAGE 3</b>		
<b>#2935</b>	Particle size 35 µm			Particle size 21.3 µm			Particle size 14.8 µm			Particle size 9.8 µm		
	mg	% detected	% loading	mg	% detected	% loading	mg	% detected	% loading	mg	% detected	% loading
Ce	0.0413	15.0	10.3	0.0212	21.8	10.8	0.0251	31.9	19.8	0.0727	26.4	24.6
Cu	0.0845	30.7	21.1	0.0400	41.2	20.3	0.0231	29.4	18.2	0.0380	13.8	12.8
Zr	0.0156	5.7	3.9	0.0071	7.3	3.6	0.0065	8.3	5.1	0.0210	7.6	7.1
Fe	0.0592	21.5	14.8	0.0270	27.8	13.7	0.0234	29.8	18.4	0.0660	24.0	22.3
Al	0.0687	25.0	17.2	0.0000	0.0	0.0	0.0000	0.0	0.0	0.0746	27.1	25.2
Mg	0.0013	0.5	0.3	0.0000	0.0	0.0	0.0002	0.3	0.2	0.0007	0.3	0.2
Cr	0.0005	0.2	0.1	0.0001	0.1	0.1	0.0000	0.0	0.0	0.0001	0.0	0.0
Ni	0.0002	0.1	0.1	0.0001	0.1	0.1	0.0000	0.0	0.0	0.0002	0.1	0.1
Mn	0.0008	0.3	0.2	0.0003	0.3	0.2	0.0000	0.0	0.0	0.0007	0.3	0.2
Sn	0.0010	0.4	0.3	0.0005	0.5	0.3	0.0000	0.0	0.0	0.0004	0.1	0.1
Mo	0.0002	0.1	0.1	0.0001	0.1	0.1	0.0000	0.0	0.0	0.0000	0.0	0.0
Ti	0.0004	0.1	0.1	0.0000	0.0	0.0	0.0000	0.0	0.0	0.0004	0.1	0.1
Li	0.0000	0.0	0.0	0.0000	0.0	0.0	0.0000	0.0	0.0	0.0000	0.0	0.0
Pb	0.0002	0.1	0.1	0.0001	0.1	0.1	0.0000	0.0	0.0	0.0000	0.0	0.0
Cs	0.0011	0.4	0.3	0.0006	0.6	0.3	0.0003	0.4	0.2	0.0003	0.1	0.1
Sr	0.0000	0.0	0.0	0.0000	0.0	0.0	0.0000	0.0	0.0	0.0000	0.0	0.0
Ru	0.0000	0.0	0.0	0.0000	0.0	0.0	0.0000	0.0	0.0	0.0000	0.0	0.0
mg, Metals Found	<b>0.2750</b>	<b>100.0</b>	<b>68.8</b>	<b>0.0971</b>	<b>100.0</b>	<b>49.3</b>	<b>0.0786</b>	<b>100.0</b>	<b>61.9</b>	<b>0.2751</b>	<b>100.0</b>	<b>92.9</b>
mg, Filter Loading	<b>0.4000</b>			<b>0.1970</b>			<b>0.1270</b>			<b>0.2960</b>		

**Table A1.8.16 Test 2/8D, Marple #2935 (high) Elemental Analyses, Stages 4-7**

<b>2/8D</b>	<b>STAGE 4</b>			<b>STAGE 5</b>			<b>STAGE 6</b>			<b>STAGE 7</b>		
<b>#2935</b>	Particle size 6.0 µm			Particle size 3.5 µm			Particle size 1.55 µm			Particle size 0.93 µm		
	mg	% detected	% loading	mg	% detected	% loading	mg	% detected	% loading	mg	% detected	% loading
Ce	0.0624	32.1	19.6	0.0510	17.5	9.0	0.0299	3.4	1.7	0.0135	2.2	1.0
Cu	0.0453	23.3	14.2	0.1309	45.0	23.2	0.5872	66.8	33.9	0.3559	57.2	26.1
Zr	0.0231	11.9	7.3	0.0289	9.9	5.1	0.0400	4.6	2.3	0.0265	4.3	1.9
Fe	0.0613	31.5	19.3	0.0740	25.4	13.1	0.1370	15.6	7.9	0.1222	19.7	9.0
Mg	0.0000	0.0	0.0	0.0000	0.0	0.0	0.0645	7.3	3.7	0.0860	13.8	6.3
Al	0.0000	0.0	0.0	0.0000	0.0	0.0	0.0000	0.0	0.0	0.0013	0.2	0.1
Cr	0.0001	0.1	0.0	0.0002	0.1	0.0	0.0005	0.1	0.0	0.0004	0.1	0.0
Ni	0.0002	0.1	0.1	0.0007	0.2	0.1	0.0006	0.1	0.0	0.0002	0.0	0.0
Mn	0.0006	0.3	0.2	0.0012	0.4	0.2	0.0026	0.3	0.2	0.0022	0.4	0.2
Sn	0.0005	0.3	0.2	0.0012	0.4	0.2	0.0054	0.6	0.3	0.0048	0.8	0.4
Mo	0.0000	0.0	0.0	0.0002	0.1	0.0	0.0010	0.1	0.1	0.0009	0.1	0.1
Ti	0.0005	0.3	0.2	0.0010	0.3	0.2	0.0020	0.2	0.1	0.0012	0.2	0.1
Li	0.0000	0.0	0.0	0.0000	0.0	0.0	0.0001	0.0	0.0	0.0000	0.0	0.0
Pb	0.0000	0.0	0.0	0.0002	0.1	0.0	0.0008	0.1	0.0	0.0008	0.1	0.1
Cs	0.0005	0.3	0.2	0.0015	0.5	0.3	0.0068	0.8	0.4	0.0058	0.9	0.4
Sr	0.0000	0.0	0.0	0.0000	0.0	0.0	0.0000	0.0	0.0	0.0000	0.0	0.0
Ru	0.0000	0.0	0.0	0.0000	0.0	0.0	0.0000	0.0	0.0	0.0000	0.0	0.0
mg, Metals Found	<b>0.1945</b>	<b>100.0</b>	<b>61.2</b>	<b>0.2910</b>	<b>100.0</b>	<b>51.6</b>	<b>0.8784</b>	<b>100.0</b>	<b>50.7</b>	<b>0.6217</b>	<b>100.0</b>	<b>45.6</b>
mg, Filter Loading	<b>0.3180</b>			<b>0.5640</b>			<b>1.7330</b>			<b>1.3640</b>		

**Table A1.8.17 Test 2/8D, Marple #2935 (high) Elemental Analyses, Stages 8-9**

<b>2/8D</b>	<b>STAGE 8</b>			<b>STAGE 9</b>								
<b>#2935</b>	Particle size 0.52 µm			Particle size final, >0.5 µm								
	<b>mg</b>	<b>% detected</b>	<b>% loading</b>	<b>mg</b>	<b>% detected</b>	<b>% loading</b>						
Ce	0.0180	2.4	1.2	0.0015	3.6	1.0						
Cu	0.3561	47.7	22.8	0.0217	52.5	14.6						
Zr	0.0377	5.0	2.4	0.0025	6.1	1.7						
Fe	0.1688	22.6	10.8	0.0142	34.4	9.5						
Mg	0.1446	19.4	9.2	0.0000	0.0	0.0						
Al	0.0000	0.0	0.0	0.0000	0.0	0.0						
Cr	0.0004	0.1	0.0	0.0000	0.0	0.0						
Ni	0.0003	0.0	0.0	0.0000	0.0	0.0						
Mn	0.0032	0.4	0.2	0.0002	0.5	0.1						
Sn	0.0071	1.0	0.5	0.0004	1.0	0.3						
Mo	0.0013	0.2	0.1	0.0001	0.2	0.1						
Ti	0.0014	0.2	0.1	0.0000	0.0	0.0						
Li	0.0002	0.0	0.0	0.0000	0.0	0.0						
Pb	0.0008	0.1	0.1	0.0001	0.2	0.1						
Cs	0.0073	1.0	0.5	0.0006	1.5	0.4						
Sr	0.0000	0.0	0.0	0.0000	0.0	0.0						
Ru	0.0000	0.0	0.0	0.0000	0.0	0.0						
mg, Metals Found	<b>0.7472</b>	<b>100.0</b>	<b>47.8</b>	<b>0.0413</b>	<b>100.0</b>	<b>27.7</b>						
mg, Filter Loading	<b>1.5647</b>			<b>0.1490</b>								

**Table A1.8.18 Test 2/8D, Marple #2935 Particle Cerium and Fission Product Distributions**

<b>2/8D #2935 high</b>	<b>Cerium</b>		<b>Cesium</b>		<b>Strontium</b>		<b>Ruthenium</b>	
	<b>mg</b>	<b>wt%</b>	<b>mg</b>	<b>wt%</b>	<b>mg</b>	<b>wt%</b>	<b>mg</b>	<b>wt%</b>
35µm and >	0.0413	12.3	0.0011	4.4	0.0000	0.0	0.0000	0.0
21.3µm	0.0212	6.3	0.0006	2.4	0.0000	0.0	0.0000	0.0
14.8µm	0.0251	7.5	0.0003	1.2	0.0000	0.0	0.0000	0.0
9.8µm	0.0727	21.6	0.0003	1.2	0.0000	0.0	0.0000	0.0
6.0µm	0.0624	18.5	0.0005	2.0	0.0000	0.0	0.0000	0.0
3.5µm	0.0510	15.2	0.0015	6.0	0.0000	0.0	0.0000	0.0
1.55µm	0.0299	8.9	0.0068	27.4	0.0000	0.0	0.0000	0.0
0.93µm	0.0135	4.0	0.0058	23.4	0.0000	0.0	0.0000	0.0
0.52µm	0.0180	5.3	0.0073	29.4	0.0000	0.0	0.0000	0.0
Final filter	0.0015	0.4	0.0006	2.4	0.0000	0.0	0.0000	0.0
<b>Sum</b>	<b>0.3366</b>		<b>0.0248</b>		<b>0.0000</b>		<b>0.0000</b>	

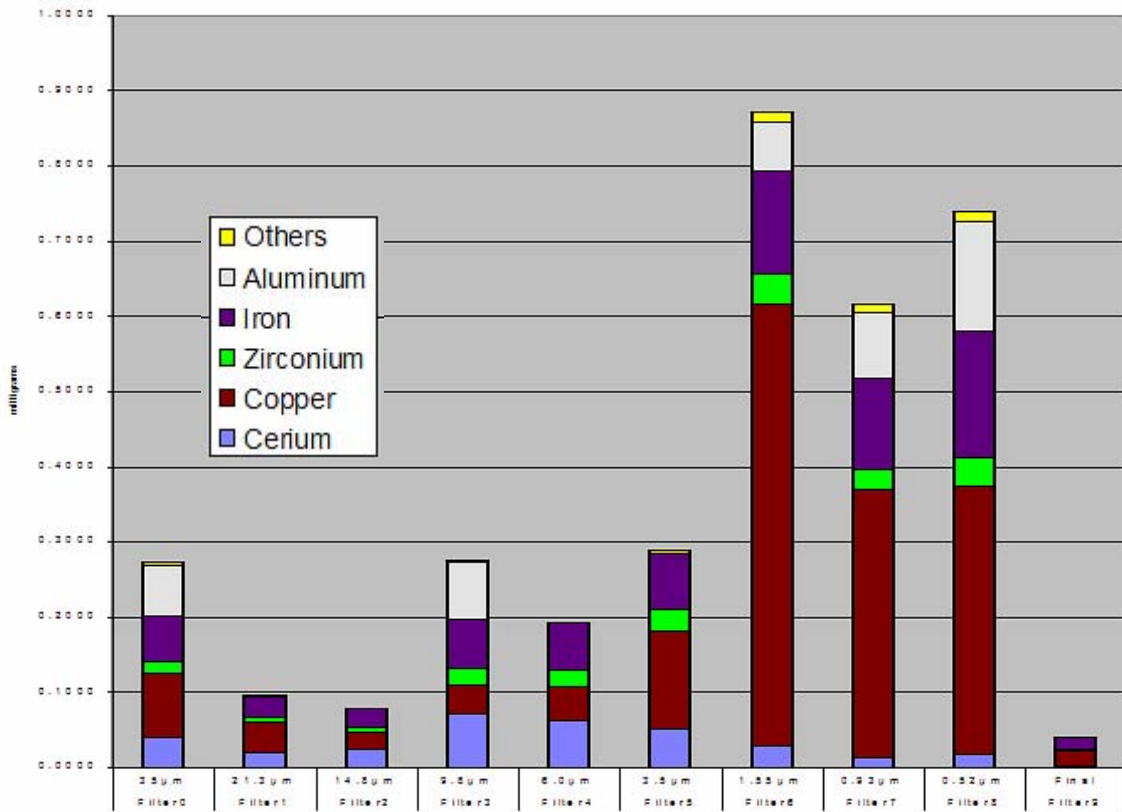


Figure A1.8.35 Test 2/8D, Marple #2935 (high) Metals Analysis Distribution, milligrams

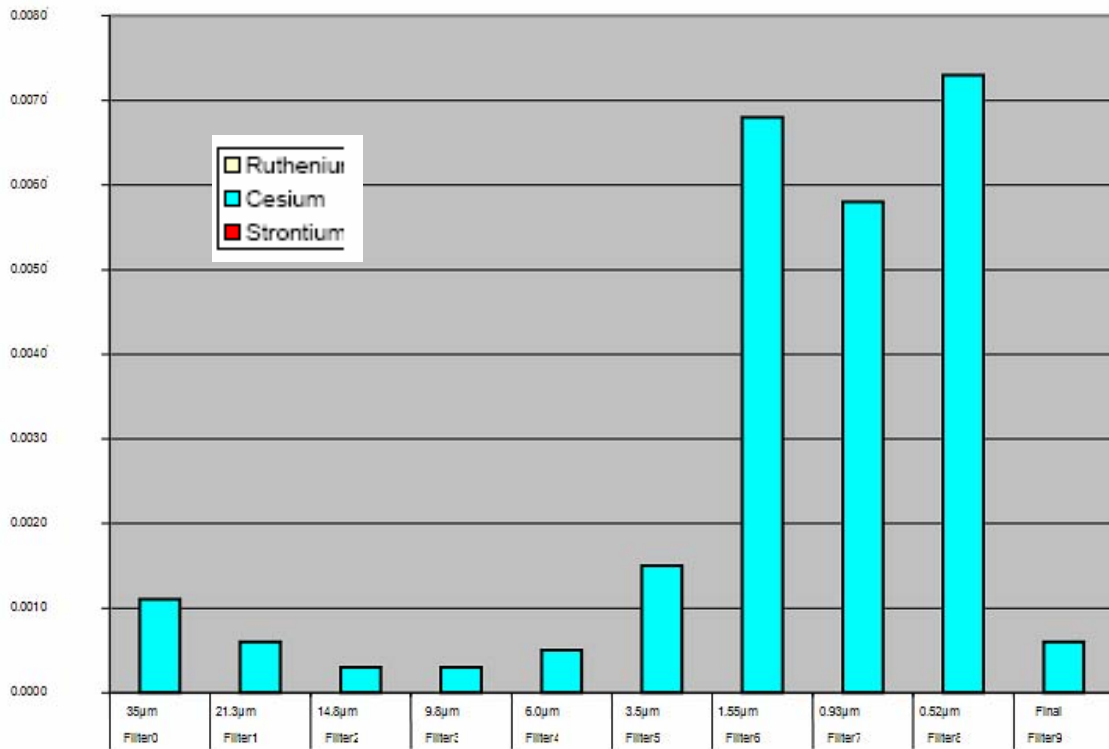


Figure A1.8.36 Test 2/8D, Marple #2935 (high) Fission Product Dopant Analysis Distrib, mg

**Table A1.8.19 Test 2/8D, Marple #2937 (low) Elemental Analyses, Stages 0-3**

2/8D	STAGE 0			STAGE 1			STAGE 2			STAGE 3		
#2937	Particle size 35 µm			Particle size 21.3 µm			Particle size 14.8 µm			Particle size 9.8 µm		
	mg	% detected	% loading	mg	% detected	% loading	mg	% detected	% loading	mg	% detected	% loading
Ce	0.3031	37.8	22.9	0.0986	24.7	16.2	0.0522	38.4	22.8	0.0873	39.9	24.9
Cu	0.1286	16.1	9.7	0.0663	16.6	10.9	0.0256	18.8	11.2	0.0361	16.5	10.3
Zr	0.0616	7.7	4.7	0.0239	6.0	3.9	0.0115	8.5	5.0	0.0231	10.6	6.6
Fe	0.2586	32.3	19.5	0.1931	48.3	31.7	0.0437	32.1	19.1	0.0692	31.6	19.7
Al	0.0268	3.3	2.0	0.0000	0.0	0.0	0.0000	0.0	0.0	0.0000	0.0	0.0
Mg	0.0000	0.0	0.0	0.0000	0.0	0.0	0.0000	0.0	0.0	0.0000	0.0	0.0
Cr	0.0080	1.0	0.6	0.0080	2.0	1.3	0.0013	1.0	0.6	0.0005	0.2	0.1
Ni	0.0044	0.5	0.3	0.0045	1.1	0.7	0.0007	0.5	0.3	0.0004	0.2	0.1
Mn	0.0031	0.4	0.2	0.0018	0.5	0.3	0.0005	0.4	0.2	0.0007	0.3	0.2
Sn	0.0021	0.3	0.2	0.0007	0.2	0.1	0.0000	0.0	0.0	0.0007	0.3	0.2
Mo	0.0011	0.1	0.1	0.0011	0.3	0.2	0.0002	0.1	0.1	0.0001	0.0	0.0
Ti	0.0019	0.2	0.1	0.0010	0.3	0.2	0.0000	0.0	0.0	0.0003	0.1	0.1
Li	0.0000	0.0	0.0	0.0000	0.0	0.0	0.0000	0.0	0.0	0.0000	0.0	0.0
Pb	0.0004	0.0	0.0	0.0001	0.0	0.0	0.0000	0.0	0.0	0.0000	0.0	0.0
Cs	0.0014	0.2	0.1	0.0008	0.2	0.1	0.0003	0.2	0.1	0.0003	0.1	0.1
Sr	0.0000	0.0	0.0	0.0000	0.0	0.0	0.0000	0.0	0.0	0.0000	0.0	0.0
Ru	0.0000	0.0	0.0	0.0000	0.0	0.0	0.0000	0.0	0.0	0.0000	0.0	0.0
mg, Metals Found	<b>0.8009</b>	<b>100.0</b>	<b>60.5</b>	<b>100.0</b>	<b>65.7</b>	<b>100.0</b>	<b>0.1360</b>	<b>100.0</b>	<b>59.4</b>	<b>0.2187</b>	<b>100.0</b>	<b>62.3</b>
mg, Filter Loading	<b>1.3229</b>			<b>0.6090</b>			<b>0.2290</b>			<b>0.3510</b>		

**Table A1.8.20 Test 2/8D, Marple #2937 (low) Elemental Analyses, Stages 4-7**

2/8D	STAGE 4			STAGE 5			STAGE 6			STAGE 7		
#2937	Particle size 6.0 µm			Particle size 3.5 µm			Particle size 1.55 µm			Particle size 0.93 µm		
	mg	% detected	% loading	mg	% detected	% loading	mg	% detected	% loading	mg	% detected	% loading
Ce	0.0677	33.2	22.6	0.0496	21.4	15.1	0.0332	5.1	2.2	0.0130	3.0	1.1
Cu	0.0434	21.3	14.5	0.0704	30.4	21.4	0.4350	67.2	28.8	0.2918	66.7	25.7
Zr	0.0240	11.8	8.0	0.0260	11.2	7.9	0.0387	6.0	2.6	0.0241	5.5	2.1
Fe	0.0640	31.4	21.3	0.0701	30.3	21.3	0.1235	19.1	8.2	0.0952	21.8	8.4
Mg	0.0000	0.0	0.0	0.0000	0.0	0.0	0.0000	0.0	0.0	0.0000	0.0	0.0
Al	0.0000	0.0	0.0	0.0091	3.9	2.8	0.0000	0.0	0.0	0.0000	0.0	0.0
Cr	0.0011	0.5	0.4	0.0005	0.2	0.2	0.0004	0.1	0.0	0.0003	0.1	0.0
Ni	0.0006	0.3	0.2	0.0010	0.4	0.3	0.0003	0.0	0.0	0.0002	0.0	0.0
Mn	0.0007	0.3	0.2	0.0014	0.6	0.4	0.0023	0.4	0.2	0.0018	0.4	0.2
Sn	0.0011	0.5	0.4	0.0010	0.4	0.3	0.0050	0.8	0.3	0.0045	1.0	0.4
Mo	0.0002	0.1	0.1	0.0002	0.1	0.1	0.0008	0.1	0.1	0.0007	0.2	0.1
Ti	0.0004	0.2	0.1	0.0011	0.5	0.3	0.0016	0.2	0.1	0.0005	0.1	0.0
Li	0.0000	0.0	0.0	0.0000	0.0	0.0	0.0000	0.0	0.0	0.0000	0.0	0.0
Pb	0.0677	33.2	22.6	0.0001	0.0	0.0	0.0005	0.1	0.0	0.0004	0.1	0.0
Cs	0.0005	0.3	0.2	0.0009	0.4	0.3	0.0063	1.0	0.4	0.0052	1.2	0.5
Sr	0.0000	0.0	0.0	0.0000	0.0	0.0	0.0000	0.0	0.0	0.0000	0.0	0.0
Ru	0.0000	0.0	0.0	0.0000	0.0	0.0	0.0000	0.0	0.0	0.0000	0.0	0.0
mg, Metals Found	<b>0.2037</b>	<b>100.0</b>	<b>67.9</b>	<b>0.2314</b>	<b>100.0</b>	<b>70.3</b>	<b>0.6476</b>	<b>100.0</b>	<b>42.9</b>	<b>0.4377</b>	<b>100.0</b>	<b>38.5</b>
mg, Filter Loading	<b>0.3000</b>			<b>0.3290</b>			<b>1.5080</b>			<b>1.1370</b>		

**Table A1.8.21 Test 2/8D, Marple #2937 (low) Elemental Analyses, Stages 8-9**

2/8D	STAGE 8			STAGE 9								
#2937	Particle size 0.52 µm			Particle size final, >0.5 µm								
	mg	% detected	% loading	mg	% detected	% loading						
Ce	0.0035	2.7	1.5	0.0048	3.7	1.3						
Cu	0.0732	55.7	31.6	0.0861	65.8	24.0						
Zr	0.0084	6.4	3.6	0.0085	6.5	2.4						
Fe	0.0318	24.2	13.7	0.0281	21.5	7.8						
Mg	0.0000	0.0	0.0	0.0000	0.0	0.0						
Al	0.0103	7.8	4.4	0.0000	0.0	0.0						
Cr	0.0001	0.1	0.0	0.0000	0.0	0.0						
Ni	0.0002	0.2	0.1	0.0000	0.0	0.0						
Mn	0.0007	0.5	0.3	0.0004	0.3	0.1						
Sn	0.0014	1.1	0.6	0.0011	0.8	0.3						
Mo	0.0002	0.2	0.1	0.0002	0.2	0.1						
Ti	0.0001	0.1	0.0	0.0000	0.0	0.0						
Li	0.0000	0.0	0.0	0.0000	0.0	0.0						
Pb	0.0002	0.2	0.1	0.0001	0.1	0.0						
Cs	0.0014	1.1	0.6	0.0016	1.2	0.4						
Sr	0.0000	0.0	0.0	0.0000	0.0	0.0						
Ru	0.0000	0.0	0.0	0.0000	0.0	0.0						
mg, Metals Found	<b>0.1315</b>	<b>100.0</b>	<b>56.7</b>	<b>0.1309</b>	<b>100.0</b>	<b>36.5</b>						
mg, Filter Loading	<b>0.2318</b>			<b>0.3590</b>								

**Table A1.8.22 Test 2/8D, Marple #2937 Particle Cerium and Fission Product Distributions**

2/8D #2937 low Particle Size	Cerium		Cesium		Strontium		Ruthenium	
	mg	wt%	mg	wt%	mg	wt%	mg	wt%
35µm and >	0.3031	42.5	0.0014	7.5	0.0000	0.0	0.0000	0.0
21.3µm	0.0986	13.8	0.0008	4.3	0.0000	0.0	0.0000	0.0
14.8µm	0.0522	7.3	0.0003	1.6	0.0000	0.0	0.0000	0.0
9.8µm	0.0873	12.2	0.0003	1.6	0.0000	0.0	0.0000	0.0
6.0µm	0.0677	9.5	0.0004	2.2	0.0000	0.0	0.0000	0.0
3.5µm	0.0496	7.0	0.0009	4.8	0.0000	0.0	0.0000	0.0
1.55µm	0.0332	4.7	0.0063	33.9	0.0000	0.0	0.0000	0.0
0.93µm	0.0130	1.8	0.0052	28.0	0.0000	0.0	0.0000	0.0
0.52µm	0.0035	0.5	0.0014	7.5	0.0000	0.0	0.0000	0.0
Final filter	0.0048	0.7	0.0016	8.6	0.0000	0.0	0.0000	0.0
<b>Sum</b>	<b>0.7130</b>		<b>0.0186</b>		<b>0.0000</b>		<b>0.0000</b>	

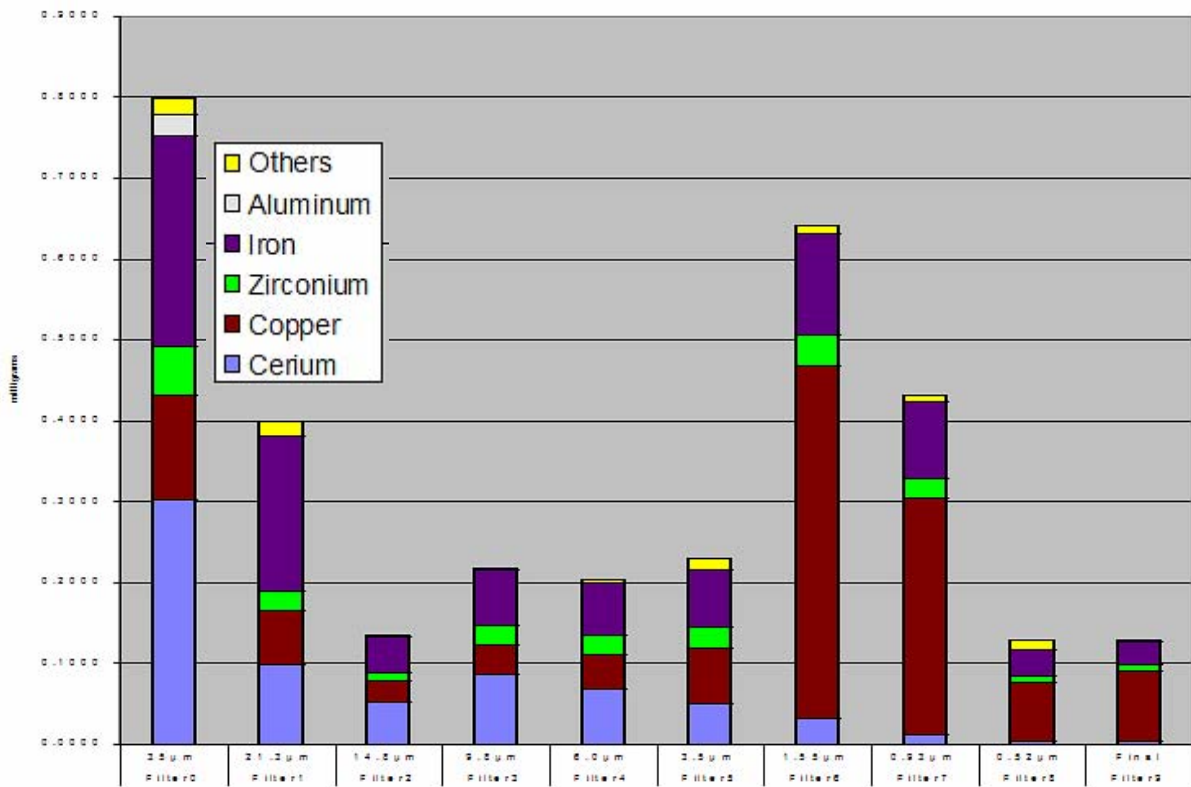


Figure A1.8.37 Test 2/8D, Marple #2937 (low) Metals Analysis Distribution, milligrams

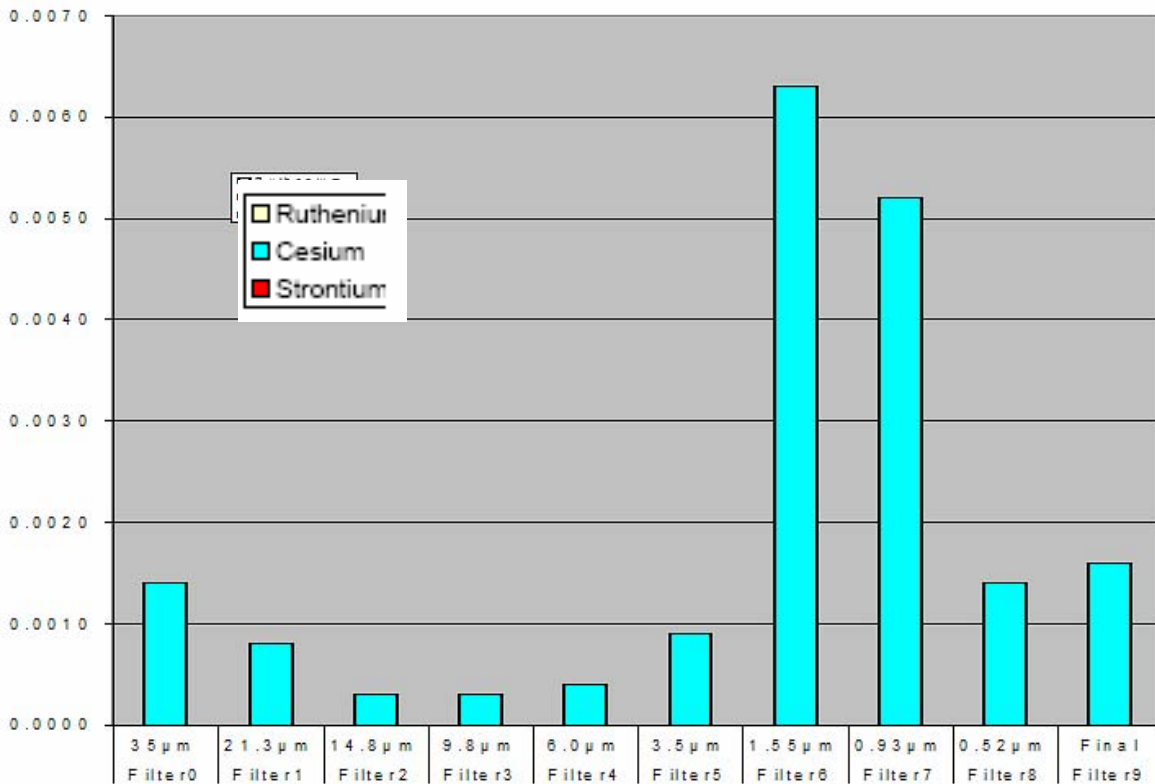


Figure A1.8.38 Test 2/8D, Marple #2937 (low) Fission Product Dopant Analysis Distrib, mg

**Table A1.8.23 Test 2/8D, Weight Distribution of Impact Debris**

Sieve Fraction	Weight, g	%
1000 µm	6.127	29.6
500 µm	3.4223	16.5
250 µm	4.3237	20.9
125 µm	2.7536	13.3
100 µm	0.5944	2.9
74 µm	0.9401	4.5
37 µm	1.5277	7.4
25 µm	0.282	1.4
<25 µm	0.7556	3.6
<b>Total</b>	<b>20.7264</b>	<b>100.0</b>

**Table A1.8.24 Test 2/8D, Elemental Analysis. Wt% of Sieved Impact Debris**

Test 2/8d Sieve Fraction		125 µm	100 µm	74 µm	37 µm	25 µm	<25 µm
Cerium		12.870	23.160	25.680	30.220	32.790	30.400
Iron		47.390	38.230	35.880	30.070	24.740	20.340
Copper		3.346	3.267	3.476	4.089	5.229	7.372
Zirconium		1.112	1.288	1.467	2.036	2.929	3.685
Aluminum		2.036	2.204	2.601	3.472	4.263	4.734
Manganese		0.569	0.426	0.374	0.289	0.241	0.209
Tin		0.040	0.036	0.041	0.055	0.077	0.112
Chromium		0.087	0.068	0.063	0.054	0.052	0.046
Magnesium		0.079	0.074	0.078	0.083	0.093	0.103
Boron		0.027	0.024	0.020	0.011	0.005	0.005
Lithium		0.012	0.009	0.007	0.004	0.001	0.003
Nickel		0.083	0.057	0.051	0.038	0.031	0.025
Titanium		0.231	0.170	0.163	0.151	0.156	0.155
Molybdenum		0.018	0.012	0.011	0.009	0.009	0.012
Lead		0.002	0.002	0.002	0.002	0.003	0.005
Barium		0.000	0.001	0.001	0.000	0.011	0.001
Strontium		0.007	0.007	0.009	0.010	0.013	0.015
Cesium		0.012	0.011	0.013	0.017	0.024	0.043
Ruthenium		0.000	0.000	0.000	0.000	0.000	0.001
<b>Total *</b>		<b>67.953</b>	<b>69.079</b>	<b>69.967</b>	<b>70.634</b>	<b>70.690</b>	<b>67.289</b>
Lanthanum		0.014	0.013	0.011	0.007	0.005	0.003
Praseodymium		0.003	0.003	0.002	0.002	0.001	0.001
Neodymium		0.009	0.008	0.007	0.005	0.003	0.002
Samarium		0.002	0.002	0.002	0.000	0.000	0.000
Europium		0.002	0.003	0.004	0.006	0.009	0.012
Terbium		0.002	0.004	0.004	0.004	0.005	0.005

\* includes "minor" lanthanides shown in Table

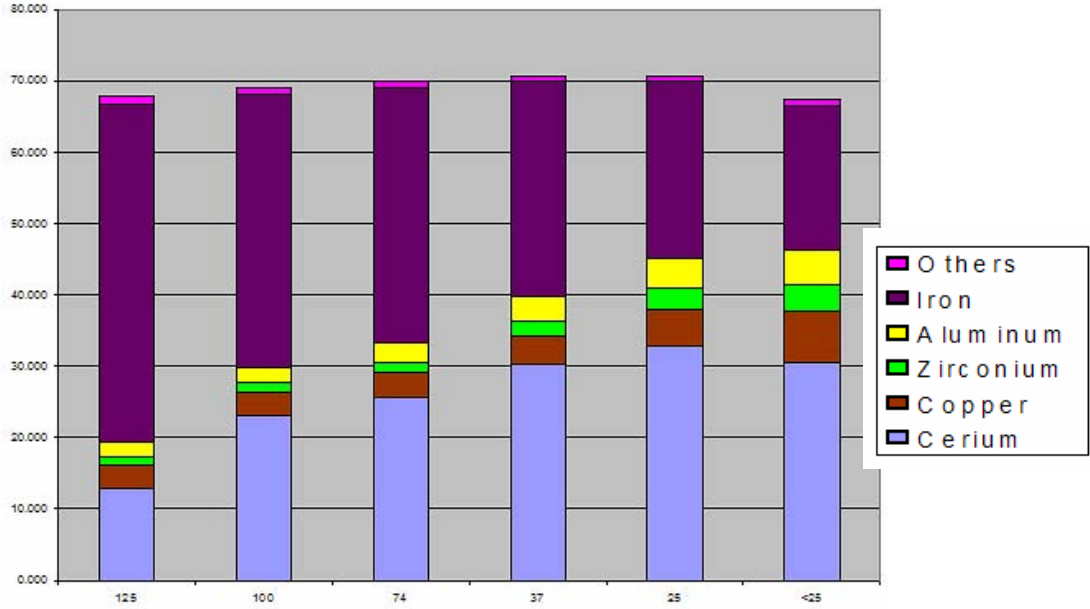


Figure A1.8.39 Test 2/8D Weight % Distribution of Metals in Impact Debris

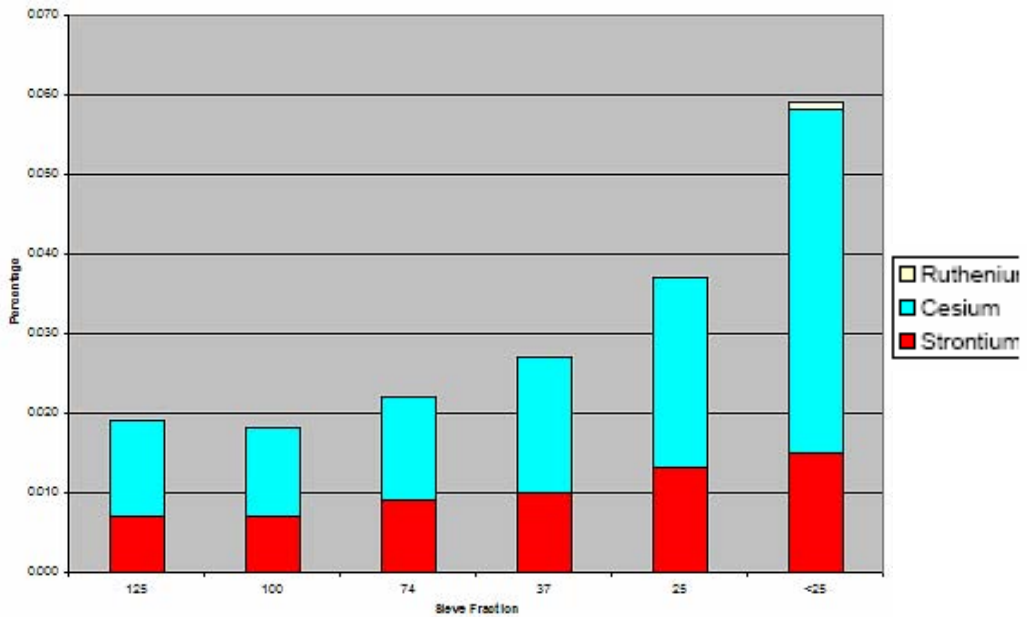


Figure A1.8.40 Test 2/8D Weight % Distribution of Fission Products in Impact Debris

### A.1.9A Test 2/9A Analyses and Results

The available aerosol data from test 2/9A is presented, following. Complete aerosol test data and chemical analyses will be documented at a later date.

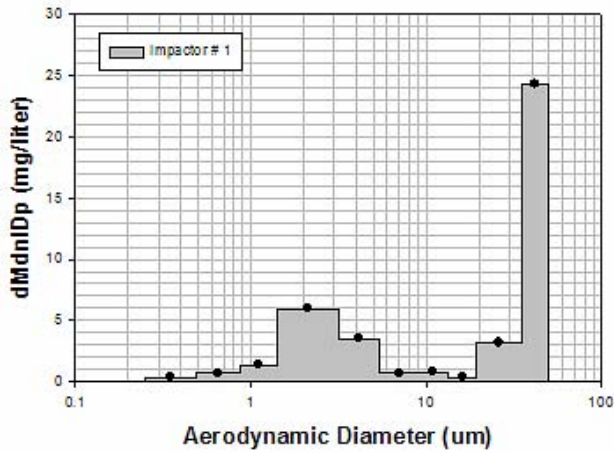


Figure A1.9.1 Test 2/9A Marple #1 Particle Size Distribution

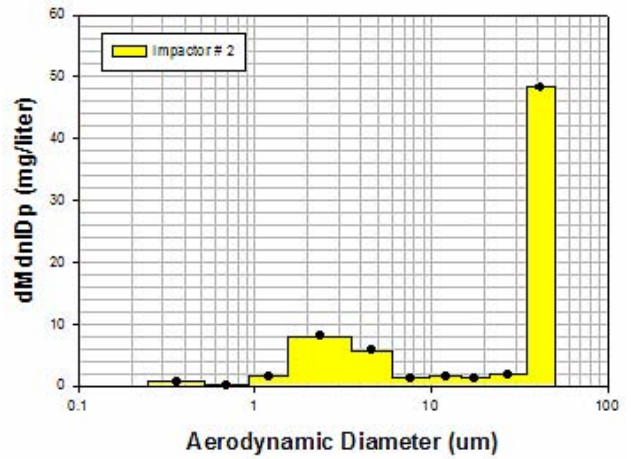


Figure A1.9.2 Test 2/9A Marple #2 Particle Size Distribution

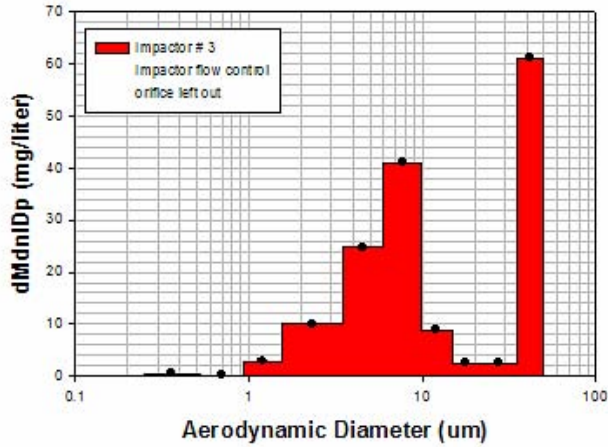


Figure A1.9.3 Test 2/9A Marple #3 Particle Size Distribution

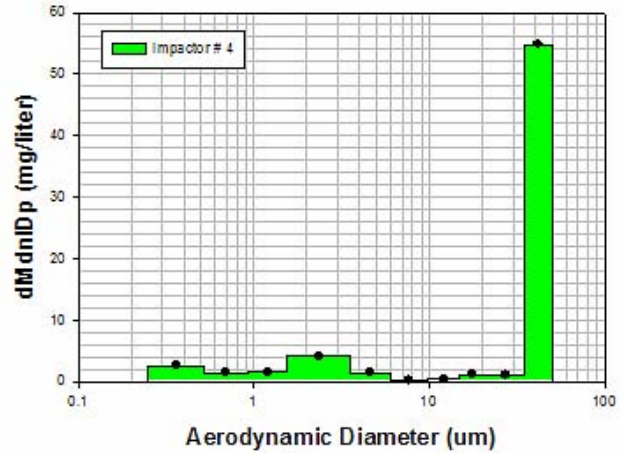


Figure A1.9.4 Test 2/9A Marple #4 Particle Size Distribution

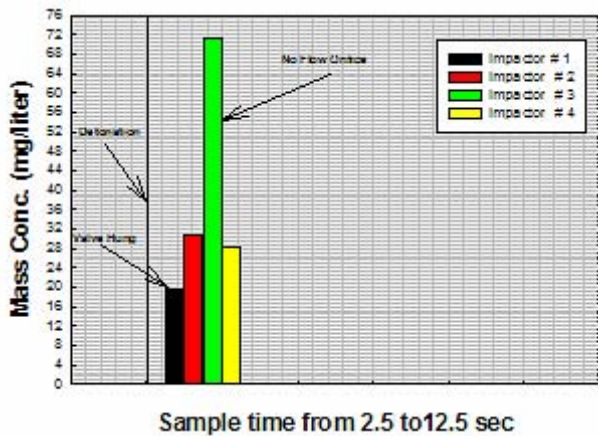


Figure A1.9.5 Test 2/9A Marple Impactors Mass Concentration

### A.1.9B Test 2/9B Analyses and Results

The available aerosol data from test 2/9B is presented, following. Complete aerosol test data and chemical analyses will be documented at a later date.

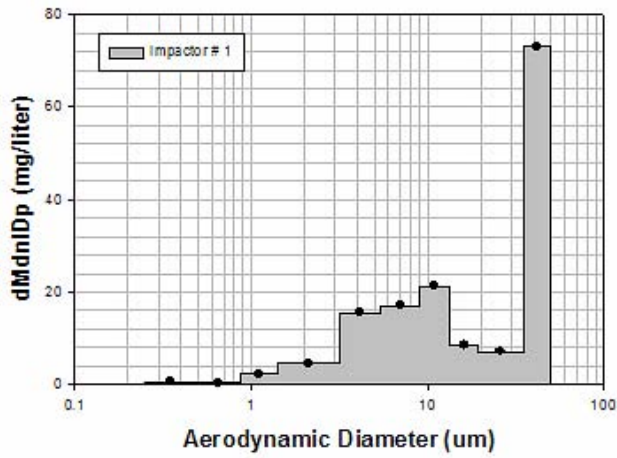


Figure A1.9.6 Test 2/9B Marple #1 Particle Size Distribution

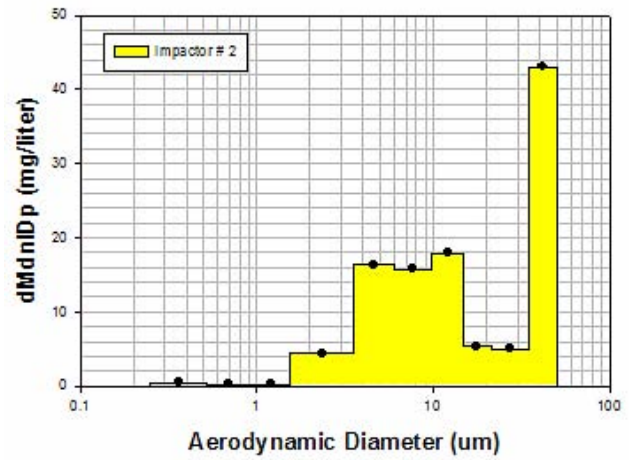


Figure A1.9.7 Test 2/9B Marple #2 Particle Size Distribution

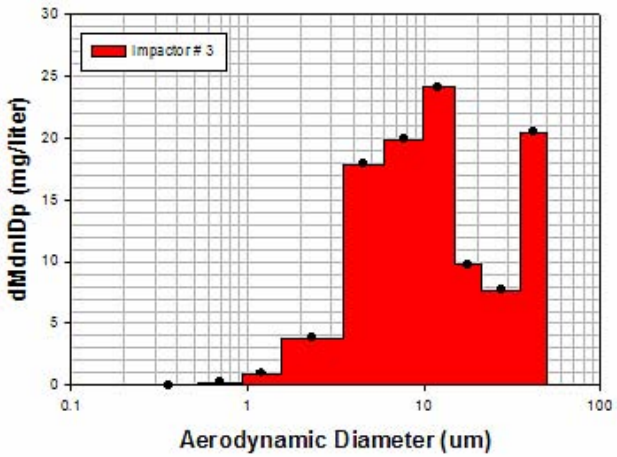


Figure A1.9.8 Test 2/9B Marple #3 Particle Size Distribution

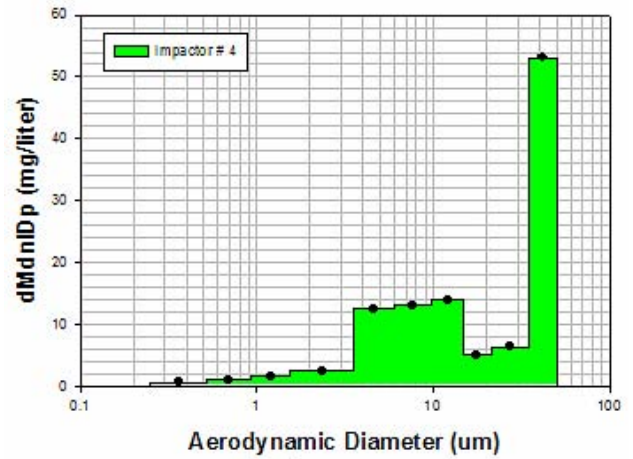


Figure A1.9.9 Test 2/9B Marple #4 Particle Size Distribution

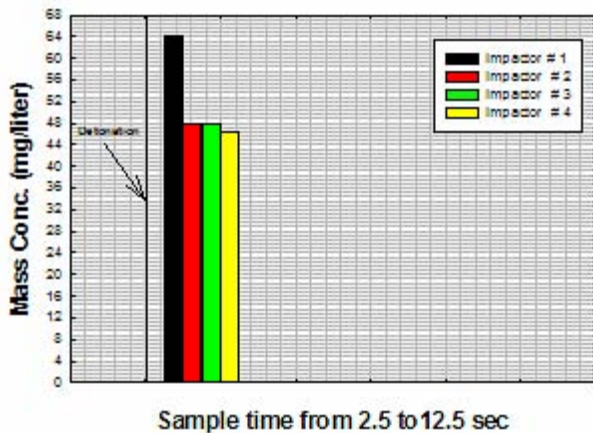


Figure A1.9.10 Test 2/9B Marple Impactors Mass Concentration

## REFERENCES

- Alfa Aesar, *Research Chemicals, Metals, and Materials Catalog*. Ward Hill, MA. 2003-2004.
- Alvarez et al., 1982. Alvarez, J.L., et al. *Waste Form Response Project Correlation Testing*. EGG-PR-5590. Idaho National Engineering Laboratory. Idaho Falls, ID. September 1982.
- Billone and Tsai, 2003. Billone, M.C, and H. Tsai, Argonne National Laboratory, Argonne, IL. Personal communication. September 2003.
- Blejwas, 2003. Blejwas, T.E., Sandia National Laboratories. Letter "Management of HEDD Project DU Waste," to N. Slater Thompson, Department of Energy. May 15, 2003.
- Brockmann et al., 2004. Brockmann, J.E, D.A. Lucero, R.E. Luna, T.T. Borek, and M.A. Molecke, *Aerosol Sampling and Results*, SAND2004-6008C. Presented at the 8th Technical Meeting of the International Working Group for Sabotage Concerns of Transport and Storage Casks, WGSTSC, November 17-18, 2004, Albuquerque, NM.
- Dickey, 2004. "Surrogate/Spent Fuel Sabotage: Aerosol Ratio Sandia Engineering Report," internal document. Sandia National Laboratories. Albuquerque, NM. July 2004.
- Einzigler et al., 2003. Einzigler, R.E., H. Tsai, M. C. Billone and B.A. Hilton. *Examination of Spent PWR Fuel Rods After 15 Years in Dry Storage*, NUREG/CR-6831. September 2003.
- Einzigler, 2003. Einzigler, R.E., Consultant, personal communication. 2003.
- EPRI, 2001. *Design, Operation, and Performance Data for High Burnup PWR Fuel from the H. B. Robinson Plant for Use in the NRC Experimental Program at Argonne National Laboratory*. EPRI, Palo Alto, CA. 2001. 1001558.
- Ewsuk and Diantonio, 2002. Ewsuk, K. and C. DiAntonio, memorandum to M.A. Molecke, Sandia National Laboratories, "Cerium Oxide (CeO<sub>2</sub>) Pellet Fabrication," September 24, 2002.
- Hagan and Dickey, 2004. Hagan, R. And R. Dickey, SNL internal memo. "Qualifications of Design of SFR Chamber R769-000," to Roger W. Smith, Sandia National Laboratories, Albuquerque, NM. June 29, 2004.
- Lange et al., 1994. Lange, F., G., Pretzsch, J. Döhler, E. Hörmann, H. Busch, W. Koch. *Experimental Determination for UO<sub>2</sub>-Release from a Spent Fuel Transport Cask after Shaped Charge Attack*. Proc. INMM 35<sup>th</sup> Meeting, Naples, Florida. July 17-20, 1994.
- Luna, 2004. Luna, R.E., Consultant, Albuquerque, NM. Unpublished. 2004.
- Mädler et al., 1999. Mädler, L., W. Koch, F. Lange, and K. Husemann, *In-Situ Aerodynamic Size Classification of Aerosols in the Size Range Between 0.1 and 100 μm for Dustiness Tests and Powder Characterization*, Journal of Aerosol Science, 30: 451-465, 1999.
- Molecke, 2004. Molecke, M.A., *Spent Fuel Sabotage Aerosol Ratio Test Program, Status Update November 2004*, SAND2004-5740C. Presented at the 8th Technical Meeting of the International Working Group for Sabotage Concerns of Transport and Storage Casks, WGSTSC, November 17-18, 2004, Albuquerque, NM.
- Molecke et al., 2004a. Molecke, M.A., K.B. Sorenson, T.T. Borek, G. Pretzsch, F. Lange, W. Koch, O. Nolte, B. Autrusson, D. Brochard, N. Slater Thompson, R. Hibbs, and F.I. Young, *Surrogate/Spent Fuel Sabotage: Aerosol Ratio Test Program and Phase 2 Test Results*, SAND2004-1832. June 2004.

Molecke et al., 2004b. Molecke, M.A., K.B. Sorenson, T.T. Borek, W. Koch, O. Nolte, G. Pretzsch, F. Lange, W. B. Autrusson, O. Loiseau, N. Slater Thompson, and F.I. Young, *Spent Fuel Sabotage Aerosol Ratio Program and Surrogate Material Test Results*, SAND2004-4061C. Presented at the 45<sup>th</sup> Annual Meeting Institute of Nuclear Materials Management, INMM, July 18-22, 2004, Orlando, FL.

Molecke et al., 2004c. Molecke, M.A., M.W. Gregson, K.B. Sorenson, H. Tsai, M.C. Billone, Koch, O. Nolte, G. Pretzsch, F. Lange, W. B. Autrusson, O. Loiseau, N. Slater Thompson, R. Hibbs, F.I. Young, and T. Mo, *Initiation of Depleted Uranium Oxide and Spent Fuel Testing for the Spent Fuel Sabotage Aerosol Ratio Program*, SAND2004-4286C. Presented at PATRAM, 14th International Symposium on the Packaging and Transportation of Radioactive Materials, September 20-24, 2004, Berlin, Germany. (Note: Not documented by PATRAM, but published by Ramtrans Publishing, UK, following).

Molecke et al., 2004d. Molecke, M.A., M.W. Gregson, K.B. Sorenson, H. Tsai, M.C. Billone, Koch, O. Nolte, G. Pretzsch, F. Lange, W. B. Autrusson, O. Loiseau, N. Slater Thompson, R. Hibbs, F.I. Young, and T. Mo, *Initiation of Depleted Uranium Oxide and Spent Fuel Testing for the Spent Fuel Sabotage Aerosol Ratio Program*, SAND2004-4227J. Packaging, Transport, Storage and Security of Radioactive Material, Vol 15(2), pp. 131-139 (2004). Ramtrans Publishing, UK.

Molecke, Sorenson, and Gregson, 2004. Molecke, M.A., K.B. Sorenson, and M.W. Gregson, *Spent Fuel Sabotage Aerosol Ratio Test Program, Progress and Status, May 2004*, SAND2004-2090C. Presented at the 7th Technical Meeting of the International Working Group for Sabotage Concerns of Transport and Storage Casks, WGSTSC, May 18-20, 2004, Edinburgh, Scotland, UK.

NAC, 2002. NAC International, UMS Safety Analysis Report for the UMS Universal Transport Cask, EA790-SAR-001, Docket No. 71-9270, Dec. 2002, Rev. 1, Vol 1 of 2, p. 7.1-6, steps 21-24. December 2002.

Naegeli, 2004. Naegeli, R.E. *Calculation of the Radionuclides in PWR Spent Fuel Samples for SFR Experiment Planning*. SAND2004-2757. Sandia National Laboratories. Albuquerque, NM. June 2004.

Olander, 1976. Olander D.R., *Fundamental Aspects of Nuclear Reactor Fuel Elements*, TID 26711-PI, TIC/ERDA, p. 180. 1976.

Peacock et al., 2002. Peacock, H.B., M.L. Hyder, and M.E. Hodges. Treatment of Off-Gases from Melting Reactor Fuel, WSRC-MS-2002-00405. Westinghouse Savannah River Company, Aiken, SC. 2002.

Philbin et al., 2002a. Philbin, J.S., Hoover, M.D., Newton, G.J. *The Need for Confirmatory Experiments on the Radioactive Source Term from Potential Sabotage of Spent Nuclear Fuel Casks*, SAND2002-1027. Sandia National Laboratories. Albuquerque, NM. April 2002.

Sandia, NEPA, 2004. High-Energy Density Device Research Tests: Addendum to SNA 03-0193, NEPA ID: SNA04-0308. Sandia National Laboratories. July 2004.

Sandoval et al., 1983. Sandoval, R.P., J.P. Weber, H.S. Levine, A.D. Romig, J.D. Johnson, R.E. Luna, G.J. Newton, B.A. Wong, R.W. Marshall, Jr., J.L. Alvarez, and F. Gelbard. *An Assessment of the Safety of Spent Fuel Transportation in Urban Environs*, SAND82-2365. Sandia National Laboratories. June 1983.

Schmidt et al., 1981. Schmidt, E.W., M.A. Walters, and B.D. Trott. *Shipping Cask Sabotage Source Term Investigation*, BMI-2089, NUREG/CR-2472. Battelle Columbus Laboratory, Columbus, OH. December 1981.

Tsai and Billone, 2003. Tsai, H. and M. C. Billone. *Characterization of High-Burnup PWR and BWR Rods, and PWR Rods after Extended Dry-Cask Storage*. Proceedings of the 2002 Nuclear Safety Research Conference, NUREG/CP-0180, March 2003.

## DISTRIBUTION

U.S. Dept. of Energy, NNSA (4)  
Sandia Site Office  
MS-0184 P.O. Box 5400  
Albuquerque, NM 87185-5400  
Patty Wagner  
Kevin T. Gray  
Roy Lybarger (2)

U.S. Dept. of Energy, NNSA (4)  
Office of International Safeguards  
1000 Independence Ave., SW  
Washington, DC 20585  
Ronald C. Cherry, NA-243  
Russell S. Hibbs, NA-243 (3)

U.S. Department of Energy, OCRWM  
1000 Independence Ave., SW (7)  
Washington, DC 20585  
Nancy Slater-Thompson, RW-30E (5)  
J. Gary Lanthrum, RW-30E  
Deborah Dawson, RW, route OA-10

U.S. Department of Energy  
1000 Independence Ave., SW  
Washington, DC 20585  
Diana D. Clark, GC-53

U.S. Department of Energy, AL  
Albuquerque Service Center (3)  
P.O. Box 5400  
Albuquerque, NM 87185-5400  
A. K Kapoor  
S. C. Hamp  
M.D. Lineback

U.S. Nuclear Regulatory Commission  
Washington, DC 20555-0001 (12)  
Branch Chief, RPERWMB, MS T-9F31  
William R. Ott, MS T-9F31  
Tin Mo, RES, MS T-9F31 (5)  
F.I. Young, NSIR, MS T4-D8 (3)  
Bernard H. White, SFPO, MS O13-D13  
Robert E. Einziger, SFPO, MS O13-D13

Idaho National Laboratory, INL  
P.O. Box 1625  
Idaho Falls, ID  
E. David Houck (3)

Institut de Radioprotection et de Surete (7)  
Nucleaire, IRSN/DEND/SATE, BP17  
92262 Fontenay-aux-Roses Cedex, France  
Bruno Autrusson (4)  
Pierre Funk  
Jerome Joly  
Olivier Loiseau

Gesellschaft für Anlagen- und (4)  
Reaktorsicherheit (GRS) mbH  
Kurfuerstendamm 200  
10719 Berlin, Germany  
Gunter Pretzsch (4)

Gesellschaft für Anlagen- und (5)  
Reaktorsicherheit (GRS) mbH  
Schwertnergasse 1  
50667 Köln, Germany  
Florentin Lange (2)  
Wenzel Brücher (2)  
Eugen Hörmann

Fraunhofer-Institut für Toxikologie und  
Experimentelle Medizin, ITEM (4)  
Nikolai-Fuchs-Str. 1  
D-30625 Hannover, Germany  
Wolfgang Koch (3)  
Oliver Nolte

Office for Civil Nuclear Security  
Department of Trade & Industry (3)  
146 Harwell  
Didcot, OX11 0RA, UK  
John M. Reynolds (2)  
Bryan M. Reeves

Argonne National Laboratory (4)  
Energy Technology Div., Bldg 212  
9700 S. Cass Ave  
Argonne, IL 60439-3838  
Mike C. Billone (3)  
Tatiana Burtseva

Robert E. Luna, Consultant (2)  
10025 Barrinson NE  
Albuquerque, NM 87111

**Sandia Internal:**

1380, MS 1145 R. Brandhuber  
1382, MS 1143 R.F. Seylar  
1382, MS 1143 D.T. Berry  
1382, MS 1143 W.R. Strong  
1382, MS 1136 D.W. Vehar  
1383, MS 1141 J.E. Dahl  
1383, MS 1141 R.L. Coats  
1383, MS 1141 M.W. Gregson (4)  
1384, MS 1146 K.O. Reil  
1384, MS 1146 P.H. Helmick  
1517, MS 0836 J.E. Brockman (2)  
1517, MS 0836 D.A. Lucero  
1517, MS 0836 M.N. Luu  
1815, MS 1349 W.F. Hammetter  
1815, MS 1349 K.G. Ewsuk  
1822, MS 0886 R. Goehner  
1822, MS 0886 T.T. Borek  
2551, MS 1455 S.F. Bender  
2554, MS 1454 L.L. Bonzon  
2554, MS 1454 R.R. Dickey  
2554, MS 1454 M. Steyskal  
2554, MS 1454 M.G. Vigil  
6100, MS 0701 P.B. Davies  
6140, MS 1089 F.B. Nimick  
6141, MS 0718 D.R. Miller (4)  
6141, MS 0718 M.A. Molecke (10)  
6141, MS 0718 C. Lopez  
6141, MS 0718 I. Khalil  
6141, MS 0718 J. Sprung  
6141 MS 0719 S.W. Webb  
6142, MS 0718 K.B. Sorenson (3)  
6143, MS 0718 J.J. Danneels  
6143, MS 0718 D. Osborn  
6143, MS 0718 R.H. Yoshimura  
6143, MS 0718 R.F. Weiner (2)

6800, MS 0771 D.L. Berry  
6860, MS 0736 M.C. Walck  
6923, MS 1361 J.C. Matter  
6923, MS 1361 D.R. Ek  
6923, MS 1361 D.D. Glidewell  
8945-1, MS 9018 Central Technical Files (1)  
9616, MS 0899 Central Technical Library (2)  
9612, MS 0612 Review & Approval Desk  
for DOE/OSTI  
10264, MS 1122 C.I. Kajder  
10328, MS 1094 H.T. Barclay  
10328, MS 1094 M. Callahan  
10328, MS 1142 D. Siddoway  
12342, MS 1453 C.E. Esparza